MALACOLOGIA, 1992, 34(1–2): 143–342

THE POMATIOPSIDAE OF HUNAN, CHINA (GASTROPODA: RISSOACEA)

George M. Davis[1], Cui-E Chen[2], Chun Wu[3] ,Tie-Fu Kuang[4], Xin-Guo Xing[5], Li Li[6], Wen-Jian Liu[7], Yu-Lun Yan[8]

ABSTRACT

This is a monograph involving the systematics of the 17 species of pomatiopsid snails thus far found in Hunan Province, the People's Republic of China. The Triculinae and Pseudobythinellini (new tribe) of the Pomatiopsinae dominate the pomatiopsid fauna. Four new species are described, three of *Neotricula* and one of *Tricula*. Detailed anatomical data are the basis for describing each species. The anatomies of "*Akiyoshia*" and *Lithoglyphopsis* are presented for the first time. *Guoia* is a new genus for some species previously considered to be *Lithoglyphus* (a strictly European hydrobiid genus) or *Lithoglyphopsis* (restricted to China). The anatomical data are the basis for phenetic and cladistic analyses to provide insight into those characters and character-states that serve to distinguish taxa, and to assess relationships among genera of the tribes Pachydrobiini (*Halewisia*, *Neotricula*, *Pachydrobia*, *Jinhongia*, *Robertsiella*, *Guoia*, *Wuconchona*, *Gammatricula*) and Triculini (*Tricula*, *Delavaya*, *Fenouilia*, *Lithoglyphopsis*, *Lacunopsis*). *Hubendickia* served as the outgroup genus of the remaining tribe of the Triculinae, the Jullieniini. Biogeographic deployment of the genera of all three tribes of the Triculinae is mapped on an area cladogram of relevant river systems. Genera of the Jullieniini dominate the lower Mekong River. *Tricula* extends from Northern India down the Yangtze and upper Mekong rivers. *Tricula* and *Neotricula* primarily flourish along the Yangtze River drainage. Four genera have shells that are so similar that shell characters cannot be used to distinguish among the genera: *Tricula*, *Neotricula*, *Jinhongia* and *Gammatricula*. Most of the species treated here are of medical importance because they either transmit or are suspected of transmitting lung flukes of the genus *Paragonimus*, or blood flukes of the genus *Schistosoma*.

Key words: Pomatiopsidae, biogeogrpahy, phenetics, cladistics, China, Hunan, *Schistosoma*, *Tricula*, *Neotricula*, *Paragoniumus*, Yangtze River

INTRODUCTION

This work is one of a series of papers dedicated to establishing the detailed anatomy and systematic relationships of genera of southeast Asian and Chinese freshwater prosobranch snails suspected of being members of the Pomatiopsidae as defined in Davis (1979, 1980). It is one more step in documenting the extensive speciation that has occurred within the tribes Triculini and Pachydrobiini of the Triculinae, which occur primarily throughout southern China, in contrast to the extensive Jullieniini adaptive radiation documented in the lower Mekong River in Thailand, Laos, and Cambodia (Davis, 1979).

In this work, *Guoia* is established as a new genus. The anatomies of "*Akiyoshia*" and *Lithoglyphopsis* are presented for the first time. Anatomical data are provided for clarification of the genus *Pseudobythinella*. Several nomenclatural problems are clarified or presented relative to necessary future work. Seventeen nominal species are treated.

Phenetic and cladistic analyses are done to provide insight into those characters and character-states that serve to distinguish taxa, and to assess relationships among genera of the tribes Pachydrobiini and Triculini,

[1]The Academy of Natural Sciences of Philadelphia, 1900 Benjamin Franklin Parkway, Philadelphia, Pennsylvania 19103-1195 U.S.A.
[2]Institute of Parasitic Diseases, Zhejiang Academy of Medical Sciences, Hangzhou, Zhejiang Province, People's Republic of China
[3]Hunan Medical University, Changsha, Hunan Province
[4]Hengshan County Anti-Epidemic Station, Hengshan, Hunan, People's Republic of China
[5]Anhua County Anti-Epidemic Station, Zhuzhou, Hunan, People's Republic of China
[6]Zhuzhou City Anti-Epidemic Station, Zhuzhou, Hunan, People's Republic of China
[7]Cili County Anti-Epidemic Station, Cili, Hunan, People's Republic of China
[8]Shimen County Anti-Epidemic Station, Shimen, Hunan, People's Republic of China

with one genus of the Jullieniini serving as the outgroup. Biogeographic deployment of the Triculinae is considered in conjunction with an assessment of the evolution of river systems in continental south Asia.

Most of the taxa treated here are of medical importance because they either transmit or are suspected of transmitting lung flukes of the genus *Paragonimus* or blood flukes of the genus *Schistosoma*.

MATERIAL AND METHODS

Localities are provided with the synonymy section for each species. Sites 1 to 12 are found on Figure 1. With reference to Figure 1, be aware that maps published at different times may provide different spellings for standard Chinese characters. Relevant here are: Hsiang = Xiang; Tzu = Zi; Lin = Li. The Yangtze River = the Chang Jiang (jiang = river; shui = river). Dong Ting Lake (Lake = Hu) = Tung t'ing Hu.

Abbreviations for institutions housing voucher species are: ANSP = Academy of Natural Sciences of Philadelphia (the A- number sequence indicates alcohol-preserved specimens); IZAS = Institute of Zoology, Academica Sinica; SMF = Senckenberg Museum, Frankfurt A.M. Germany; ZAMIP = Zhejiang Academy of Medical Sciences, Institute of Parasitic Diseases, Hangzhou, China. Voucher catalog numbers are provided in the synonymy section for each species.

Methods are those of Davis & Carney (1973), Davis et al. (1976), Davis (1979), and Davis & Greer (1980). All dissections were done with living material in Hunan, China using a Wild dissecting microscope and a Nikon high intensity lamp. Scanning electron microscopical analyses, photography of shells, radular preparations and computer analyses were done in Philadelphia.

Descriptions of taxa employ only those character and character-states useful to discriminate among species of Pomatiopsidae. Character-states common to all are not repeated here but are described elsewhere (Davis, 1979, 1980).

Relative sizes of organs or shells are defined by range in size (as in shells) or ratios to facilitate comparison among taxa using terms such as "small, " "elongate, " etc. This practice follows Davis et al. (1986) and all later papers in this series of studies. The sizes and ratio used are:

1. Shell length: large (≥ 5.0 mm), medium (4.0–4.9 mm), small (2.1–3.9 mm), minute (≤ 2.0 mm) (based on mean size of the mature size class with the greatest number of individuals, realizing that mature snails may occur with different numbers of whorls, e.g. 5.0, 5.5, 6.0 whorls).

2. Operculum attachment pad: width of attachment pad ÷ width of operculum: narrow (≤ 0.35), wide (0.36–0.55), very wide (≥ 0.56).

3. Osphradium length: length of osphradium ÷ length of gill (Davis et al. 1976, 1982, 1983): long (≥ 0.40), short (≤ 0.35).

4. Length of gill filament section Gf_2: length of Gf_2 ÷ length of Gf_1 and Gf_2: long (≥ 0.51), medium (=normal) (0.31–0.50), short (≤ 0.30).

5. Gill filament number: few (≤ 15), numerous moderate (16–25), numerous (≥ 26).

6. Bursa copulatrix length: length of bursa ÷ length of the pallial oviduct: long (≥ 0.40), short (≤ 0.38).

7. Albumen gland length: length of the albumen gland (Ppo) ÷ length of the entire pallial oviduct: standard (≥ 0.45), short (≤ 0.42).

8. Male gonad length: gonad length ÷ length of digestive gland: short (< 0.50), long (≥ 0.50).

9. Seminal receptacle duct length: very short or absent (≤ 0.02 mm), long (> 0.02 mm).

10. Radula length: short (≤ 0.40 mm), medium (0.41–0.59 mm), long (0.60–0.79), very long (≥ 0.80 mm).

11. Radula; mean rows of teeth: few (≤ 59), moderate (60–69), many (70–84), very many (≥ 85).

12. RPG ratio: length of the supraesophageal connective ÷ sum of the length of the right pleural ganglion, the supraesophageal connective, and the supraesophageal ganglion; concentrated (≤ 0.29), moderately concentrated (0.30–0.49), elongate (0.50–0.67), extremely elongate (≥ 0.68) (Davis et al. 1984, 1985).

13. Subesophageal connective length: usual or standard triculine (0.02–0.09 mm); none; long (≥ 0.10 mm) [based on average of several measurements].

Multivariate Analysis

Shell data were analyzed for populations of *Guoia*. The first data matrix involved 33 OTUs (operational taxonomic units) (individual shells) and 11 characters. The OTUs were:

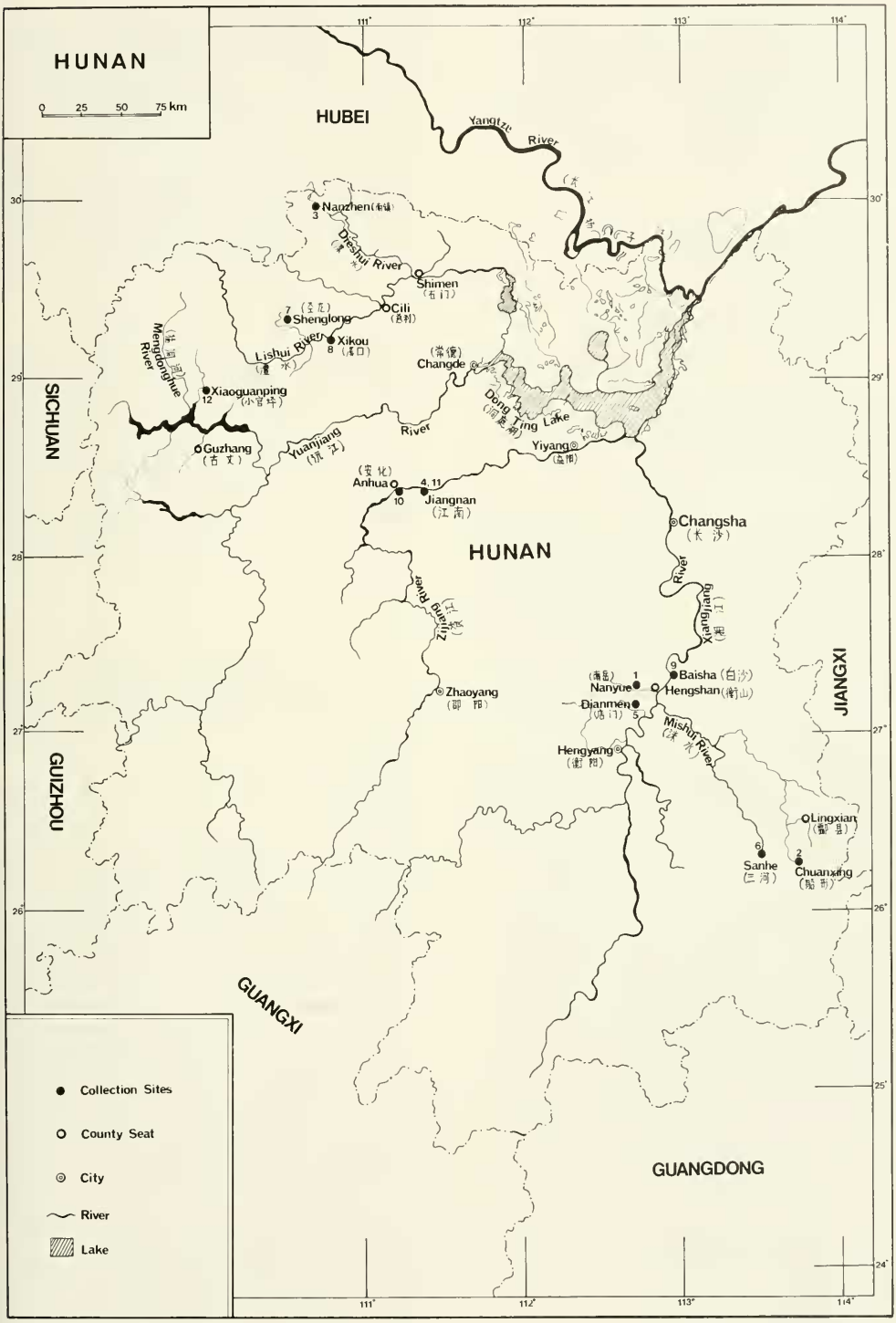

FIG. 1. Map of Hunan, China, showing localities from which specimens described in this monograph were collected.

Guoia viridulus, large class snails, males (1–7), females (8–12); ANSP cataloged specimens of *Guoia viridulus* collected over 90 years ago (18–21); small class snails, males (22–26), females (27–32). *Guoia fuchsianus* males (13, 14), females (15–17). ANSP cataloged historic *G. fuchsianus* (33).

The characters were:

1. Number of whorls
2. Length
3. Width
4. Length of body whorl
5. Length of penultimate whorl
6. Width of penultimate whorl
7. Width of 3rd whorl
8. Length of last three whorls
9. Length of aperture
10. Width of aperture
11. Width of columellar shelf

The second matrix included individuals of two populations from historic collections, *Guoia fuchsianus* cataloged in the ANSP collections: ANSP 98205 (34–38), ANSP 45961 (39–41). These OTUs were added to the OTUs of matrix one to give a total OTU count of 41. The character matrix was reduced because all OTUs 34–41 had eroded apices, thus characters 1, 2, 7, and 8 could not be measured for all individuals.

Computations were made using the 1974 version of NT-SYS (Rohlf et al., 1972). Characters were standardized (standard deviation and mean values). Similarity and distance coefficients were calculated and phenograms produced using UPGMA. Cophenetic correlations were calculated. Principal Component Analysis (PCA) was done with components extracted until eigenvalues became less than 1.0. A transposed matrix of the first three principal components with their character loading was postmultiplied by the standardized matrix to yield a matrix of OTU projections in the principal component space (Rohlf et al., 1972). The OTU locations in the three-dimensional space were used as the initial configuration for a nometric multidimensional scaling (MDS) placement of Q-mode taxonomic distances between OTUs (Kruskal, 1964). Ordination was done followed by a Prim Network (minimum Spanning Tree = MST). Subsequently a phenogram was produced based on MDS and the cophenetic correlation calculated.

A similar multivariate analysis was used to assess phenetic relationships among 30 OTUs on the basis of shell data. The OTUs involved species of *Tricula*, *Neotricula* or species the shells of which resembled those of species of *Tricula*. The analysis was done as an aid for distinguishing among species on the basis of shell characters.

Another similar multivariate analysis was done to assess phenetic relationships among the same species for which the shell analysis was done. However, this analysis involved 48 anatomical character-states.

Cladistic Analysis

Scorings were not done in binary alone but involved six multistate characters (Table 85). Analysis was first done using the computer-mediated program Hennig-86 (Farris, 1988). *Hubendickia* served as the outgroup. Options run were cc-. (character-states all unordered); ie; tplot; tsave; nelsen. A final non-computer-mediated cladogram was made after weighting one character following establishing the direction of evolution of its states.

Shell Characters

Shell character-states is illustrated in Figs. 2, 3. Aside from shell measurements there are a number of diagnostic qualitative character-states of use to discriminate among shells (Tables 1, 2).

Triculine shells have three predominant shapes (Fig. 2A): globose, ovate-conic, ovate-turreted. Many character-states involve the aperture. The adapical end may be regularly rounded or slightly constricted to form an adapical apertural notch (Adn, Fig. 3D). The constriction may be less pronounced (Fig. 3E). The adapical aperture and apertural notch may be extended to form the adapical apertural beak (Adb, Fig. 3A). The apertural notch may have a noticeable internal groove (Ngr, Fig. 3E) or lack a groove (Fig. 3A). The adapical apertural notch may be bounded by an adapical tooth or node on the inner lip (Adt, Fig. 3A, D); or the adapical inner lip may lack such a thickening (Fig. 3E, H).

The inner lip may (Ari, Fig. 3A) or may not be fused (Gap, Figs. 3D, E) to the body whorl. When separated from the body whorl the gap (Gap) may be narrow (Fig. 3E) or wide (Fig. 3D). The inner lip may be straight, arched (Fig. 3A), sigmoid or undulating (Fig. 3E), or angled (Fig. 3D). The adapical part of the inner lip may be thickened (Adil, Fig. 3D) or thin; the abapical part of the inner lip the

TABLE 1. Twenty-six shell character and character-states useful for describing shells of Triculinae as illustrated in Figures 2 and 3.

Abil	Abapical inner lip
Abs	Abapical spout
Adb	Adapical apertural beak
Adil	Adapical part of inner lip
Adt	Adapical tooth or node
Adn	Adapical apertural notch
Agp	Adapical apetural gap
Aol	Adapical outer lip angle
Aols	Adapical outer lip sinus
Ari	Arched inner lip
Cr	Crenulated suture
Ct	Columellar tooth
Gap	Gap between the body whorl and the inner lip
L	Length
Mln	Mid-lip notch
Nab	Normal adapical aperture
Ngr	Adapical notch groove
Ol	Outer lip
Sfo	Scooped forward
Sin	Sinuate outer lip
Stl	Straight lip
Umc	Umbilical chink
Var	Varix
W	Width
x	distance from base of body whorl to abapical end of aperture
y	distance from edge of outer lip to edge of body whorl

same. The inner lip may have a mid-lip notch (Mln, Fig. 3D).

The abapical end of the aperture may project noticeably beyond the base of the body whorl when the shell is viewed in apertural view (Fig. 3E); it may not (Fig. 3F). The abapical end of the aperture may be spout-like (Figs. 3D, E); it may not (Fig. 3A, F). The columella may have a tooth (Ct, Fig. 3F). It is necessary to break open the body whorl of some shells from a population to determine whether or not there is an internal columellar node, tooth, or keel.

The adapical end of the aperture may be pulled away from the body whorl leaving an adapical gap (Agp, Fig. 3D, F) or the adapical aperture may be fused to the body whorl (Fig. 3A).

In side view the outer lip may be straight (Stl, Fig. 3H) or sinuate (Sin, 3B). The outer lip may be aligned with the axis of coiling (Fig. 3C, H) or scooped forward (Sfo, Fig. 3B). In side view there may be an adapical depression or sinus in the outer lip (Aols, Fig. 3H) caused by an adapical apertural notch.

Rotating the shell from apertural view to the right (apex up) so that the inner lip is perpendicular to the horizontal, the abapical part of the inner lip may be deflected away from the columella causing a lip deflection angle (Fig. 3G, 2B). Such an angle may not occur.

Gill Filament Shape

Considering the longest (thus mid-gill) gill filaments, three shapes are found when the filaments are examined so as to see the entire leaflet (Fig. 4). The Gf_2 section may be flat, have a modest dome, or be high domed.

Vital Staining

Davis (1967) discussed using aqueous methylene blue and neutral red as vital stains. The exact methods are as follows: small quantities of powdered stain are dumped into a quantity of tap water (approximately 500 ml) and stirred until dissolved. Sufficient powder is added so that when the solution is placed before a light the solution is opaque. Wide-mouth jars are used, one each for the two stains. Wide mouth containers are specified because the stain is used over and over again. With the living animal pinned out on the black parafin-wax layer in a 9-cm Petri dish, the water covering the animal is poured off and the stain poured on to cover the animal. The stain is left on for 30 seconds to a minute, then poured back into the storage bottle. The animal is rinsed five to ten times to remove excess stain and then covered with water to continue the dissection.

Neutral red is used first to deliniate glandular tissue and the ducts of the female reproductive system. The two regions of the pallial oviduct are differentiated; the oviduct is stained as well as the gonad and oocytes.

Methylene blue is used next; it seems to harden and delineate the ducts of the female reproductive system. The slender duct of the seminal receptacle and the various other components of the bursa copulatrix complex of organs are made to stand out.

Bouins Solution

When all work with the living animal is finished, Bouins solution is most useful to eliminate problems caused by mucus, to delineate mantle cavity structures, such as the gill filaments, and to dissect the nervous system. The nerves and ganglia stain bright yellow enabling one to see them better and to differen-

TABLE 2. Shell character-states scored for 29 characters used for a multivariate analysis of phenetic relationships among 21 species of Triculinae, the shells of which either are classified as *Tricula* or *Neotricula* or resemble the shells of these two genera.

1. Size:	small (0), medium (1), minute (2), long (3)
2. Shape:	ovate-conic (0), ovate-turreted (1), turreted (2), cylindrical-conic (3), globose-conic (4)
3. Aperture shape:	ovate (0), pyriform (1), distorted (2)
4. Umbilicus:	none (0), chink (1), clearly open (2)
5. Whorl at suture:	smooth (0), crenulated (1)
6. Teleoconch sculpture:	none (0), spiral microsculpture at suture (1)
7. Spiral sculpture at mid body-whorl to shell base	none (0), with (1)
8. Protoconch whorls:	smooth (0), wrinkled (1), malleated and/or pitted (2)
9. Adapical aperture:	normal (0), with notch (1), with beak (2)
10. Adapical aperture:	normal (0), with internal groove (1)
11. Adapical aperture:	normal (0), with sinus (1)
12. Abapical aperture:	normal (0), with spout (1)
13. Inner lip:	straight (0), arched (1), sinuate (2), angled (3)
14. Outer lip-side view:	straight (0), sinuate (1)
15. Outer lip-side view:	parallel with axis of coiling (0), scooped forward (1), slanted back (2)
16. Inner lip:	no tooth (0), with tooth (1)
17. Inner lip:	no notch (0), with notch (1)
18. Base of inner lip, side view:	straight (0), angled to form lip deflection angle (1)
19. Inner lip:	thin (0), thick [≥ 0.10mm] (1), differentially thickened (2)
20. Inner lip:	fused to body whorl (0), partly separated (1), totally separated by narrow gap (2), widely separated (3)
21. Adapical aperture:	fused to body whorl (0), slightly separated (1), widely separated (2)
22. Columella within body whorl:	smooth (0), tooth or node (1), spiral keel (2), lamellae on aperture side of columella (3)
23. Varix:	none (0), slight (1), pronounced (2)
24. Adapical aperture:	normal (0), with beak tubercle (1)
25. Adapical outer lip angle:	none (0), slight (1), extended (2)
26. Base of body whorl:	normal (0), with keel spiraling down from umbilical area (1)
27. Base of shell at umbilicus:	normal (0), with wide columellar shelf (1)
28. Base of shell at abapical lip:	normal (0), with basal post (1)
29. Shell attains 7.0 whorls:	no (0), yes (1)

tiate nerves from muscle fibers. Bouins solution strengthens the nerves such that they can be handled better. Dissections of the head involving the buccal mass, salivary glands and associated nerves are facilitated.

Body Measurements

How the lengths of the gonad, digestive gland, and body are measured is illustrated in Davis & Carney (1973). Lengths of mantle cavity organs are measured with the mantle cut along the right side of the neck from the mantle edge to the rear of the mantle cavity. The mantle is then reflected to the left and pinned out as shown in Figure 5. How lengths of mantle cavity structures are measured is illustrated in Figure 5. The ocular micrometer is positioned and rotated along the dotted trajectory. As shown in Figure 5, not all gill filaments may be illustrated.

Abbreviations

a	line perpendicular to mid-line "x" at posterior edge of eye lobes
a′	Line perpendicular to mid-line "x" at the anterior edge of penial base
Adb	Adapical apertural beak
Ae	Abapical embayment
Af	Anterior foot;
Algo	Anterior lobes of gonad
Als	Adapical outer lip sinus
Apg	Anterior pedal glands.
Apo	Anterior pallial oviduct = capsule gland
Apo-1	Anterior pallial oviduct = capsule gland
Apo-2	Different tissue type anterior to capsule gland.
Ast	Anterior chamber of stomach
Au	Auricle
Bc	Basal crescent
Bg	Beak groove

Bm Buccal mass
Bp Base of penis
Bu Bursa copulatrix
Cc Cerebral commissure
Cl Columellar muscle
Coi Oviduct coil
Cr Crescent ridge
Cs Columellar shelf
Csd Common sperm duct
Dbu Duct of bursa
Di Digestive gland
Dsr Duct of seminal receptacle
Ebr Eyebrow
Ebv Efferent branchial vein
Edi Anterior edge of digestive gland (Figs. 141, 142)
Edi Dashed line indicates anterior limit of digestive gland
Ej Ejaculatory duct
Emc Posterior end of mantle cavity
Epr Dashed line indicates posterior limit of prostate gland
Es Esophagus
Ey Eye
Eyb Eyebrow
Fp Fecal pellet
Gf_1 Thickened basal bar of gill filament
Gf_2 Slender terminal part of gill filament
Glo Glandular lobe
Go Gonad
Go-a Section of gonad, the extent of which is indicated by the dashed line, removed to show seminal vesicle
Go-b Gonad
Gr Patch of white granules
Gra Granules or glands, white to lemon yellow
Grv Groove
Gs Grey streak on Ast
Il Inner lip
In Intestine
In_1 Intestine looping around anterior end of style sac
In_2 Fecal pellet compressor section of intestine
In_3 Anterior intestine
Ki Kidney
L Length
Lap Length of aperture
Lbw Length of body whorl
LGf_1 Length of gill filament section Gf_1
LGf_2 Length of gill filament section Gf_2
LGi Length of gill
LMa Length (= width) of mantle collar anterior to gill
Lm Dashed line is trajectory used to measure length of gill and length of mantle cavity
LofA Length of shell with aperture pressed down on a horizontal surface
LOs Length of osphradium
Lpl Left pleural ganglion
Lpw Length of penultimate whorl
Ma Mantle collar
Ne Neck
Ngr Adapical notch groove
Odi Opening from stomach to digestive gland
Oki Opening of kidney into mantle cavity
Ol Outer lip
Omc Opening of spermathecal duct into mantle cavity
Omn Osphradiomantle nerve
Ooc Oocyte(s)
Oop Opening into albumen gland (Ppo)
Oov Opening of oviduct to albumen gland (enlarged in Fig. 10)
Ope Opening for sperm entry to pericardium
Opo Opening of oviduct into albumen gland
Opr Opening to vas deferens
Os Osphradium
Osd Opening of spermathecal duct to mantle cavity (Figs. 11, 21)
Osd Point where oviduct fuses to, and opens into pericardium
Osm Osphradiomantle nerve
Osr Oviducal seminal receptacle
Ov Oviduct
Pa Papilla
Pbu Pericardial bursa
Pc Pellet compressor (= In_2)
Per Pericardium
Pe Penis
Pf Penial filament
Ppo Posterior pallial oviduct = albumen gland
Pr Prostate
Psc Pleurosupraesophogeal connective
Pst Posterior chamber of stomach
Rcg Right cerebral ganglion
Ri Yellow ridge
Rpl Right pleural ganglion
Rs Radular sac
Sd Spermathecal duct
Sdo Opening of oviduct into the pericardium
Sdu Sperm duct
Sec Pleurosupraesophageal connective
Seg Supraesophageal ganglion
Sg Salivary gland
Sn Snout
Sr Seminal receptacle
Sts Style sac
Sty Stylet
Suc Pleurosubesophageal connective

Sug	Subesophageal ganglion
Sv	Seminal vesicle
Tn	Tentacle
Twv	Thin walled vestibule
Uc	Umbilical chink
Vd	Vas deferens
Vd_1	Posterior vas deferens
Vd_2	Anterior vas deferens
Ve	Vas efferens
Vei	Vein
Ven	Ventricle
W	Width (Fig. 110)
Wap	Width of aperature
Wgr	White granular inclusions
Wg	White granules
WofA	Width of shell with aperature pressed down on a horizontal surface
W	Wall of neck
x	Mid-line of snout-neck with snout anterior (up).
x	Marks the same point in Figs. 20, 21 A and B; 117A, 118
Yri	Yellow ridge along anterior and posterior ends of the Ast

SYSTEMATICS

Taxa Treated

POMATIOPSIDAE

Pomatiopsinae
  Pomatiopsini
    Oncomelania
      Oncomelania hupensis Gredler, 1881
  Pseudobythinellini, Davis & Chen new tribe
    Akioyshia
      "*Akiyoshia*" *chinensis* Liu, Zhang & Chen, 1982
    Pseudobythinella
      Pseudobythinella chinensis (Liu & Zhang, 1979)
      P. shimenensis Liu, Zhang & Chen, 1982
Triculinae
  Pachydrobiini
    ***Guoia* Davis & Chen gen. nov.**
      G. fuchsianus (Moellendorff, 1885)
      G. viridulus (Moellendorff, 1888)
    Neotricula
      N. cristella (Gredler, 1887)
      ***N. dianmenensis* Davis & Chen, sp. nov.**
      ***N. duplicata* Davis & Chen, sp. nov.**
      ***N. lilii* Chen & Davis, sp. nov.**
      N. minutoides (Gredler, 1885)

Triculini
  Lithoglyphopsis
    L. modesta (Gredler, 1886)

  Tricula
    T. gredleri Kang, 1986
    ***T. maxidens* Chen & Davis, sp. nov.**
    T. odonta Liu, Zhang & Wang 1983a

Nomina nuda:
  Tricula gredleri
  Akiyoshia odonta

Nomina Nuda

Two names were introduced into the literature for presumed Pomatiopsidae from Hunan Province but without photographs, illustrations, designation of types, or descriptions that would permit one to identify the species in question. Accordingly these are nomina nuda. The nominal taxa involved are:

Tricula gredleri Feng et al., 1985 [Kang sp. nov.]
Tricula gredleri Feng et al., 1986 [Kang sp. nov.]
Akiyoshia (*Saganoa*) *odonta* Feng et al., 1985 [Kang sp. nov.]
Akiyoshia (*Saganoa*) *odonta* Feng et al., 1986 [Kang sp. nov.]

Higher Taxa Defined

The family Pomatiopsidae was differentiated from the Hydrobiidae in Davis (1979); two subfamilies were recognized, the Pomatiopsinae and Triculinae. Both subfamilies have a spermathecal duct, a pomatiopsid type central tooth (square to rectangular) with pronounced basal cusps arising from the face of the tooth (an exception includes the Pseudobythinellini discussed below), cover eggs (laid singly) with sand grains, and do not brood young. The penis is without complex glands or lobes. The differentiation of the pomatiopsid subfamilies from other higher taxa with spermathecal ducts was given in Davis et al.(1985: 74–75). These higher taxa are the Hydrobiidae: Littoridininae and Amnicolinae (also see Hershler & Thompson, 1988).

The Pomatiopsinae are Gondwanian in distribution. Pomatiopsinae snails have an elon-

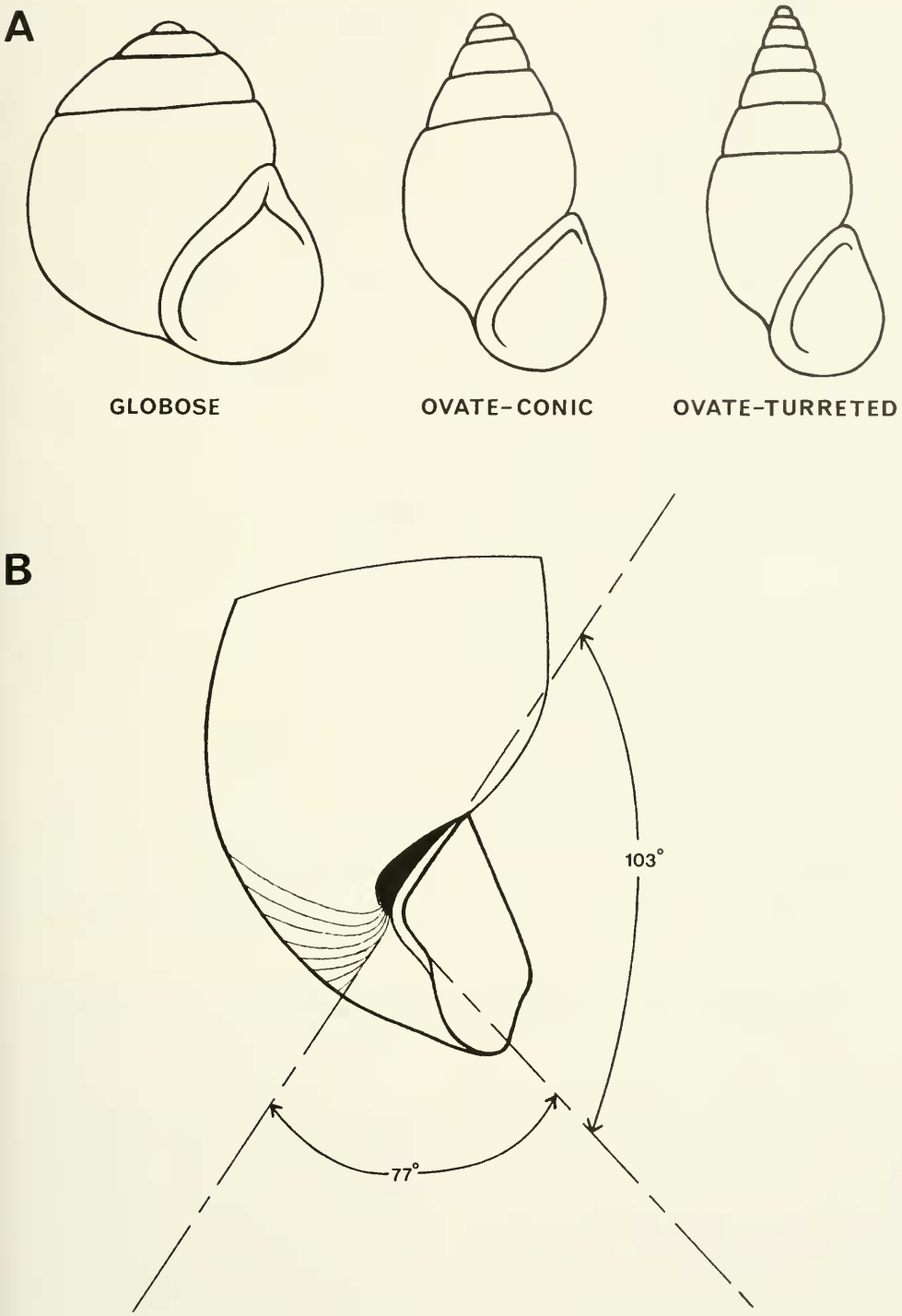

FIG. 2. Shell characters used in describing species of Hunan Triculinae. A. Three major shell shapes. B. Inner lip in side view showing a pronounced lip deflection angle.

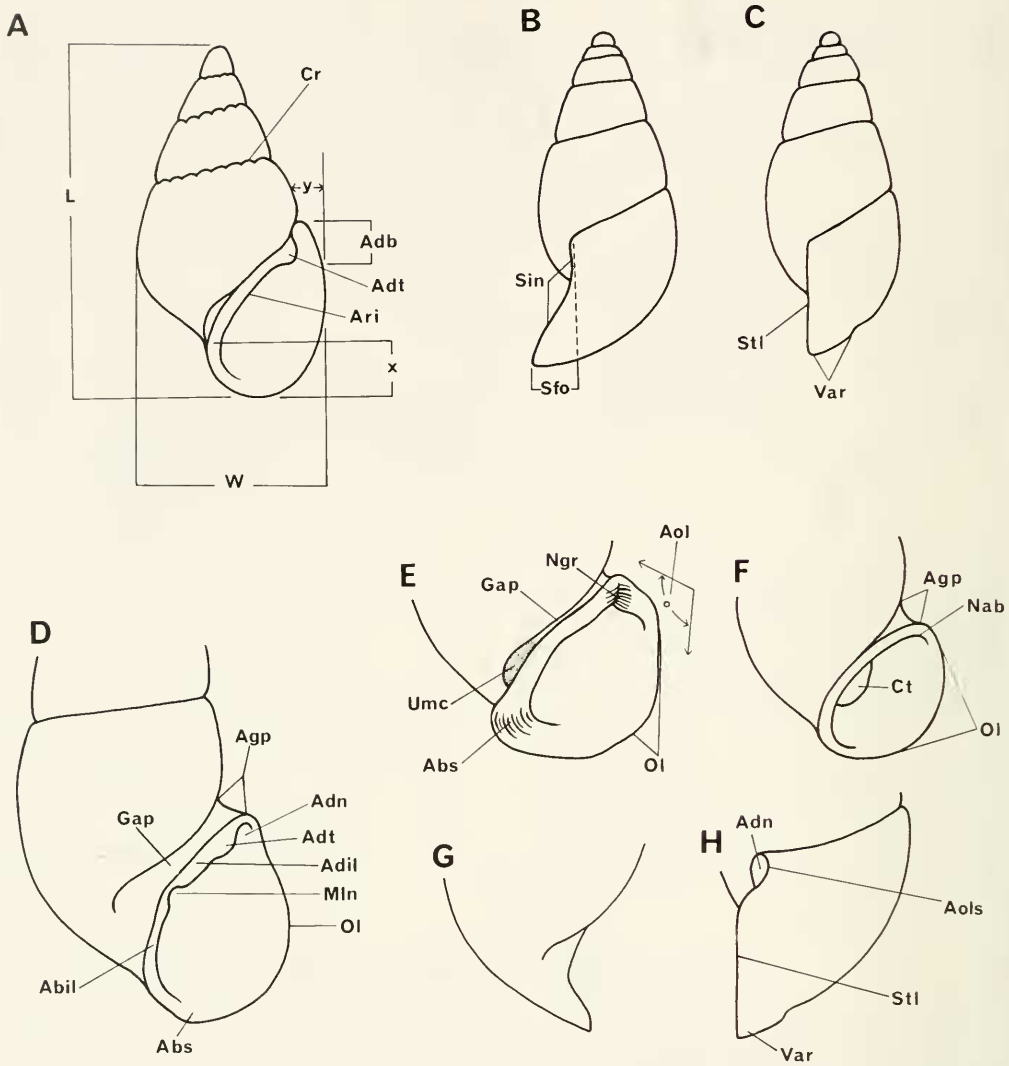

FIG. 3. Shell characters used in describing species of Hunan Triculinae. Labels are defined in Table 1.

gated spermathecal duct extending to the anterior end of the mantle cavity. In the tribe Pomatiopsini, the eyes are in pronounced bulges. These snails have a pedal crease, suprapedal fold and omniphoric groove. They move by a step-wise mode. They have evolved from freshwater to an amphibious mode of existence, and in Japan *Blanfordia* has become terrestrial (Davis, 1979, 1981). The tribe Pseudobythinellini is placed in the Pomatiopsinae because of the elongated spermathecal duct. The central tooth is of the *Hydrobia* type with a pair of cusps arising from the lateral angles. The eyes are not in pronounced eye lobes. There is no suprapedal fold, omniphoric groove or pedal crease. Animals move by ciliary glide. The penis of species classified here as Pseudobythinellini lacks a penial lobe with functioning duct (in addition to the vas deferens) that widens to form a wide coiled mass or penial gland in the cephalic haemocoel. The acces-

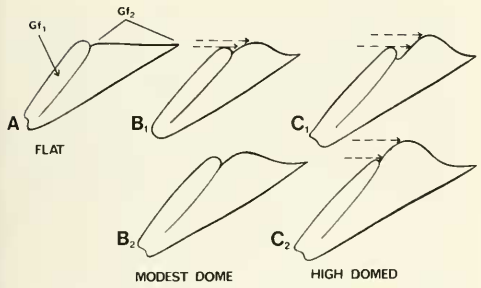

FIG. 4. Shapes of the Gf_2 segment of the largest gill filaments.

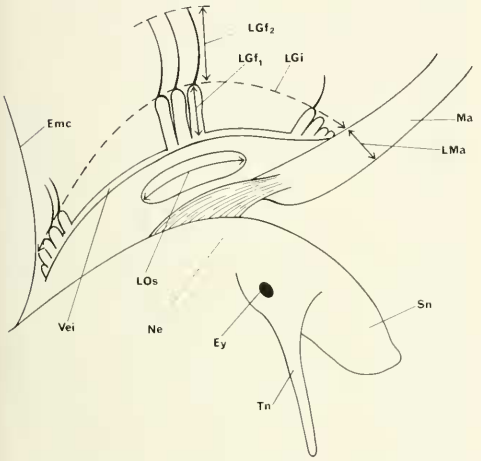

FIG. 5. Mantle reflected to reveal mantle cavity organs and how their lengths were measured. The dashed line is the trajectory for measuring the length of the gill. The length of the mantle cavity is measured from Emc along the LGi plus LMa.

sory penial lobe and penial gland are characteristic of the European genus *Bythinella* and North American genus *Amnicola* of the Hydrobiidae: Amnicolinae (Davis et al., 1985; Hershler & Thompson, (1988).

The Triculinae are Asian with a distribution from northern India throughout South China and southeast Asia. No Triculinae are found in Japan (Shikoku to Okinawa). Ioganzen & Starobogatov (1982) refer their new genus *Sibirobythinella* to the Triculidae. However, given the extensive convergences in structure such as the spermathecal duct and central tooth of the radula (reviewed in Davis et. al., 1985) it is not at all certain that taxa from Siberia or northeastern Russia relegated to the Triculidae by Russian workers are Triculinae sensu Davis (1979, 1980). *Sibirobythinella* is not, based on data provided, a triculine snail. The shell and radula might indicate placement in the Pseudobythinellini. Ioganzen & Starobogatov (1982) place their taxon in the family Triculidae apart from taxa they erected to family status such as Littoridinidae, Pomatiopsidae and Stenothyridae, all characterized by having a spermathecal duct running independently of the pallial oviduct from the mantle cavity to the bursa copulatrix. Unfortunately, they do not provide sufficient data to differentiate their taxon from European Hydrobiidae: Littoridininae, Amnicolinae, or Pomatiopsinae: Pseudobythinellini.

Triculinae snails have a short spermathecal duct opening to the posterior end of the mantle cavity. The snails are aquatic, do not have a suprapedal fold, pedal crease, or omniphoric groove. Only in a few derived genera are the eyes in pronounced lobes. Snails progress by ciliary glide.

Tribal, Generic and Species Descriptions

POMATIOPSINAE

Pomatiopsini

Type genus. Pomatiopsis Tryon 1862

Diagnosis. Ovate-conic to turreted shells. Shell length greater than 2.5 mm; most greater than 3.0 mm. Apical whorls are not flattened. Spermathecal duct runs from the bursa copulatrix to the anterior end of the mantle cavity. Spermathecal duct not tightly pressed to pallial oviduct. Sperm duct running posteriorly from oviduct to the bursa or the spermathecal duct at the bursa. Eyes are in pronounced eye lobes. There is a suprapedal fold, an omniphoric groove, and pedal crease. Basal cusps of the central tooth of the radula arise from the face of the tooth.

Oncomelania Gredler 1881

Type Species. Oncomelania hupensis Gredler 1881: 120-121; pl. 6, fig. 5

Type locality. U—tschang—fu, March 1879. [= Hubei Province; Wu—Tshan—fu; Yen, 1939].

Designation. By monotypy

Types. Bozen; lectotype and two paralectotypes

Bozen No. 89. No. types at SMF (Zilch, 1974: 197)

Oncomelania hupensis Gredler, 1881

No detailed study of this well-known species is presented here. This species is included for completeness sake in monographing the Pomatiopsidae of Hunan, China. This species is the vector for *Schistosoma japonicum* and abounds in the marshes around Dong Ting Lake and along the Yangtzee River (Fig. 1) (Lou et al., 1982; Liu et al., 1981). Detailed anatomical data for *Oncomelania* have been published elsewhere (Davis 1967, 1968a, 1969a; Davis & Carney 1973).

Pseudobythinellini Davis & Chen New Tribe

Type genus. Pseudobythinella Liu & Zhang 1979.

Diagnosis. Ovate shells less than 2.5 mm long, with flattened apical whorls. The sperm duct runs anteriorly from the oviduct to the spermathecal duct; it is so tightly pressed to the pallial oviduct that it is difficult to differentiate it. Unlike the Pomatiopsini, the sperm duct enters the spermathecal duct far anterior to the bursa copulatrix; the duct of the bursa is thus elongated (the continuation of the spermathecal duct to the bursa from the point of entry of the sperm duct). Eyes are not in pronounced eye lobes. There is no suprapedal fold, no omniphoric groove or pedal crease. Animals are aquatic and move by ciliary glide. Basal cusps of the central tooth of the radula arise from the lateral angles of the tooth.

Synonymy. Erhaiini Davis et al. 1985: 69.

Discussion. The genera included in this tribe are *Akiyoshia* and *Pseudobythinella* from China. Liu & Zhang, 1979, described certain species from China and classified them as *Bythinella* and *Pseudobythinella*. They provided no anatomical data aside from penis and radular illustrations. *Pseudobythinella* Liu & Zhang, 1979, was described as different from so-called *Bythinella* of China by (1) having a tooth or node on the inner lip, and (2) the central tooth having two pairs of basal cusps, those on each side on the same level (not *Hydrobia*-like).

The so-called *Bythinella* of China lack the complex male reproductive system characters that serve to define the Hydrobiidae: Amnicolinae of Europe and North America including genuine *Bythinella* (Europe) and *Amnicola* (North America). Because *Bythinella* does not occur in China, Davis & Kuo,[1] (in Davis et al., 1985) described the genus *Erhaia* to accommodate new species that Liu and Zhang would have considered to be *Bythinella*. Davis & Kuo (1985) raised the tribe Erhaiini to accommodate *Erhaia*.

As a result of this study, *Erhaia* is placed in the synonymy of *Pseudobythinella*. It is clear that at least one species described as *Bythinella* from China (*B. chinensis* Liu & Zhang, 1979) has a tooth on the columella; it is observed when the aperture is tilted. Upon breaking open the shell it is seen that this "tooth" is the terminus of a thick, glassy, spiral columellar shelf or ledge. In summary, there appears to be no basis for placing those taxa with an overall similar anatomical ground plan in separate genera on the basis of presence or absence of a tooth on the columella, or where the tooth is prominently seen in the aperture contrasted with the presence of a columellar thickening seen only upon breaking the shell. The type species of *Erhaia*, *E. daliensis* Davis & Kuo (in Davis et al., 1985) has no columellar "tooth" in evidence in the aperture even when the aperture is rotated to examine as deeply as possible into the shell. However, upon breaking open the body whorl, a pronounced thickened columellar ridge is seen. This glassy ridge is also found in *Erhaia kunmingensis* Davis & Kuo 1985, but it is not very pronounced and forms no node.

The same situation involves the basal cusps of the central tooth. The two basal cusps on a side being on the same level or one above the other is irrelevant to generic definition. Most species of *Pseudobythinella* (including the Chinese taxa described as *Bythinella*) have only one pair of basal cusps on the lateral angles.

The Pseudobythinellini are not classified as Hydrobiidae but are in the Pomatiopsidae for the following reasons: (1) There is evidence that the position of the basal cusps of the cen-

[1]Due to a change in China affecting the manner of spelling Chinese words in English, Dr. Y. H. Kuo in the literature until 1985 changed the spelling of his name to Y. H. Guo (see Davis et al., 1985, 1986).

tral tooth derived from the pomatiopsine condition, i.e. from the face of the tooth. In *Pseudobythinella kunmingensis* from Yunnan, China most central teeth of most snails had a single pair of basal cusps. However, some central teeth had two pairs (Davis et al., 1985: fig. 16F), the innermost arising from the face of the tooth and lower than the outermost pair arising from the laternal angle. This has not, to our knowledge, been seen in any taxon of Hydrobiidae that has a spermathecal duct. (2) The position of the connections of the spermathecal duct, duct of the bursa, and oviduct are unlike any seen in the Hydrobiidae. These Chinese species lack the complex penial lobes, three to four differentiated regions of the pallial oviduct, and tendency to brooding seen in the Hydrobiidae: Littoridininae. (3) There is the biogeographic overlap of these snails with at least one genus of the Pomatiopsini, more if *Akiyoshia*, originally described from Japan, is also a member of the *Pseudobythinella* clade.

Akiyoshia Kuroda & Habe 1954

Type Species. Akiyoshia uenoi Kuroda & Habe, 1954: 71–73, figs. 1–4

Type locality. Akiyoshi limestone cave, Yamaguchi Prefecture, Japan

Designation. By monotypy

Saganoa Kuroda, Habe & Tamu, 1957

Type species. Akiyoshia (*Saganoa*) *kishiiana* Kuroda, Habe & Tamu in Kuroda & Habe, 1957: 186–187, figs. 5–8.

Type locality. Saga (= Arashiyama), western foothills of Kyoto City, Japan

Designation. By original designation

Discussion. Species from China were described as *Akiyoshia* (*Saganoa*) by Liu et al. (1982). They were thus described because the shells of those species are minute, turreted, with roundish apertures, i.e. generally corresponded to the conchological descriptions given by Kuroda & Habe (1957). We doubt that the Chinese species are *Akiyoshia*, *s.s.*, or *Akiyoshia* (*Saganoa*) due to the distance and differences in geological events creating environments now inhabited by the Chinese and Japanese snails. We are reminded that species once described as *Tricula* from India, China, and the Ryukyu Archipelago are now classified in four genera on the basis of detailed anatomical data. We note that *Saganoa* species are blind cave- or well-dwelling snails; those collected from China are stream-dwelling and not blind. However, we will not describe a new genus until the relevant Japanese snails are studied and the data dictate such a course.

Akiyoshia (*Saganoa*) *chinensis*
Liu et al., 1982

Holotype. IZAS, HN 798002; Liu, Zhang & Chen, 1982: 367, figs. 2–5 (in Liu et at. 1982).

Type Locality. Guzhang, Hunan Province, Sept. 1979

Assigned Species. China only: *Akiyoshia* (*Saganoa*) *chinensis* Liu, Zhang & Chen, 1982; *A.* (*S.*) *yunnanensis* Liu, Wang & Zhang, 1982. N = 2 (in Liu et at. 1982).

Habitat

Refer to *Tricula gredleri*, D87-3. This species was sympatric with *T. gredleri* and *T. maxidens*. Snails were collected from a village close to the type locality, approximately 5 km; the type locality is across the valley and on the opposite hillside from D87-3.

Depository

Specimens are catalogued into the collections of ZAMIP, M0010; ANSP 373142, A12658.

Description

Shell. Shells are minute, smooth, turreted with deep sutures and slightly convex whorls (Figs. 6A–E, 7A–E, 8). Shells of mature animals have 4.5–5.5 whorls; the majority are 5.0–5.5 whorls. Shell lengths of mature snails of 5.0 or more whorls range from 1.60–1.86 mm (Table 3). There is a slight umbilical chink. The aperture is sub-circular; there is a trace of a varix on some shells. In side view the outer lip is slightly sinuate (Fig. 7B). With the outer lip down (90° to the horizontal), the outer lip is either straight or angled. There are no apertural teeth or adapical notches.

Under SEM the following are observed: (1) Spiral microsculpture can be seen at the base of the shell (Fig. 7C), and on some whorls (Fig. 7D). (2) The protoconch is smooth (Fig. 7D, E). (3) Breaking open the body whorl reveals no internal columellar teeth or spiral ledges (Fig. 8A–E). The columella of the pen-

TABLE 3. Shell measurements (mm) of topotypical *Akioyshia chinensis*. Mean ± standard deviation (range). N = number measured.

	Large class		Small class		
	N = 3	N = 5	N = 1	N = 5	N = 1
No. Whorls	5.0–5.25	5.5	4.5	5.0	5.5
Length (L)	1.77±0.02 (1.76–1.80)	1.84±0.01 (1.82–1.86)	1.64	1.66±0.04 (1.60–1.68)	1.68
Width (W)	0.73±0.01 (0.72–0.74)	0.70±0.02 (0.68–0.74)	0.70	0.66±0.02 (0.64–0.68)	0.66
L last three whorls	1.53±0.02 (1.52–1.56)	1.51±0.03 (1.48–1.56)	1.44	1.44±0.02 (1.40–1.46)	1.40
L body whorl	0.91±0.03 (0.88–0.94)	0.88±0.03 (0.84–0.92)	0.86	0.85±0.02 (0.84–0.88)	0.80
L penultimate whorl	0.36 No. Var.	0.37±0.01 (0.36–0.38)	0.34	0.34±0.02 (0.32–0.36)	0.32
W penultimate whorl	0.59±0.01 (0.58–0.60)	0.58±0.01 (0.58–0.60)	0.58	0.56±0.01 (0.54–0.56)	0.54
W 3rd whorl	0.48±0.02 (0.46–0.50)	0.49±0.04 (0.44–0.54)	0.48	0.46 No Var.	0.46
L aperture	0.61±0.02 (0.60–0.64)	0.59±0.02 (0.56–0.60)	0.60	0.55±0.02 (0.52–0.58)	0.54
W aperture	0.49±0.01 (0.48–0.50)	0.46±0.04 (0.40–0.48)	0.46	0.31±0.01 (0.44–0.48)	0.44
x	0.20 No Var.	0.15±0.04 (0.10–0.22)	0.16	0.17±0.08 (0.16–0.24)	0.18
y	0.09±0.03 (0.06–0.12)	0.10±0.04 (0.04–0.14)	0.12	0.07±0.04 (0.06–0.08)	0.12

ultimate whorl has minute calcareous nodes (Fig. 8F). The inner edge of the inner lip has raised calcareous pitted nodes (Figs. 8G, H); the inner surface of the aperture is regularly pitted (Fig. 8G, I).

External features. The head is white; there are no white granules about the eye. There is no *Oncomelania*–type "eyebrow." The operculum is corneous and paucispiral (Fig. 7F.). The inner-lip edge is straight, i.e. the operculum shape is sub rectangular, not ovate. The inner muscle attachment callus is comparatively small and weakly developed, about 27% the diameter of the operculum.

Mantle cavity. Measurements and counts of mantle cavity organs are given in Table 4; see Figure 9. The gill is central in the mantle cavity and symmetrical about the osphradium. The osphradium is short in females, long in males relative to the length of gill. Being long in this case is an artifact of the much reduced gill. If the gill was the usual length, i.e. filling most the length of the mantle cavity, the osphradium would (and should) be classified as short.

There are only 11–14 gill filaments. Gf_2 is long in females, medium (or normal) in males. The total lengths of the longest gill filaments are 0.22 ± 0.03 mm. There is no patch of white granules anterior to the osphradium near to or partially on the mantle collar.

Female reproductive system. The body of an uncoiled female without head or kidney tissue is shown in Figure 10A. Measurements of relevant organs are given in Table 4. Important features are: (1) The gonad (Go) is a simple sac located posterior to the stomach. (2) The bursa copulatrix (Bu) is clearly seen posterior to the pallial oviduct (Ppo). It is small. (3) There are three histologically different sections to the pallial oviduct; the albumen gland (Ppo), capsule gland (Apo-1), and a dense white anterior region (Apo-2). These areas are clearly discernable in gross dissection of living animals. (4) The bursa complex of organs is shown in Figure 11 in the same relative position as in Figure 10. The usual pomatiopsid seminal receptacle is lost; the function of the seminal receptacle is relocated within a U-shaped bend or twist of the oviduct (Osr, Figs. 10, 11). (5) There is a pronounced, elongated sperm duct (Sdu) connecting the oviduct (Ov) to the spermathecal duct. The oviduct enters the albumen gland (Ppo) just posterior to the posterior end of the mantle cavity (Emc). (6) The spermathecal duct (Sd)

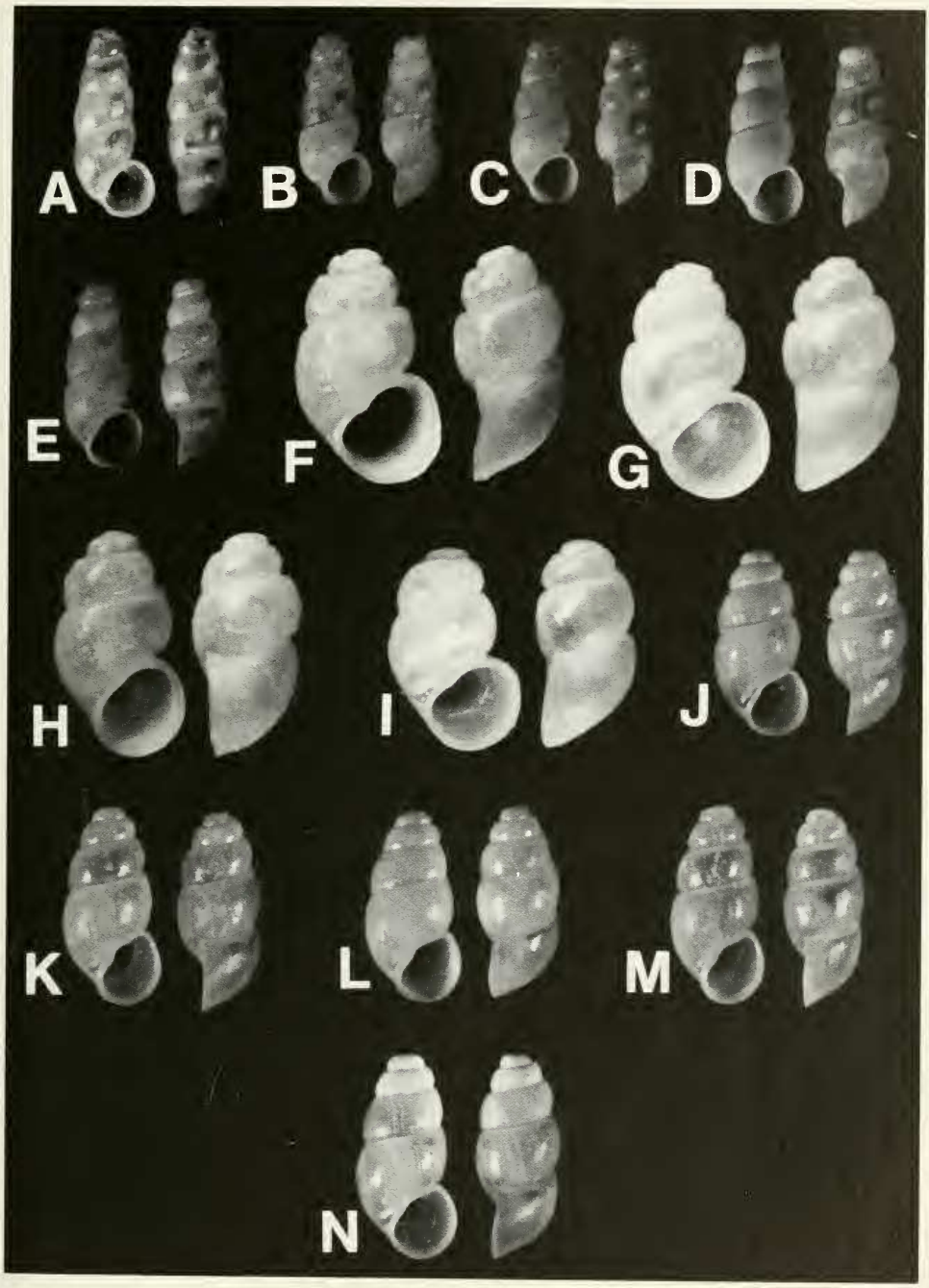

FIG. 6. Shells of *Akiyoshia chinensis* (A–E); *Pseudobythinella shimenensis* (F–I), and *P. chinensis* (J–N). The length of shell A is 1.77 mm; others are printed to same scale.

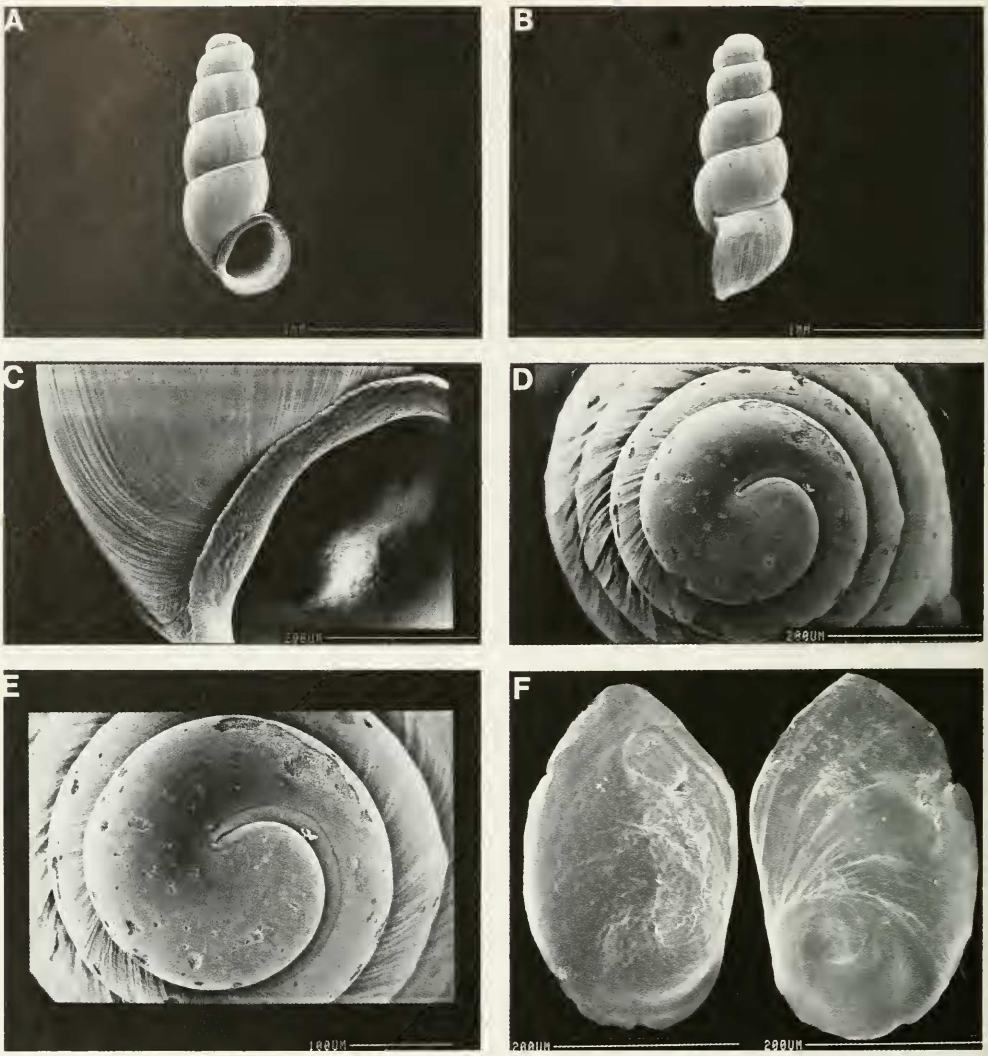

FIG. 7. SEM pictures of shell (A–E) and operculum (F) of *Akiyoshia chinensis*. C. Enlargement of base of shell showing rough growth lines crossed by fine spiral microsculpture. D, E. The apical whorls are smooth; teleoconch roughened sculpture starts at 1.5 whorls. Spiral microsculpture is seen at 1.5 to 1.75 whorls. F. Inner surface of operculum to left showing modestly developed attachment pad for muscles. Outer surface is to right showing paucispiral coil.

runs to the anterior end of the mantle cavity to open independently of the pallial oviduct.

Male reproductive system. An uncoiled male is shown in Figure 12 without head and with kidney tissue removed. Measurements of relevant organs are given in Table 4. Important features are: (1) The anterior lobes of the gonad (Go) are ventral to the posterior chamber of the stomach. (2) There are numerous lobes of the gonad that drain into a vas efferens (Ve). (3) The vas deferens leaves the vas efferens at mid-gonad to slightly posterior to

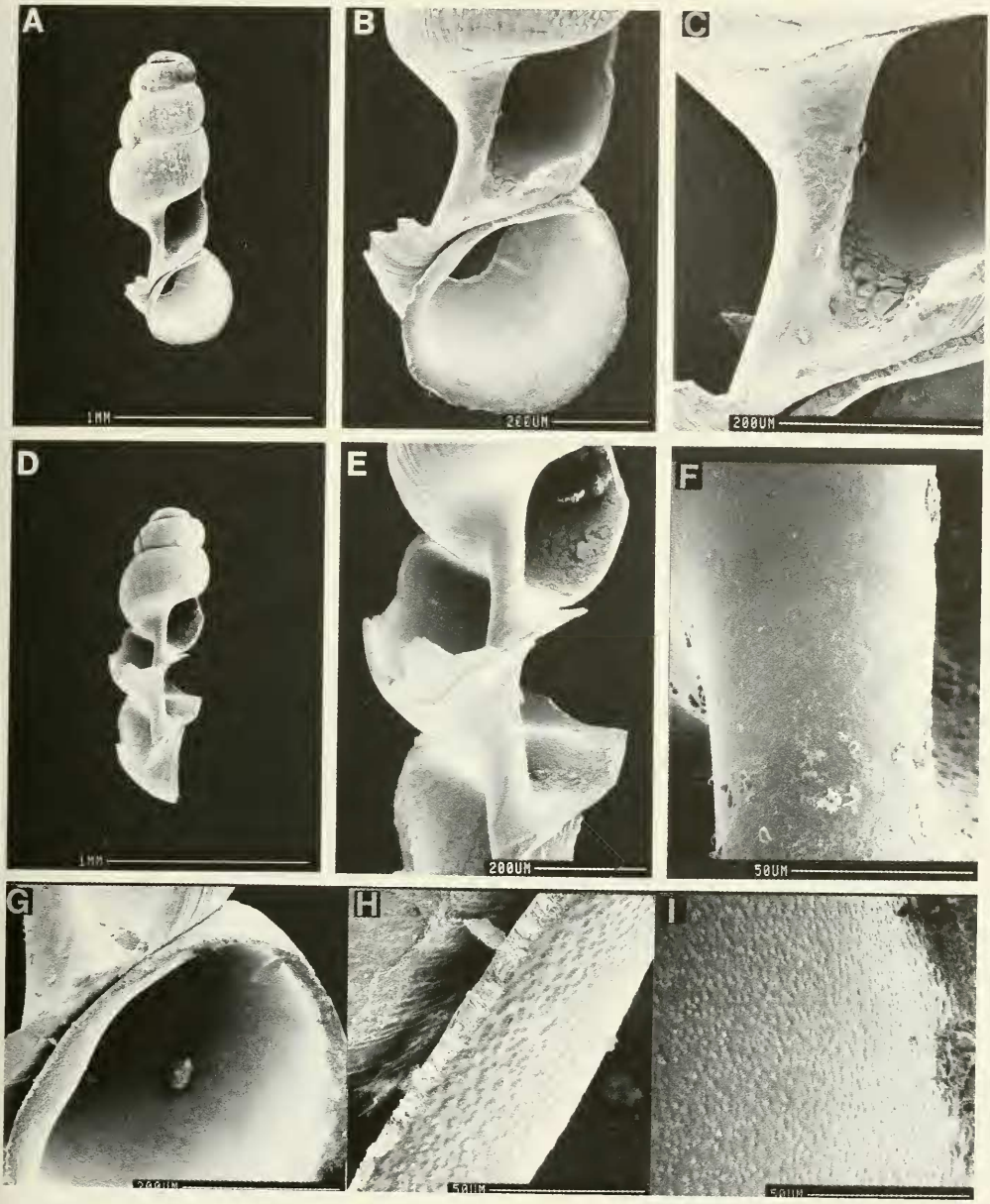

FIG. 8. SEM analysis of columella inside body whorl of *Akiyoshia chinensis* and sculptural attributes of columella and inner lip. See text for details.

mid-gonad to begin coiling as the seminal vesicle (Sv) dorsal to the gonad. (4) The prostate (Pr) overlies the posterior end of the mantle cavity. (5) The prostate consists of discernable lobes. (6) The anterior vas deferens (Vd_2) leaves the prostate close to mid-prostate. (7) The penis (Fig. 13 C) is simple with a long penial filament (Pf) and small papilla (Pa). A penial filament is defined as a terminal length of penis that is distinctly narrowed compared with the rest of the penis. This narrowing is not simply due to the gradual taper-

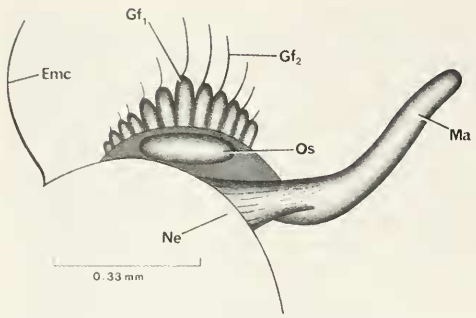

FIG. 9. Mantle cavity structures of *Akiyoshia chinensis*

ing of the penis. No ejaculatory duct was seen. An ejaculatory duct is a distinctly swollen muscle wrapped section of the vas deferens found in the base of the penis or neck. (8) The base of the penis (Bp) is to the right at the snout-neck mid-line (x, Fig. 13A, B) and oriented 65°–90° to the mid-line.

Digestive System. The digestive gland (Di) covers the posterior chamber of the stomach (Fig. 12). The stomach is shown in Figure 14 in the same relative position as in Figure 12. There is no caecal appendix; the style sac (including the intestinal loop) is 48% the length of the stomach.

Radular statistics are given in Tables 5 and 6. Refer to Figures 15, 16. The cusp formula most frequently encountered is

$$\frac{4(5)\text{-}1\text{-}(5)4}{1(2)\text{-}1(2)};\ 4\text{-}1\text{-}4;\ 19\text{-}24;\ 16\text{-}21.$$

There are numerous cusps on the marginals but there are significantly more on the inner

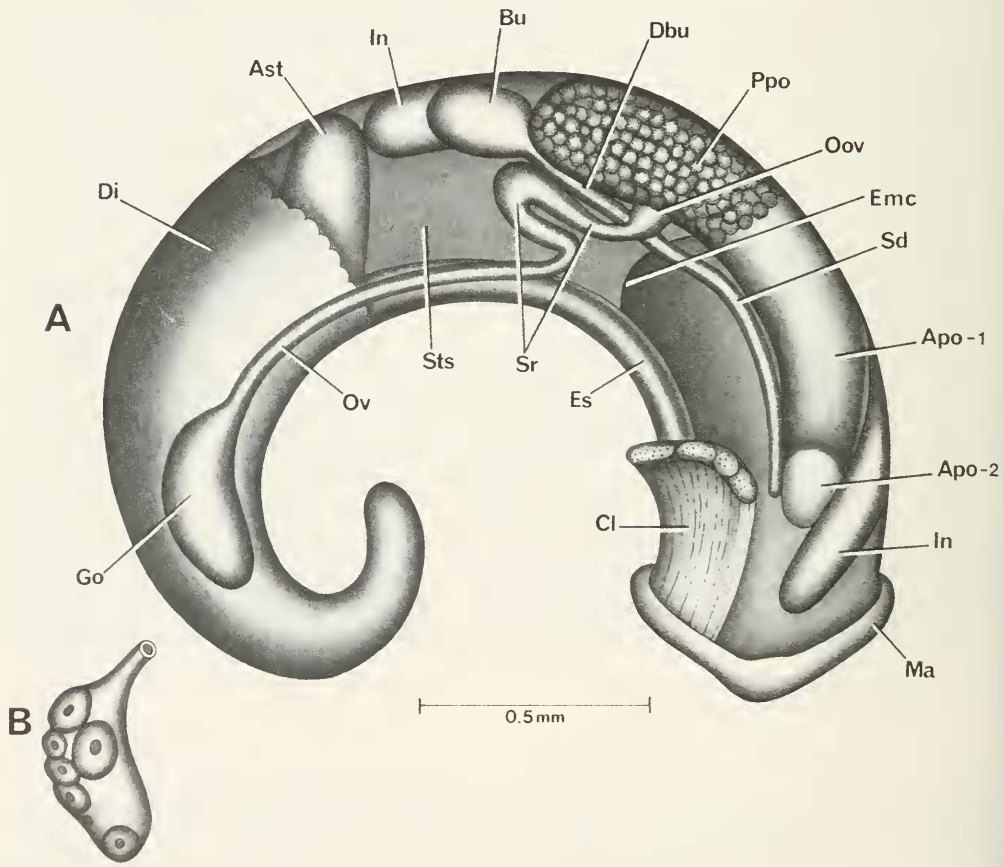

FIG. 10. Uncoiled female of *Akiyoshia chinensis* with head and kidney tissue removed (A) and gonad showing oocytes (B).

TABLE 4. Lengths (mm) or counts of non-neural organs and structures of *Akiyoshia chinensis*. N = number of snails used. Mean ± standard deviation (range).

	Females (N = 4)	Males (N = 2)
Body	3.27±0.20 (N = 3)	3.06
	(3.04–3.40)	(3.02, 3.10)
Gonad	0.40±0.11 (N = 3)	1.36
	(0.28–0.50)	(1.30, 1.42)
Digestive gland	1.59±0.19 (N = 3)	0.80 (N = 1)
	(1.40–1.78)	
Posterior pallial oviduct	0.57±0.06 (N = 3)	—
(= albumen gland)	(0.50–0.60)	
Anterior pallial oviduct	0.52±0.07 (N = 3)	—
(= capsule gland)	(0.46–0.60)	
Total pallial oviduct	1.09±0.10	—
= OV	(0.96–1.20)	
Bursa copulatrix	0.24±0.03	—
BU	(0.20–0.28)	
Duct of BU	0.43±0.08	—
	(0.32–0.50)	
BU ÷ OV	0.22±0.02	—
	(0.20–0.25)	
Seminal receptacle	—	—
	—	
Duct of seminal receptacle	—	—
	—	
Mantle cavity	0.73±0.05	0.70
	(0.70–0.80)	(0.60, 0.80)
Gill (G)	0.52±0.04	0.44
	(0.50–0.58)	(0.40, 0.48)
Osphradium (OS)	0.17±0.04	0.21
	(0.12–0.20)	0.20, 0.22
OS ÷ G	0.32±0.07	0.48
	(0.25–0.39)	(0.42, 0.55)
No. of filaments	12±1.4	11.5
	(11–14)	(11, 12)
Gf_2	0.11±0.03 (N = 5) M+F	0.12
	(0.08–0.12)	(0.10, 0.14)
Gf_1	0.10±0.02 (N = 5) M+F	0.11
	(0.08–0.14)	(0.10, 0.12)
Total Gf = TGF	0.22±0.03	0.23
	(0.18–0.26)	(0.20, 0.26)
Gf_2 ÷ TGF	0.54±0.08	0.48
	(0.46–0.67)	(0.46, 0.50)
Prostate	—	0.73
		(0.70, 0.76)
Seminal vesicle	—	—
Penis	—	0.76 (N = 1)

marginals ($\bar{X}$ of 21.3 vs. 18.1 for the outer marginals). The central tooth is featured in Figure 15C, E, H. The central raised "tongue" running anterior—posterior on the face of the tooth is flanked by deep eye-socket-like depressions (contrast lack of such deep holes on each side of the "tongue" in *Pseudobythinella kunmingensis* and *P. daliensis* (Davis et al., 1985: figs. 9, 16). Whether one or two basal cusps, they arise from the lateral angle of the central tooth. The bases of the lateral angles are flared as in the above mentioned species of *Pseudobythinella*.

The shape of the lateral teeth is emphasized in Figure 15G, H. Marginals are featured in Figure 16. The outermost cusp of the outer marginal is extremely elongated, a unique feature (Fig. 16F–H).

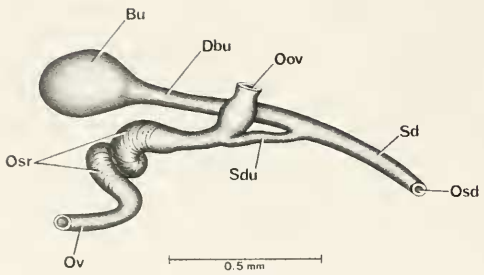

FIG. 11. Bursa copulatrix complex of organs of *Akiyoshia chinensis* positioned as in Figure 10.

Nervous system. No data.

Remarks

This species differs from those classified as *Pseudobythinella* by possessing a slender high-turreted shell without a trace of a tooth or node on the columella as examined in the aperture or within the body whorl. The standard seminal receptacle is lost; its function is moved into the oviduct. The bursa is a comparitively small sphere clearly visible posterior to the pallial oviduct in contrast to the elongated tubular bursa mostly, if not entirely, buried dorsal to the albumen gland in *Pseudobythinella.* The central tooth of the radula has deep-set socket-like depressions on either side of the "tongue" on the face of the tooth; these deep holes are lacking in *Pseudobythinella.*

Pseudobythinella Liu & Zhang, 1979

Synonymy. Erhaia Davis & Kuo, 1985.

Type species. Pseudobythinella jianouensis Liu & Zhang, 1979: 135-136, figs. 1–3.

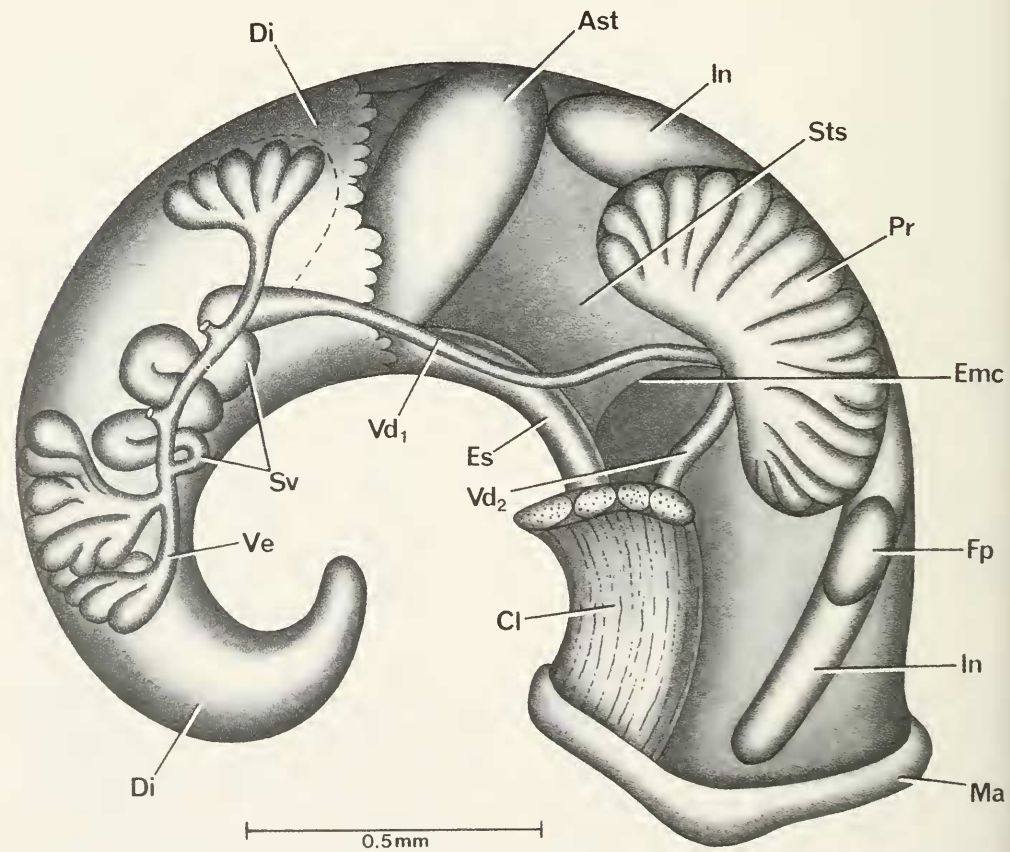

FIG. 12. Uncoiled male of *Akiyoshia chinensis* without head and kidney tissue removed. Some lobes of gonad are removed to reveal seminal vesicle (Sv). Dashed line shows contour of gonad.

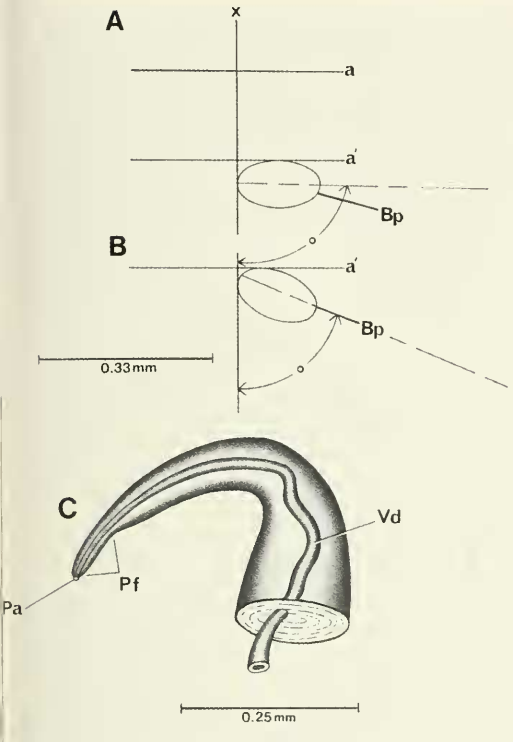

FIG. 13. Position of base of penis of *Akiyoshia chinensis* on neck (A, B) relative to snout-neck midline (x); penis (C).

Type locality. Jian'ou, Fujian Province, People's Republic of China.

Designation. By monotypy with designated type species.

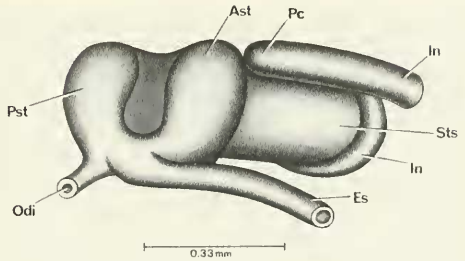

FIG. 14. Stomach of *Akiyoshia chinensis* positioned as in Figures 10 and 12.

Types. IZAS, FJ767701, holotype, plus paratypes.

Assigned Species. China only: *P. jianouensis* Liu & Zhang, 1979; *Bythinella chinensis* Liu & Zhang, 1979; *B. hubeiensis* Liu, Zhang & Wang, 1983b; *B. gongjianguoi* Kang, 1983b; *B. wufengensis* Kang, 1983a; *B. watanensis* Kang, 1983a; *P. liui* Kang, 1983b; *P. shimenensis* Liu, Zhang & Chen, 1982; *B. lii* Kang, 1985; *Erhaia daliensis* Davis & Kuo, 1985; *E. kunmingensis* Davis & Kuo, 1985. N = 11.

Diagnosis. Bythinella—like shell, minute, with smooth, flattened apical whorls. Apical whorls may have faint spiral microsculpture. Columella with spiral glassy thickening that may form a considerable keel or spiral ledge; the ledge may terminate in the aperture appearing as a "tooth" on the inner lip. Anatomical criteria are based on four species for which

TABLE 5. Radular statistics for *Akiyoshia chinensis*. Mean ± standard deviation (range). N = number used. In mm except for width of central tooth in μm.

	Females (N = 7)	Males (N = 4)
Shell length	1.71±0.09 (1.60–1.78)	—
Radular length	0.39±0.02 (0.36–0.42)	0.39±0.02 (0.37–0.40)
Radular width	0.04±0.003 (0.038–0.048)	0.04±0.005 (0.036–0.046)
Total rows of teeth	90.4±4.3 (84–96)	84.5±5.1 (81–92)
No. rows of teeth forming	33±1.6 (31–35)	31.3±1.3 (30–33)
Central tooth width	10.5±0.5 (N = 21) (9.5–10.7)	9.8±0.5 (N = 19) (8.9–10.2)

FIG. 15. Radula of *Akiyoshia chinensis*. A–E, males; F–H, females. C, E, H. features central teeth; G, H. Lateral teeth. D. features inner marginals.

FIG. 16. Radula of *Akiyoshia chinensis*. A, B, F = males; C–E, G, H = females. A. features inner marginals. B, D. Basal morphology of attachment zone of marginals. F–H. Outer marginals. See text for details.

TABLE 6. Cusp formulae for the radular teeth of *Akiyoshia chinensis* with the percent of radulae in which a given formula was found at least once.

Central Teeth		Lateral Teeth		Inner Marginal teeth		Outer Marginal teeth
4-1-4 / 1-1	57%	4-1-4	100%	14	—	14%
				15	—	14%
5-1-5 / 1-1	57%			16	—	29%
5-1-4 / 1-1	29%			17	—	71%
				18	14%	43%
5-1-5 / 2-2	29%			19	43%	71%
4-1-4 / 2-2	14%			20	71%	43%
				21	86%	29%
5-1-5 / 1-2	14%			22	71%	—
				23	86%	—
						—
				24	57%	—
				25	29%	
				$\bar{X}$ * = 21.3±1.8		18.1±1.7
				N = 70		N = 70

*Mean ± standard deviation of cusp number for all teeth counted.

TABLE 7. Shell measurements (mm) of *Pseudobythinella chinensis*. Mean ± standard deviation (range). Number measured = 5. All shells of mature animals had 4.5 whorls.

Length (L)	1.77±0.06 (1.68–1.84)
Width (W)	0.85±0.03 (0.83–0.90)
L last three whorls	1.64±0.06 (1.56–1.68)
L body whorl	1.07±0.06 (1.00–1.16)
L penultimate whorl	0.36±0.01 (0.34–0.36)
W penultimate whorl	0.69±0.07 (0.56–0.74)
L 3rd whorl	0.53±0.01 (0.52–0.54)
L aperture	0.70±0.03 (0.66–0.72)
W aperture	0.54±0.04 (0.52–0.60)
x	0.16±0.03 (0.12–0.20)
y	0.04±0.01 (0.02–0.06)

we have data; the two species of this study and *P. daliensis* and *P. kunmingensis* described in Davis et al. (1985). The female gonad is a simple tube or tube with low lobes. The oviduct has a wide 360° loop dorsal to the bursa copulatrix. There is the standard generalized seminal receptacle. Hydrobiid—type central tooth. The lateral tooth lacks a pronounced intermediate cusp. A lateral tooth has a pronounced curved process projecting posterior from the face of the tooth. The process is slight, or if large it is straight in *Akiyoshia chinensis*. Stomach without caecal appendix. There is a tendency for hypertrophy of the radular sac.

Pseudobythinella chinensis (Liu and Zhang)

Holotype. IZAS, HN766602, Liu & Zhang, 1979: fig. 4.

Type locality. Lengshuijiang, Xinhua, Hunan Province; July 1976. (approximately 27°4′N, 111°25′E)

Synonymy. *Bythinella chinensis* Liu & Zhang, 1979: 134, 136.
Erhaia chinensis, Davis et al., 1985
Pseudobythinella chinensis, this paper

Habitat

Snails were collected from Shen Keng Village, Sanhe Town, Lingxian County, Zhu Zhou Prefecture; 26°17′18″ N, 113°31′50″ E; Figure 1, site 6. The field collection number

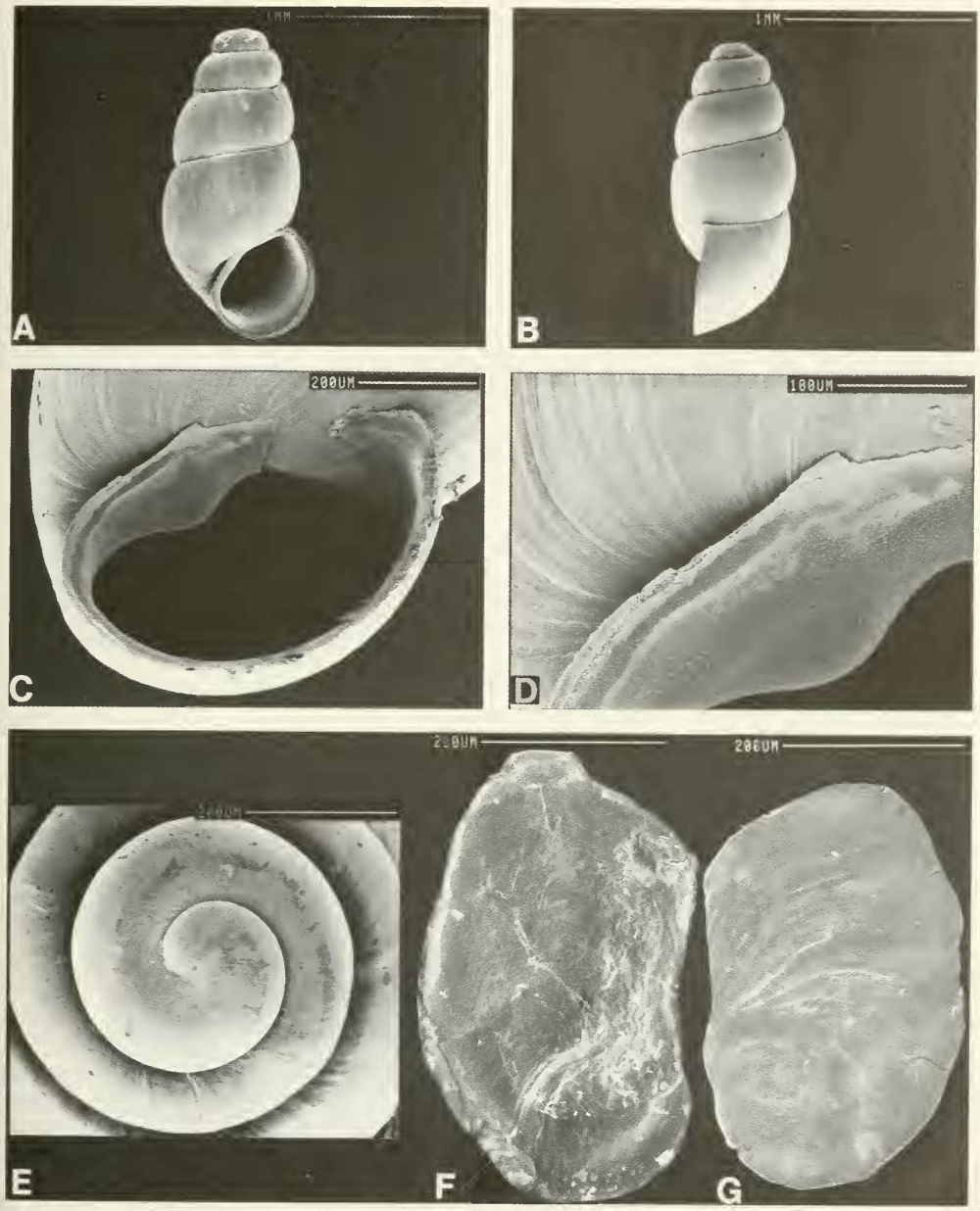

FIG. 17. SEM picture of shells (A–E) and opercula (F, G) of *Pseudobythinella chinensis*. Note that in A, no "tooth" is seen on columella. Tilting shell to look inside body whorl reveals a swelling or "tooth" on columella. C, D reveal no spiral microsculpture. See text for details. The apical whorls are smooth (E). Inner surface of operculum (F); outer surface (G).

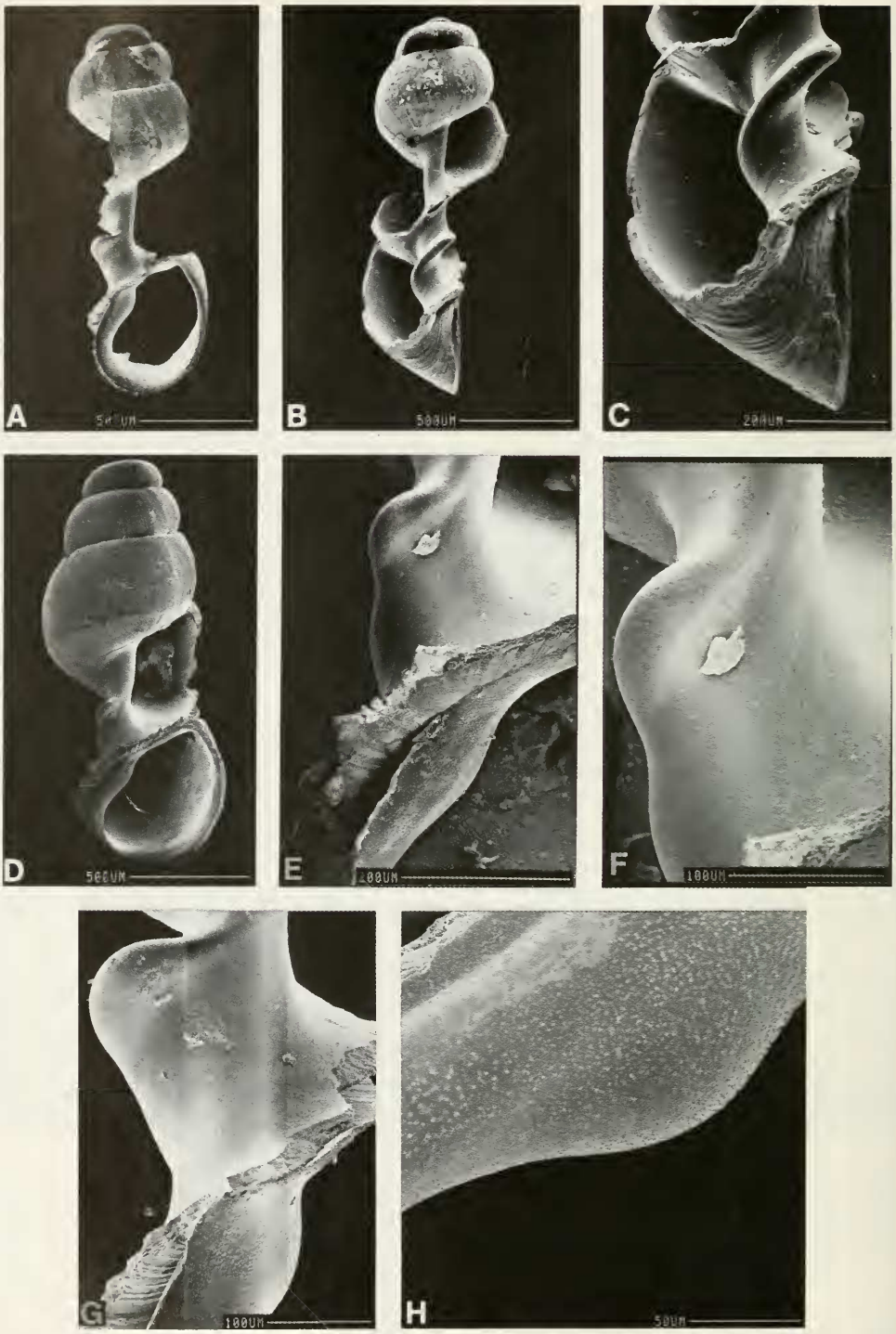

FIG. 18. SEM of shells of *Pseudobythinella chinensis* broken to show raised spiral ridge and "tooth" on columella inside body whorl. See text for discussion of sculpture on columella and inner lip.

TABLE 8. Lengths (mm) or counts of non-neural organs and structures of *Pseudobythinella chinensis*. N = number of snails used. Mean ± standard deviation (range).

	Females (N = 2)	Males (N = 1)
Body	3.68	3.28
	(3.42,3.94)	—
Gonad	0.32	0.90
	(0.30,0.34)	—
Digestive gland	1.72	1.80
	(1.70,1.74)	—
Posterior pallial oviduct (= albumen gland)	—	—
Anterior pallial oviduct (= capsule gland)	—	—
Total pallial oviduct = OV	1.20 (No. Var.)	—
Bursa copulatrix BU	0.38 (0.36,0.40)	—
Duct of BU	—	—
BU ÷ OV	0.32 (0.30,0.33)	—
Seminal receptacle	0.04(N=1)	—
Duct of seminal receptacle	0.12(N=1) —	—
Mantle cavity	—	0.52 —
Gill (G)	—	0.24
Osphradium (OS)	—	—
OS ÷ G	—	—
No. of filaments	—	12
Gf_2	—	0.10
Gf_1	—	0.10
Total Gf = TGF	—	0.20
Gf_2 ÷ TGF	—	0.50
Prostate	—	0.64
Seminal vesicle	—	0.40
Penis	—	0.52

assigned was D85-81. Snails came from a small stream that flowed between the peaks of big mountains; the elevation was 500 m. The stream was heavily shaded by vegetation lining the banks. The stream was 20–30 cm wide, 10–20 cm deep with a bottom paved with small rocks, leaves and mud.

Depository

Specimens are housed at ZAMIP, M0011; ANSP, 373139, A12655.

Description

Shells. Shells are minute, smooth, and conic-turreted (Figs. 6J–N; 17A–E; 18A–H). They are 4.5 whorls ranging in length from 1.68 to 1.84 mm (Table 7); they are umbilicate with a sub-ovate to sub-circular aperture. The sutures are moderately deep; whorls with slightly convex whorls. No tooth is visible in the aperture in 60% of the shells while a thickening on the columella is seen in the aperture of 40% of the shells. Tipping the aperture up, one can see a considerable tooth-like swelling on the columella, the terminus of the pronounced internal columellar keel. In side view the outer lip is straight to slightly sinuate; in the contrasting view the inner lip is straight (outer lip down, 90° to the horizontal).

SEM analyses show the apical whorls to be smooth (Fig. 17E). With the aperture tilted,

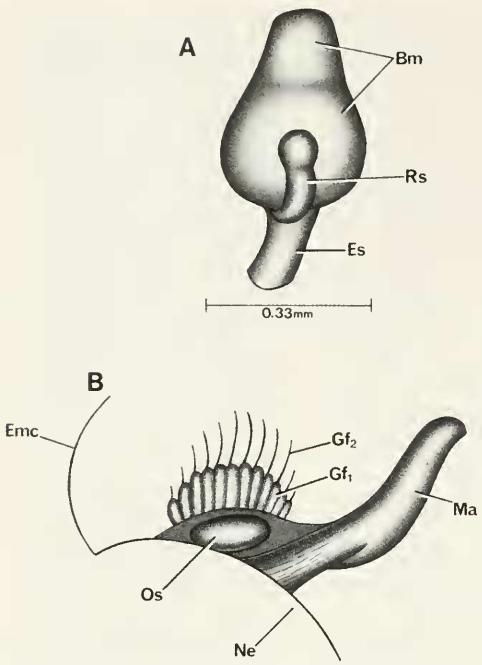

FIG. 19. The buccal mass of *Pseudobythinella chinensis* with pronounced radular sac (A) and reflected mantle showing mantle cavity organs (B).

the columeller "tooth" is seen (Fig. 17C, D); note the numerous calcareous pitted pustules on the columella and "tooth". With the shell broken open, it is seen that the "tooth" seen in the aperture is the terminus of a pronounced columellar keel starting at mid-body whorl and spiralling down to the aperture (Fig. 18A–E). An enlargement of the area of highest concentration of pitted calcareous pustules on the "tooth" (Fig. 18G) is given in Fig. 18H. The entire surface of the keel is roughened with calcareous pustules or micro-ridges.

External features. The head-neck is white; there are no white granules about the eyes. The operculum is corneous and paucispiral (Fig. 17F, G). The shape is sub-rectangular. The columeller edge is somewhat concave, especially where the operculum passes over the columeller "tooth" (Fig. 17C). The callus on the inner surface is weakly developed, but wide, 69% the width of the operculum (Fig. 17F).

Mantle cavity. The opened and reflected mantle cavity is shown in Figure 19B. Measurements and counts of relevant organs are given in Table 8. The gill is centrally located in the mantle cavity and the osphradium (Os) is centered against the gill. The osphradium by definition is long but this is an artifact of the much reduced size of the gill. The usual pomatiopsid gill nearly fills the length of the mantle cavity. On this criterion the osphradium is here considered short (circa 0.32 ratio). The Gf_2 is medium (= normal) length. The length of the longest gill filament is approximately 0.20 mm.

Female reproductive system. The body of an uncoiled female snail is shown in Figure 20 without head and with kidney tissue removed. Measurements of relevant organs are given in Table 8. Important features are: (1) The gonad (Go) is posterior to the stomach (Pst). (2) The gonad consists of a simple sac with four to five small undivided lobes protruding from the posterior end. (3) The bursa (Bu) is either completely covered by the albumen gland (Ppo) or only protrudes slightly posterior to the albumen gland (as in Fig. 20). (4) The oviduct (Ov) makes a pronounced bend pressing against the posterior edge of the bursa (Bu). (5) The spermathecal duct (Sd) runs to the anterior end of the mantle cavity to open independently of the pallial oviduct. (6) The sperm duct (Sdu) is unique in that it branches off the spermathecal duct near the anterior end of the spermathecal duct, far forward of the posterior end of the mantle cavity (Fig. 21). (7) The seminal receptacle (Sr) is unique in that it branches from the sperm duct (Sdu), not the oviduct, and in that it is entirely anterior to the posterior end of the mantle cavity (Fig. 21).

Male reproductive system. An uncoiled male is shown in Figure 22 without head or kidney tissue. Part of the gonad (Go) has been cut away to reveal the seminal vesicle (Sv) coiled dorsal to it. Measurements of relevant organs are given in Table 8. Important features are: (1) The gonad is posterior to the stomach. (2) There is no vas efferens in the usual sense. Thick lobes arise from a wide collecting gutter that functions as a vas efferens. (3) The seminal vesicle (Sv) arises from mid-gonad and makes a small knot dorsal to the gonad. (4) The posterior vas deferens (Vd_1) runs as a wide tube, swollen with sperm, from the seminal vesicle to become a slender duct only at the style sac. (5) The prostate overlies the

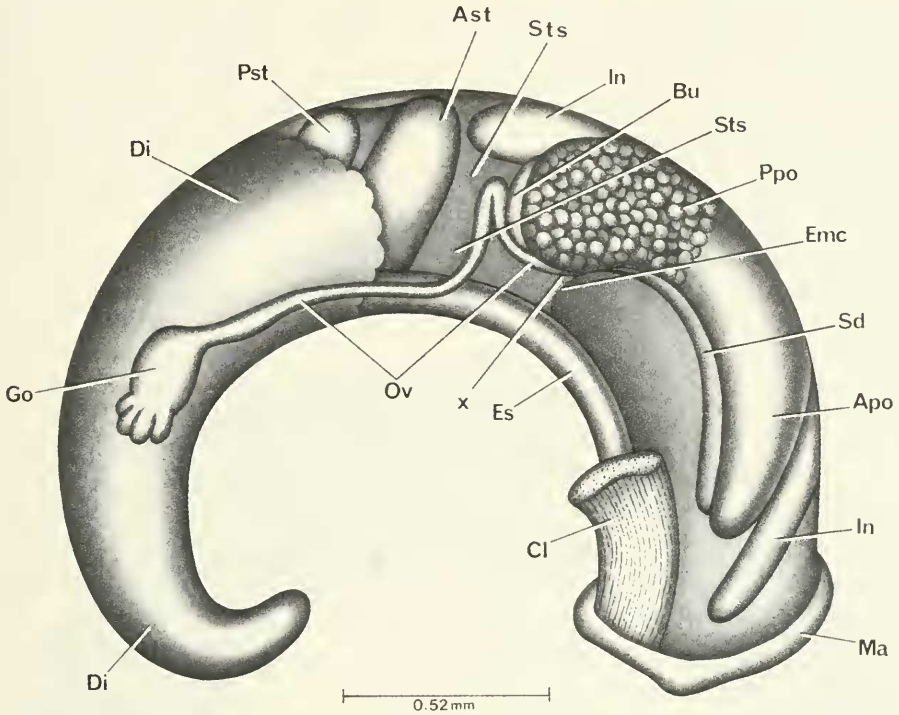

FIG. 20. Uncoiled female *Pseudobythinella chinensis* with head and kidney tissue removed.

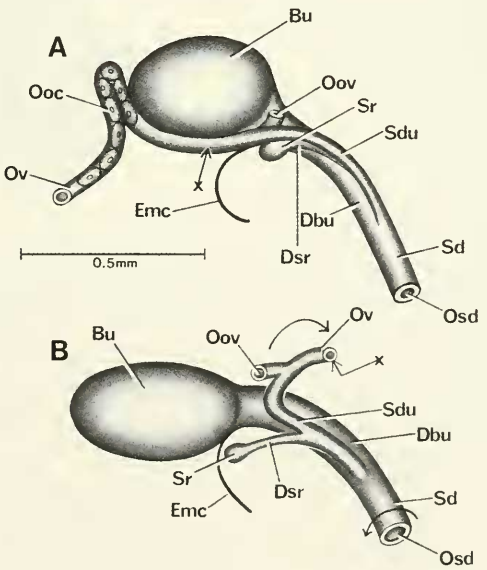

FIG. 21. Details and variation of bursa copulatrix complex of organs of *Pseudobythinella chinensis*. Figure 21A is in same orientation as in Figure 20. In B, oviduct cut and reflected in direction of arrow to show opening of oviduct (Oov) that attaches to albumen gland

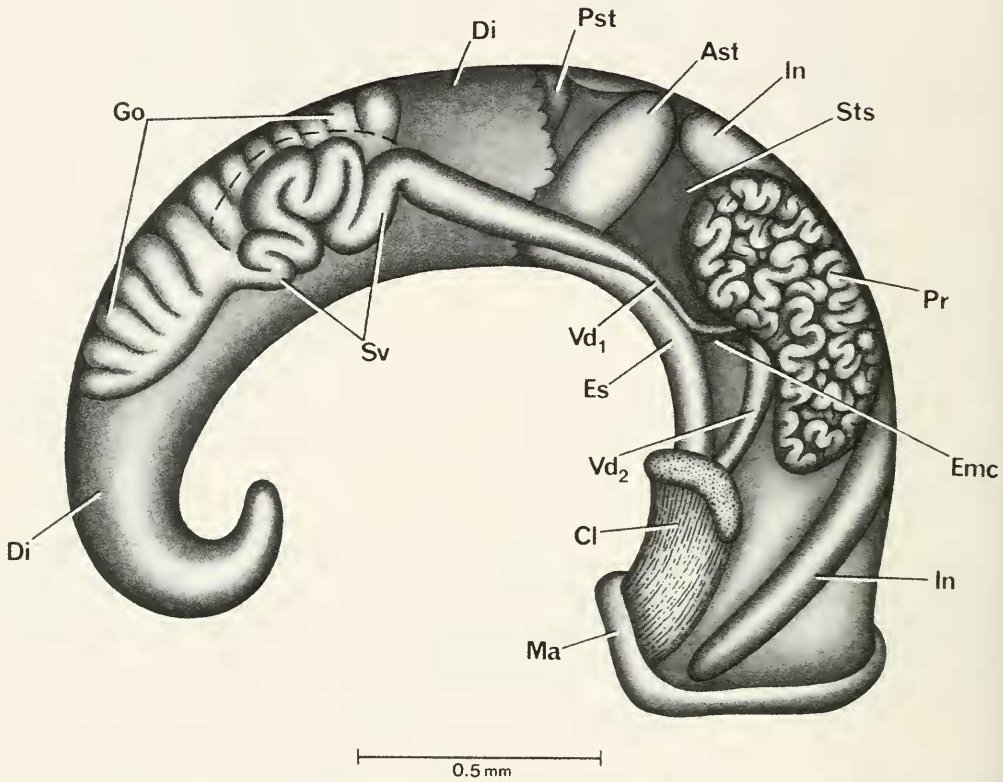

FIG. 22. Uncoiled male of *Pseudobythinella chinensis* without head or kidney tissue. Some of lobes of anterior gonad are cut away (- - -) to show knot of seminal vesicle (Sv) dorsal to gonad.

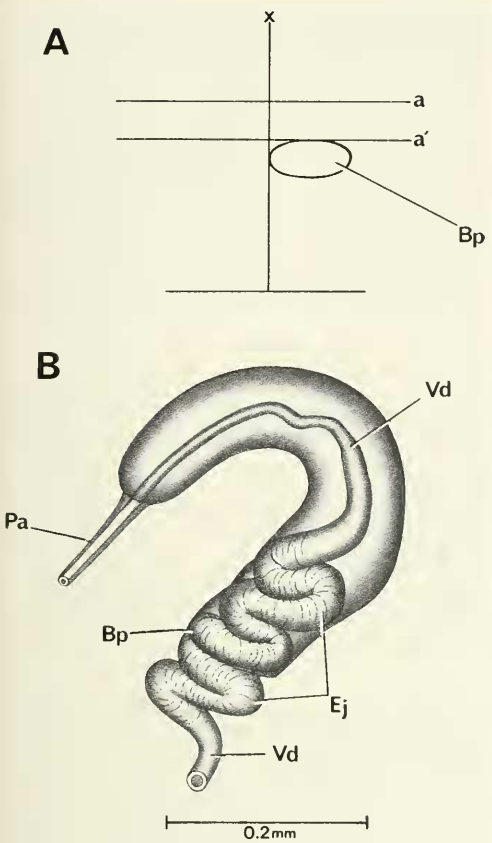

FIG. 23. A. The orientation of base of penis (Bp) of *Pseudobythinella chinensis* to snout-neck mid-line (x) and lobes of eyes (a). B. Penis.

posterior end of the mantle cavity. (6) The anterior vas deferens (Vd_2) separates from the prostate at mid-prostate. (7) The penis (Fig. 23B) has an enormous muscular ejaculatory duct (Ej) in the base that continues to coil for a short distance in the neck. (8) The penis has an enormously elongated papilla, a unique feature. (9) The base of the penis (Bp, Fig. 23A) arises to the right of the snout-neck mid-line x and at 90° to it.

Digestive system. The digestive gland (Di) covers the posterior chamber of the stomach (Pst, Figs. 20, 22). The radular sac (Rs) loops up over the buccal mass (Bm, Fig. 19 A). Radular statistics are given in Tables 9, 10. The radula is minute, with an extraordinary number of rows of teeth (97 per 0.48 mm)

TABLE 9. Radular statistics for *Pseudobythinella chinensis*. Mean ± standard deviation (range). N = number used. In mm except for width of central tooth in μm.

	Sex Unknown (N = 4)
Shell length	1.79±0.001
Radular length	0.48±0.01
Radular width	0.06±0.004
Total rows of teeth	97.3±6.7 (N = 3)
No. rows of teeth forming	10.3±4.0
Central tooth width	12.0±0.5 (N = 9)

(Fig. 24). The most commonly encountered cusp formula is $\frac{(4)5\text{-}1\text{-}5(4)}{1\text{-}1}$; 4(5)-1-(5, 6)4;

24-29; 17-22.

The inner marginal teeth have significantly more cusps(mean of 26) than do the outer marginals (mean of 20). The two outer cusps of the outer marginals are specialized to form a pincer-like process (Fig. 24G, H). The "tongue" on the face of the central tooth is broad and is not flanked by deep-set holes (Fig. 24A, B).

Nervous system. No data.

Remarks

This species differs from the other three for which we have anatomical data by the following: (1) The bursa may somewhat protrude posterior to the albumen gland. (2) the oviduct makes a pronounced bend near the bursa; the ascending and descending arms of the bend are pressed together (contrast the open 360° loops or complex oviduct loops of the other species). (3) The sperm duct is elongated and extends anterior to the posterior end of the mantle cavity to enter the spermathecal duct, a unique character-state. (4) The seminal receptacle branches off the sperm duct, not the oviduct, a unique character-state. (5) There is no vas efferens. (6) The penis has an extremely elongated papilla, a unique character-state.

Pseudobythinella shimenensis Liu, Zhang & Chen

Holotype. IZAS, HN797904; Liu et al., 1982: 254, 256, fig. 1.

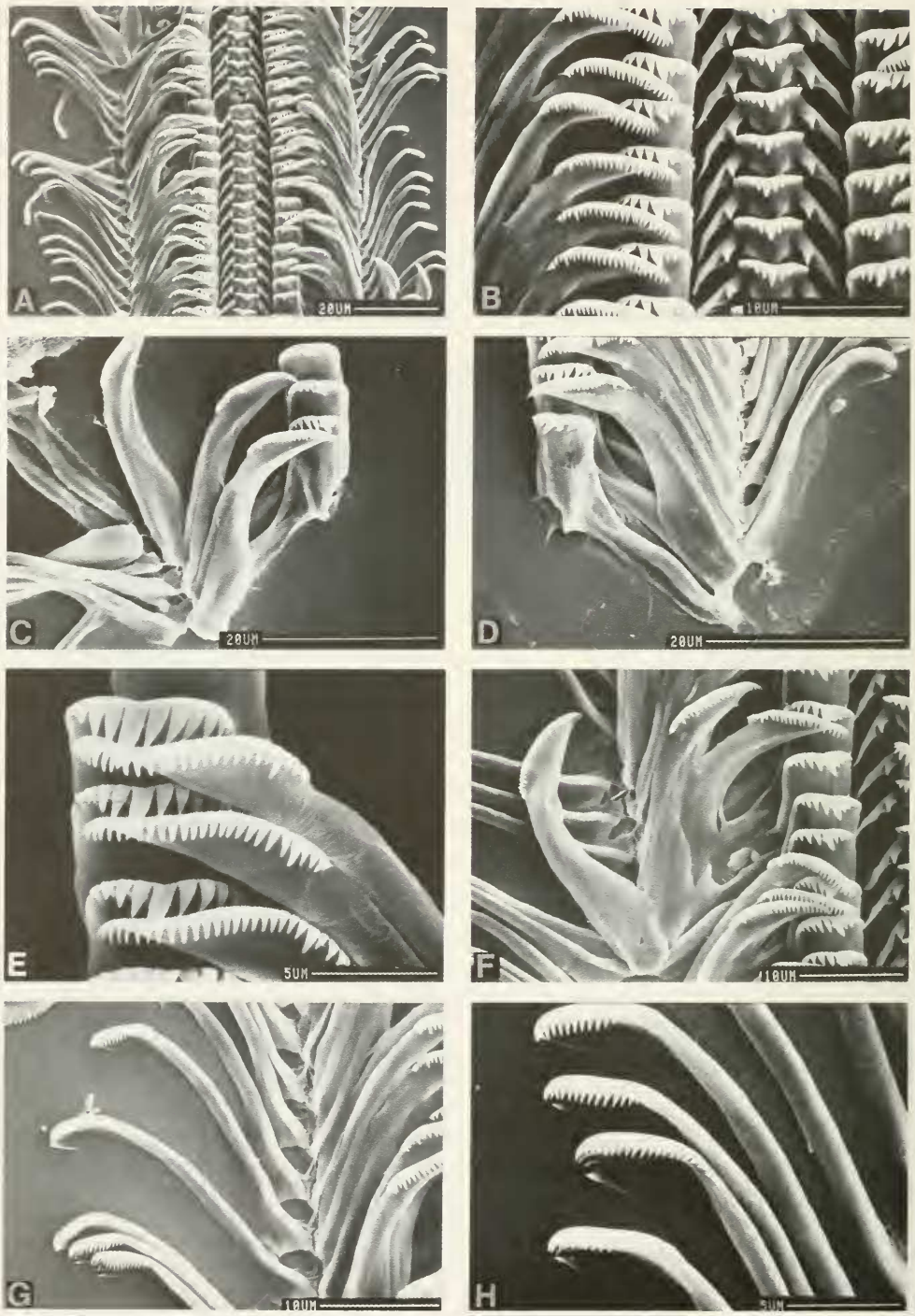

FIG. 24. Radula of *Pseudobythinella chinensis*. B. Central and inner marginal teeth emphasized. C, D. Details of morphology of lateral teeth. E, F. Inner marginals emphasized. G, H. Outer marginals. See text for details.

TABLE 10. Cusp formulae for the radular teeth of *Pseudobythinella chinensis* with the percent of the four radulae in which a given formula was found at least once.

Central Teeth		Lateral Teeth		Inner Marginal Teeth		Outer Marginal Teeth
5-1-5 / 1-1	75%	4-1-4	100%	17	—	75%
		5-1-5	75%	18	—	75%
5-1-4 / 1-1	50%					
		6-1-5	50%	19	—	75%
4-1-4 / 1-1	25%	4-1-5	50%	20	—	75%
		5-1-4	50%	21	—	50%
		6-1-4	25%	22	—	50%
				23	—	25%
				24	25%	25%
				25	100%	—
				26	100%	—
				27	75%	—
				28	25%	—
				29	25%	—
				$\bar{X}$ * = 26±1.0		20.0±2.1
				N = 40		N = 33

*Mean ± standard deviation of cusp number for all teeth counted.

Type locality. Shimen, Hunan Province, October 1979.

Synonymy. Pseudobythinella shimenensis Liu, Zhang & Chen, 1982: 254–256. *Pseudobythinella shimenensis* Davis et al., 1985: 68.

Habitat

Snails were collected from Qingguandu Village, Nanzhen Town, Shimen County, Changde Prefecture; 29°56′36″ N, 110°41′42″ E; Figure 1, site 3; topotypes. Snails were collected from under stones and leaves at the edge of a small pool of a stream. The water was clean, clear, cool.

Depository

Specimens are housed at ZAMIP, M0012, ANSP 373137, A12653.

TABLE 11. Shell measurements (mm) of *Pseudobythinella shimensis.* Mean ± standard deviation (range). Five shells measured, all 4.0 whorls.

Length (L)	1.98±0.04 (1.94–2.04)
Width (W)	1.17±0.02 (1.14–1.20)
L last three whorls	1.95±0.04 (1.92–2.02)
L body whorl	1.44±0.03 (1.41–1.48)
L penultimate whorl	0.38±0.01 (0.38–0.40)
W penultimate whorl	0.82±0.02 (0.80–0.84)
L 3rd whorl	0.48±0.02 (0.45–0.50)
L aperture	0.99±0.02 (0.96–1.00)
W aperture	0.76±0.03 (0.73–0.80)
x	0.24±0.12 (0.10–0.38)
y	0.07±0.04 (0.04–0.12)

Description

Shells. Shells are minute, smooth, ovate with flattened apex (Figs. 6F–I, 25, 26). Shell measurements are given in Table 11; shell lengths range from 1.94 to 2.04 mm for shells of 4.0

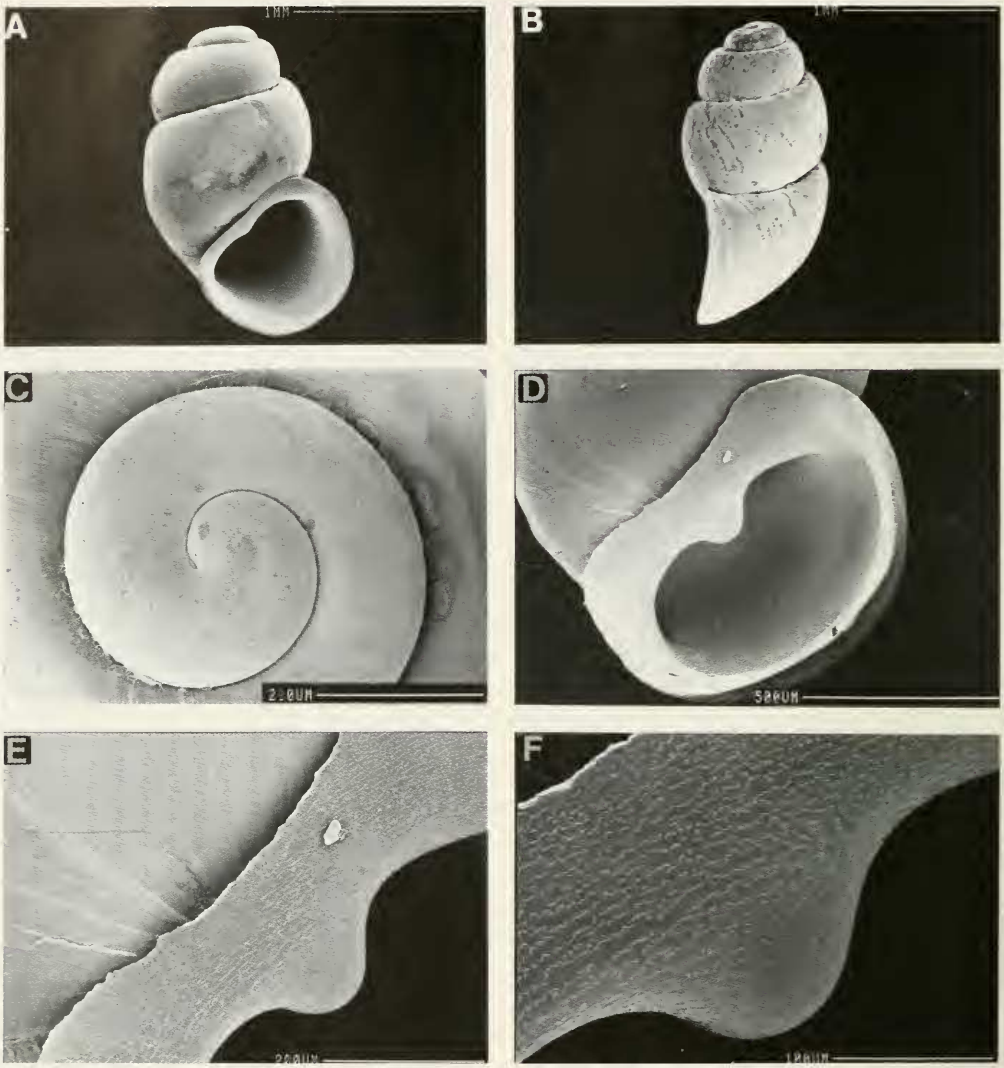

FIG. 25. SEM photographs of shells of *Pseudobythinella shimenensis*. A. Note slight swelling or tooth on columella. C. Apical whorls showing spiral microsculpture starting at 0.5 whorls. D. Aperture rotated to expose fully tooth on columella. E, F. Columella highly magnified to show sculpture pattern on inner lip, columella, and tooth.

whorls. The aperture is broadly ovate to subcircular. The sutures are deep and the whorls shouldered, convex. The inner lip is straight to saddle-shaped with a narrow umbilicus above the center of the saddle of 33%; no umbilicus, 66%. The columella has a tooth plainly in view in the aperture. The face of the body whorl is flattened in most specimens. The outer lip is straight to slightly arched (Fig. 25B). In side view, the adapical outer lip is fused to the body whorl in 40%; separated by 0.05 mm ± 0.03 mm (N = 5) from the body whorl in 60%.

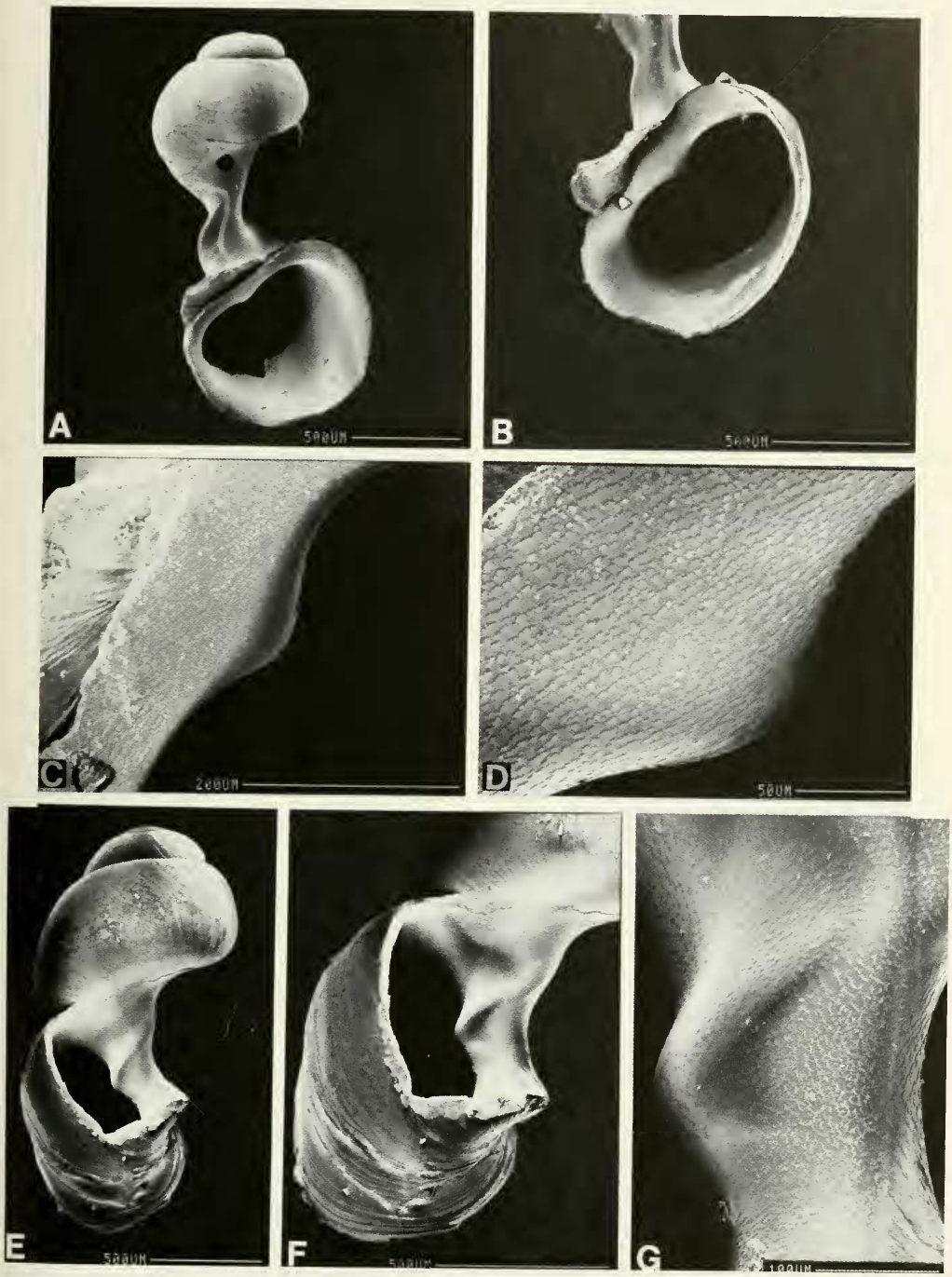

FIG. 26. SEM photographs of shells of *Pseudobythinella shimenensis* broken open to reveal raised spiral ridge on columella of body whorl that terminates as tooth. C, D. Large scale-like sculptural plates on columella at aperture contrast with thin line-like raised ridges on spiral ridge within body whorl (G).

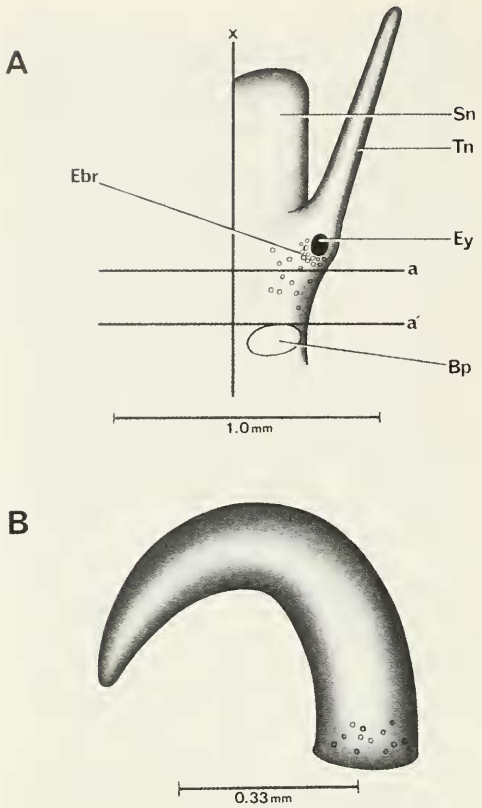

FIG. 27. Head (A) and penis (B) of *Pseudobythinella shimenensis*. A. Relationship of base of penis to mid-line of snout-neck (x) and to posterior end of eye lobes (a).

The inner lip is straight (outer lip down 90° to horizontal).

SEM examination shows that the tip of the apical whorl is smooth with fine spiral sculpture seen starting in less than half a whorl (Fig. 25C). Tilting the aperture somewhat, the columellar "tooth" is clearly seen (Fig. 25D–F). It is covered with raised calcareous lappets (Fig. 25E), contrasted with the pustules seen in *P. chinensis*. Upon breaking open several shells, it is seen that the "tooth" is the terminus of a columellar keel that starts mid-body whorl (Fig. 26A, B, E–G). The calcareous lappets begin on the columellar keel and extend to the aperture (Fig. 26D, G); above the keel there are minute raised calcareous ridges (Fig. 26G).

External features. The head is white with a small cluster of white granules about the medial edge of the eye, i.e. an "eyebrow" (Ebr, Fig. 27). There is a scattering of white granules posterior to the eyebrow at the side of the neck. The operculum is corneous, paucispiral and kidney-bean shaped with the columellar—side concavity corresponding to the tooth on the columella (Fig. 28). On the inner surface of the operculum the attachment pad for the muscle has a pronounced ridge (Fig. 28A, C). The pad is relatively narrow, some 40% the width of the operculum.

Mantle cavity. The reflected mantle showing mantle cavity organs is given in Figure 29; measurements and counts are given in Table 12. There are relatively few gill filaments (12–13) yet these take up 78% the length of the mantle cavity. The osphradium is mid-gill and is long. Gf_2 is long; the longest gill filaments are 0.36 mm long. There is no cluster of white granules just anterior to the osphradium close to the neck (Ne)—mantle collar (Ma) junction.

Female reproductive system. The body of an uncoiled female with head and kidney tissue removed is shown in Figure 30. Measurements and counts of organs are given in Table 12. Important features, to note are: (1) The gonad is located posterior to the stomach. It is a single small sac that has three or four small protruding lobes created by pressure of individual oocytes at the posterior end of the gonad. (2) The albumen gland (Ppo) covers most of the bursa copulatrix (Bu) and extends beyond the bursa to cover most of the style sac. The albumen gland curves around the bursa leaving the posterior end of the bursa exposed. Only in a few cases is the bursa completely covered by the albumen gland. (3) The spermathecal duct (Sd) is tightly pressed to the pallial oviduct and opens into the mantle cavity close to the anterior end of the capsule gland (Apo). (4) The bursa copulatrix complex of organs is shown in Figure 31 oriented in the same relative positions as in Figure 30. The bursa is short. (5) The oviduct enters (Oov) the albumen gland posterior to the posterior end of the mantle cavity (Emc). The sperm duct is short and branches off the spermathecal duct posterior to the posterior end of the mantle cavity. (6) The duct of the seminal receptacle (Dsr) branches off the oviduct posterior to the sperm duct (Fig. 31). The seminal receptacle

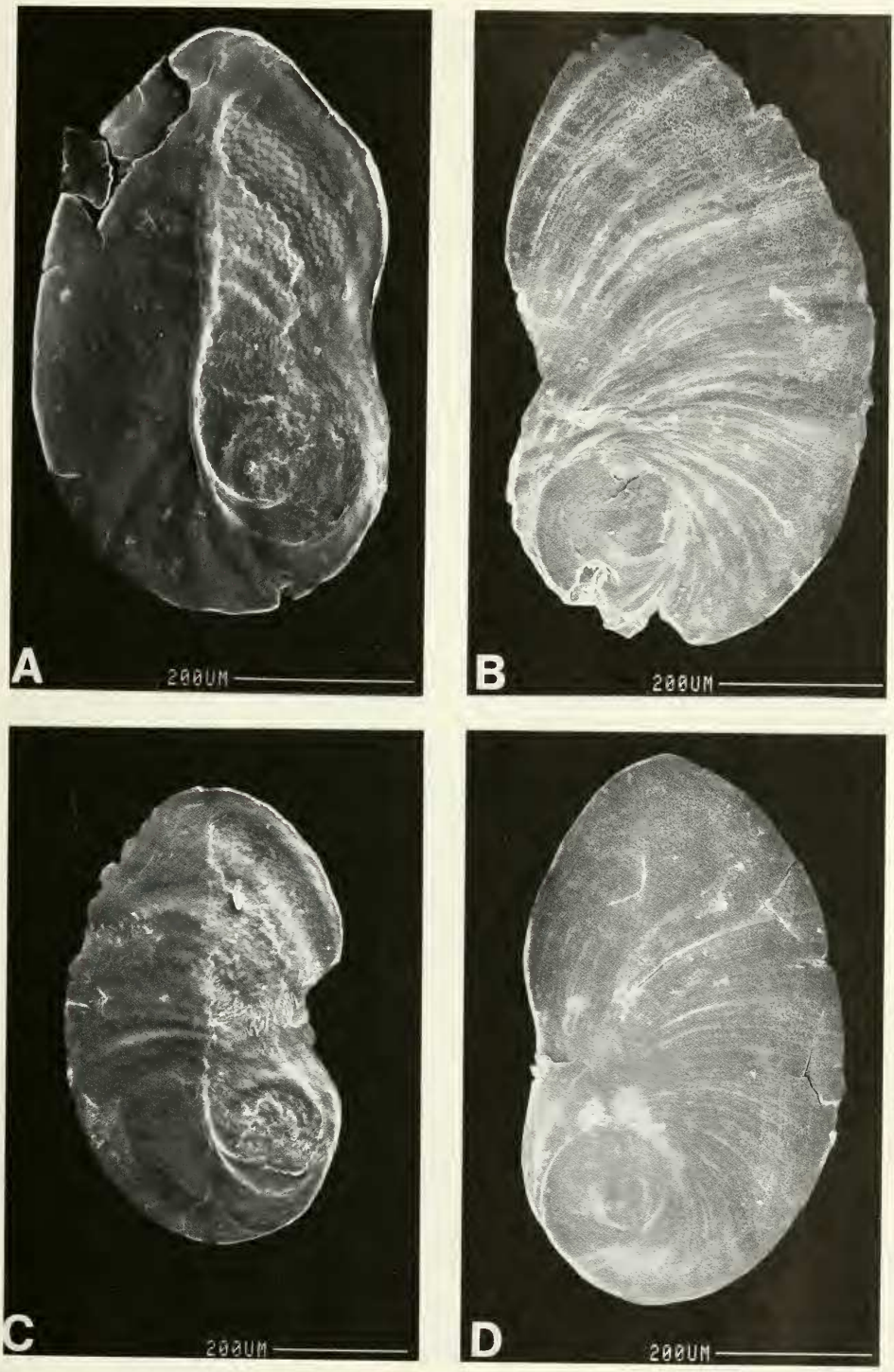

FIG. 28. Opercula of *Pseudobythinella shimenensis*. A, C. Inner surface. B, D. Outer surface. Note prominent ridge on inner surface running along inner edge of attachment pad.

TABLE 12. Lengths (mm) or counts of non-neural organs and structures of *Pseudobythinella shimenensis*. N = number of snails used. Mean ± standard deviation (range).

	Females (N = 5)	Males (N = 1)
Body	3.62±0.34 (3.26–4.04)	3.94
Gonad	0.47±0.09 (0.34–0.60)	2.00
Digestive gland	1.78±0.15 (1.68–2.04)	2.10
Posterior pallial oviduct (= albumen gland)	—	—
Anterior pallial oviduct (= capsule gland)	—	—
Total pallial oviduct = OV	1.52±0.09 (1.40–1.60) N = 4	—
Bursa copulatrix BU	0.49±0.11 (0.36–0.60) N = 4	—
Duct of BU	0.26 (N = 2) No. var.	
BU ÷ OV	0.33±0.08 (0.23–0.40) N = 4	—
Seminal receptacle	0.11±0.02 (0.08–0.13) N = 4	—
Duct of seminal receptacle	0.16±0.05 (0.10–0.22) N = 4	—
Buccal Mass	0.46 (N = 1)	—
Mantle cavity	0.98±0.11 (0.84–1.10) N = 4	.90
Gill (G)	0.76±0.07 (0.70–0.84) N = 4	.70
Osphradium (OS)	0.31±0.08 (0.20–0.40)	.28
OS ÷ G	0.40±0.08 (0.29–0.48) N = 4	.40
No. of filaments	12.3±0.5 (12–13)	.28
Gf_2	0.20 (N = 2)	—
Gf_1	0.16 (N = 2)	—
Total Gf = TGF	0.36 (N = 2)	—
Gf_2 ÷ TGF	0.55 (N = 2)	—
Prostate	—	1.00
Seminal vesicle	—	.80
Penis	—	.90

TABLE 13. Radular statistics for *Pseudobythinella shimenensis*. Mean ± standard deviation (range). N = number used. In mm except for width of central tooth in μm.

	Sex Unknown
Shell length	2.1±0.12 (1.9–2.2) N = 9
Radular length	0.79±0.46 (0.71–0.84) N = 5
Radular width	0.071±0.005 (0.064–0.076) N = 6
Total rows of teeth	113±1.7 (111–115)
No. rows of teeth forming	9±3 (6–14)
Central tooth width	14.1±0.82 (13.2–15.3) N = 13

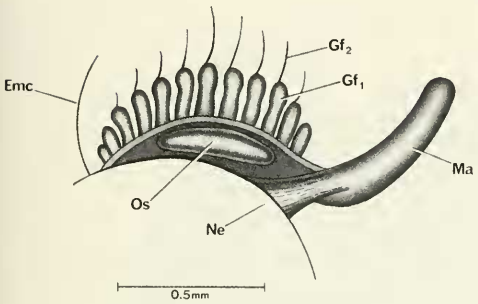

FIG. 29. Mantle cavity of *Pseudobythinella shimenensis*. Mantle cut and reflected to show mantle-cavity structures.

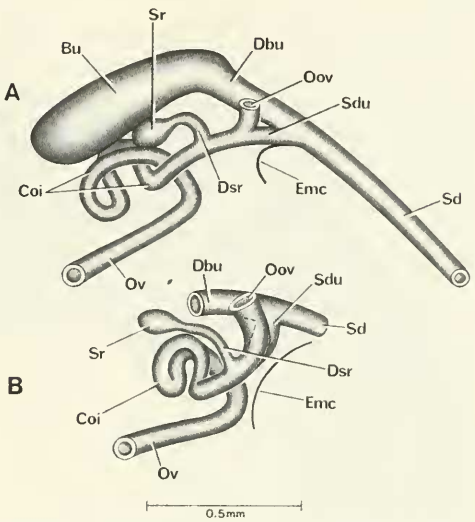

FIG. 31. Details and variation of bursa copulatrix complex of organs of *Pseudobythinella shimenensis*. Figure 31A is in same orientation as in Figure 30. B. Bursa cut away to show seminal receptacle (Sr) and oviduct coil (Coi).

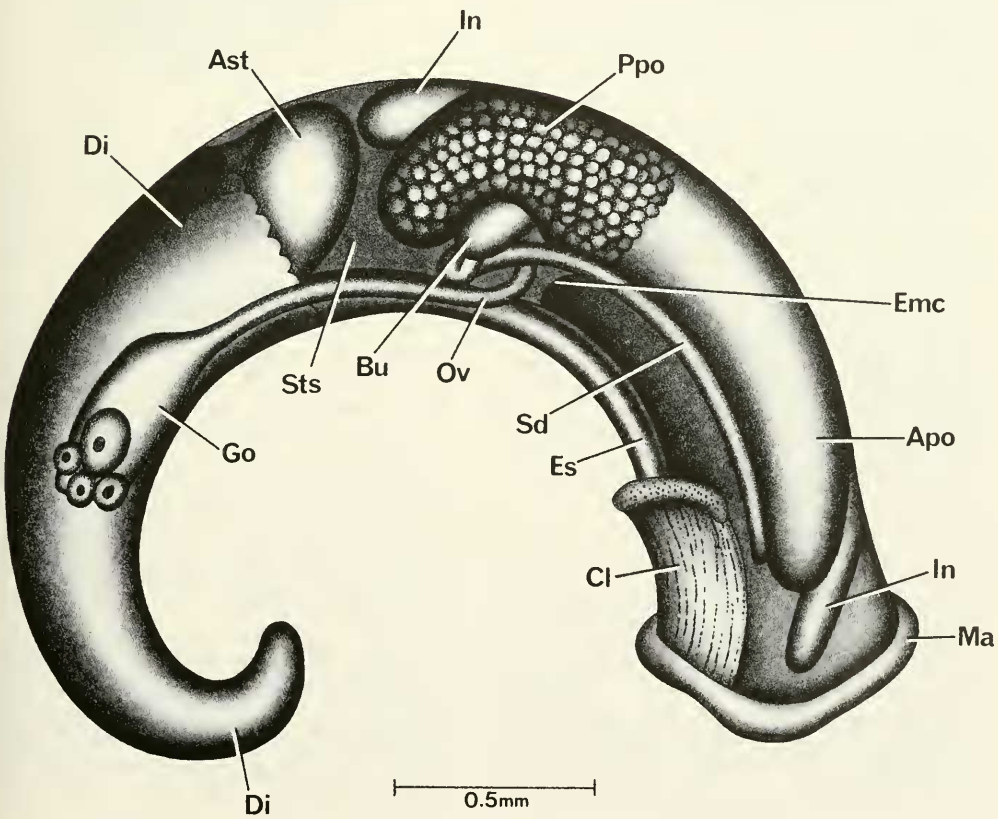

FIG. 30. Uncoiled female *Psuedobythinella shimenensis* with head and kidney tissue removed.

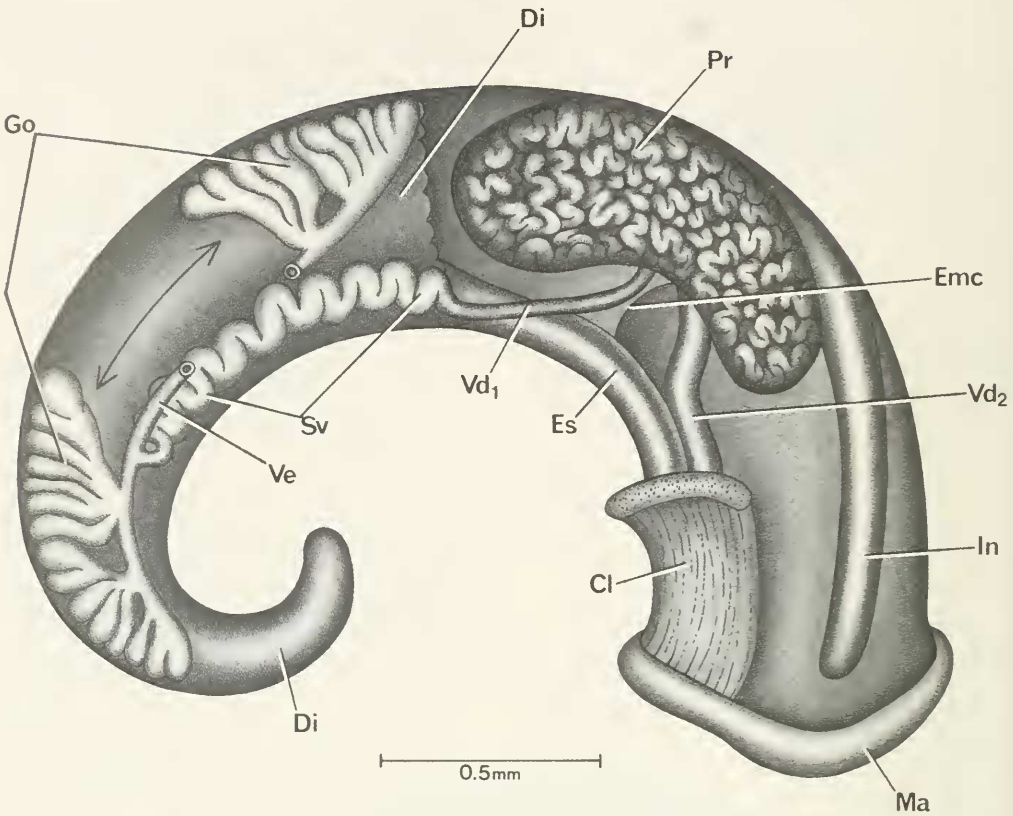

FIG. 32. Uncoiled male of *Pseudobythinella shimenensis* without head or kidney tissue. Some lobes of gonad removed (iine with arrows) to reveal seminal vesicle (Sv).

and the duct of the seminal receptacle are well developed. (7) Posterior to the duct of the seminal receptacle the oviduct makes an irregular loop or double coil that is dorsal to the bursa. In Figure 31A, the coil has been pulled out a little from beneath (dorsal to) the bursa to show the pattern of coiling. The coil is shown in actual position in Figure 30.

Male reproductive system. The body of an uncoiled male is shown in Figure 32 with head and kidney tissue removed. Measurements and counts of organs are given in Table 12. Important features to note are: (1) The gonad covers the stomach. (2) A portion of the gonadal lobes has been cut away to show the seminal vesicle (Sv) that coils regularly dorsal to the gonad. (3) There is a well-defined vas efferens (Ve) with the posterior vas deferens arising from the vas efferens at mid—to slightly posterior to mid-gonad. (4) There are a number of bundles of testicular lobes arising from the vas efferens. (5) The prostate overlies the posterior end of the mantle cavity (Emc). (6) The anterior vas deferens (Vd_2) leaves the prostate (Pr) close to the posterior end of the mantle cavity. (7) The penis is simple and without discernable papilla (Fig. 27B). (8) The base of the penis (Bp) arises from the neck to the right of the snout-neck mid-line (x) and at 90° to it (Fig. 27A). There is no discernable ejaculatory duct.

Digestive system. The digestive gland covers the posterior chamber of the stomach of females (Di, Fig. 30), and the entire stomach in males (Fig. 32). The radular sac (Rs, Fig. 33) is highly elongated, coiling dorsal to the buccal mass (Bm).

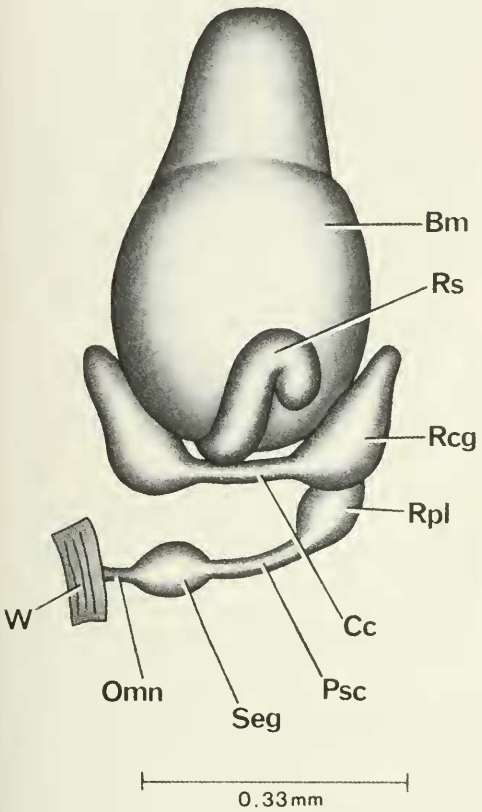

FIG. 33. Dorsal aspect of buccal mass of *Pseudobythinella shimenensis* with dorsal part of nerve ring. Note radular sac (Rs) coiling dorsally over buccal mass (Bm).

Radular statistics are given in Tables 13 and 14. The most commonly encountered cusp formula is

$$\frac{4(5)\text{-}1\text{-}(5)4}{1\text{-}1};\ 2(3)\text{-}1\text{-}\ 3(4);\ 17\text{-}20,\ 16\text{-}18.$$

There is a very large number of rows of teeth for the comparatively short length of radula (113 per 0.79 mm). The radula is illustrated in Figures 34, 35. Fig. 34B, D, E feature the central tooth. The face of the tooth is moderately raised as a tongue with a slight concavity on either side extending beneath the basal cusps. The lateral angles have the flared ends typical of *Pseudobythinella*.

The lateral teeth are featured in Figures 34C, D, F and 35A, B, E. Two points are important. (1) The basal process of the lateral tooth is prominent and curved towards midradula as also seen in *P. chinensis* but in contrast to the weak or slighly developed straight basal process seen in *Akiyoshia chinensis*. (2) As in the above mentioned taxa, there is a gradation in size of the cusps on the lateral tooth. The "1" of the 3-1-3 is not considerably larger than the flanking cusps. Inner marginal teeth (Figs. 34B, C, F; 35C, D, E, F) and outer marginals (Figs. 34C, E; 35C, G) have numerous small cusps. No one cusp is extra long (i.e. with derived specialization).

Nervous system. A segment of the nervous system is shown in Figure 33. The cerebral commissure (Cc) is elongated. The dorsal nerve ring is moderately concentrated (RPG of 0.38, Table 15). Otherwise the dorsal aspect of the nerve ring is typical for the Triculinae.

Remarks

This species differs from the others for which we have anatomical data as follows: (1) The glands about the eye form an "eyebrow". *Pseudobythinella chinensis* and *P. daliensis* lack any glands about the eyes; there is a scatter of glands in *P. kunmingensis*. (2) A tooth is clearly visible in the aperture of the shell. (3) The bursa is an elongated tube; it is an elongated ovoid sac in the other species. (4) The penis lacks an ejaculatory duct.

Pseudobythinella daliensis differs from the other three species by having a small, not minute shell. It does not have an elongated radular sac as do the others.

Pseudobythinella kunmingensis differs from the other three species by having a scatter of glands about the eyes. The spermathecal duct shares a common opening with the capsule gland (Apo) (not shown in Fig. 31 where the spermathecal duct is cut short).

TRICULINAE

Pachydrobiini Davis & Kang, 1990

Type genus. Pachydrobia Cross & Fischer, 1876

Diagnosis. Genera of Triculinae in which the spermathecal duct bypasses the pericardium and the oviduct does not make a closed 360° twist. With the exception of *Wuconchona*,

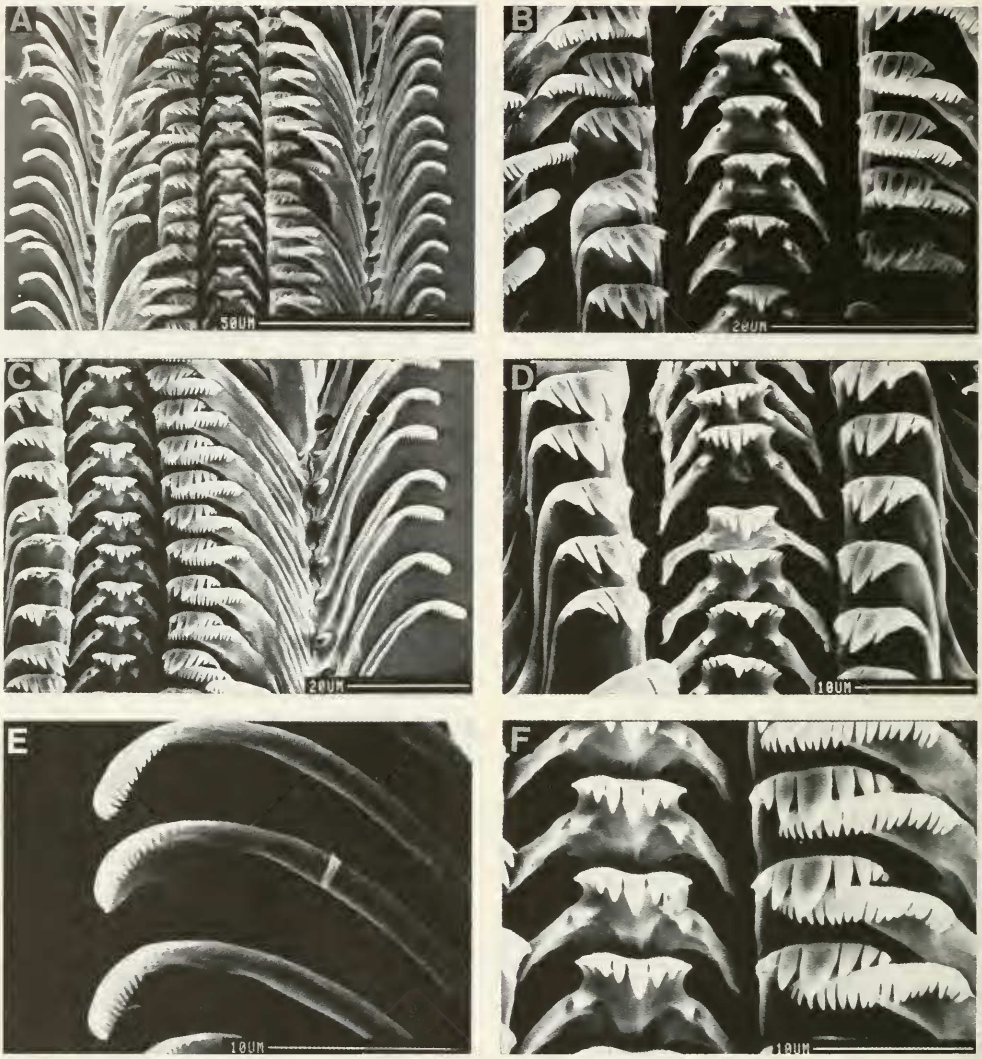

FIG. 34. Radula of *Pseudobythinella shimenensis* featuring central and lateral teeth (B–D, F) and outer marginal teeth (E).

there is a sperm duct. The seminal receptacle arises from the bursa or the duct of the bursa in the plesiomorphic state; the seminal receptacle is lost in the derived state and its function taken over by new structures.

Genera assigned. Guoia, *Halewisia*, *Neotricula*, *Pachydrobia*, *Robertsiella*, *Jinhongia*, *Gammatricula*, *Wuconchona* (N = 8).

The *Lithoglyphopsis* Problem

Considering all Asian genera of freshwater rissoacean snails, it has been especially important to locate and study the type species of *Lithoglyphopsis* for two reasons. (1) *Lithoglyphopsis* was the taxon that caused early European workers to include within the family Hydrobiidae those Asian taxa now known to

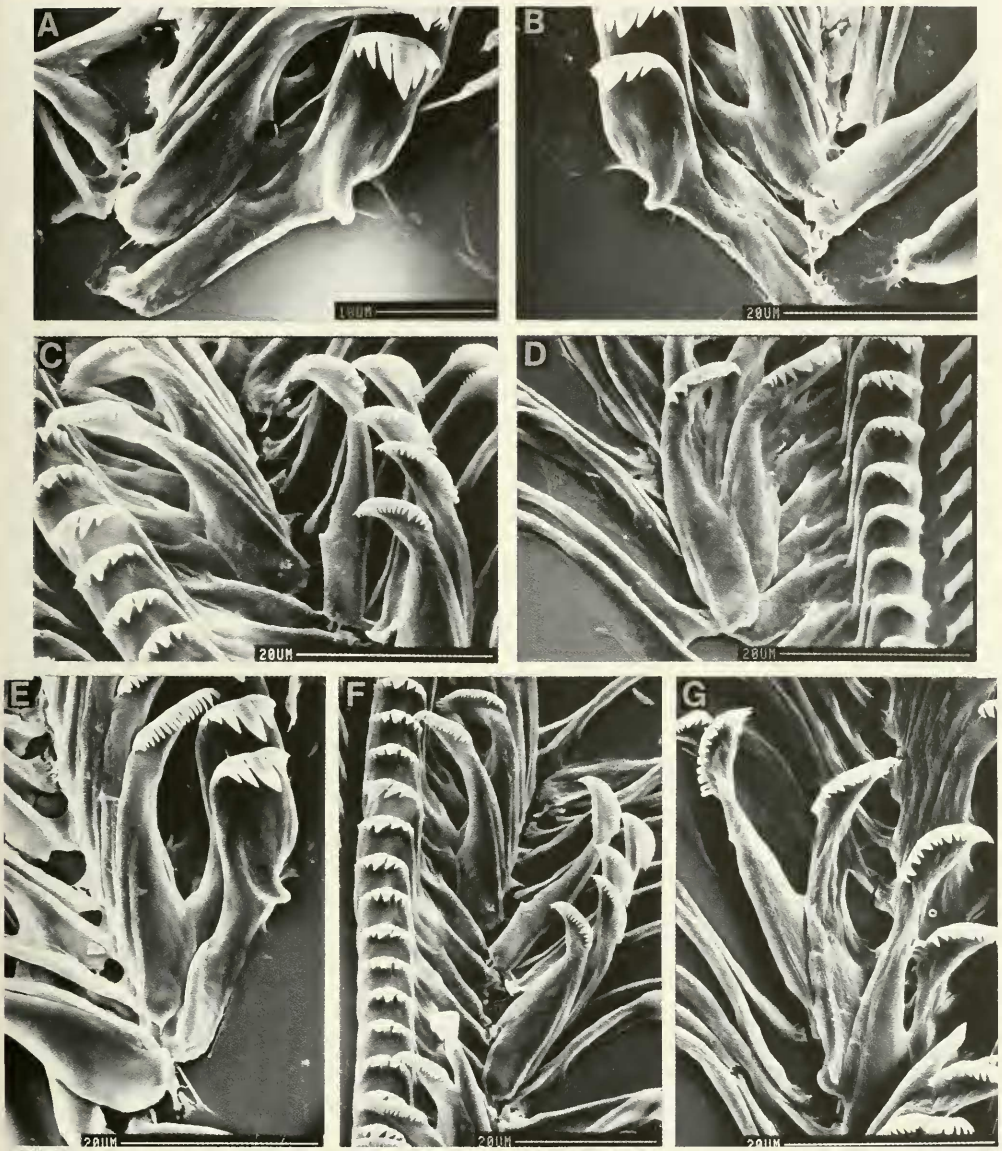

FIG. 35. Radula of *Pseudobythinella shimenensis* featuring entire lateral tooth (A, B, E), inner marginals (C–F), outer marginals (G).

be Pomatiopsidae: Triculinae. (2) The snail transmitting *Schistosoma mekongi* Voge et al., 1978, was originally described as *Lithoglyphopsis aperta* Temcharoen, 1971.

Considering the first, the shells of certain Chinese species from Hunan Province so much resembled shells of European *Lithoglyphus* that they were described as species of *Lithoglyphus* (Gredler, 1881, 1886; Moellendorff, 1888). Subsequently Thiele (1928) noted that the morphology of the central tooth of *L. modestus* differed slightly from that of European *Lithoglyphus* and he therefore established the genus *Lithoglyphopsis*, with *L. modestus* Gredler, 1886, as its type species by original designation. However, overall shell

TABLE 14. Cusp formulae for the radular teeth of *Pseudobythinella shinenensis* with the percent of the radulae in which a given formula was found at least once.

Central Teeth		Lateral Teeth		Inner Marginal Teeth		Outer Marginal Teeth
4-1-4 / 1-1	80%	2-1-3	60%	14	—	20%
5-1-5 / 1-1	40%	2-1-4	60%	15	—	40%
5-1-4 / 1-1	20%	3-1-3	60%	16	—	60%
4-1-4 / 1-1	20%	3-1-4	40%	17	80%	100%
				18	100%	80%
				19	100%	40%
				20	60%	20%
				21	40%	—
				$\bar{X}$ * = 18.7±1.2 N = 50		17.2±1.3 N = 49

*Mean ± standard deviation of cusp number for all teeth counted.

TABLE 15. Lengths of neural structures of *Pseudobythinella shimenensis*. The mean is given and with data when N = 2. N = number used.

Cerebral ganglion	0.20 (N = 2) (No. Var.)
Cerebral commissure	0.09 (N = 2) (0.08, 0.10)
Pleural ganglion	
Right (1)*	0.10 (N = 1)
Left	—
Pleuro-supraesophageal connective (2)*	0.12 (N = 1)
Pleuro-subesophageal connective	—
Supraesophageal ganglion (3)*	0.10 (N = 1)
Subesophageal ganglion	—
Osphradio-mantle nerve	0.04 (N = 1)
RPG ratio* = 2 ÷ 1+2+3	0.38 (N = 1)

and radular characters persuaded Thiele (1928) to include *Lithoglyphopsis* of the Hydrobiidae along with 12 other Asian Triculinae genera within the Tribe Lithoglypheae along with European *Lithoglyphus*. As late as 1974, Brandt included the Asian genera in question in the family Hydrobiidae, subfamilies Triculinae, Cohilopinae, Rehderiellinae, and Lithoglyphinae.

As for the second, Davis et al. (1976) studied this species and stated that it was most closely related to *Tricula*, especially *Tricula burchi* Davis, 1968b; they stated that *Tricula* might be a suitable genus for "*L.*" *aperta*. In 1980, Davis referred *L. aperta* to *Tricula*. Davis et al. (1976) pointed out that on the basis of both shell and radula, *Tricula aperta* could not be considered a species of *Lithoglyphopsis*. However, the questions have remained: What is *Lithoglyphopsis*? To which genera is *Lithoglyphopsis* most closely related? Can one establish once and for all that *Lithoglyphopsis* is a member of the Triculinae, not a member of the Hydrobiidae: Lithoglyphinae? What is the potential for species of *Lithoglyphopsis* to transmit a species of *Schistosoma*?

As a result of our studies in Hunan Province, it was clear that species historically considered to be *Lithoglyphus* in Hunan belong to two genera: *Lithoglyphopsis* and a new genus described here as *Guoia*.

Guoia Davis & Chen, genus nov.

Type Species. Lithoglyphus viridulus Moellendorff, 1888

Etymology. Named for Dr. Guo Yuan Hua, Institute of Parasitic Diseases, China National Center for Preventive Medicine, Shanghai, for his tireless efforts to discover and understand species of snails involved in disease transmission.

Diagnosis. Shells small (<3.6 mm long), and globose-conic. The spermathecal duct opens into the rear of the mantle cavity. A long, slender sperm duct connects the spermathecal duct (at a position close to the posterior end of the mantle cavity) to the oviduct close to where the oviduct opens into the albumen gland. Duct of the bursa is massive, running directly anterior from the large bursa to form the short spermathecal duct opening at the rear of the mantle cavity. There is no seminal receptacle; sperm are stored in a swelling of the oviduct just posterior to the juncture of the sperm duct and oviduct, or they are stored in an outpocketing of the sperm duct at the juncture to the oviduct. There is a thin corneous stylet at the tip of the penis. The penis has a glandular lobe. The ejaculatory duct is massive, extending posteriorly along the neck from the base of the penis. Radula *Tricula*-like.

Relationships. A member of the *Neotricula* clade by virtue of (1) the oviduct travels from gonad to albumen gland straight, without twist or coil (contrast the *Tricula* clade), and (2) the spermathecal duct does not enter the pericardium. The closest generic similarity is with *Robertsiella* of Malaysia in that (1) the penis of the males has a similar stylet, and (2) the spermathecal duct-duct of bursa-bursa connections and relative postitions are the same. There are differences. In *Robertsiella*, the seminal receptacle is encapsulated in the muscular wrapped duct of the bursa (*Guoia* lacks a seminal receptacle). A section of the oviduct of *Guoia* serves as a seminal receptacle. The shell of *Robertsiella* is ovate-conic, not globose-conic. The sperm duct of *Guoia* is elongated, twisting over the bursa; it is very short in *Robertsiella*. The duct of the bursa is very short in *Robertsiella*, elongated in *Guoia*.

Assigned Species.
Lithoglyphus fuchsianus Moellendorff, 1885
Lithoglyphus viridulus Moellendorff, 1888

Thiele (1928: 365) noted that of Asian species described as *Lithoglyphus*, *L. fuchsianus* and *L. viridulus*, had radulae that corresponded to the European *Lithoglyphus*, whereas the radulae of *L. modestus* and *L. tonkinianus* Bavay & Dautzenberg (a Vietnamese species) had an entirely different type of central tooth. He created the genus *Lithoglyphopsis* to include the latter two species and named "*L. modesta*" as the type species. Yen (1929) placed all Chinese taxa described as *Lithoglyphus* in the genus *Lithoglyphopsis* including *L. liliputanus* Gredler, 1881 from "Kwangtung" (= Guangdong). The shell of this last species is a miniature version of *L. modestus*. Until the anatomy is known its generic placement is *incertae sedis*.

Guoia viridulus (Moellendorff, 1888).

Lithoglyphus viridulus Moellendorff, 1888: 141, pl. 4, fig. 6, 6a-b
Lithoglyphus viridulus (Moellendorff, 1888). Thiele 1928
Lithoglyphopsis viridulus, Yen, 1939

Types: S.I.; Lectotype, 4129, fig. in Yen, 1939: pl. 4, fig. 9
Paralectotypes, 4130, figured here; Figure 36 A–C.
Type Locality: Hunan

Habitat

Anhua County, Anhua Town, Zijiang River; 28°23′46″ N, 111°12′41″ E., Figure 1, Site 10. Collected by Chen and Davis, 16 March 1987; field collection number D87-1. Catalog numbers are: large class, ANSP 373147, A12663; small class, ANSP 373148, A12664. D85-78, small class, ANSP 373149, A 12665; ZAMIP M0055. Snails were collected 1.6 km upstream from the town boat landing, along the shores of a small island in the middle of the river. Water flows through a stone breakwater at the upstream end of the island. Between the breakwater and the cobbles of the island was a protected area with water some 30 cm deep and with emergent vegetation. On the undersides of rocks at the breakwater on the protected side were numerous *Guoia viridulus* and *Lithoglyphopsis modesta.* Associated snail fauna included *Stenothyra hunanensis* (Davis et al. 1988), *Gyraulus* sp., *Radix* sp., *Semisulcospira* sp., and a viviparid.

Introduction

There were two size classes of fully mature snails living intermixed at the site (Fig. 37). Throughout the description these will be referred to as the large class and small-class snails. There are slight shape differences between the classes, yet we have felt it prudent not to consider them belonging to different

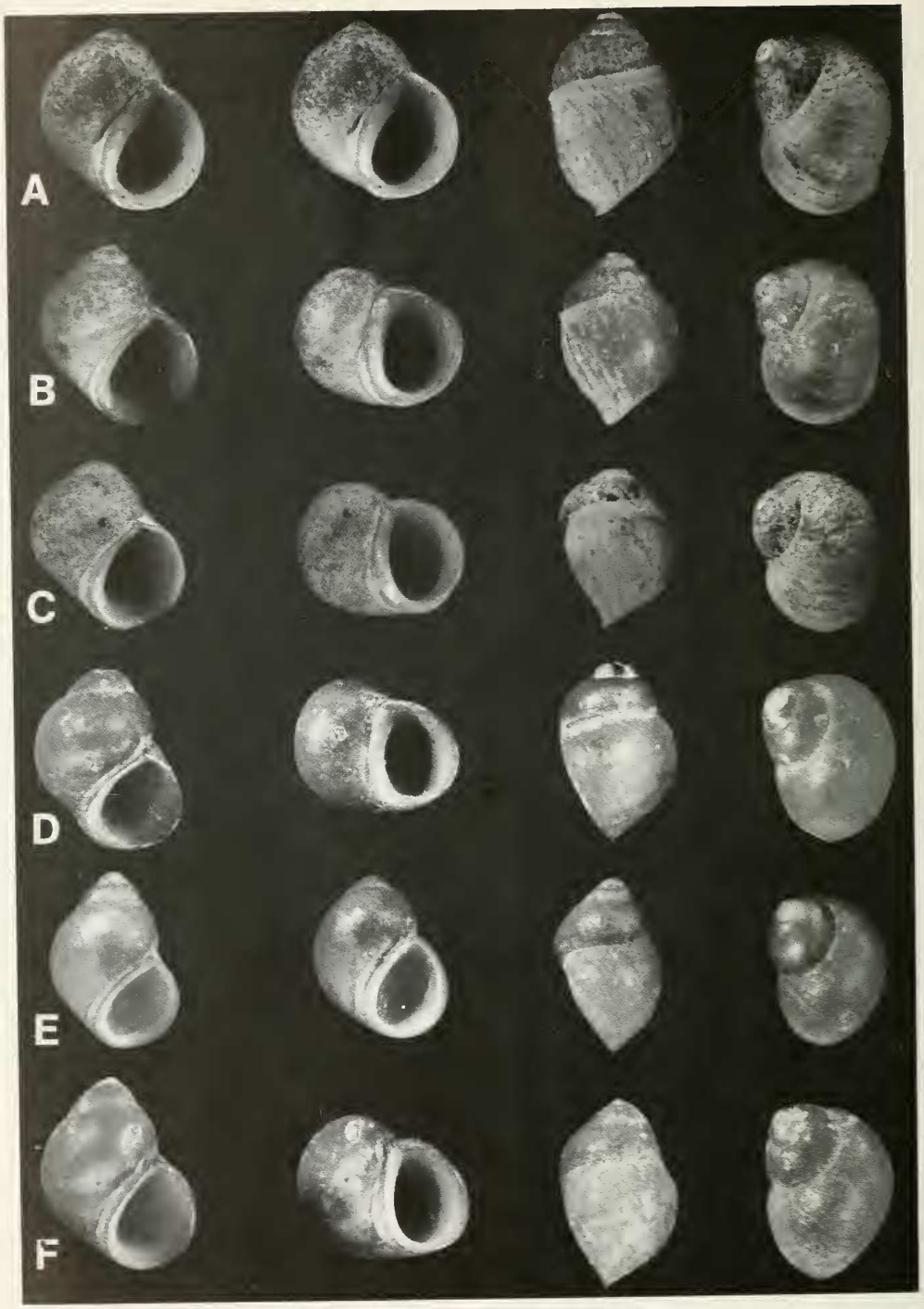

FIG. 36. Lectotype and paralectotypes of species of *Guoia*. A–C. Paralectotypes of *Guoia viridulus* (SMF 4130); A = 3.50 mm long. *Guoia fuchsianus*, D–F. D. Lectotype, L = 3.24 mm. E, F. Paralectotypes.

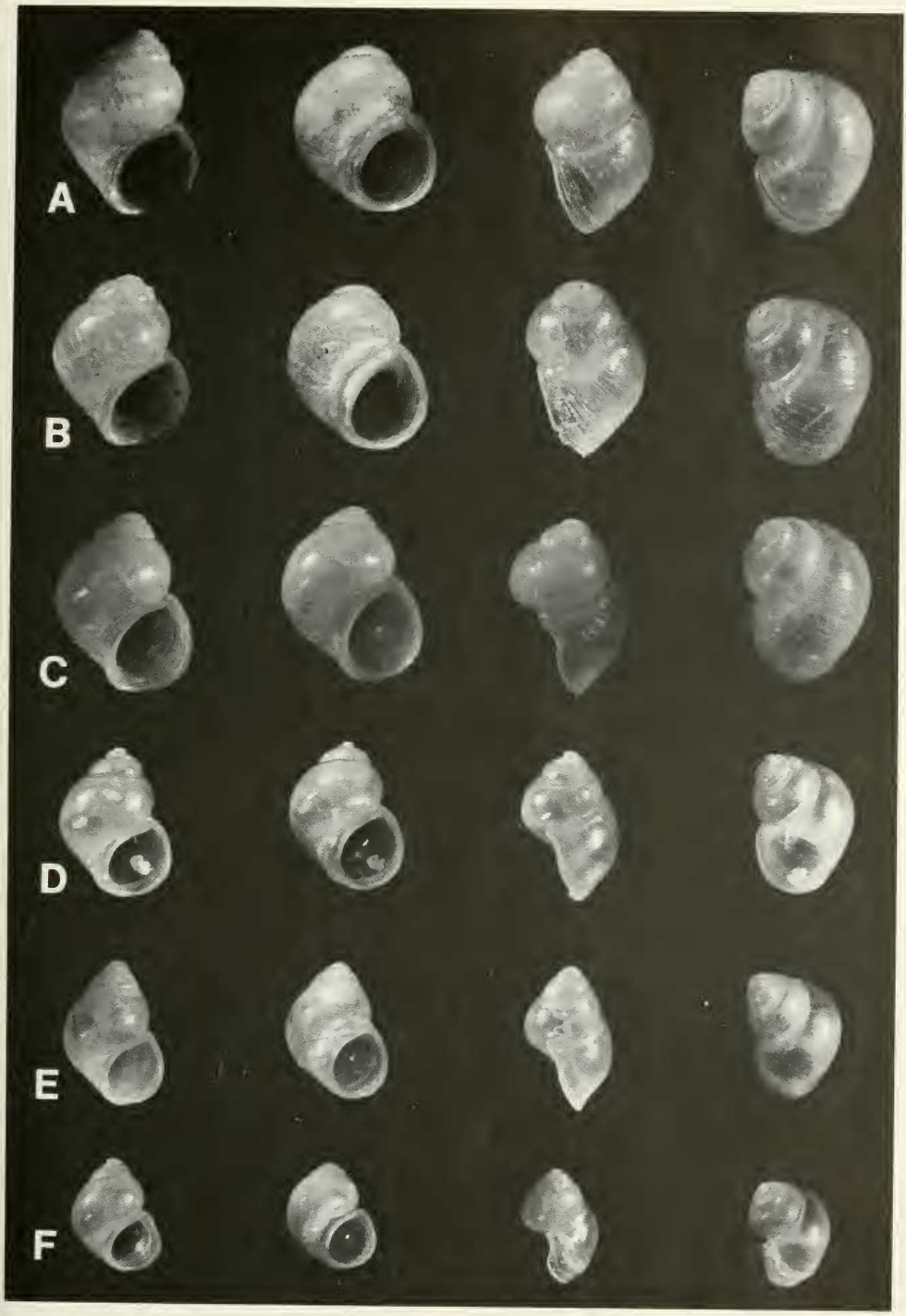

FIG. 37. Four aspects of each of six shells of *Guoia viridulus*. A–C. Large class; A = 3.6 mm long. D–F. Small class; D = 2.8 mm long. A, B, D, E = females; C, F = males.

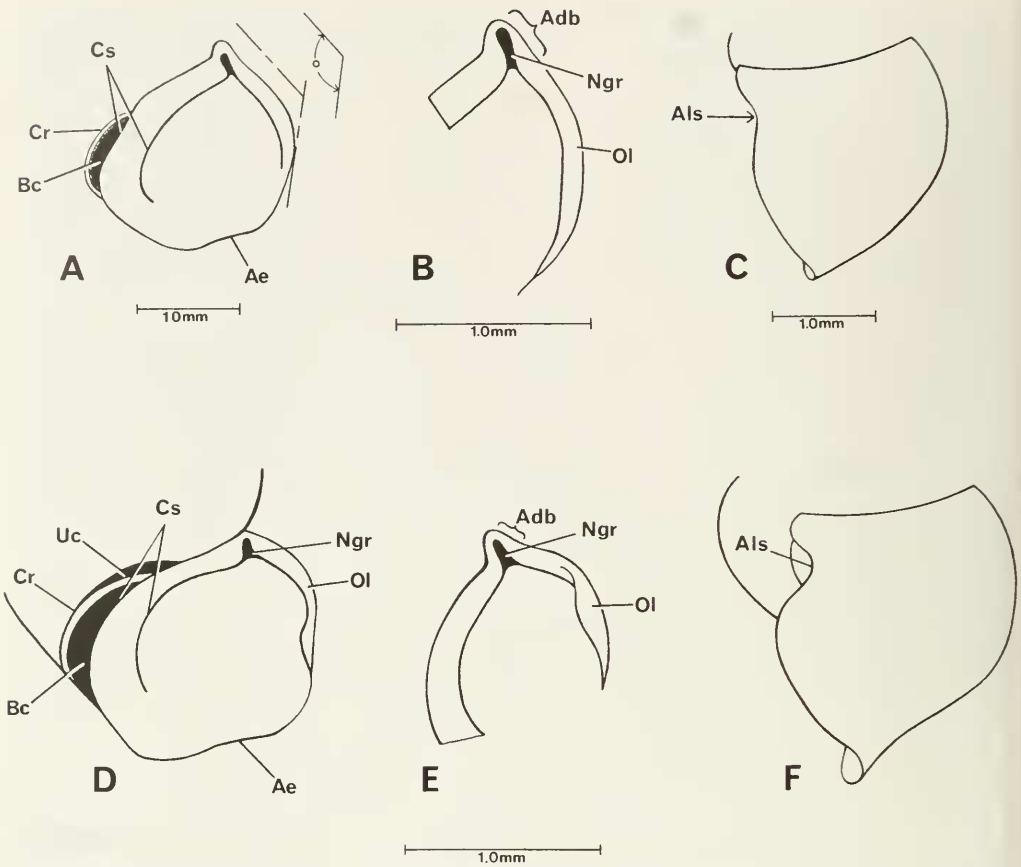

FIG. 38. Illustrated details of the apertural region of shells of *Guoia viridulus* characteristic of the species.

species as we could find no anatomical differences between them, and as they live in micro-sympatry. The greater amount of anatomical data was from the large-class snails based on living specimens. Subsequently, anatomical data were gathered in Philadelphia from alcohol-preserved small class snails.

As there is considerable similarity among shells of the two size classes of snails that we refer to as *G. viridulus*, as well as *G. fuchsianus*, we did a multivariate analysis of shell measurements of these taxa as well as older museum specimens of these species in order to attempt to assess differences among them. The following anatomical description is based on large class snails. Small class snails are contrasted with large class individuals in the remarks section for this species.

Description

Shells. Figures 36–39. Large-class (Figs. 37A–C, 39A–C). Shells small, globose-conic, 4.0–4.5 whorls, smooth but with rough growth lines. Aperture sub-circular with complete peristome, with pronounced apertural beak (Fig. 38, Adb) and a pronounced beak groove (Ngr). There is a wide columellar shelf (Cs), a small basal crescent (Bc) with crescent ridge (Cr). Some shells have an umbilical chink (Uc), others do not. The abapical lip has an embayment (Ae). The adapical outer lip is flared out making somewhat of an angle with the remaining outer lip. In side view, the lip is sinuate forming a slight sigmoid embayment (Als).

Females are larger than males (Table 16). Size ranges (lengths) are: males, 2.8 to 3.6

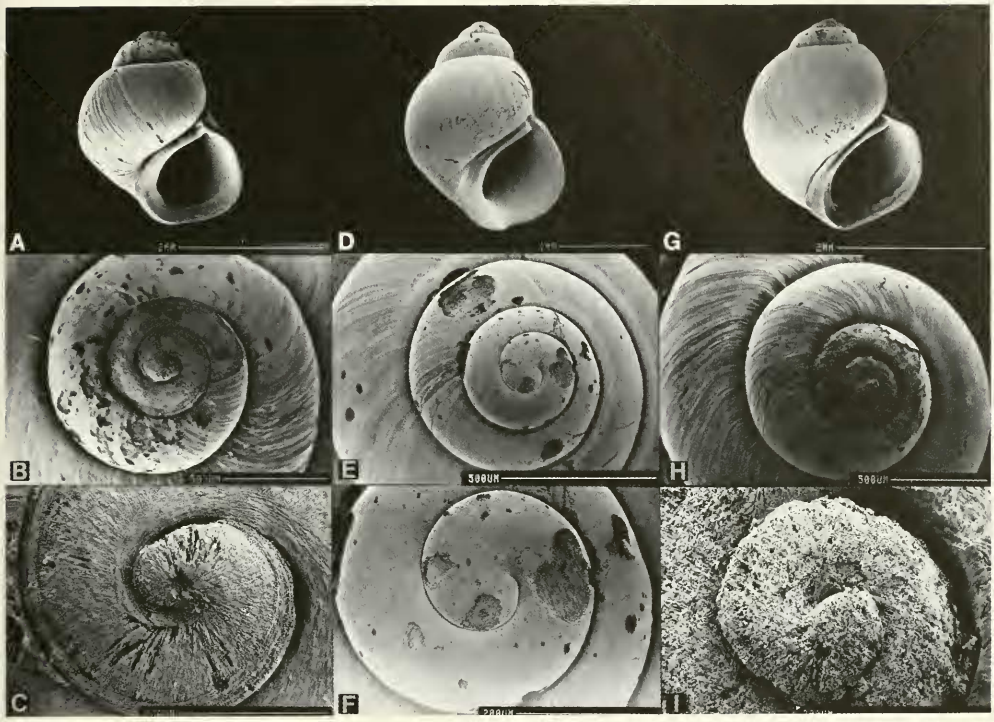

FIG. 39. SEM photos of shells of *Guoia viridulus* (A–F) and *G. fuchsianus* (G–I). A–C. Large form; D–F. Small form. B, C, E, F, H, I = enlargements of apical whorls.

mm; females, 2.8–3.8 mm. Our samples compare well with two lots of *G. viridulus* from the collections (Table 16, column 3). They compare well with paralectotypes (Figs. 36A–C compared with Fig. 37A–C).

Small-class (Figs. 37D–F). Shells as in the large class with the following differences. Length is substantially smaller (Table 16) with males 2.0–2.1 mm long, females 2.2–2.8 mm long. The small-class shells appear somewhat more conic than large class shells (compare Fig. 37E vs. 37A). However, the width to length ratio is not significantly different between classes; the length of the body whorl to total height is slightly greater in the large size class (0.84 ± 0.03, 0.84 ± 0.05 for large-class; 0.80 ± 0.02, 0.80 ± 0.03 for small class). The basal crescent and columellar shelf are deeply depressed in small class shells (Fig. 37D). The outer lip in side view has a deep sigmoid embayment (Fig. 38F).

SEM pictures of the apical whorls are shown in Figure 39B, C, E, F. The large class individuals inevitably had eroded apices; the small class shell apices were smooth. Some spiral microsculpture was noted at the shoulder of the body whorl of small class shells.

Multivariate analysis. The phenogram based on distance coefficients (cophenetic correlation 0.77) is given in Figure 40. Note the following: (1) Historic *G. viridulus* (nos. 18-21) form a discrete unit within the wider variance of 9 large-class Anhua *G. viridulus* collected by us. (2) One Anhua *G. viridulus* (no. 5) clusters with Baisha *G. fuchsianus* collected by us. (3) The one historic *G. fuchsianus* that had complete whorls so that it could be included in this analysis clusters in the middle of the *G. fuchsianus* variance. (4) Two small-class Anhua *G. viridulus* (nos. 27, 28) and two snails classified by us as large-class Anhua *G. viridulus*

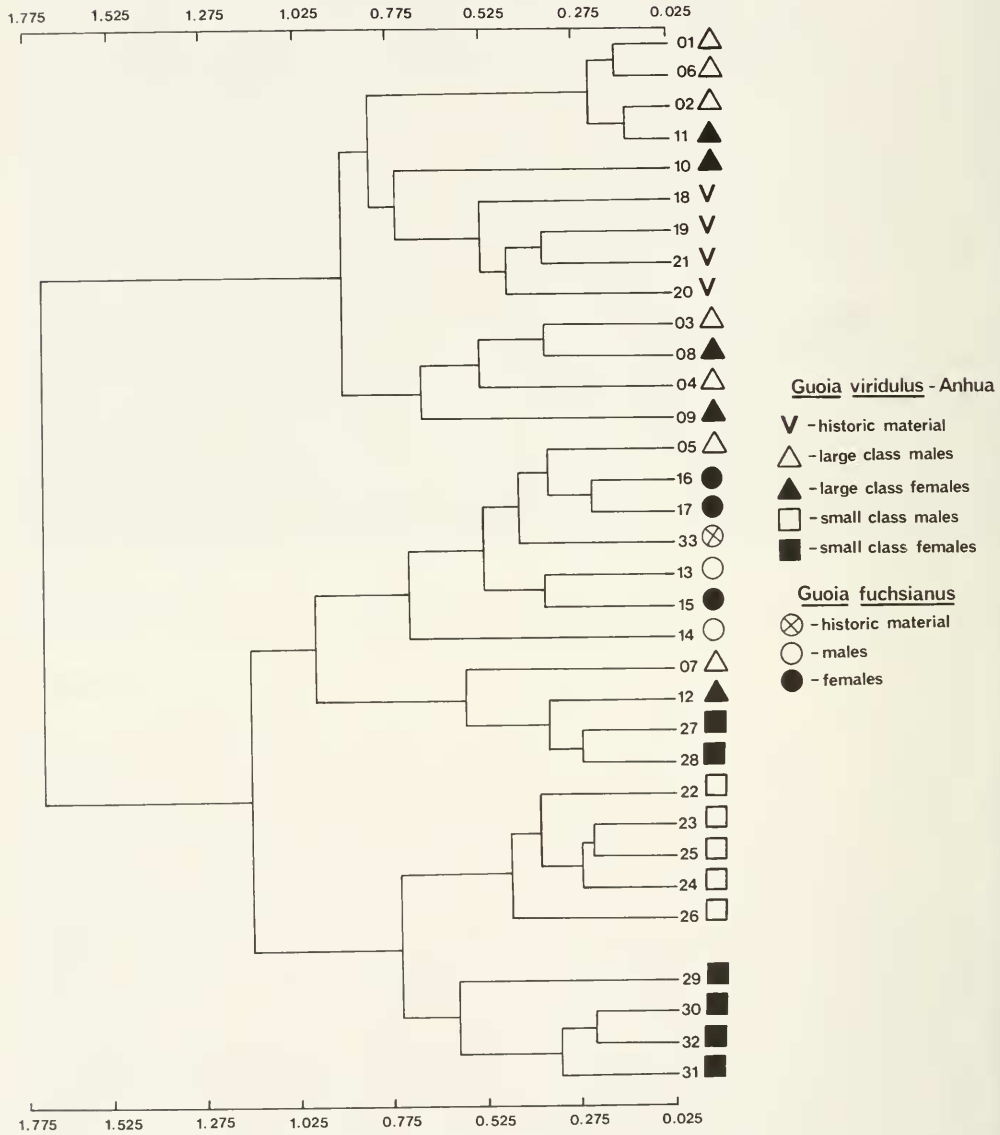

FIG. 40. UPGMA phenogram of distances for shell measurements of two species of *Guoia*. See text for details.

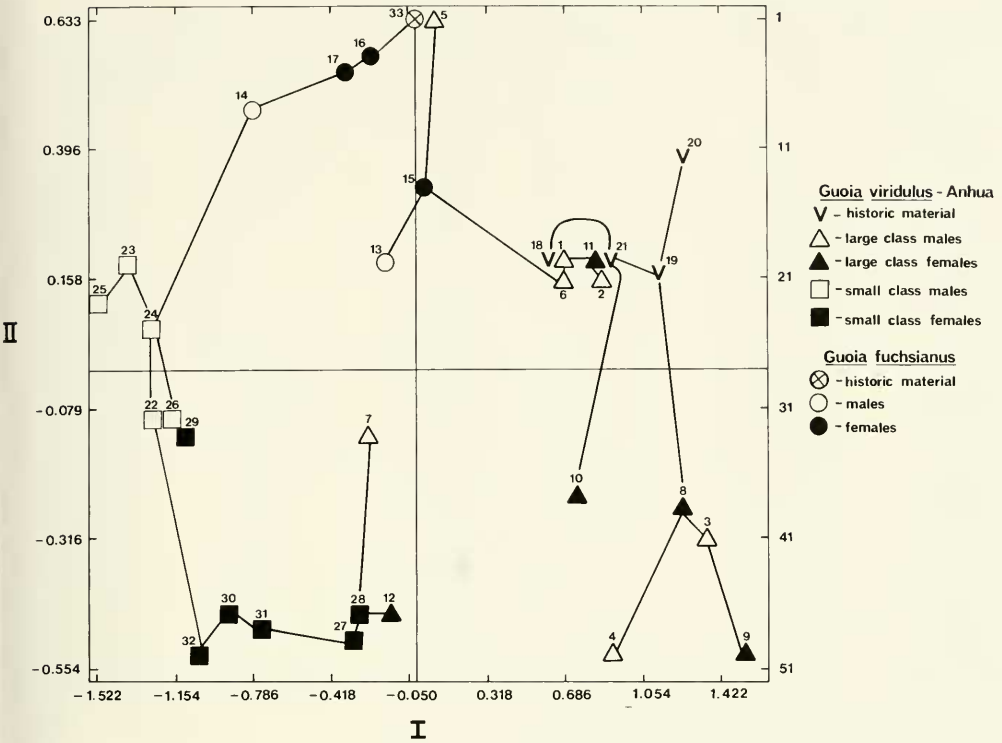

FIG. 41. Ordination diagram following three dimensional scaling. The first two principal components are given. Taxa are connected by a MST. See text for details.

(nos. 7, 12) form a sub cluster with *G. fuchsianus*. (5) Most (82%) of the small-class *G. viridulus* form a discrete cluster at the bottom.

In the PCA analysis, there were three significant components (Table 17); the first with 76.6% of the variance, the second with 13.49, the third with 5.69 (total of 95.8%). Character loadings showed the first component to be one of size (Table 18); characters loading heavily on the second component-axis are number of whorls and length of the penultimate whorl. Ordination on the first two PCA axes following MDS is given in Figure 41. The MST connects OTUs. Size increases from left to right. Along the second axis, relative to length, shells with more whorls, longer penultimate whorls, and wider 3rd whorls are to the bottom. Proportionally shorter penultimate whorls and narrower 3rd whorls are to the top. The second axis is one of changes in translation, whorl expansion, and whorl number. We deduce the following from the ordination diagram and table of character loadings. (1) We consider the small-class and large-class snails to belong to the same species, *G. viridulus*. With only two exceptions (nos. 5, 20) the variance along the second axis ranges from −0.554 to +0.182 for both size classes showing the same considerable variance in whorl translation and expansion. The only differences between the size classes are clear-cut differences in size, and the qualitative differences of deeper lip sinuation and depressed lip sinuation and depressed cres-

TABLE 16. Shell measurements for populations of *Guoia viridulis*.

	Large Class (D87-1)		ANSP 45501	Small Class (D87-1)	
	Males (N = 7)	Females (N = 5)	& 98206 (N = 4)	Males (N = 5)	Females (N = 6)
No. Whorls	4.0–4.5	4.0–4.5	4.5	4.0–4.25	4.5
Length (L)	3.21±0.28 (2.76–3.56)	3.36±0.38 (2.84–3.84)	3.44±0.16 (3.28–3.60)	2.12±0.06 (2.02–2.16)	2.48±0.24 (2.24–2.80)
Width (W)	2.57±0.16 (2.32–2.76)	2.61±0.29 (2.12–2.88)	2.89±0.19 (2.72–3.12)	1.66±0.08 (1.54–1.76)	1.86±0.14 (1.68–2.08)
L body whorl	2.69±0.28 (2.12–2.92)	2.82±0.31 (2.32–3.12)	2.99±0.11 (2.88–3.12)	1.70±0.06 (1.62–1.76)	1.99±0.22 (1.80–2.32)
L penultimate whorl	0.33±0.07 (0.20–0.38)	0.40±0.05 (0.36–0.48)	0.29±0.02 (0.28–0.32)	0.24±0.02 (0.22–0.28)	0.28±0.03 (0.24–0.32)
W penultimate whorl	1.16±0.13 (0.96–1.28)	1.22±0.13 (1.04–1.36)	1.11±0.04 (1.08–1.16)	0.80±0.04 (0.76–0.84)	0.90±0.10 (0.78–1.04)
W 3rd whorl	0.56±0.08 (0.48–0.68)	0.56±0.08 (0.48–0.68)	0.53±0.04 (0.48–0.56)	0.44±0.04 (0.40–0.50)	0.51±0.06 (0.40–0.56)
L last 3 whorls	3.15±0.26 (2.72–3.48)	3.28±0.34 (2.80–3.68)	3.38±0.17 (3.20–3.52)	2.05±0.06 (1.96–2.12)	2.41±0.23 (2.20–2.72)
L aperture	1.95±0.19 (1.56–2.12)	2.00±0.19 (1.68–2.20)	2.29±0.12 (2.16–2.44)	1.26±0.05 (1.20–1.32)	1.44±0.11 (1.32–1.60)
W aperture	1.56±0.17 (1.24–1.76)	1.62±0.22 (1.24–1.76)	1.83±0.12 (1.68–1.96)	0.94±0.05 (0.88–1.00)	1.10±0.09 (0.96–1.20)
W columellar shelf	0.33±0.04 (0.28–0.40)	0.31±0.10 (0.14–0.40)	0.33±0.05 (0.28–0.40)	0.13±0.02 (0.12–0.16)	0.11±0.03 (0.09–0.16)
W ÷ L	0.80±0.03 (0.77–0.84)	0.78±0.03 (0.75–0.81)	0.84±0.02 (0.82–0.87)	0.78±0.03 (0.76–0.82)	0.75±0.03 (0.71–0.79)

TABLE 17. Percent of variance accounted for by each principal component (PC).

PC	%	Accumulated %
1	76.6	76.6
2	13.5	90.1
3	5.7	95.8

cent-columellar callus in the small-class snails. Note that two shells (nos. 7, 12) where originally selected as large-class snails based on visual impression of shape and apertural characters, yet are clearly small-class snails when measured. The length variance for small-class shells was 2.02–2.84 mm, for

TABLE 18. Character loading on each PC axis.

	Components		
	1.	2.	3.
1. No. Whorls	0.293	−0.724	−0.624
2. Length	0.996	0.012	−0.015
3. Width	0.965	0.210	−0.092
4. Length of body whorl	0.970	0.192	−0.059
5. Length of penultimate whorl	0.700	−0.579	0.307
6. Width of penultimate whorl	0.944	−0.209	0.210
7. Width of 3rd whorl	0.745	−0.525	0.249
8. Length of last three whorls	0.994	0.054	−0.026
9. Length of aperture	0.994	0.271	−0.113
10. Width of aperture	0.949	0.270	−0.098
11. Width of columellar shelf	0.874	0.274	−0.034

TABLE 19. Lengths (mm) or counts of non-neural organs and structures of large-class *Guola viridulus*. Mean ± standard deviation (range). N = number of snails used.

	Females	Males (N = 1)
Body	5.69±1.29 (4.36–7.24) N = 4	6.0
Digestive gland	2.23±0.49 (1.80–2.9) N = 4	2.8
Gonad	0.89±0.46 (0.46–1.44)	1.4
Total pallial oviduct PO	2.09±0.21 (1.80–2.30) N = 4	—
Bursa copulatrix = Bu	0.61±0.11 (0.50–0.76) N = 4	—
Bu ÷ PO	0.29±0.03 (0.27–0.33) N = 4	—
Duct of bursa	0.12±0.06 (0.06–0.18) N = 3	—
Buccal mass	0.67±0.03 (0.64–0.70) N = 3	—
Mantle cavity	1.51±0.18 (1.30–1.66) N = 5	2.30
Osphradium = Os	0.53±0.09 (0.46–0.68) N = 5	1.00
Gill = G	1.35±0.17 (1.14–1.50) N = 5	2.00
Os ÷ G	0.40±0.05 (0.32–0.45) N = 5	0.50 (0.26–0.36)
No. gill filaments	24.4±2.1 (22–27) N = 5	25
Gf_2	0.25±0.09 (0.12–0.34) N = 8	male + female
Gf_1	0.37±0.07 (0.30–0.42) N = 8	male + female
Total Gf = TGF	0.57±0.17 (0.42–0.74) N = 8	male + female
Gf_2 ÷ TGF	0.39±0.08 (0.29–0.49)	male + female
Prostate	—	1.80
Seminal vesicle	—	1.20
Penis	—	3.33 (N = 2) (3.06–3.60)

large-class, 2.92-3.84 mm; thus for the species there is a 90% increase in size from shortest to longest mature specimen.

2) We consider the shells at the top of the ordination clustered around mid-axis 1 as belonging to *G. fuchsianus*. They differ considerably from *G. viridulus* in that all have 4.0 whorls, relatively narrower 3rd whorls and shorter penultimate whorls. Only 1 individual (no. 5) of *G. viridulus* (7%) grouped with shells of *G. fuchsianus*.

External features. The head is shown in Figure 42. The snout is transparent but flecked with spots of melanin pigment on the dorsal snout and bars of pigment along the tentacles. There is a small dense eyebrow (Eyb) about each eye comprised of yellow glands. The operculum is shown in Figures 43, 44C–F. It is ovate, paucispiral, with a modest internal attachment pad.

Mantle cavity. The reflected mantle is shown in Figure 45A. The mantle cavity structures are typical for taxa of the *Neotricula* clade. The opening of the spermathecal duct (Osd) is next to the pericardium (Pe). The osphradium (Os) is long and situated mid-gill. The terminal gill filaments (Gf_2) are normal length (Tables 19, 20). The length of the longest filaments is 0.57 ± 0.17 mm long. The filaments are not pleated and lack a pronounced crest (Fig. 45B).

TABLE 20. Lengths (mm) or counts of non-neural organs and structures of alcohol-preserved small-class *Guoia viridulus*. N = number of snails used.

	Females	Males (N = 1)
Body	6.3 (5.60, 6.98) N = 2	—
Digestive gland	2.75 (2.4, 3.1) N = 2	—
Gonad	1.10 (N = 1)	—
Posterior pallial oviduct (= albumen gland)	1.2 (1.1, 1.3) N = 2	—
Anterior pallial oviduct (= capsule gland)	1.3 (1.2, 1.34) N = 2	—
Total pallial oviduct	2.28±0.33 (1.9–2.5) N = 3	—
Bursa copulatrix	0.43±0.16 (0.25–0.56) N = 3	—
Mantle cavity	1.81 (1.62, 2.00) N = 2	1.50
Osphradium = Os	0.67 (0.58, 0.76) N = 2	0.62
Gill = G	1.61 (1.42, 1.80) N = 2	1.24
Os ÷ G	0.41 (0.41, 0.42) N = 2	0.41
No. gill filaments	22 (21, 23) N = 2	19
Gf_2	0.23±0.07 (0.16–0.30) N = 3	male & female
Gf_1	0.30±0.08 (0.24–0.36) N = 3	male & female
Total Gf = TGF	0.53±0.13 (0.40–0.66) N = 3	male & female
Gf_2 ÷ TGF	0.43±0.03 (0.40–0.46) N = 3	male & female
Prostate	—	1.04
Penis	—	2.24

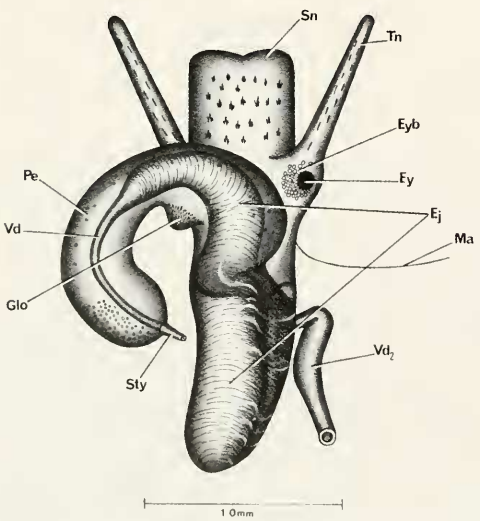

FIG. 42. Head and penis of *Guoia viridulus*.

Female reproductive system. The body of an uncoiled female without head and with kidney tissues removed is shown in Figure 46A. Measurements of relevant organs are given in Tables 19, 20. Important features to note are: (1) The body is not squat, but regularly tubular (contrast *Lithoglyphopsis modesta*). (2) The posterior pallial oviduct (Ppo) does not bend over the style sac (contrast *L. modesta*). (3) The gonad (Go) is posterior to the stomach. (4) Sperm enter the system at the rear of the mantle cavity (Emc) through the opening of the spermathecal duct. The spermathecal duct does not enter the pericardium (contrast taxa of the *Tricula* clade). (5) The pericardium does not swell out into the mantle cavity. The bursa copulatrix complex of organs is shown in Figure 47. (6) The terminal end of the muscular spermathecal duct (Sd) is a thin walled vestibule (Twv). The spermathecal duct is short or long; it is that section of duct between

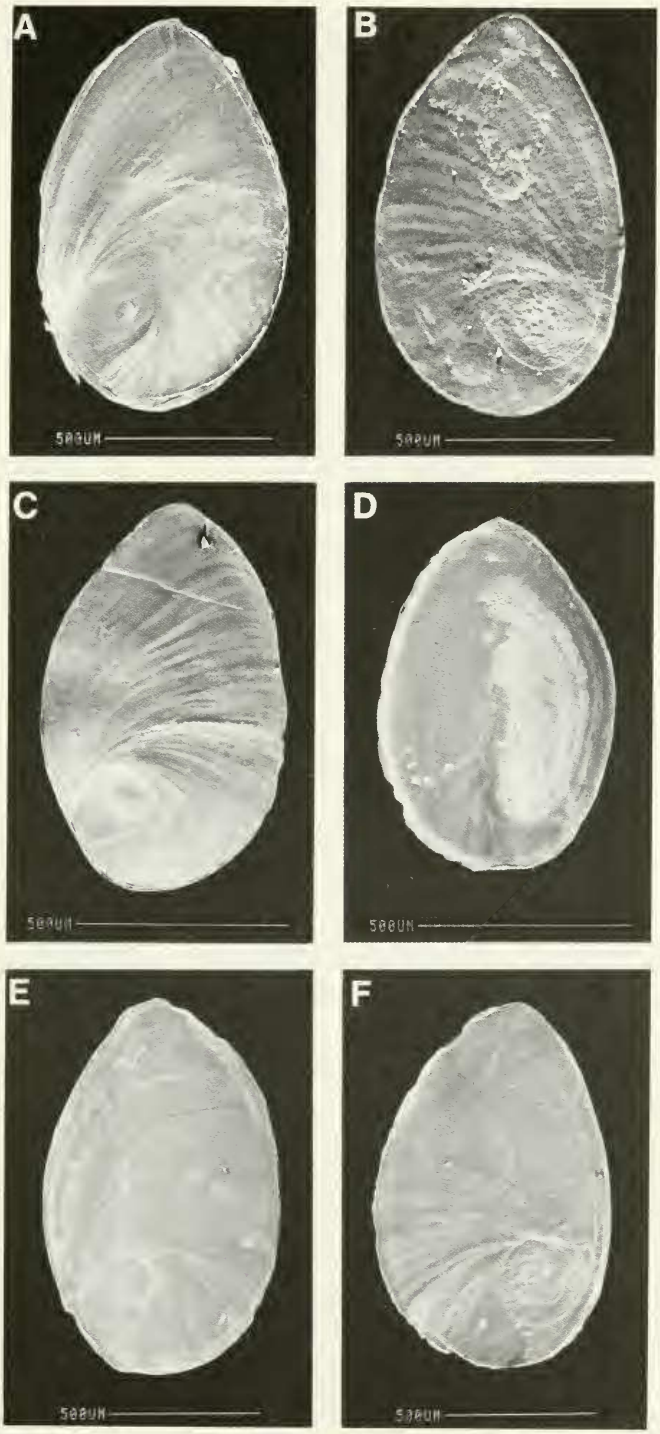

FIG. 43. Opercula of *Guoia viridulus* (A–D) and *Guoia fuchsianus* (E, F). A, B from large-class specimens; C, D from small-class specimens. A, C, E. Outer surfaces; B, D, F. Inner surfaces.

TABLE 21. Radular statistics for *Guoia viridulus* snails. Mean ± standard deviation (range). In mm except for width of central tooth in μm.

	Large Class	
	Females (N = 4)	Males (N = 3)
Radular length	0.96±0.11 (0.84–1.08)	0.94±0.02 (0.92–0.96)
Radular width	0.12±0.01 (0.104–0.132)	0.12±0.01 (0.112–0.128)
Total rows of teeth	70±4 (66–75)	71.7±2.5 (69–74)
Rows of teeth forming	10±1.8 (8–12)	9.7±0.06 (9–10)
Central tooth width	27±3.5 (24–32)	26±2 (24–28)
	Small Class	
Radular length	0.67±0.05 (0.64–0.72)	0.61±0.05 (0.60–0.62)
Radular width	0.09±0.01 (0.08–0.10)	0.08±0.01 (0.07–0.09)
Total rows of teeth	69±3.6 (66–73)	69.7±6.7 (64–77)
Rows of teeth forming	7.5±0.6 (7–8)	8.7±0.6 (8–9)
Central tooth width	18±1.6 (16–20)	17.3±1.2 (16–18)

the end of the mantle cavity (Emc) and the point where the sperm duct (Sdu) arises from the spermathecal duct. (7) The spermathecal duct runs directly posterior from the mantle cavity to become the duct of the bursa (Dbu) directly posterior to which the thin-walled bursa copulatrix (Bu) swells as a large oval sac. (8) The sperm duct (Sdu) is a long convoluted duct transporting sperm from the spermathecal duct to the oviduct close to where the latter (Opo) enters the albumen gland (Ppo). (9) The usual seminal receptacle has been lost. When dissecting living specimens one often observes a bright pink sheen or glittering within a section of the oviduct (Ov) just posterior to the juncture of the sperm duct (Sdu) and oviduct (Osr, Fig. 47). This section of oviduct assumes the function of the seminal receptacle and is called the oviducal seminal receptacle (Osr). The duct may be considerably swollen with sperm (Fig. 47D, E). (10) Posterior to the sperm storage area (Osr) the oviduct is convoluted (Fig. 47B). (11) The bursa is posterior to the posterior pallial oviduct (Bu, Fig. 46). (12) The bursa is short.

Male reproductive system. The body of an uncoiled male is shown in Figure 48 without head but with kidney tissue (Ki) left in place. Measurements of relevant organs are given in Tables 19, 20. Important features are: (1) The gonad consists of relatively large lobes draining into a vas efferens (Ve, Fig. 49). (2) The seminal vesicle arises from the vas efferens (Ve) approximately one third of the way posterior from the anterior end of the gonad (Fig. 49). The juncture of the vas efferens and the beginning seminal vesicle may be swollen (Fig. 48). The coils of the seminal vesicle may be ventral to or dorsal to the lobes of the gonad. (3) The gonad is posterior to the stomach. (4) The prostate (Pr) overlaps the posterior end of the mantle cavity (Emc). (5) The penis has a glandular lobe (Fig. 42 Glo) on the concave edge near the base. (6) The penis has a stylet (Sty, Fig. 42).

The stylet requires some comment. It is very much like the stylet observed in *Robertsiella* (Davis & Greer, 1980). It is corneous and very fragile. In the living-moving male, it is very obvious at 50X, projecting from the tip of the penis (Fig. 42). However, in relaxed and fixed specimens it is not in evidence. Rarely at 50X one observed a pin-prick of light reflecting from the tip of the stylet mostly retracted into the penis. To observe the stylet in preserved specimens, the penis is cut from

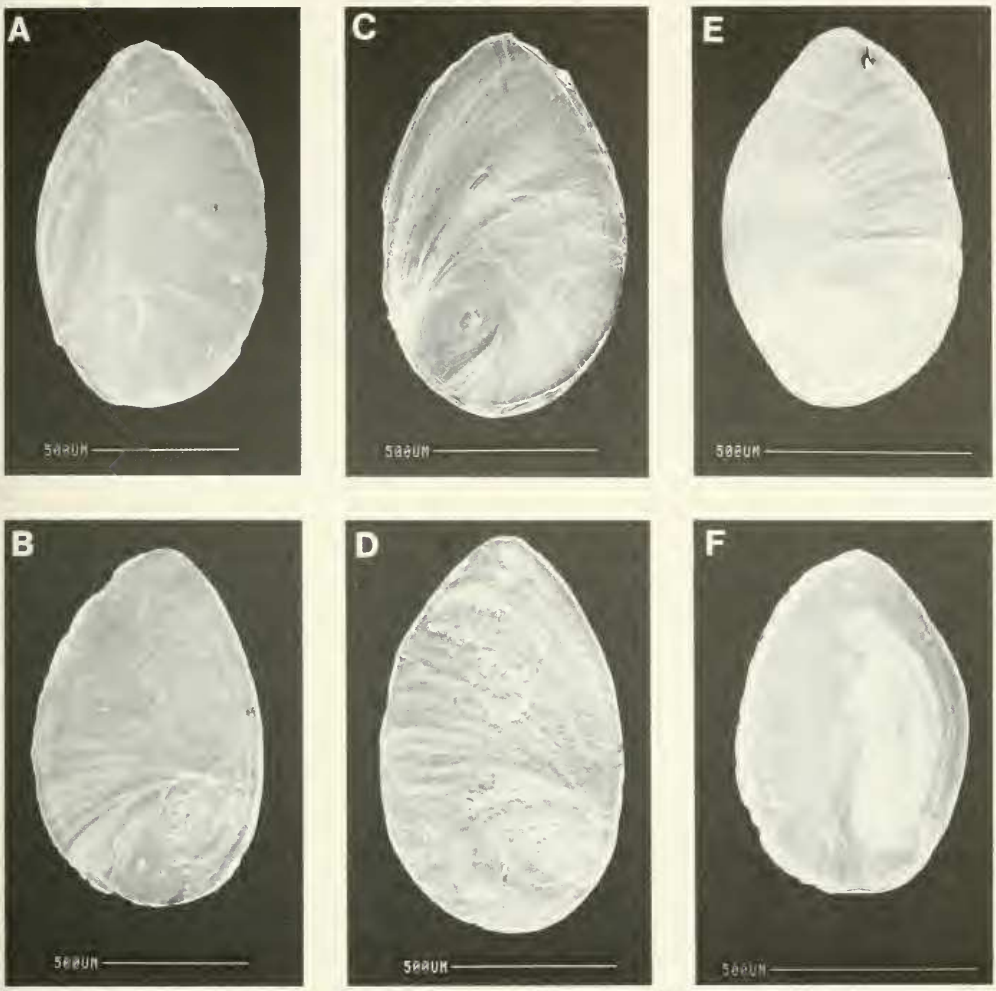

FIG. 44. Opercula of *Guoia viridulus* (C–F) and *G. fuchsianus* (A, B). C, D from large-class snails; E, F from small-class snails. A, C, E. Outer surfaces; B, D, F. Inner surfaces.

the animal, mounted in water on a slide with cover slip, and examined at 400 X (Fig. 50). The stylet is quickly dissolved when the penis is placed in Clorox (0.5% Na hypochlorite). Thus the stylets of *Robertsiella* and *Guoia* are not robust as those found in *Stenothyra* (Davis et al. 1986, 1988).

(7) The ejaculatory duct is massive and highly muscularized (Ej, Figs. 42, 51). It extends out of the base of the penis and from the posterior penis along the entire length of the dorsal neck. The circular ejaculatory duct is slightly left (Fig. 52), central, or to the right of the snout-neck mid-line (Fig. 51).

Digestive system. The digestive gland covers the posterior chamber of the stomach. The paired salivary glands are the standard triculine type. The radular sac does not coil up over the buccal mass.

The radulae of large-class snails are shown in Figures 53E–H and 54A–H. Teeth counts and statistics are given in Tables 21, 22. The most frequently encountered formula is:

$$\frac{3\text{-}1\text{-}3;}{3\text{-}3}\ 3(4)\text{-}1[2]\text{-}3(4);\ 10\text{-}13;\ 8\text{-}10.$$

The inner pair of basal cusps of the central tooth are comparatively enormous. The cen-

TABLE 22. Cusp formulae for the radular teeth of *Guoia viridulus* with the percent of the radulae in which a given formula was found at least once.

Central Teeth		Lateral Teeth		Inner Marginal Teeth		Outer Marginal Teeth	
Large Class (N = 5 radulae)							
3-1-3 / 3-3	60%	3-1[2]-4	60%	8		8	40%
3-1-3 / 4-3	20%	4-1[2]-3	60%	9	20%	9	60%
3-1-4 / 4-4	20%	3-1[2]-3	40%	10	60%	10	40%
4-1-3 / 3-3	20%	3-1[2]-5	20%	11	80%	11	20%
4-1-4 / 3-3	20%	4-1[2]-4	10%	12	60%	12	0
5-1-5 / 3-3	20%			13	40%	13	20%
5-1-4 / 3-3	20%			14	20%	14	20%
5-1-5 / 3-3	20%			$\bar{X}$ = * 1.5±1.6 N = 50		10.4±2.3	
Small Class (N = 5 radulae)							
4-1-4 / 3-3	40%	4-2-3	100%	11	20%	11	0
		3-2-4	80%	12	60%	12	40%
4-1-3 / 4-3	40%	4-2-4	60%	13	80%	13	80%
4-1-5 / 3-3	40%	5-2-3	60%	14	100%	14	100%
3-1-5 / 4-4	40%	5-2-4	60%	15	80%	15	60%
3-1-3 / 4-3	20%	3-2-3	40%	16	60%	16	0
		4-2-4	40%				
3-1-4 / 4-4	20%	4-2-5	20%	$\bar{X}$ = *7.40±0.9 N = 30		6.3±0.6 N = 30	
3-1-3 / 4-4	20%						
4-1-4 / 4-4	20%						
4-1-3 / 3-4	20%						
4-1-4 / 4-3	20%						

*Mean ± standard deviation of cusp number for all teeth counted.

tral cusp at the anterior edge of the central tooth is frequently grooved or split.

The radulae of small-class snails are shown in Figures 54E–H and 55. Teeth counts and statistics are given in Tables 21, 22. The most frequently encountered formula is:

3(4)-1-(4)3; 3(4)-1[2]-3(4); 12-16; 12-15.
3-3

Comparing both size classes, as one would expect, the small-class has a smaller radula except for total rows of teeth, which are not significantly different between classes. The

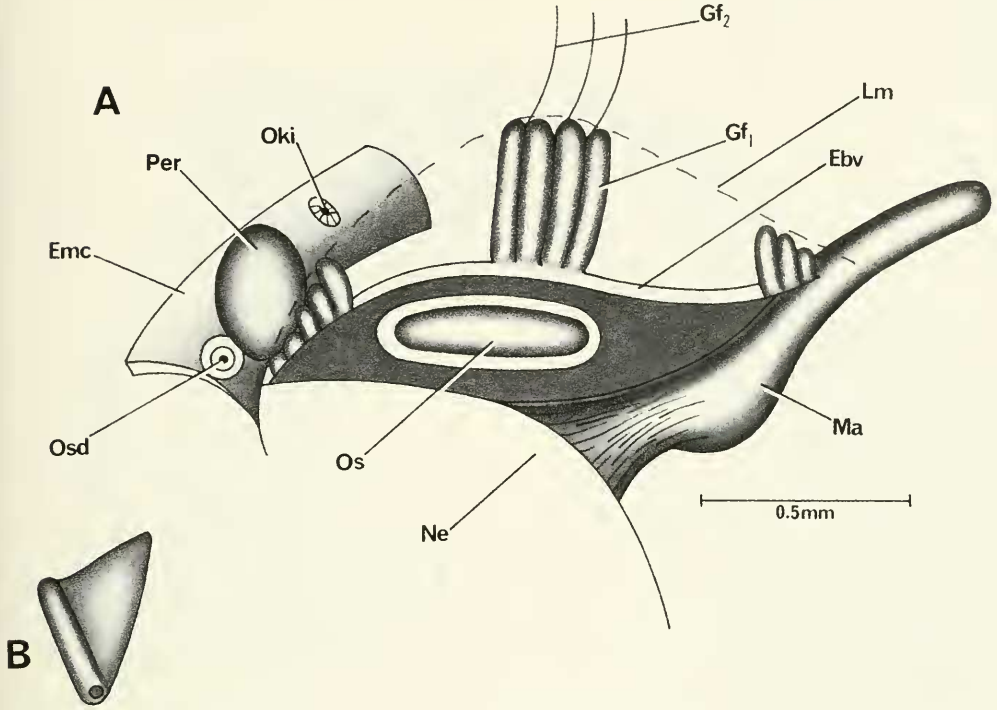

FIG. 45. Cut and reflected mantle to show mantle cavity organs of *Guoia viridulus* (A). Not all gill filaments are shown. B. Single gill filament.

morphologies of the teeth of both size classes are the same.

Nervous system. Measurements are given in Table 23. The RPG ratio is 0.229 ± 0.11, that is, the pleuro-supraesophageal connective is concentrated. The pleuro-subesophageal connective is lost in the fusion of ganglia. The osphradio-mantle nerve is elongated (>0.12 mm) thus compensating for the low RPG ratio.

Remarks

In comparing small- and large-class snails, no qualitative anatomical differences were found. The sizes of the bodies and organs were not significantly different. However, the small class animals were relaxed with sodium nembutol prior to fixing in 8% formalin and grading up to 70% ethyl alcohol. Presumably, the extended fixed bodies would measure longer than animals removed living from the shells and pinned out in a contracted state. Because the animals of the two size classes do not differ in details of anatomy, and because they live in microsympatry, they are considered the same species.

While the shells are significantly different in size, the range of variance along the second principal component is the same for both size classes indicating that the substantive difference is only one of size. What could account for this? Has this phenomenon been seen before? A similar situation was reported for *Tricula xianfengensis* Davis & Guo, 1986, in which large and small class mature snails with the same anatomy and shell shape were found in a narrow ditch alongside a kitchen garden in Xiaguan City, Yunnan Province. In both of these cases, we suspect that the size classes resulted from two different cohorts when egg laying occurred at different seasons. It is possible that eggs laid late in the season with growth extending into the cold weather months resulted in a small size class due to stunting caused by decreased rate of growth in the fall and winter. Presumably egg laying and growth in the late spring and summer would result in optimal growth. A comparative molecular genetic analysis of these size classes would be most instructive and desirable.

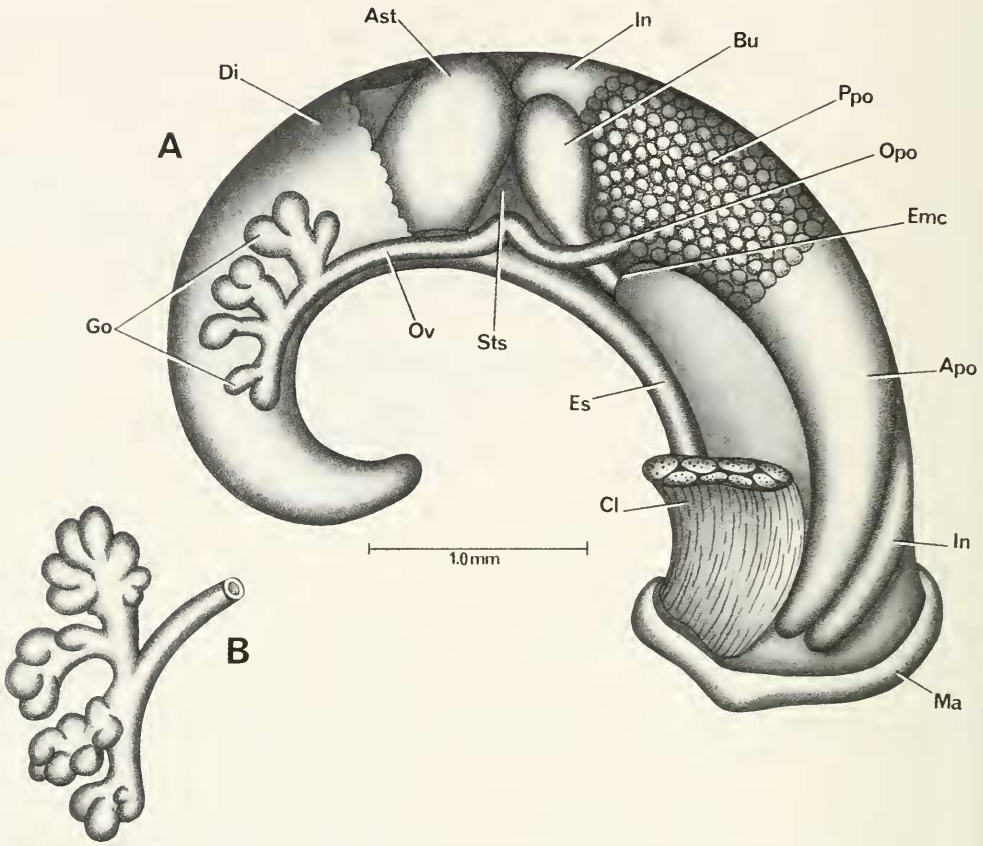

FIG. 46. Uncoiled female of *Guoia viridulus* with head and kidney tissue removed (A). B. Variation in gonad morphology.

TABLE 23. Lengths of neural structures from four individuals of large class *Guoia viridulus*. Mean ± standard deviation (range).

Cerebral ganglion	0.31±0.03	(0.26–0.32)
Cerebral commissure	0.07±0.02	(0.06–0.10)
Pleural ganglion		
Right (1)	0.15±0.04	(0.10–0.12)
Left	0.11±0.01	(0.10–0.12)
Pleuro-supraesophageal connective (2)	0.08±0.04	(0.04–0.14)
Pleuro-subesophageal connective	0	0
Supraesophageal ganglion (3)	0.12±0.02	(0.10–0.14)
Subesophageal ganglion	0.12±0.02	(0.10–0.14)
Osphradio-mantle nerve	0.15±0.03	(0.12–0.18)

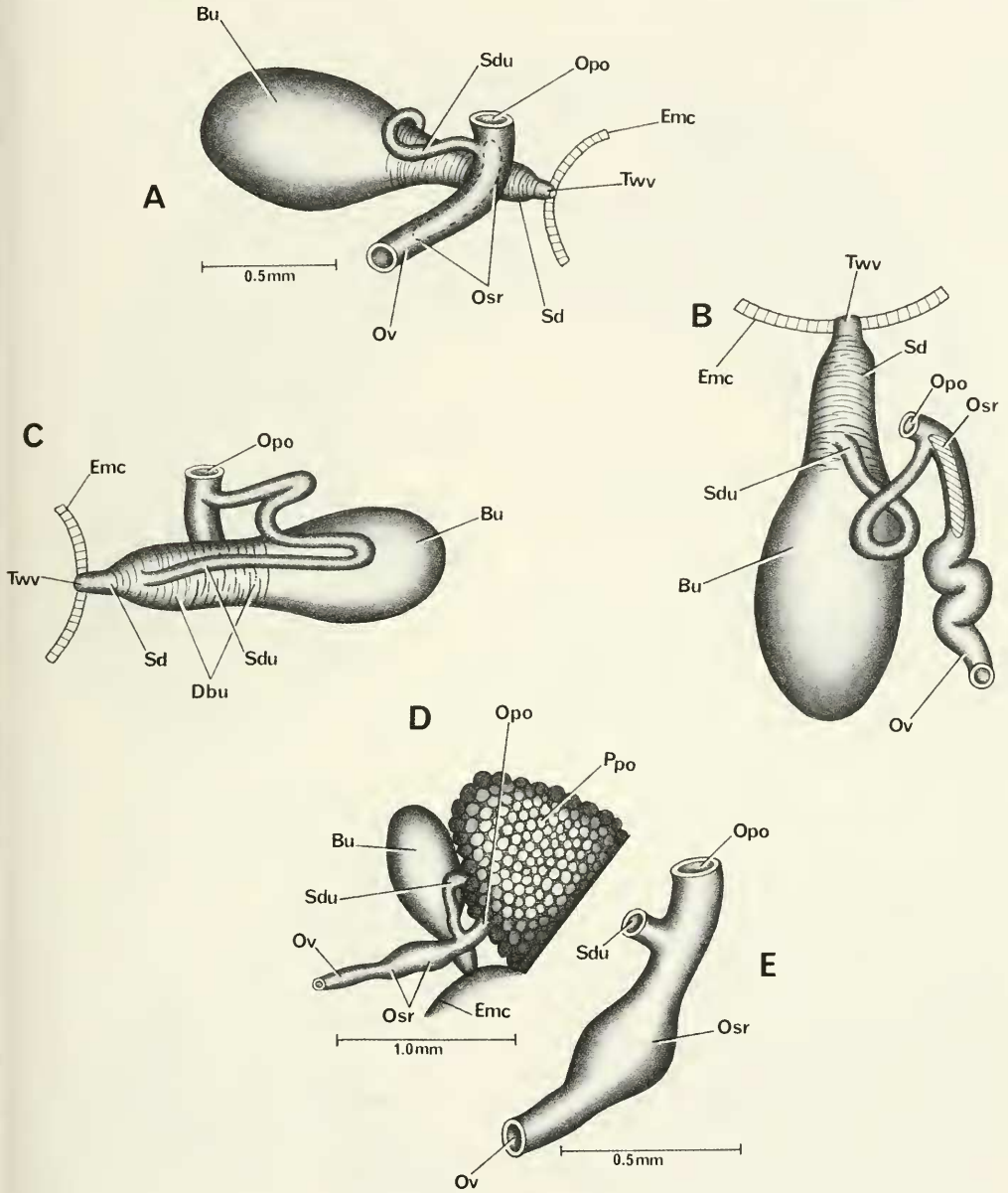

FIG. 47. Bursa copulatrix complex of organs of *Guoia viridulus*. Organs in A are in same orientation as in Figure 46. Figures B, C shows bursa flipped over to show dorsal aspect to reveal origin of elongated and twisting sperm duct (Sdu). Figure D most closely approximates organ position in Figure 46 but with tissue cleared away to show relationships of ducts relative to end of mantle cavity (Emc) and albumen gland (Ppo). E. Blown up section of oviduct within which sperm are stored (Osr).

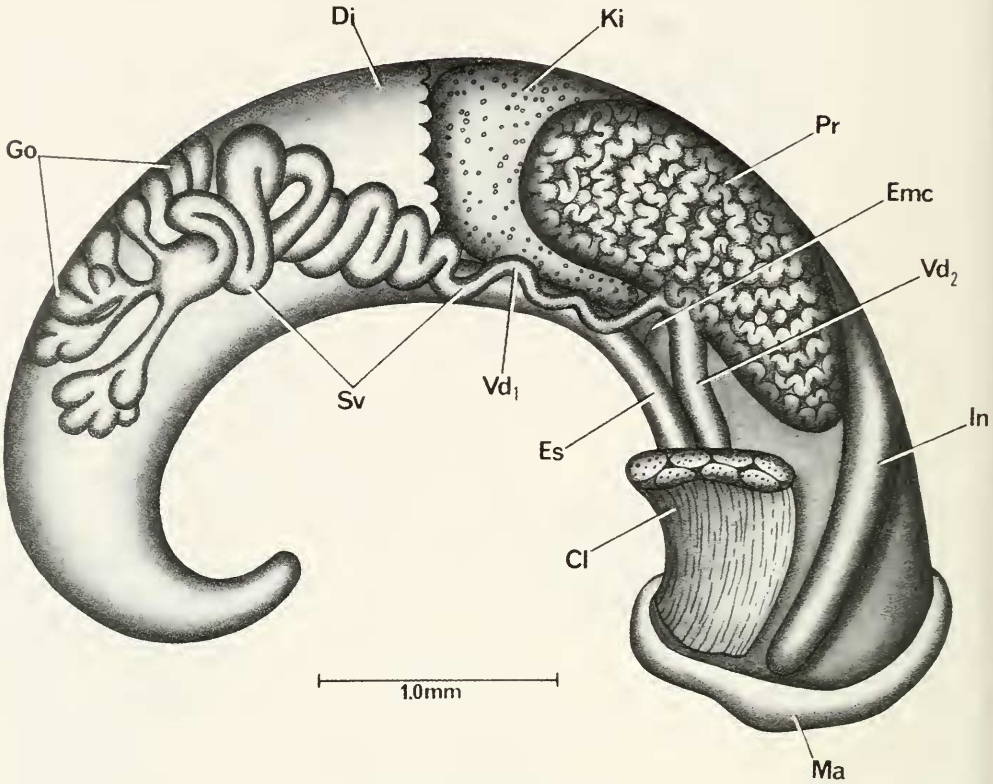

FIG. 48. Uncoiled male of *Guoia viridulus* with head removed.

Guoia fuchsianus (Moellendorff, 1885)

Lithoglyphus fuchsianus Moellendorff, 1885: 169, 170
Lithoglyphus, fuchsianus, Moellendorff, 1888: 140. pl. 4, fig. 5, 5a–b.
Lithoglyphus fuchsianus, Thiele, 1928
Lithoglyphopsis fuchsianus, Yen, 1939

Type locality. Moellendorff, 1885: Hsiang-tan provinciae sinensis Hunan.
Moellendorff, 1888: Hsiangtan and Hêngshan-hsien; Hunan.
Yen, 1929: Heng-dshou-fu, Hunan

Types. Lectoype: SI, 4127. Figured by Yen (1939: pl. 4, fig. 10); paralectotypes: SMF, 4128. Figured here, Figure 36E, F.

Habitat

Xiangjiang River at Baisha, Hengshan County, 25°58′22″N, 112°45′55″E. Figure 1,

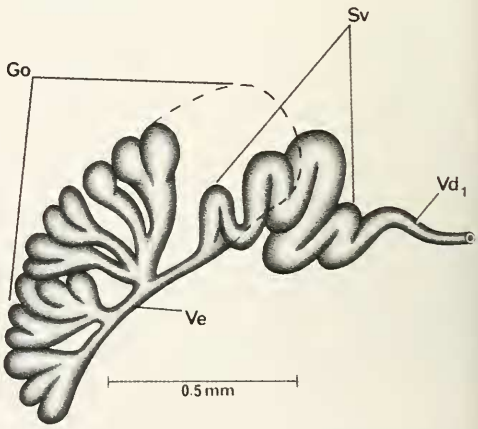

FIG. 49. Male gonad with anterior lobes cut away to show origin of vas deferens from vas efferens (Ve), and seminal vesicle (Sv) that lies dorsal to gonad. Dashed line indicates extent of gonad cut away.

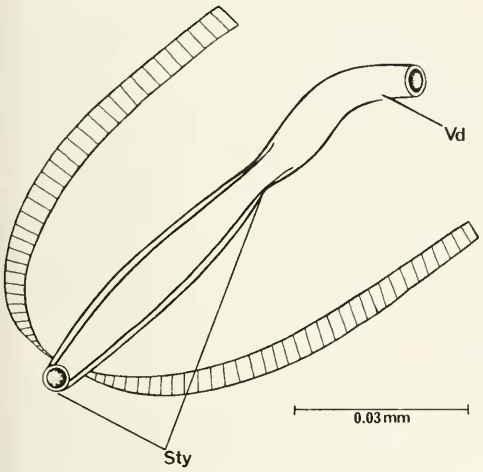

FIG. 50. Tip of penis of preserved *Guoia viridulus* as observed under compound microscope at 400X. Sty, Stylet; Vd, Vas deferens.

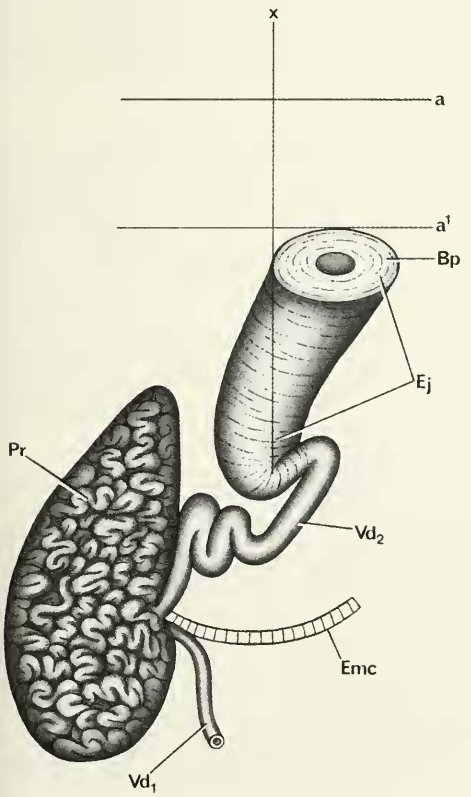

FIG. 51. Relationship of ejaculatory duct to mid-line (x) of snout-neck of *Guoia viridulus* (from small-class specimen).

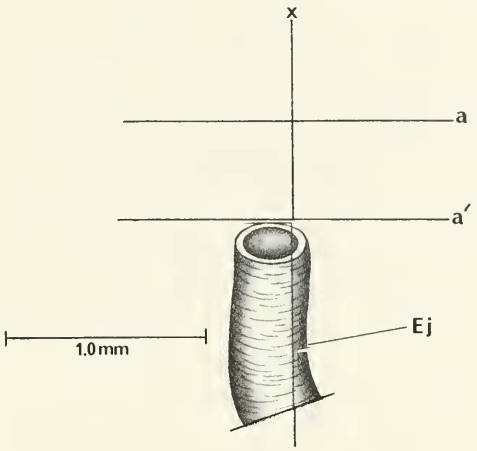

FIG. 52. Ejaculatory duct of *Guoia viridulus* slightly to left of snout-neck mid-line.

locality 9. Collected by Davis, Chen, & Wu, October 1985, field number D85-75; by Chen & Wu, 1986. Snails sympatric with *Lithoglyphopsis modesta* on stones at the bottom of the river in 2.0–2.5 m depth. Catalog numbers are: D86-B, ANSP 373145; A12661. D85-75, ANSP 373146; A12662.

Description

Shell. Shells (Figs. 36D–F, 39G–I, 56C–F, 57, 58) are small (Table 24), and generally as described for large class *L. viridulus* with the following differences. The outer lip of *G. fuchsianus* is only slightly sinuate. There is a more pronounced umbilical depression. The inner lip is separated slightly from the body whorl by a narrow depressed groove, the basal crescent (Fig. 57, Bc) paved with shell growth increments from body whorl to the inner lip (Figs. 57, 58). The penultimate whorl of the species is proportionally shorter than that of *G. viridulus* and the third whorl less wide.

Overall, however, the shells have such intrapopulation variance that the species are difficult to differentiate on the basis of shells alone. Some 10% of the shells from one population are virtually indistinguishable from shells of the other. An example of variance in shape for *G. fuchsianus* is shown in Figure 58A–D, in which camera lucida drawings of two shells from collection D86-B are illustrated with two shells from historic ANSP 98205. Because most of the historic *G. fuch-*

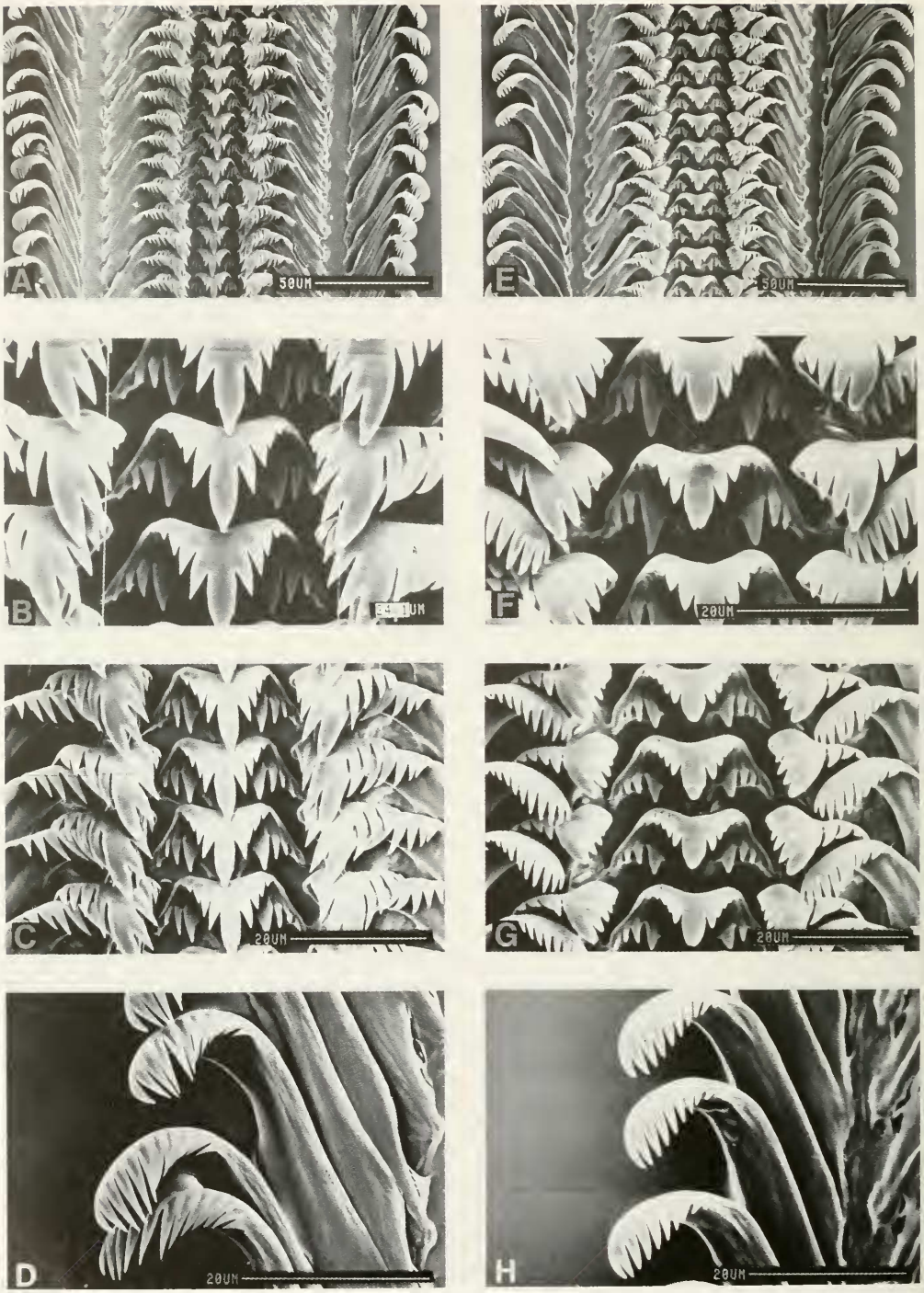

FIG. 53. Radulae of large size-class *Guoia viridulus* (E–H) and *G. fuchsianus* (A–D). A, E. = portions of radulae. B–C, F–G. Central, lateral and inner marginal teeth; D, H. Outer marginal teeth.

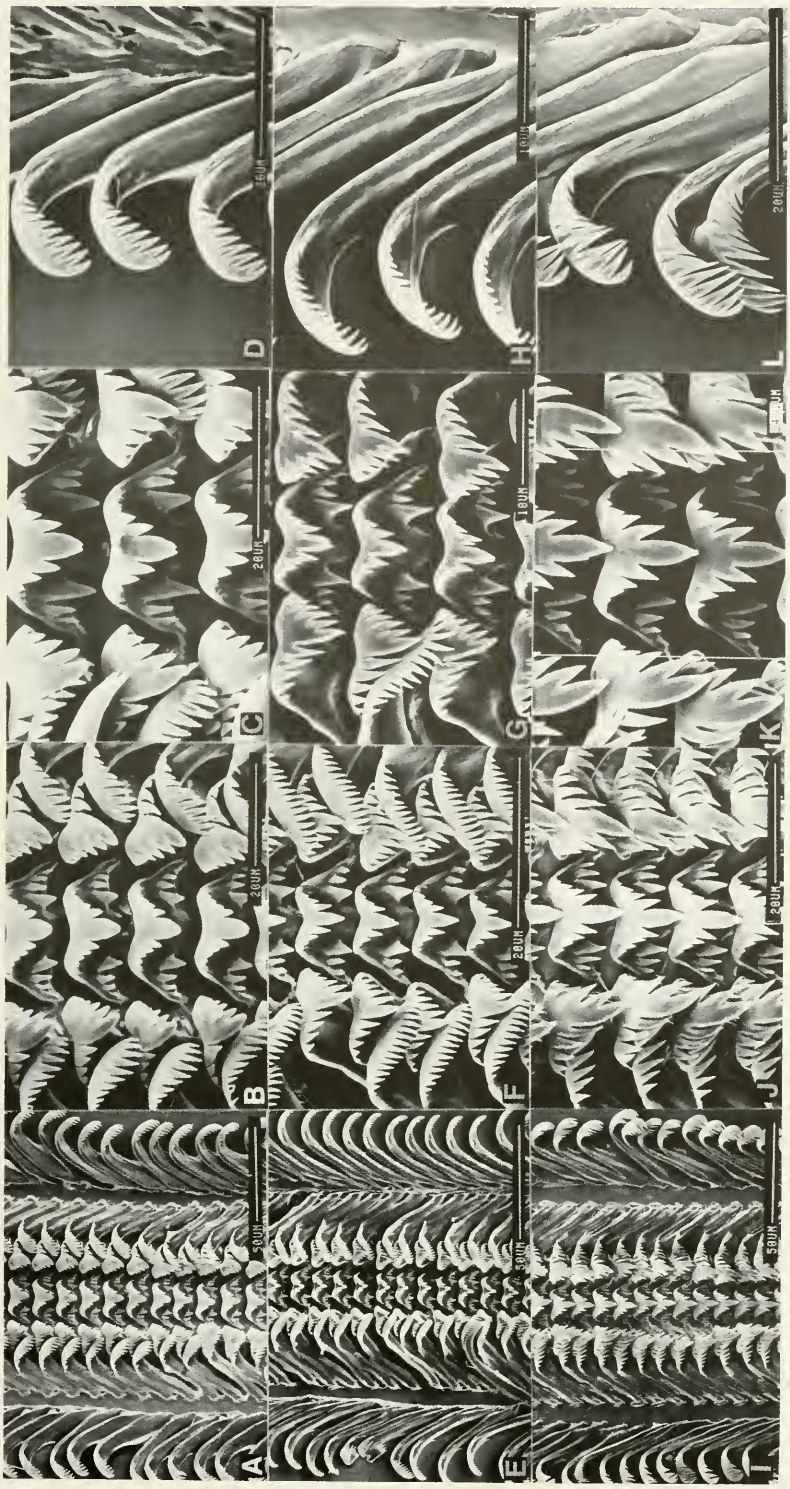

FIG. 54. Radulae of large size-class (A–E) and small size-class (E–H) *Guoia viridulus*; and *Guoia fuchsianus* (I–L). A, E, I. Segments of radulae; B, C, F, G, J, K. Central, lateral and inner marginal teeth; D, H, L. Outer marginal teeth.

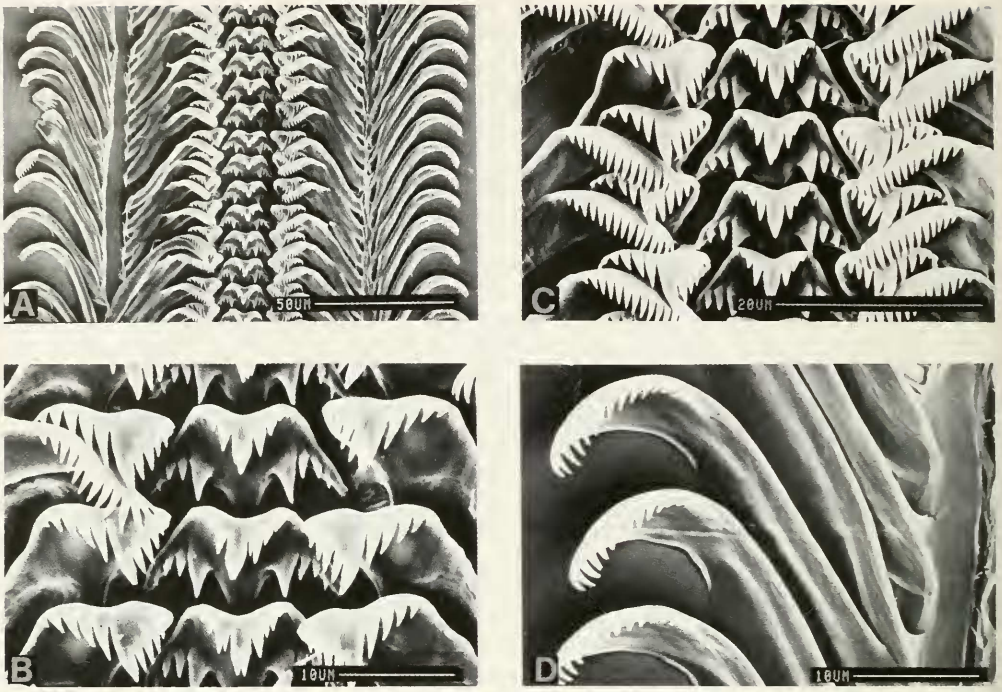

FIG. 55. Radula of small size-class *Guoia viridulus*. A. Segment of radula; B, C. Central, lateral and inner marginal teeth; D. Outer marginal teeth.

sianus had eroded shells so that characters 1, 7, and 8 could not be measured, the multivariate analyses involving all populations of *G. viridulus* and *G. fuchsianus* without these three characters did not provide differentiation of species or populations. Individuals were simply spread out along a size gradient. The historic *G. fuchsianus* specimens are larger than field-collected specimens. Still, basing size on the length of body whorl and width, this species is somewhat smaller than *G. viridulus* (compare Tables 24 and 16).

Anatomy. In 1985, most of the snails were sexually immature so that complete anatomical data could not be gathered. Organ measurements and counts that could be made are presented in Table 25. Sufficient observations were made to demonstrate that *Guoia fuchsianus* is a distinct species, not to be confused with *G. viridulus*. Only anatomical features unique to this species will be presented here.

(1) The duct of the bursa (Dbu, Fig. 59B) is a considerably swollen duct that narrows before opening into the capacious bursa (Bu). (2) The duct of the bursa is comparatively long: 0.35 mm for *G. fuchsianus*, 0.12 for *G. viridulus*. (3) The sperm storage area (Sr) is a swelling that bulges out of the sperm duct (Sdu) where the sperm duct opens into the oviduct (Ov, Fig. 59). (4) The buccal mass is longer (0.64–0.70 mm for *G. viridulus*, 0.70–0.72 for *G. fuchsianus*). (5) The central anterior cusp of the central tooth of the radula and flanking cusps are considerably more posteriorly projecting than those of *G. viridulus* (compare Fig. 54C, G, K). The anterior cusp support and cusps of *G. fuchsianus* form a prominent triangular-shaped projection posteriorly. This, coupled with the elongated central cusp, causes the tip of the central cusp to overlap the tooth immediately posterior. A ratio will demonstrate the difference between taxa. The length from anterior central edge to posterior tip of the central cusp divided by width of the anterior central cusp yields 0.75–0.88 for *G. fuchsianus* and 0.57–0.71 for *G. viridulus*. (See Tables 26, 27 for radular statistics.) (6) Measurements of neural structures are given in Table 28. The RPG ratio is 0.42, that is, the pleuro-supraesophageal

connective is moderately concentrated (contrast the concentrated condition in *G. viridulus*, RPG ratio = 0.23).

The penis of two individuals had a well-developed stylet but no glandular lobe or pronounced ejaculatory duct. The prostate was fully developed and penis length was 1.5–1.6 mm long. Because the penis of *G. viridulus* with a pronounced glandular lobe exceeded 3.0 mm in length, it is possible that the ones we observed for *G. fuchsianus* were immature, underdeveloped, or, conversely, atrophied. We are not convinced that the penis of *G. fuchsianus* lacks a glandular lobe or ejaculatory duct.

Remarks

Conchological characters that separate this species from *G. fuchsianus* are few and discussed above. Refer also to the multivariate analysis presented under *G. viridulus*.

Whereas it is clearly desirable to have more anatomical data, the available data substantiate the placement of this species in the genus *Guoia*. The six anatomical differences provided above convince us that we are dealing with a distinct species. The penial data are not of sufficient quality to permit us to make a definitive comment except that a stylet is definitely present.

Neotricula Davis, 1986

Type Species. Lithoglyphopsis aperta Temcharoen, 1971: 103–104, pl. 7, fig. 14.
Tricula aperta (Temcharoen), Davis 1979, 1980.

Type locality. Mekong River at Ban Na on Khong Island, Laos

Assigned Species. N. aperta (type for genus assigned in Davis et al., 1986a); *N. burchi* (Davis, 1968) [Thailand]; *N. cristella* (Gredler, 1887); *N. dianmenensis* Davis & Chen, sp. nov.; *N. duplicata* Davis & Chen, sp. nov.; *N. lilii* Chen & Davis, sp. nov.; *N. minutoides* (Gredler, 1885); N = 7.

Diagnosis. Shells small to medium sized, ovate conic, smooth. Central tooth of radula with several anterior cusps (contrast single triangular blade as in *Delavaya*). The oviduct runs from the gonad to the pallial oviduct without making a loop or twist. The spermathecal duct does not enter the pericardium but opens into the posterior mantle cavity; it is a narrow duct throughout. The duct of the bursa enters a U-shaped bend to run into a discrete sem-

TABLE 24. Shell measurements (mm) for populations of *Guoia fuschianus*. Mean ± standard deviation (range).

	Baisha		ANSP: 98205, 45961	
	Males (N = 2)	Females (N = 3)	Whole Shell (N = 1)	Eroded Shell (N = 8)
1. No. Whorls	4.0	4.0	4.0	—
2. Length (L)	2.26 (2.48, 2.76)	2.79±0.12 (2.72–2.79)	2.96	—
3. Width (W)	2.20 (2.08, 2.32)	2.36±0.07 (2.32–2.44)	2.32	2.44±0.12 (2.28–2.60)
4. L body whorl	2.26 (2.16, 2.36)	2.45±0.02 (2.44–2.48)	2.60	2.70±0.12 (2.56–2.88)
5. L penultimate whorl	0.24 (0.20, 0.28)	0.23±0.05 (0.20–0.28)	0.24	0.30±0.04 (0.24–0.36)
6. W penultimate whorl	0.90 (0.80, 1.00)	0.92±0.07 (0.88–1.00)	0.86	1.01±0.08 (0.92–1.12)
7. W 3rd whorl	0.46 (0.40, 0.52)	0.47±0.02 (0.44–0.48)	0.40	—
8. L last three whorls	2.60 (2.48, 2.72)	2.77±0.09 (2.72–2.88)	2.92	—
9. L aperture	1.68 (1.56, 1.80)	1.85±0.08 (1.76–1.92)	2.00	1.93±0.08 (1.80–2.04)
10. W aperture	1.38 (1.28, 1.48)	1.45±0.02 (1.44–1.48)	1.52	1.54±0.08 (1.40–1.60)
11. W columellar shelf	0.18 (0.16, 0.20)	0.25±0.02 (0.24–0.28)	0.28	0.28±0.04 (0.20–0.32)
W ÷ L	0.84 No var.	0.85±0.01 (0.84–0.85)	0.78	—

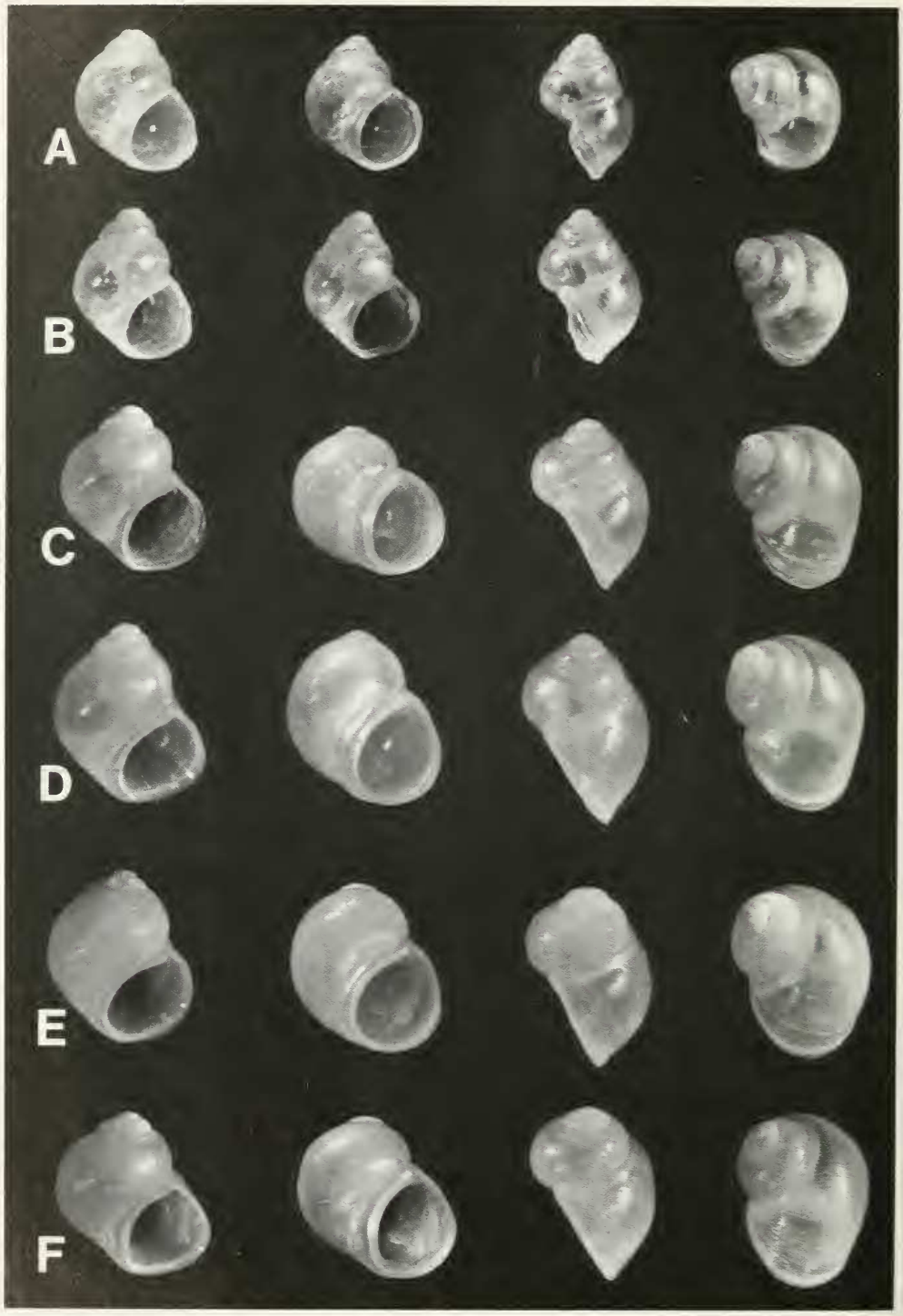

FIG. 56. Shells of small-class *Guoia viridulus* (A, B) for comparison with shells of *G. fuchsianus* (C–F). Shell A is 2.36 mm long; others printed at same scale. All are from females except E, which is from a male.

TABLE 25. Lengths (mm) or counts of non-neural organs of female *Guoia fuschianus*.

	1.	2.	3.	$\bar{X}$.
Body	4.9			
Digestive gland	2.1			
Bursa copulatrix	0.68	0.54		0.61
Duct of bursa	0.34	0.36		0.35
Buccal mass	0.70	0.72		0.71
Mantle cavity	2.0	1.70	2.20	1.97±0.25
Gill	1.8	1.50	2.00	1.77±0.25
Osphradium	0.9	0.7	0.84	0.81±0.10
Osphradium ÷ gill	0.50	0.47		0.48
No. gill filaments	25	22	25	24.0±1.7
Gf_2	0.16	0.22		0.19
Gf_1	0.48	0.46		0.47
Total Gf	0.64	0.68		0.66

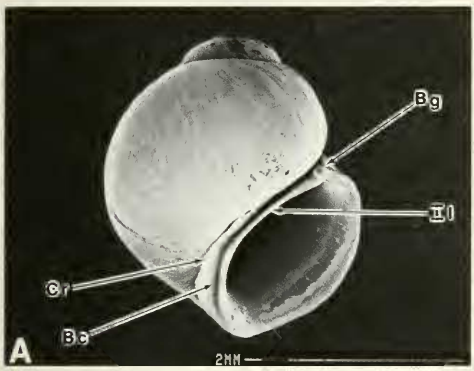

FIG. 57. SEM photograph of a shell of *Guoia fuchsianus*.

inal receptacle in most species. The duct of the seminal receptacle may shorten or become lost. The spermathecal duct joins the duct of the bursa (contrast joining the bursa as in *Halewisia*). A slender duct, the sperm duct, connects the U-shaped duct to the oviduct.

Neotricula cristella (Gredler, 1887)

Paralectotypes. SMF 4242; plate 4, fig. 3, in Yen, 1939

Type locality. Kiangshi Province, "in Quellwasser."

Synonymy. Hydrobia cristella Gredler, 1887
Tricula cristella, Yen, 1939
Neotricula cristella, this paper

Habitat

Material for this paper was collected from Mojingtai, Hengshan Mountain, Nanyue Town, Hengshan County, Hengyang Prefecture; 27°15′N, 112°39′13″E; Figure 1 site 1. Snails came from a small stream 0.4 km down the mountain road from the Mojingtai Hotel towards the Banshan Ting Temple. Collections number = D85-73; the collection was made by Dr. Chen Cui—E, 28 Sept. 1985.

Depository

Specimens are deposited in ZAMIP, M0001; in ANSP 368774 and A12146.

Description

Shell. Shells are small, narrowly ovate-conic, of 5.0 to 5.5 whorls (Figs. 60H–L, 61A–D). Lengths range from 2.40 to 2.84 mm (Table 29). The aperture is ovate; there is no umbilicus. The whorls at the suture are smooth (not crenulated). SEM analyses reveals a faint trace of spiral microsculpture on the adapical surface of the whorls at the suture. The inner lip is arched and widely separated from the body whorl, the distance increasing from abapical to adapical. Thus, the adaptical end of the aperture is widely separated from the body whorl. The adapical end of the aperture has a wide notch; there is no internal notch groove; there is no sinus. There is no abapical spout. In side view, the outer lip is slightly sinuate; it is not scooped forward. The inner lip lacks nodes, teeth or notches. The inner lip is thin throughout. In side view, the inner lip is straight on some shells, angled to form a deflection angle in others. Within the

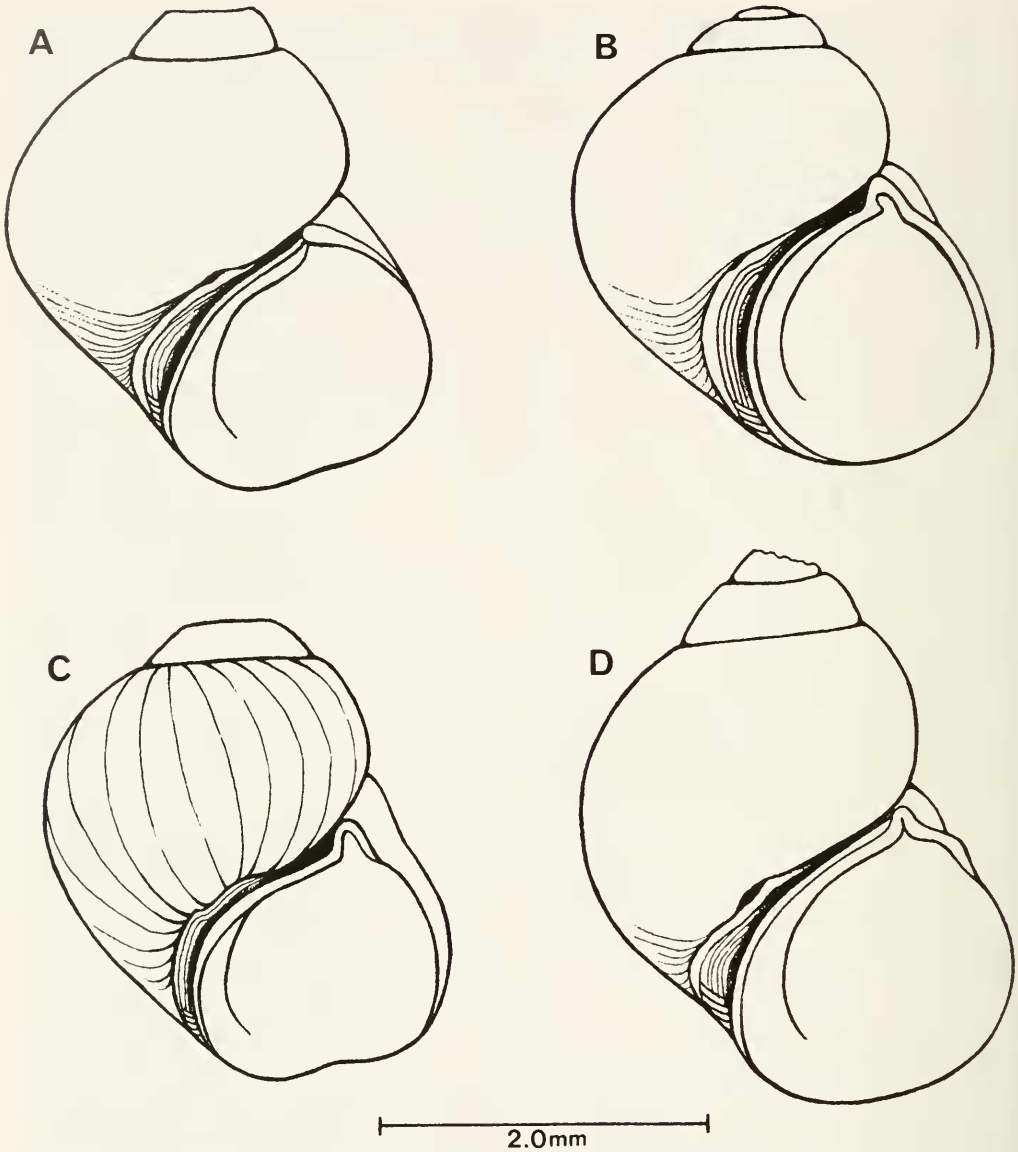

FIG. 58. Illustration of four shells of *Guoia fuchsianus* aided by camera lucida. Shells A, D from ANSP 98205 (historic collections); shells B, C from D86-B.

body whorl, the columella is smooth. There is a slight varix on some shells, no varix on others. In apertural view, the lip projects beyond the base of the shell 0.34 ± 0.06 mm. SEM analysis shows the protoconch to be slightly wrinkled (Fig. 61C, D).

External features. The head is not pigmented. There are no granules about the eyes (Fig. 62). There is a patch of white granules where the mantle margin meets the neck. The operculum is corneous, paucispiral and appears to have two layers, a larger outer layer and a

TABLE 26. Radular measurements (mm) and counts for *Guoia fuchsianus*. Mean ± standard deviation (range). In mm except for width of central tooth in μm.

	Female (N = 5)	Male (N = 2)
Radular length	0.90±0.05 (0.84–0.98)	0.80 (no variation)
Radular width	0.11±0.003 (0.11–0.12)	0.11 (0.10–0.11)
Total rows of teeth	72.6±4.3 (66–78)	68.5 (68–69)
No. rows of teeth forming	23.8±1.1 (23–25)	22.5 (22–23)
Central tooth width	23.2±2.3 (22–26)	22 (no variation)

TABLE 27. Cusp formulae for the radular teeth of *Guoia fuschianus* with the percent of radulae in which a given formula was found at least once. N = 3 radulae.

Central Teeth		Lateral Teeth		Inner Marginal Teeth		Outer Marginal Teeth	
4-1-4 / 2-2	66%	3-1[2]-4	100%	10	33%	10	33%
3-1-3 / 3-3	33%	4-1[2]-3	66%	11	66%	11	66%
		3-1[2]-3	66%	12	100%	12	100%
		4-1[2]-4	33%			13	33%
		2-1[2]-4	33%	$\bar{X}$ = * 11.4±0.7 N = 26		11.3±0.8 N = 30	

*Mean ± standard deviation of cusp number for all teeth counted.

TABLE 28. Lengths (mm) of neural structures of *Guoia fuchsianus*. Mean (data). N = 2

Cerebral ganglion	0.29 (0.28, 0.30)
Cerebral commissure	0.12 (no variation)
Pleural ganglia	
Right (1)	0.11 (0.10, 0.12)
Left	0.10 (no variation)
Supraesophageal connective (2)	0.16 (0.12, 0.20)
Subesophageal connective	0
Supraesophageal ganglion (3)	0.11 (0.10, 0.12)
Subesophageal ganglion	0.10 (no variation)
Osphradio-mantle nerve	0.12 (0.10, 0.14)
RPG ratio (2 ÷ 1+2+3)	0.42 (0.38, 0.46)

narrower inner layer (Fig. 61E, F). The internal attachment pad is prominent but only 40 to 50% the width of the operculum.

Mantle cavity. Mantle cavity organs are shown in Figure 63A. Organ measurements and counts are given in Table 30. The osphradium is slightly anterior to mid-gill; it is oval and small. There are 13 to 15 gill filaments, of which only seven or eight are fully developed, that is, with both Gf_1, and Gf_2 elements prominent. The anterior five filaments are widely separated and without the Gf_2 part. Gf_2 is long. The longest gill filaments are 0.38 ± 0.09 mm long. The largest gill filaments in lateral view are modestly domed (Fig. 63B). The pericardium (Pe), opening of the kidney into the mantle cavity (Oki) and the opening of the spermathecal duct (Sd) into the mantle cavity are shown in relationship to each other (Fig. 63A).

Female reproductive system. An uncoiled female without head and with kidney tissue removed is shown in Figure 64. Measurements of organs are given in Table 30. Important features are: (1) The gonad (Go) is posterior to the stomach, is small and consists of few lobes. (2) The bursa copulatrix (Bu) is round and situated directly posterior to the albumen gland (Ppo). (3) The albumen gland is of normal size. (4) The bursa copulatrix complex of organs is shown in Figure 65. Organs in Figure 65A have the same orientation as in Figure 64. The bursa is short. (5) The duct of the seminal receptacle (Dsr) is a U-shaped con-

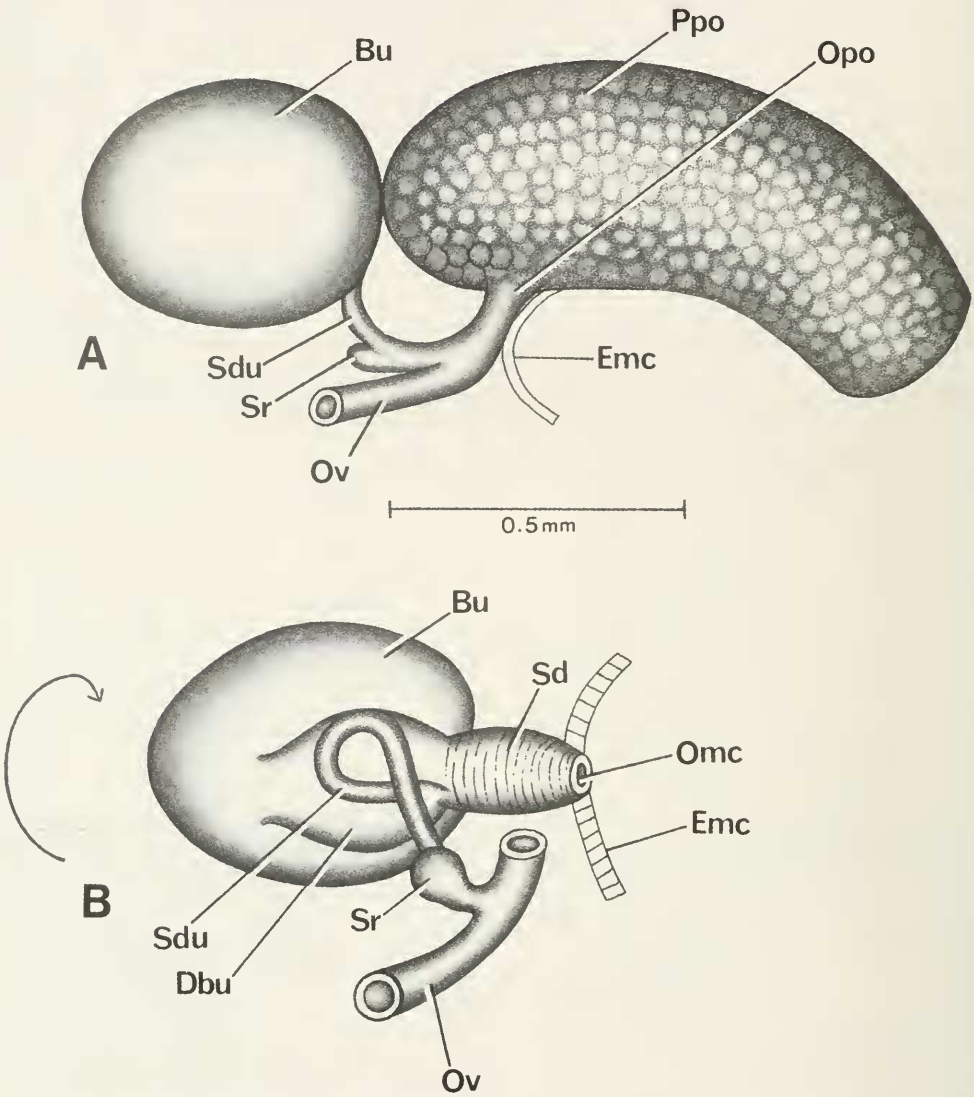

FIG. 59. Aspects of female reproductive system of *Guoia fuchsianus*. A. Female reproductive system oriented in same position as in Figure 46A. Anterior pallial oviduct not shown. B. Bursa of A turned 180° over, as indicated by the arrow, to show the relationships of ducts attaching to the bursa (Bu) and oviduct (Ov).

tinuation of the duct of the bursa (Fig. 65B, C). It turns to the right side and tucks dorsal to the bursa. (6) The duct of the seminal receptacle (Dsr) is long. The seminal receptacle (Sr) is a comparatively minute bulb. (7) The spermathecal duct (Sd) is short and opens into the posterior end of the mantle cavity (Emc). (8) The spermathecal duct opens into the bottom of the U-shaped bend formed by the duct of the bursa at a point opposite the opening of the duct of the seminal receptacle (Fig. 65A, B).

Male reproductive system. An uncoiled male snail without head and with kidney tissue removed is shown in Figure 66. Measurements of organs are given in Table 30. Important

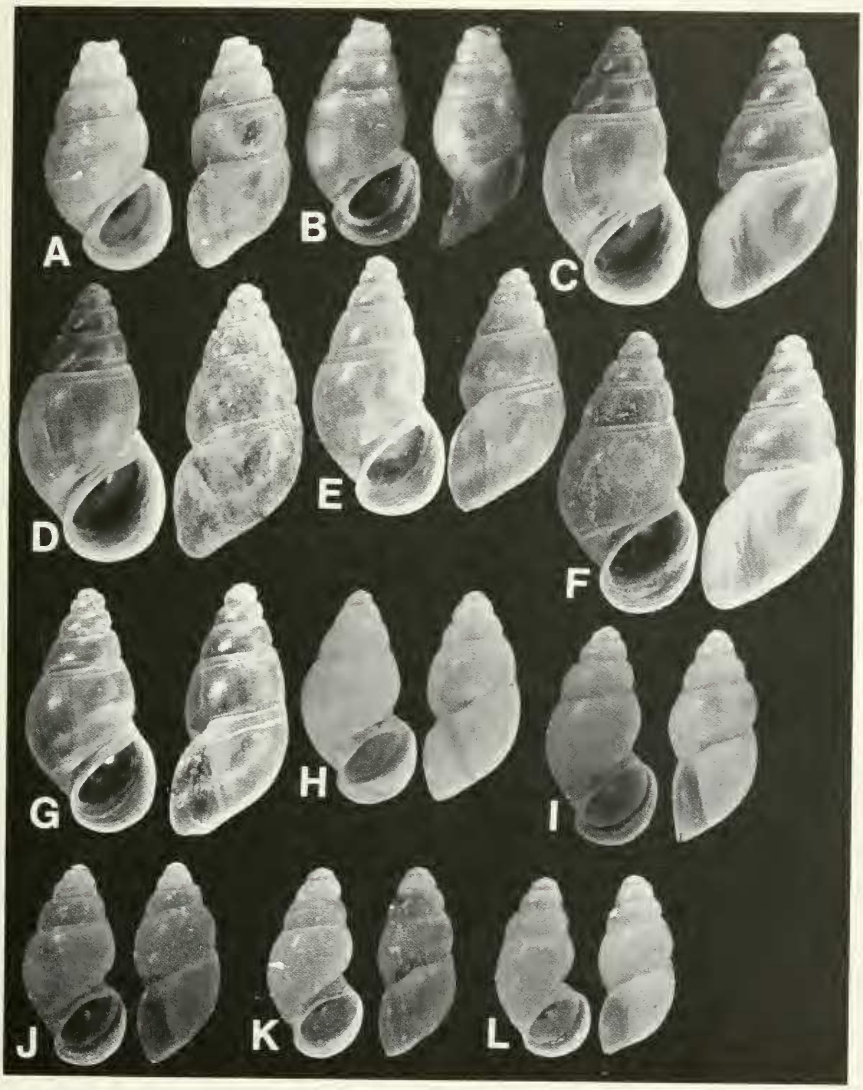

FIG. 60. Shells: *Neotricula lilii*, A, B. Paratypes. *N. minutoides*, C–G. *N. cristella*, H–L. Length of shell A is 3.12 mm; others printed to same scale.

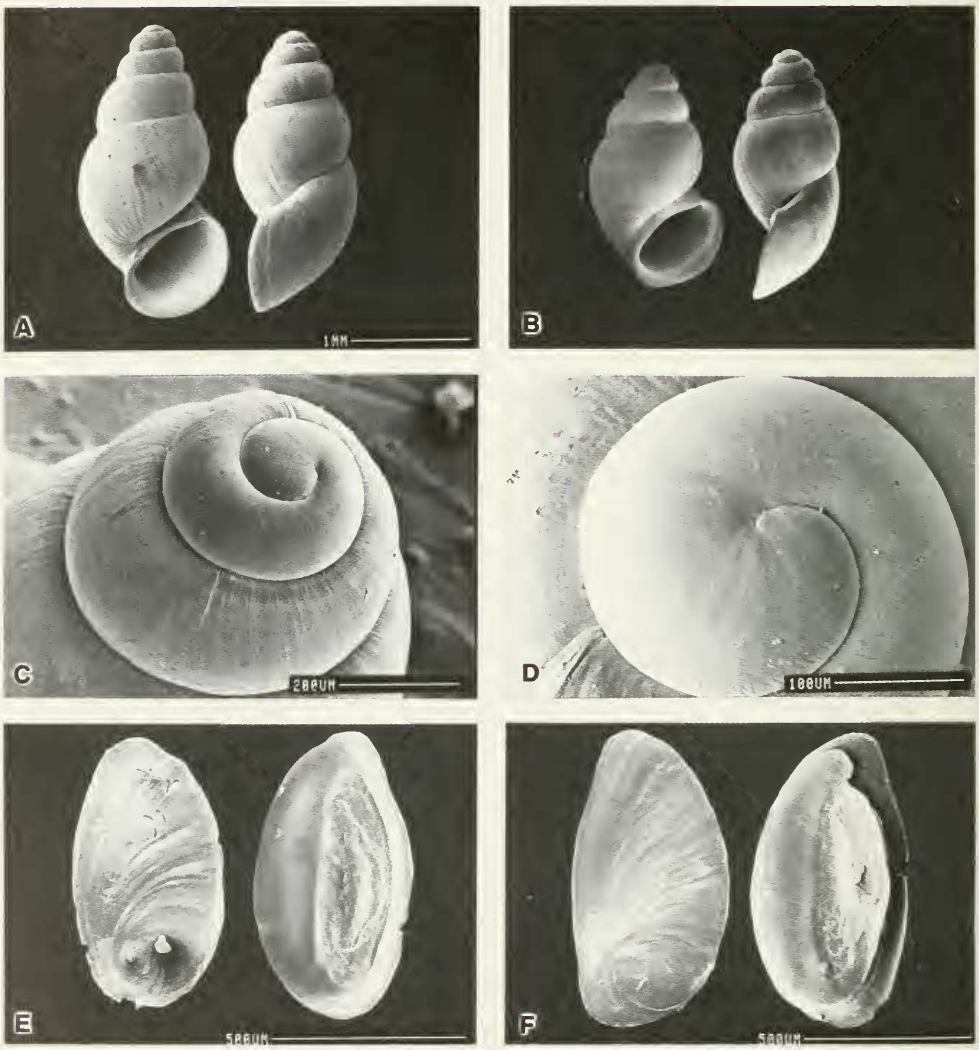

FIG. 61. SEM photographs of shells (A–D) and *opercula* (E, F) of *Neotricula cristella*. C, D. Details of apical whorls. In E, F, inside surface of opercula shown on right side.

TABLE 29. Shell measurements (mm) for male and female *Neotricula cristella*. Mean ± standard deviation (range). N = number measured.

	Females	Males	
Whorls	5.0–5.25 (N = 4)	5.5 (N = 2)	5.0 (N = 3)
Length (L)	2.64±0.10 (2.52–2.76)	2.78 (2.72–2.84)	2.37±0.02 (2.36–2.40)
Width (W)	1.33±0.09 (1.24–1.44)	1.38 (1.36–1.40)	1.21±0.08 (1.12–1.28)
L body whorl	1.85±0.11 (1.76–2.00)	1.86 (1.84–1.88)	1.61±0.02 (1.60–1.64)
L penultimate whorl	0.40±0.01 (0.38–0.40)	0.45 (0.40–0.50)	0.36±0.03 (0.34–0.40)
W penultimate whorl	0.90±0.02 (0.88–0.92)	0.94 (0.88–2.00)	0.83±0.03 (0.80–0.86)
L last three whorls	2.46±0.11 (2.36–2.60)	2.56 (2.52–2.60)	2.20±0 —
L aperture	1.21±0.08 (1.16–1.32)	1.14 (1.12–1.16)	1.07±0.06 (1.00–1.12)
W aperture	0.81±0.05 (0.76–0.88)	0.80 —	0.69±0.02 (0.68–0.72)
Tip apical whorl (W)	0.14±0.02 (0.12–0.16) N = 6*	— —	— —
Diameter 1st whorl	0.28±0.02	—	(0.26–0.30) N = 6*
x**	0.37±0.02 (0.36–0.40) N = 3*	0.34±0.06 (0.28–0.40)	

* all whorl classes
**distance from base of body whorl to abapical tip of aperture

features are: (1) The gonad (Go) is posterior to the stomach. (2) The prostate (Pr) overlaps the posterior end of the mantle cavity (Emc). (3) The seminal vesicle (Sv) arises from the vas efferens (Ve) about mid-gonad. (4) The seminal vesicle is coiled lateral to the gonad, like a spring or coils in a knot dorsal to the gonad posterior to the stomach. It does not continue onto the stomach. (5) The anterior vas deferens (Vd_2) leaves the prostate at the posterior end of the mantle cavity. (6) The penis is simple but with a very elongated penial filament. (Pf, Fig. 67). (7) The vas deferens is highly coiled passing through the center of the penis. There is no ejaculatory duct in the base of the penis or in the neck. (8) The orientation of the base of the penis (Bp) to the snout-neck midline (x) and the posterior edge of the eye bulges is shown in Figure 62. The long axis of the penial base varies from 70° to 90° from "x" as shown.

Digestive system. The digestive gland covers the posterior chamber of the stomach of females but is posterior to the stomach of males. Radular statistics are given in Tables 31 and 32. There are 99 ± 3.4 rows of teeth along a radula 0.54 mm long. The most frequently encountered formula is

$$\frac{3(2)\text{-}1\text{-}(2)3}{3(2)\text{-}(2)3};\ 3\text{-}1[2]\text{-}3(4);\ 14\text{-}17;\ 12\text{-}15.$$

SEM photographs of radulae and teeth are given in Figures 68, 69. Central teeth are featured in Figure 68C–F; they are typical of the generalized triculine type. The morphology of the entire lateral tooth is shown in Figure 68A, B. The one unusual feature seen in the radula of this species involves the dominant cusp of the lateral tooth, the "1" of the 3-1-3; it is deeply divided, almost forming two cusps. (Fig. 68A–F, 69A–C).

Nervous system. Measurements are given in Table 33. The RPG ratio of 0.36 shows that the dorsal nerve ring is moderately concentrated.

Remarks

Conchologically, this species differs from all other *Neotricula* by having a shell with (1)

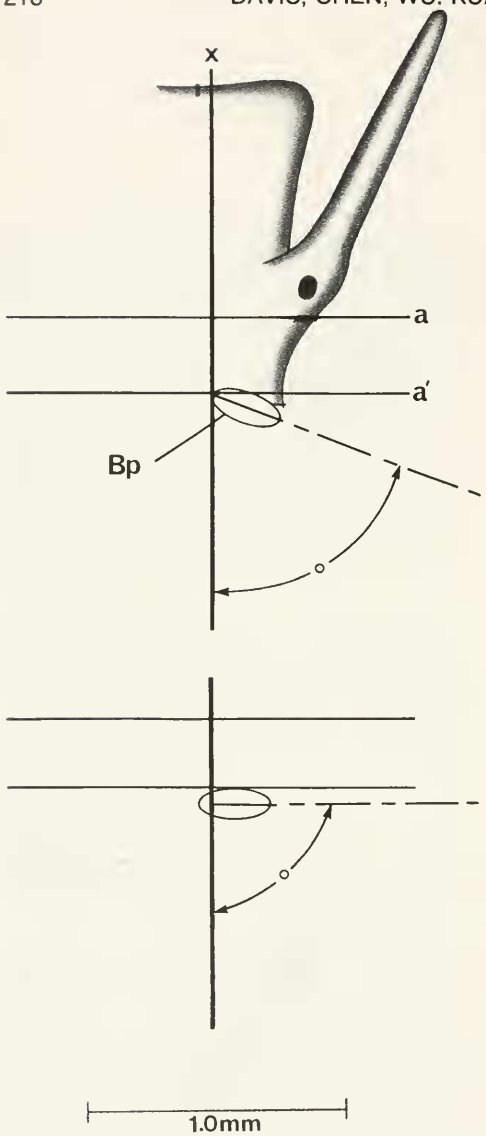

FIG. 62. Head of a male snail of *Neotricula cristella* showing the orientation of long axis of the penial base (Bp) to snout-neck mid-line x.

the inner lip widely separated from the body whorl, and (2) the adapical end of the aperture widely separated from the body whorl.

The multivariate analysis involving all species of Triculinae with shells closely resembling those of *Tricula* or *Neotricula* indicates different affinities depending on the analysis used. The phenogram based on distance coefficients (Fig. 153) shows linkage with *Gammatricula chinensis*. The differences are: (1) The sutures of *N. cristella* are smooth; those of *G. chinensis* are crenulated. (2) The adapical aperture of the former has a notch; of the latter, no notch. (3) The inner lip of the former is thin, of the latter, thick. (4) The inner lip of the former is widely separated from the body whorl, of the latter, narrowly separated. (5) The adapical end of the aperture of the former is widely separated from the body whorl, of the latter, slightly separated. (6) There is no abapical outer lip deflection angle in the former, a slight one in the latter.

The minimum spanning tree (Fig. 154) based on distance coefficients yields a different closest relationship, one with *Tricula hudiequanensis*. However, (1) *T. hudiequanensis* has a medium length shell (*N. cristella* has a small shell). (2) The adapical aperture of the former does not have a notch. (3) The outer lip of the former, in side view, is scooped forward; it is straight in the latter. (4) The inner lip of the former is thick; it is thin in the latter. (5) The inner lip and adapical aperture are not as greatly separated from the body whorl in the former as in the latter.

The most distinguishing anatomical character (considering only species of *Neotricula*) is the long penial filament. This species shares with *N. lilii* the character-state of having very many rows of teeth on the radula; with *N. minima*, the state that the digestive gland covers the posterior chamber of the stomach. The U-shaped continuation of the duct of the bursa into the duct of the seminal receptacle is shared with *N. burchi* of northwest Thailand and *N. aperta* of the lower Mekong River.

Neotricula dianmenensis Davis & Chen, sp. nov.

Holotype: ZAMIP-M0034, Figure 70A.
Paratypes: ANSP 373143, A12659; ZAMIP MOO04. Figure 70B–D; Figure 71A, B.

Type Locality: Jiepai Village, Dianmen Town, Hengshan County, Hengyang Prefecture. 27°15′16″N, 112°33′31″E. Figure 1, Site 5. Field collection D85-80.

Collection Date: October 1985.

Etymology: Named for the town of Dianmen.

Habitat

300 m above sea level. Snails were collected from a small stream 20–25 cm wide and

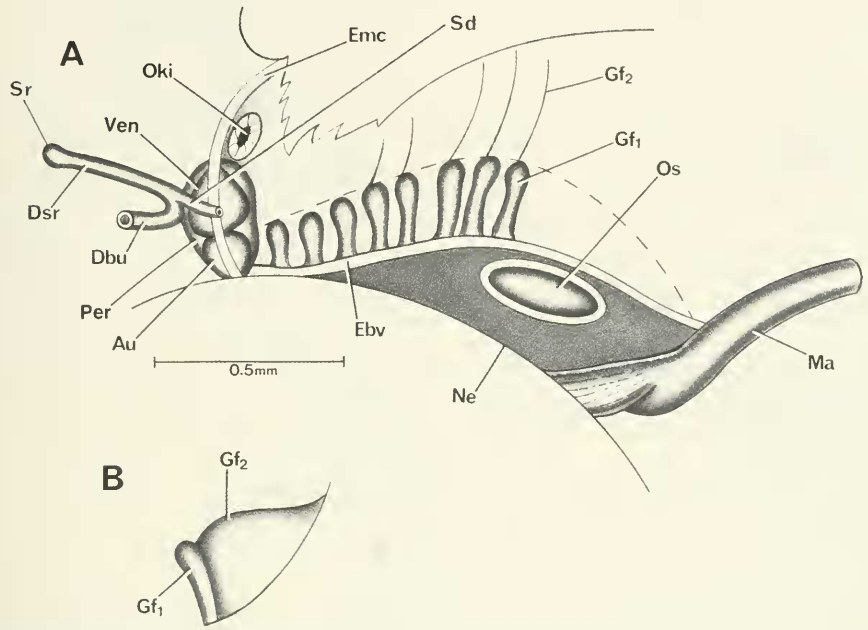

FIG. 63. A. Mantle cavity structures of *Neotricula cristella* showing the relationship of the gill to pericardium (Pe) and openings of the kidney (Oki) and spermathical duct (Sd). B. Single gill filament

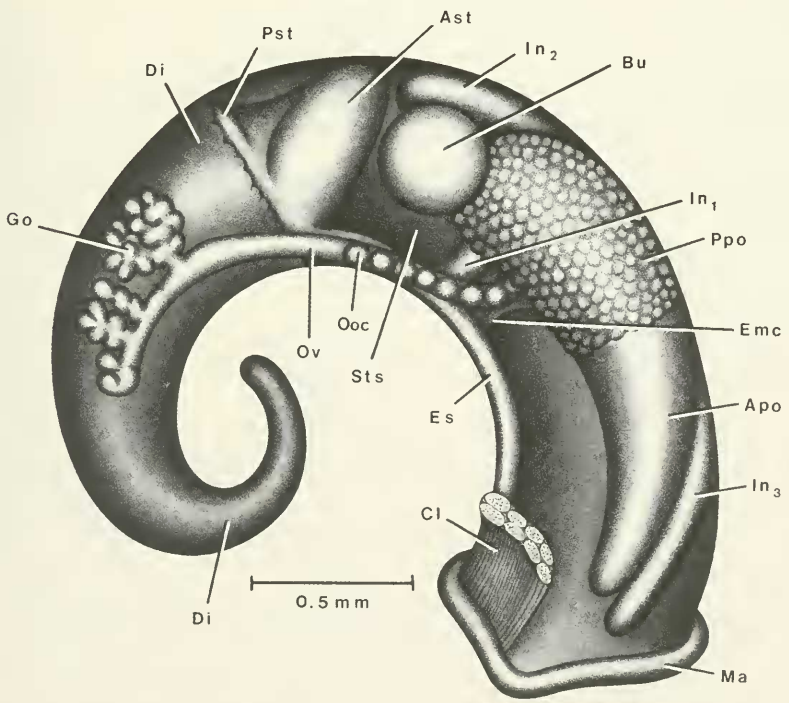

FIG. 64. Uncoiled female *Neotricula cristella* with head and kidney tissue removed.

TABLE 30. Lengths (mm) or counts of non-neural organs and structures of *Neotricula cristella*. Mean ± standard deviation, (range).

	Females (N = 5)	Males (N = 3)
Body	4.60±0.17 (4.34–4.76)	4.17±0.32 (3.80–4.36)
Gonad	0.62±0.08 (0.54–0.70)	1.03±0.21 (0.80–1.20)
Digestive gland	2.06±0.17 (1.90–2.30)	1.93±0.31 (1.60–2.20)
Posterior pallial oviduct (= albumen gland)	0.86±0.06 (0.76–0.90)	—
Anterior pallial oviduct (= capsule gland)	0.96±0.09 (0.90–1.10)	—
Total pallial oviduct = OV	1.82±0.13 (1.66–2.00)	—
Bursa copulatrix = BU	0.38±0.05 (0.34–0.46)	—
Duct of BU	0.19±0.05 (0.14–0.26)	—
BU ÷ OV	0.21±0.04 (0.17–0.20)	—
Seminal receptacle	0.10±0.02 (0.08–0.12)	—
Duct of seminal receptacle	0.19±0.04 (0.16–0.24)	—
Mantle cavity	1.11±0.28 (0.76–1.44)	1.00±0.07 (0.96–1.08)
Gill (G)	0.92±0.28 (0.60–1.28)	0.85±0.05 (0.80–0.90)
Osphradium (OS)	0.23±0.08 (0.16–0.36)	0.24±0.02 (0.22–0.26)
OS ÷ G	0.26±0.08 (0.18–0.37)	0.29±0.03 (0.26–0.33)
No. of filaments	13.6±0.9 (13–15)	13.3±1.2 (12–14)
Gf_2	0.23±0.06 (0.16–0.30)	—
Gf_1	0.16±0.03 (0.12–0.20)	—
Total Gf = TGF	0.38±0.09 (0.26–0.50)	—
Gf_2 ÷ TGF	0.61±0.04 (0.56–0.65)	—
Prostate	—	0.81±0.02 (0.80–0.90)
Seminal vesicle	—	0.38±0.07 (0.40–0.44)
Penis	—	1.53±0.18 (1.40–1.74)
Buccal mass	0.50±0.06 (0.44–0.56)	—

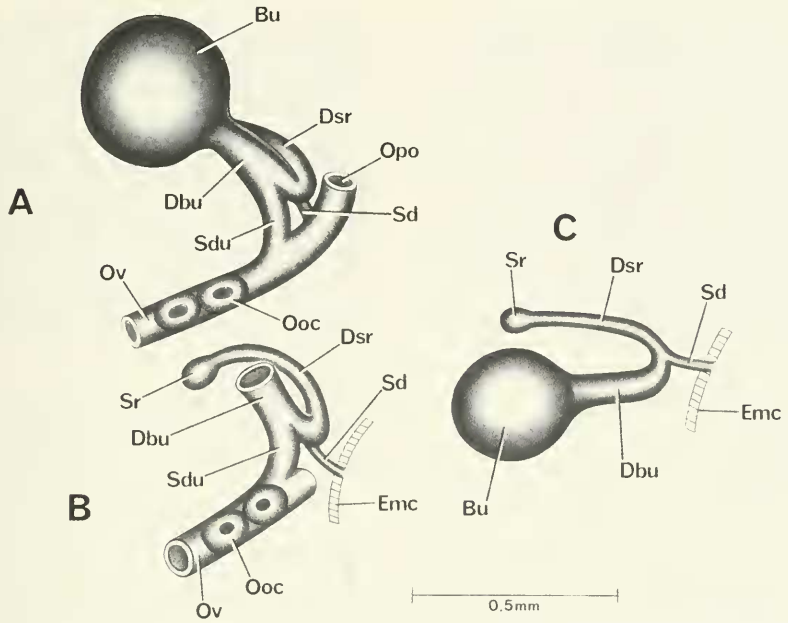

FIG. 65. Details and variation of bursa copulatrix complex of organs of *Neotricula cristella*. Figure A is in same orientation as in Figure 64. B. Bursa removed to show entire seminal receptacle (Sr) and duct (Dsr). C. Bursa rotated to show interconnection of Dbu, Dsr and the spermathical duct (Sd).

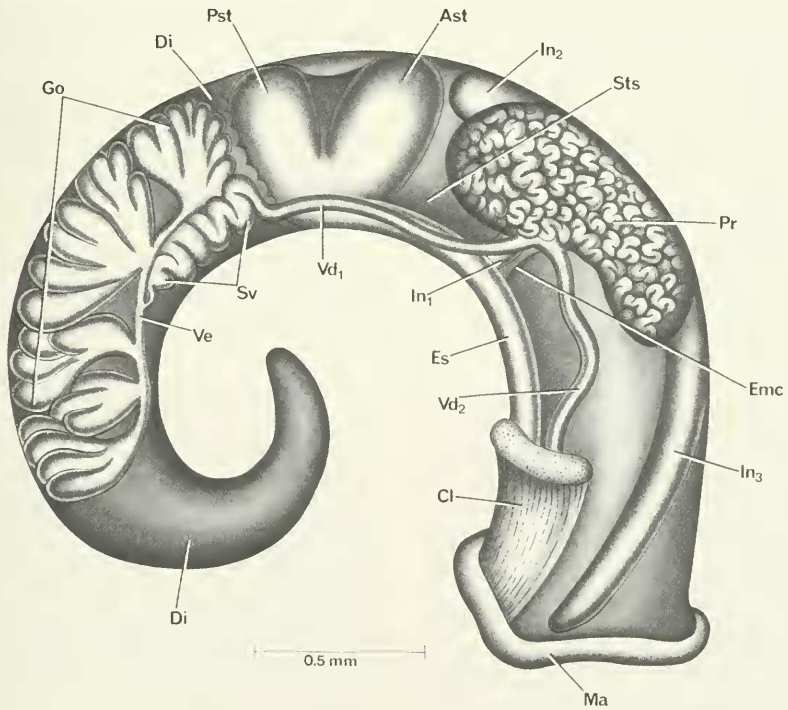

FIG. 66. Uncoiled male of *Neotricula cristella* without head or kidney tissue.

TABLE 31. Radular statistics for *Neotricula cristella*. Mean ± standard deviation (range). N = number used. In mm except for width of central tooth in μm.

	Males and females (N = 4)
Shell length	2.58±0.30 (2.16–2.88)
Radular length	0.54±0.05 (0.48–0.59)
Radular width	0.06±0.002 (0.056–0.060)
Total rows of teeth	99±3.4 (95–103)
No. rows of teeth forming	23±6.9 (16–32)
Central tooth width	12.9±0.8 (12.3–14)

TABLE 33. Lengths (mm) of neural structures of *Neotricula cristella*. Mean ± standard deviation (range). N = 3.

Cerebral ganglion	0.23±0.06 (0.16–0.28)
Cerbral commissure	0.05±0.01 (0.04–0.06)
Pleural ganglion	
Right (1)*	0.08±0.02 (0.06–0.10)
Left	0.10±0.04 (0.06–0.14)
Pleuro-supraesophageal connective (2)*	0.11±0.01 (0.10–0.12)
Pleuro-subesophageal connective	0.09±0.06 (0.02–0.14)
Supraesophageal ganglion (3)*	0.11±0.01 (0.10–0.12)
Subesophageal ganglion	0.11±0.01 (0.10–0.12)
Osphradio-mantle nerve	0.05±0.03 (0.02–0.08)
RPG ratio* = 2 ÷ 1+2+3	0.36±0.01 (0.36–0.38)

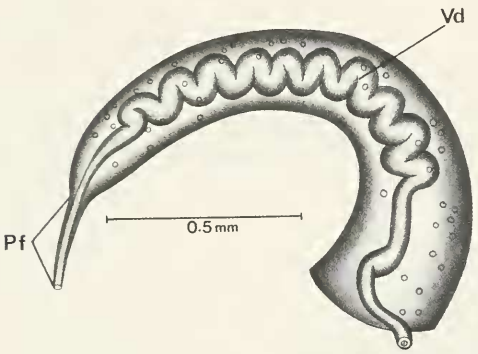

FIG. 67. Penis of *Neotricula cristella*.

10–15 cm deep. The flow was slow; the water was clean and cool. The stream flows down from Nanyue Mountain. The bottom of the stream was paved with small rocks, sand, and leaves. At stream side was short, scrubby vegetation. There were some 50 snails per stone.

Description

Shell. The shells are small, ovate-conic, of 5.0 to 5.5 whorls (Figs. 70A–D, 71A, B). Because the apices of most mature snails are eroded, it is not possible to be precise about lengths;

TABLE 32. Cusp formulae for the radular teeth of *Neotricula cristella* with the percent of radulae in which a given formula was found at least once.

Central Teeth		Lateral Teeth		Inner Marginal Teeth		Outer Marginal Teeth
3-1-3 / 3-3	93%	3-1[2]-3	79%	11	—	7%
		3-1[2]-4	21%	12	—	21%
2-1-2 / 2-2	21%			13	14%	71%
		4-1[2]-3	14%	14	43%	79%
4-1-4 / 3-3	9%	4-1[2]-4	7%	15	71%	50%
				16	71%	—
				17	50%	—
				18	21%	—
				$\bar{X}$ * = 15.1±2.7 N = 138		13.6±1.2 N = 127

*Mean ± standard deviation of cusp number for all teeth counted.

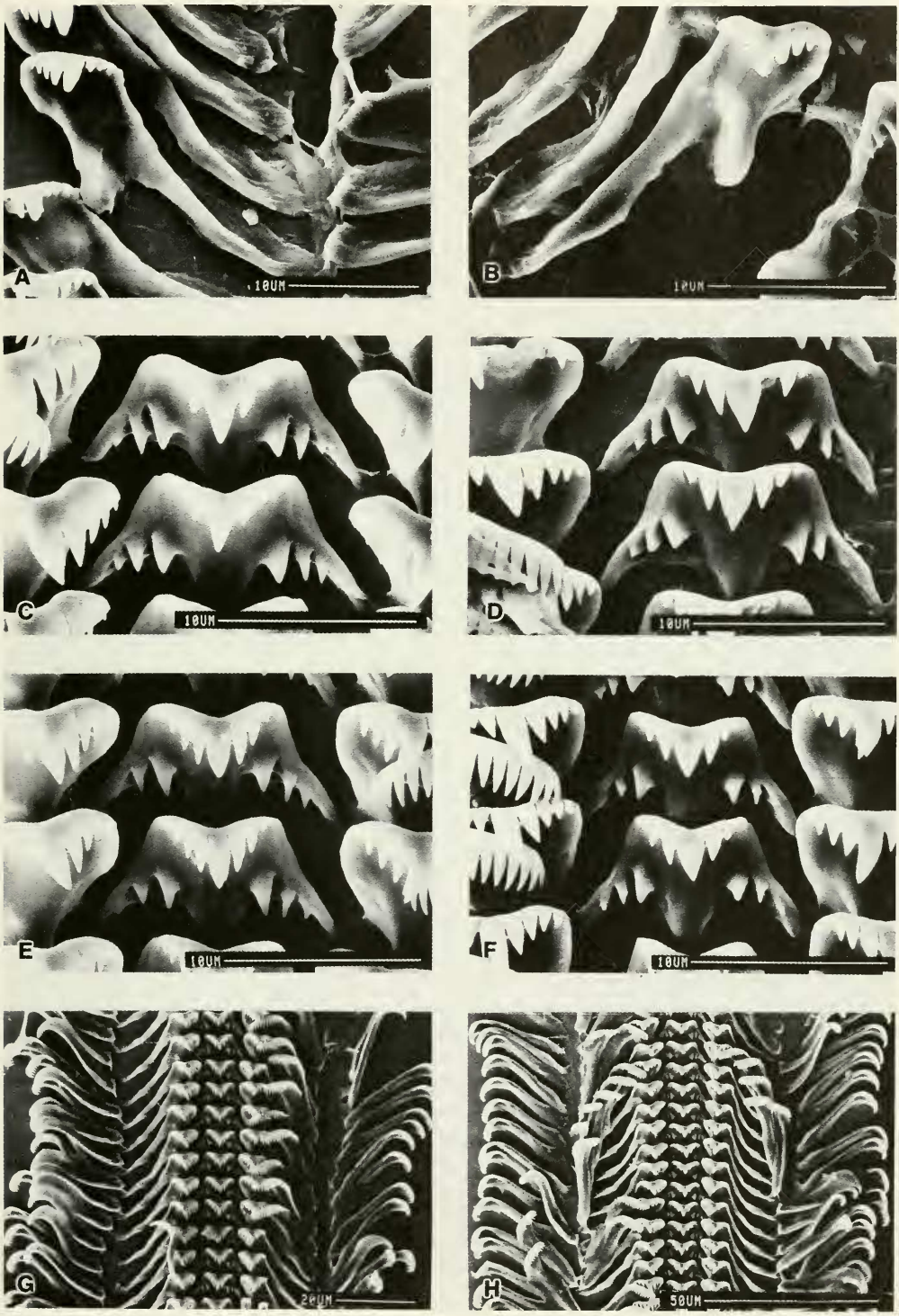

FIG. 68. Radula of *Neotricula cristella*. See text for details.

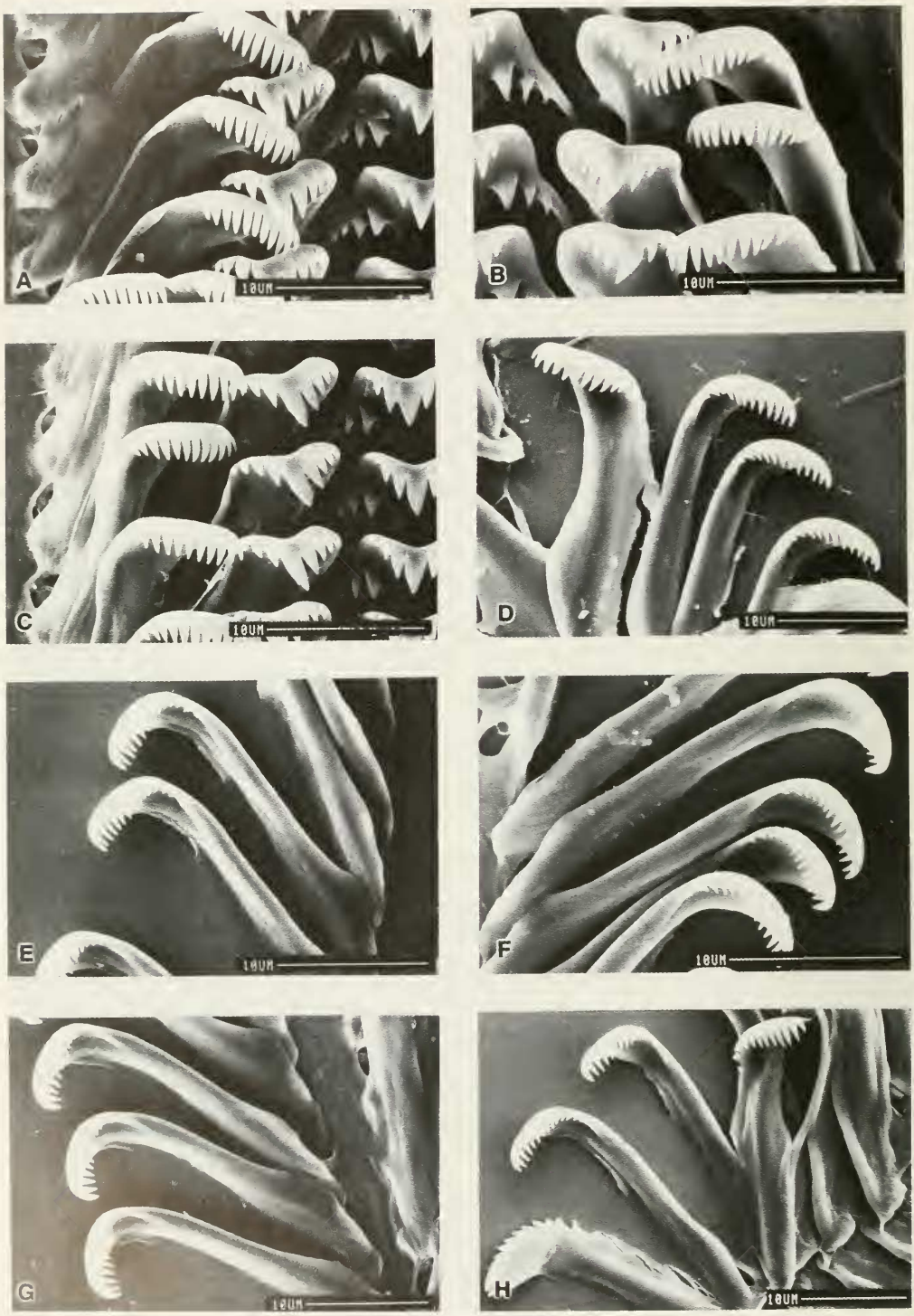

FIG. 69. Radula of *Neotricula cristella*. See text for details.

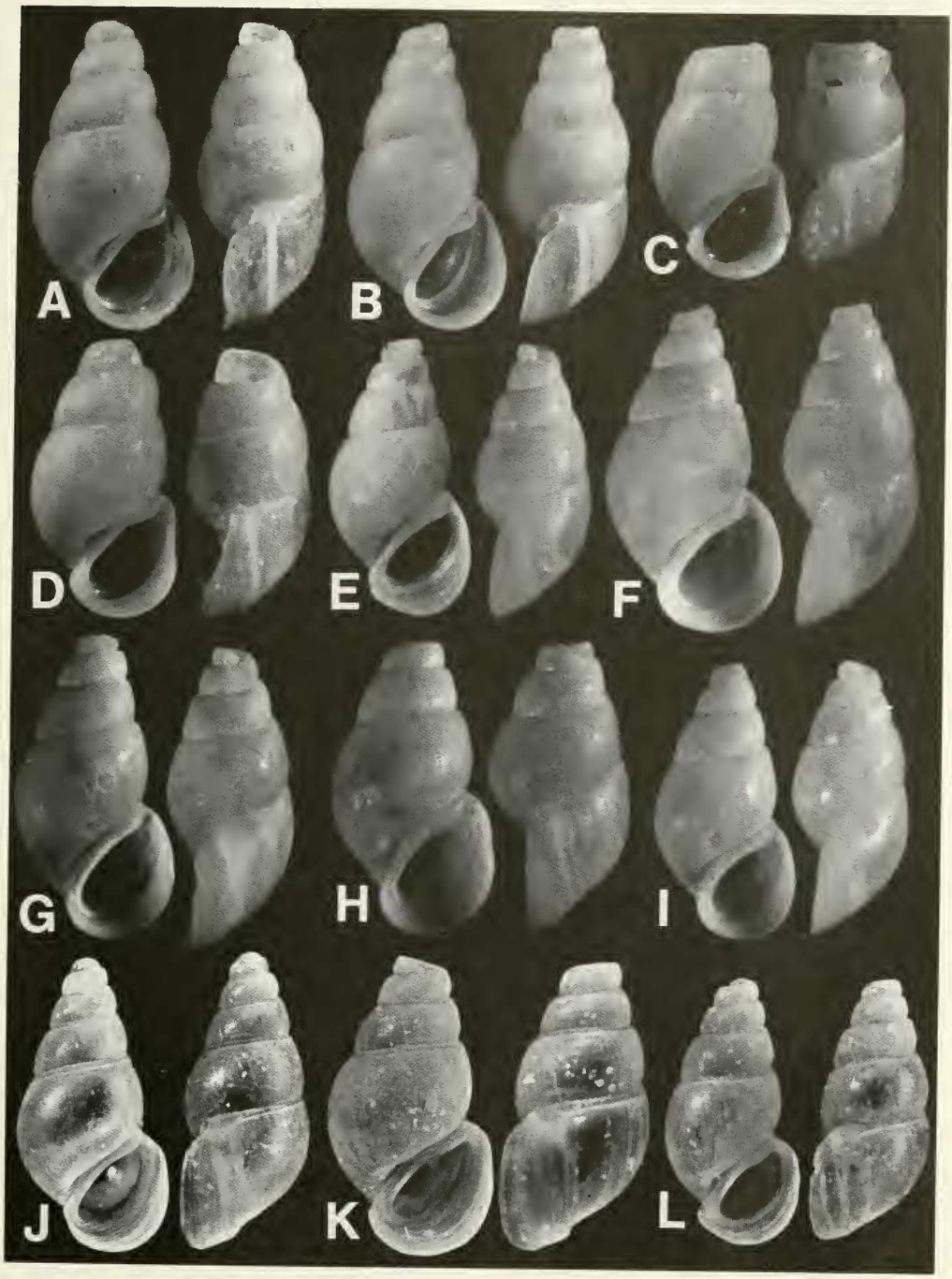

FIG. 70. Shells of: *Neotricula dianmenensis* A–D. A. Holotype. *Neotricula duplicata* E–I from D85 collections. F. Holotype. *Neotricula lilii* J–L. J. Holotype. A = 3.32 mm; other shells printed at same scale. Shells not designated as holotypes are paratypes.

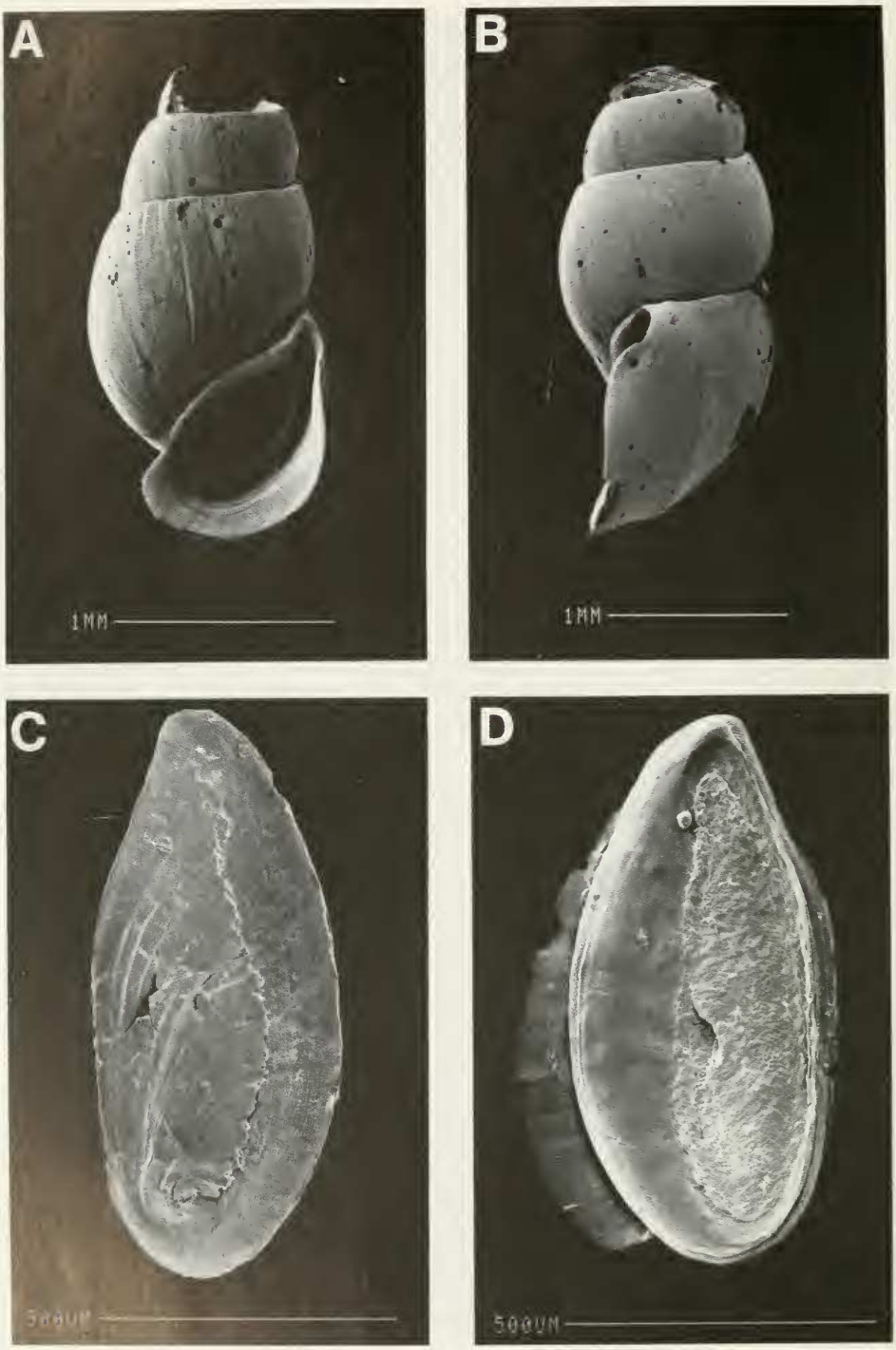

FIG. 71. SEM photographs of shells (A, B) and opercula (C, D) of *Neotricula dianmenensis*. D. Inner surface.

TABLE 34. Shell measurements (mm) for *Neotricula dianmenensis*. Mean ± standard deviation (range). All except two shells were eroded, therefore lengths are less than for entire specimens. e = eroded. *, probably a male.

	Shells used for dissections		Types		
	Females (3)	Males (1)	Holotype	Paratypes (5)	*Small Paratype (1)
No. Whorls	3e	5.5	4e	2.0–4.0e	5.0
Length (L)	2.90±0.20 (2.76–3.12)	2.72	3.32	2.89±0.25 (2.64–3.20)	2.76
Width (W)	1.50±0.08 (1.44–1.60)	1.36	1.64	1.50±0.06 (1.44–1.56)	1.28
L body whorl	2.02±0.12 (1.92–2.16)	1.76	2.20	1.96±0.08 (1.84–2.04)	1.68
L penultimate whorl	0.54±0.10 (0.48–0.62)	0.40	0.52	0.52±0.05 (0.46–0.56)	0.44
W penultimate whorl	1.10±0.10 (1.04–1.20)	0.96	1.16	1.08±0.06 (1.00–1.16)	0.96
W 3rd whorl	— —	— —	0.80	0.77±0.05 (0.72–0.80) N = 3	0.68
L last three whorls	2.90±0.20 (2.76–3.12)	2.72	3.12	2.85±0.19 (2.64–2.96) N = 3	2.40
L aperture	1.47±0.08 (1.40–1.56)	1.24	1.56	1.43±0.08 (1.32–1.52)	1.26
W aperture	0.91±0.02 (0.88–0.92)	0.80	0.96	0.91±0.03 (0.88–0.94)	0.80
x	0.42±0.05 (0.40–0.48)	0.40	0.50	0.43±0.08 (0.32–0.52)	0.36
y	—	—	0.16	0.09±0.05 (0.04–0.16)	0.08

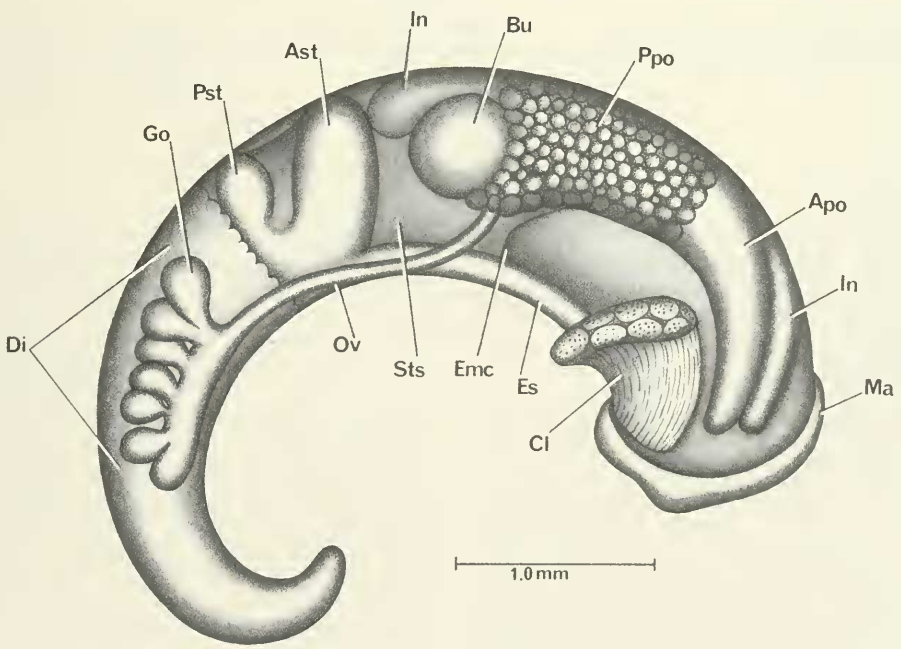

FIG. 72. Uncoiled female *Neotricula dianmenensis* with head and kidney tissue removed.

TABLE 35. Dimensions (mm) or counts of non-neural organs and structures of *Neotricula dianmenensis*. N = number of snails used. L = length. Mean ± standard deviation (range).

	Females (N = 3)	Males (N = 1)
Body L.	4.9±0.53 (4.4–5.4)	3.9
Digestive gland L	1.99±0.36 (1.76–2.4)	1.9
Gonad L.	0.75±0.08 (0.70–0.84)	1.1
Pallial oviduct L. = PO	1.58±0.16 (0.44–0.56)	—
Bursa copulatrix L. = BU	0.50±0.06 (0.44–0.56)	—
Duct of bursa L.	0.18 (0.16, 0.20) N = 2	—
BU ÷ PO	0.32±0.07 (0.26–0.40)	—
Seminal receptacle L.	0.15±0.01 (0.14–0.16)	—
Duct of seminal receptacle L. (see text)	0 to 0.12	—
Buccal mass L.	0.55±0.04 (0.52–0.60)	
Mantle cavity L.	1.41±0.20 (1.20–1.60)	1.26
Osphradium L. = Os	0.35±0.05 (0.30–0.40)	0.34
Gill L. = G	1.23±0.21 (1.00–1.40)	1.06
Os ÷ G	0.29±0.03 (0.26–0.32) N = 4	—
No. filaments	18.3±1.5 (17–20)	17
Gf_2 L	0.25 (0.20, 0.30) N = 2	(males & females)
Gf_1 L.	0.21 N = 2	(males & females)
Total Gf L. = TGF	0.46 N = 2 no variation	
Gf_2 ÷ TGF	0.54 (0.44, 0.65) N = 2	(males & females)
Prostate L.	—	1.0
Seminal vesicle L.	—	0.70
Penis L.	—	1.54

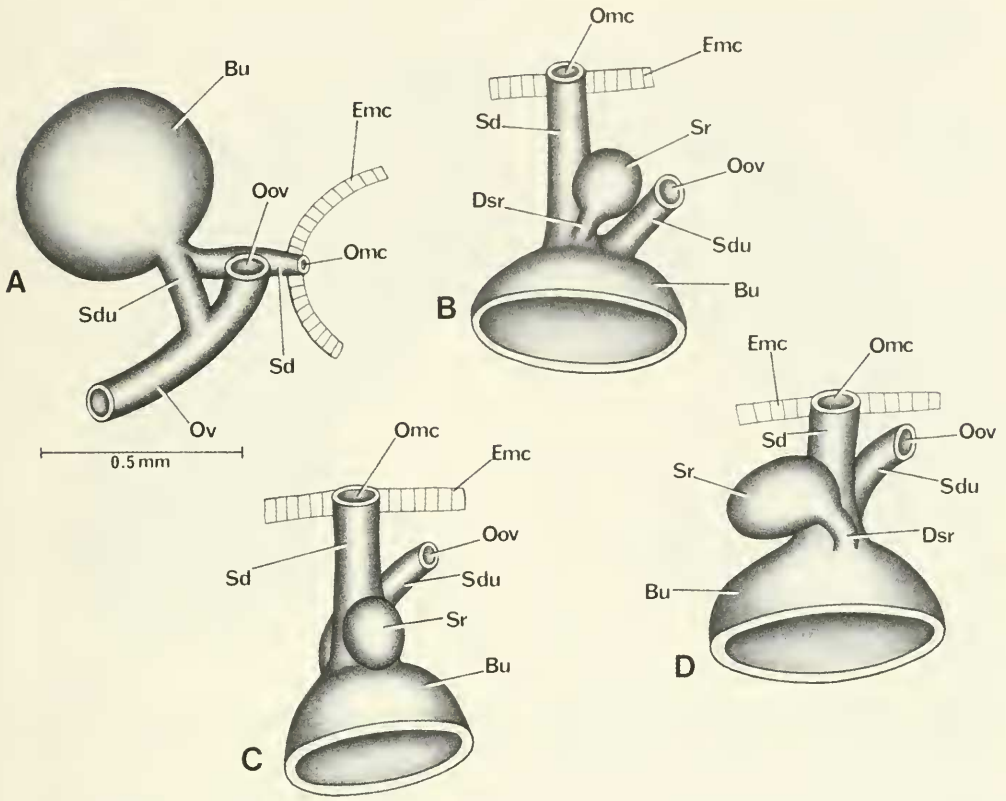

FIG. 73. Details and variation of bursa copulatrix complex of organs of *Neotricula dianmenensis*. A, same orientation as in Figure 72. B–D. Bursa complex flipped over to show where seminal receptacle enters the base of bursa, and variation.

we can give no data on apical whorl characters. Lengths probably range from 2.76 to 3.44 mm (Table 34). There is possibly sexual dimorphism, with the males smaller. The aperture shape is distorted due to the pronounced aperture beak. There is a narrow but pronounced umbilicus. The whorls at the suture are smooth (not crenulated). SEM analysis reveals a trace of spiral microsculpture below the sutures (also seen at 50X). There is an angulation of the inner lip just abapical to the pronounced beak tubercle. The inner lip is fused to the body whorl (most shells). The inner lip is slightly separated from the body whorl opposite the beak tubercle (some shells). The adapical end of the aperture is fused to the body whorl; there is a pronounced apertural beak some 0.26 mm long with a wide opening into the interior (0.12–0.16 mm wide gap); there is no internal notch groove. There is an apertural sinus. In side view, the outer lip is straight; it is slightly scooped forward. Facing the inner lip in side view, there is a strong lip deflection angle. There is no varix. In apertural view, the abapical lip extends beyond the base of the shell 0.43 ± 0.08 mm.

The whorls are slightly convex and the sutures sharply defined but shallow.

External features. Details of the head are not available. The operculum (Fig. 71C,D) is distinctive for its long, thin shape. The width to length ratio is 0.44 ± 0.03. As seen in Figure 71D, there may be an easily detached external layer. The internal attachment pad is pro-

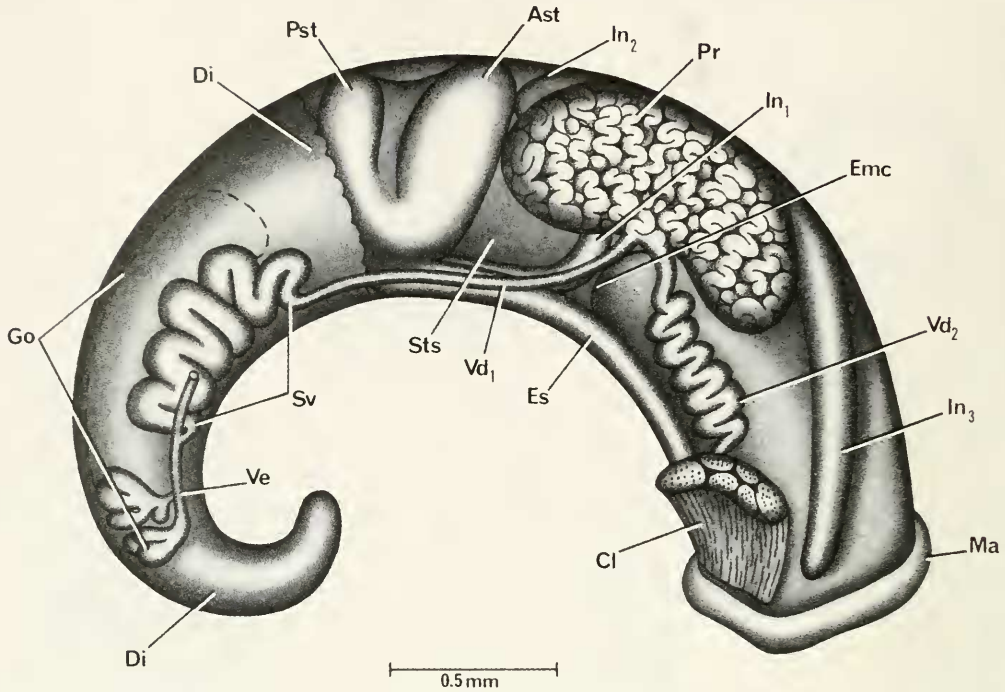

FIG. 74. Uncoiled male of *Neotricula dianmenensis* without head or kidney tissue. Some lobes of gonad cut away to show seminal vesicle that coils dorsal to gonad. Dashed line shows anterior limit of gonadal lobes.

nounced (Fig. 71D). The shape of the operculum reflects the inner lip angulation.

Mantle cavity. Measurements and statistics are given in Table 35. Mantle cavity structures and relationships are normal for those of *Neotricula*. The osphradium is mid-gill; it is short. Gill filaments are normally developed; Gf_2 is normal length. Gf_2 does not have a pronounced crest.

Female reproductive system. The body of an uncoiled female without head and with kidney tissue removed is shown in Figure 72. Measurements of organs are given in Table 35. Important features are: (1) The gonad is posterior to the stomach; it consists of few lobes. (2) The bursa (Bu) is clearly seen posterior to the posterior pallial oviduct (Ppo). (3) Sperm enter the system at the posterior end of the mantle cavity (Emc) by passing into the spermathecal duct (Sd) that bypasses the pericardium. The spermathecal duct runs a short distance to open into the bursa (Bu, Fig. 73A) dorsal to the duct of the bursa (Dbu). (4) The sperm duct (Sdu) runs from the bursa (Bu) to the oviduct (Ov); there is no duct of the bursa. (5) The seminal receptacle (Sr) arises from the spermathecal duct where the latter joins the bursa (Fig. 73B–D). (6) The duct of the seminal receptacle varies in length from 0 (Sr fused to the spermathecal duct, Fig. 73C) to moderately long (Fig. 73D). (7) The oviduct runs from gonad to pallial oviduct without making a loop or twist. (8) The oviduct opens into the pallial oviduct close to the posterior end of the pallial oviduct. (9) The bursa copulatrix is round and short. (10) The length of the albumen gland is standard (based on one individual for which this could be discerned, ratio of 0.47).

Male reproductive system. The body of an uncoiled male is shown in Figure 74 without head and with kidney tissue removed. The anterior lobes of the gonad were removed to reveal the seminal vesicle. Measurements are given in Table 35. Important features are: (1) The gonad consists of numbers of finely divided lobes that drain into a vas efferens

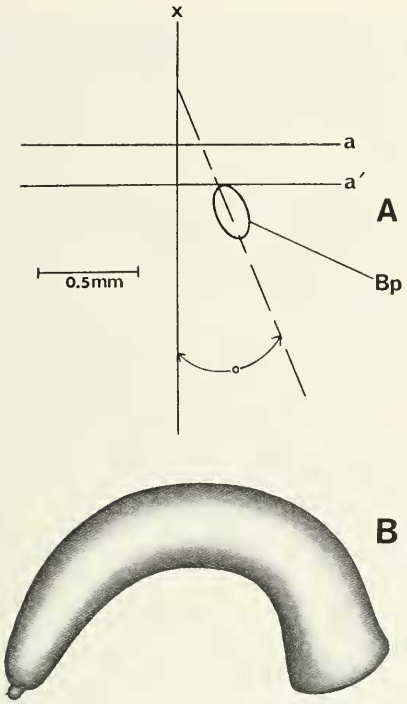

FIG. 75. The penis (B). (A), orientation of the base of the penis (Bp) of *Neotricula dianmenensis* to the snout-neck mid-line (x).

TABLE 36. Radula statistics for *Neotricula dianmenensis*. Mean ± standard deviation (range). In mm except the central tooth width in μm. N = 4. Shell lengths not available.

Radular length	0.45±0.06	(0.36–0.48)
Radular width	0.08±0.002	(0.76–0.080)
Total rows of teeth	58.8±4.2	(56–65)
No. rows of teeth forming	1.90±3.6	(14–22)
Central tooth width	14.1±0.6	(13.4–14.9) N = 11

(Ve, Fig. 74). (2) The posterior vas deferens arises from the vas efferens posterior to mid-gonad and immediately coils as the seminal vesicle (Sv) that is dorsal to the lobes of the gonad. (3) The seminal vesicle coils posterior to the stomach. (4) The gonad is entirely posterior to the stomach. (5) The prostate is massive; it overlaps the posterior end of the mantle cavity. The posterior prostate overlaps the entire style sac (Sts). (6) The penis is simple, without lobes; it has a papilla (Fig. 75B). (7) No ejaculatory duct was found. (8) The shaft of the penis arises from the neck to the right of the snout-neck mid-line (x, Fig. 75A) at an angle of 22°–23°.

Digestive system. The digestive gland is posterior to the stomach (only slight overlap on the posterior chamber (Figs. 72, 74). The rad-

TABLE 37. Cusp formulae for the radular teeth of *Neotricula dianmenensis* with the percent of radulae (N = 4) in which a given formula was found at least once.

Central Teeth		Lateral Teeth		Inner Marginal Teeth		Outer Marginal Teeth (N = 3)	
2-1-2 / 2-2	50%	3-1-4	75%	7	25%	7	0
		4-1-3	50%	8	25%	8	0
3-1-3 / 2-3	25%	4-1-2	25%	9	25%	9	33%
		2-1-3	25%	10	25%	10	33%
3-1-3 / 2-2	25%	2-1[2]-2	25%	11	100%	11	66%
2-1-3 / 2-2	25%	3-1-2	25%	12	100%	12	100%
		3-1-3	25%	13	75%	13	66%
		3-1-4	25%	14	25%	14	0
				$\bar{X}$* = 11.5±1.7 N = 38		11.6±1.2 30	

*Mean ± standard deviation of cusp number for all teeth counted.

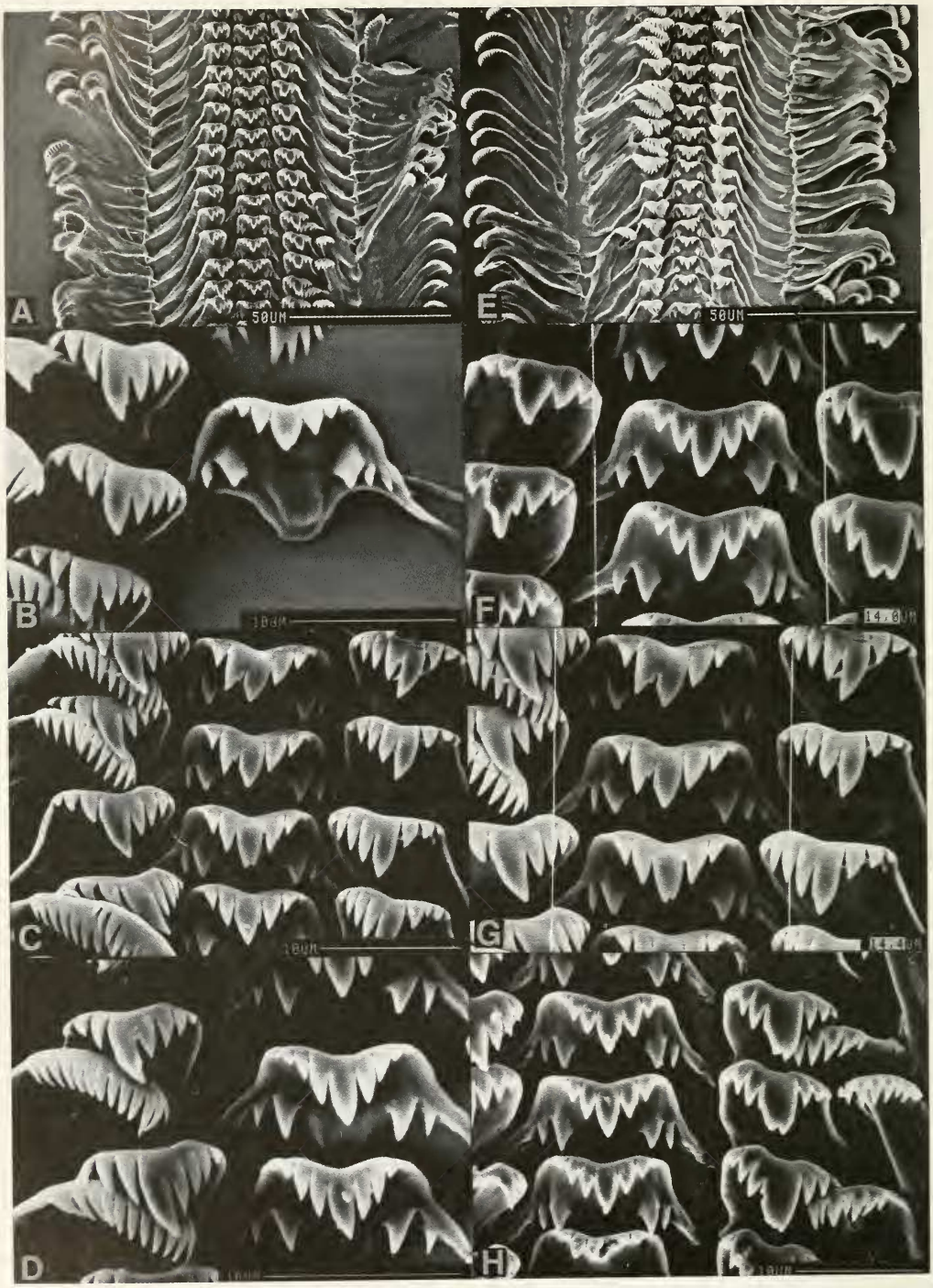

FIG. 76. Radula of *Neotricula dianmenensis*. A, E. Segments of the radula. B–D, F–H. Central, lateral and inner marginal (C, D, H) teeth. See text for details.

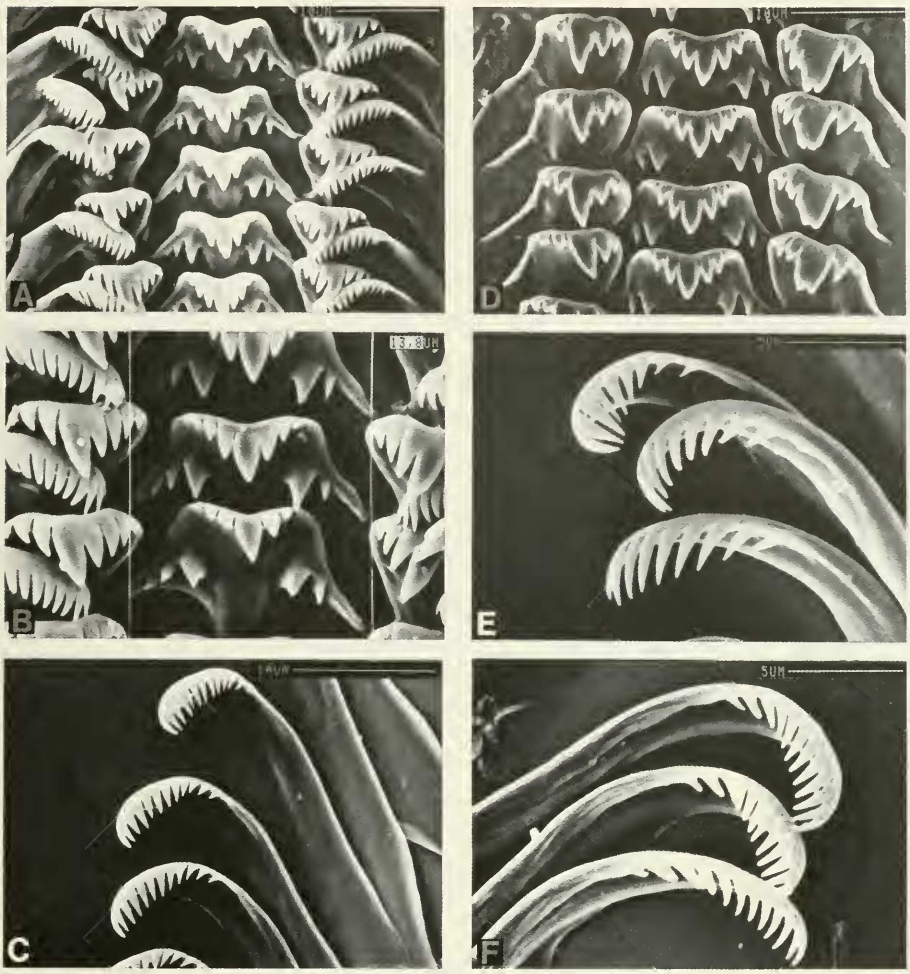

FIG. 77. Radula of *Neotricula dianmenensis*. Outer marginals are featured in C, E, F. Dominant cusp of lateral tooth (i.e. the "1" of the 3-1-2) is either massive (D) or bifurcated (B).

TABLE 38. Lengths (mm) of neural structures of *Neotricula dianmenensis*. Mean ± standard deviation (range). N = 4.

Cerebral ganglion	0.23±0.01	
Cerebral commissure	0.07±0.01	
Pleural ganglia		
Right (1)	0.13±0.01	
Left	0.12–	(no variation)
Pleuro-supraesophageal connective (2)	0.13±0.04	(0.10–0.18)
Pleuro-subesophageal connective	0.08 N = 2	(0.06–0.10)
Supraesophageal ganglion (3)	0.11±0.01	(0.10–0.12)
Subesophageal ganglion	0.12–	
Osphradio-mantle nerve	0.04±0.01	(0.02–0.04)
RPG ratio = 2 ÷ 1+2+3	0.35±0.01	(0.34–0.36)

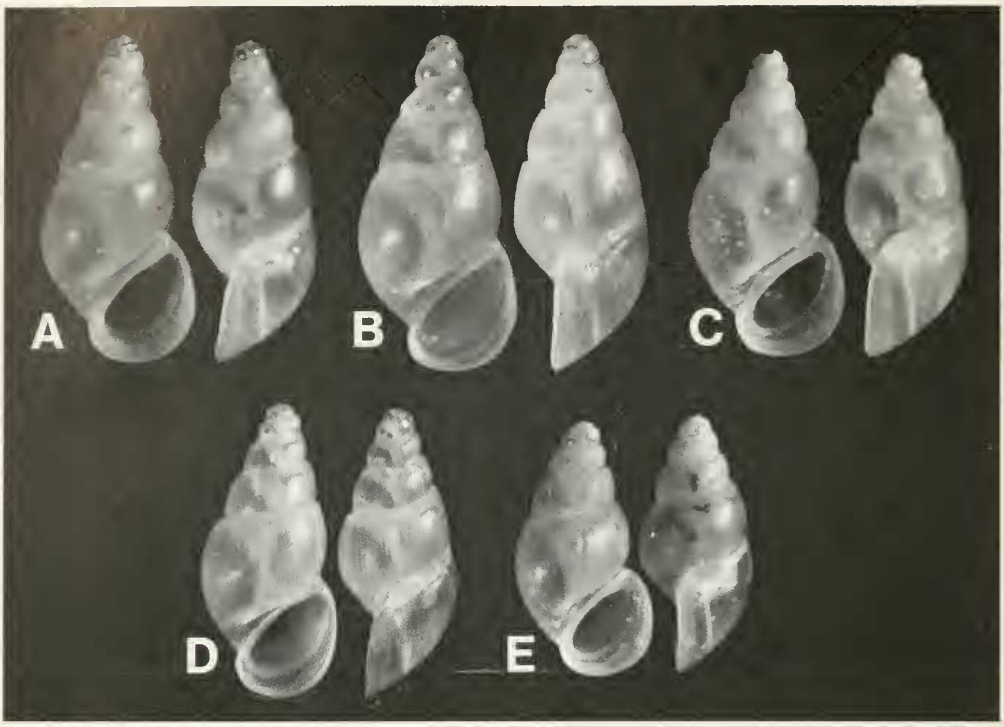

FIG. 78. Paratypes of *Neotricula duplicata* from D87-2. Shell in Figure A is 3.52 mm long; other shells printed at same scale.

ula sac does not coil dorsal to the nerve ring. The radula is shown in Figures 76, 77; radular statistics are given in Tables 36 and 37. The radula is typical Triculini. The enlarged cusp of the lateral tooth (the "1" of 3-1-2, etc.) is frequently bifid or massive (Figs. 77A, B, D). The typical radular formula is:

$$\frac{2(3)\text{-}1\text{-}(3)2}{2\text{-}2}$$, 3(4)-1[2]-2 to 4, 10-13, 10-13.

Nervous system. Standard Triculinae. Measurements are given in Table 38. The RPG ratio shows the supraesophageal connective to be moderately concentrated.

Remarks

Conchologically, *N. dianmenensis* is most similar to *N. duplicata* and *N. lilii* (Figs. 153, 154). However, it differs from the other two by having a distorted aperture shape (Table 2, char. 3), an angled inner lip (char. 13), and a pronounced beak tubercle (char. 24). Additionally, it differs from *N. duplicata* by having a clearly open umbilicus (char. 4), an adapical apertural sinus (char. 11), a sinuate outer lip (char. 14), and a thin inner lip (char. 19).

Anatomically the greatest similarity is to *N. duplicata* (Fig. 157), but it differs from that species in seven characters (15% of the 46 comparable characters, Table 80). *Neotricula. dianmenensis* has few rows of teeth whereas *N. duplicata* has many (char. 42). The gonad of the former is posterior to the stomach; it overlaps the stomach in the latter. The spermathecal duct is comparatively long in the former, short in the latter (char. 19). There is no duct of the bursa in the former; it is long in the latter (char. 16). The osphradium is long in the former, short in the latter (char. 9).

Neotricula duplicata Davis & Chen sp. nov.

Holotype. ZAMIP-M0035, Figure 70A.

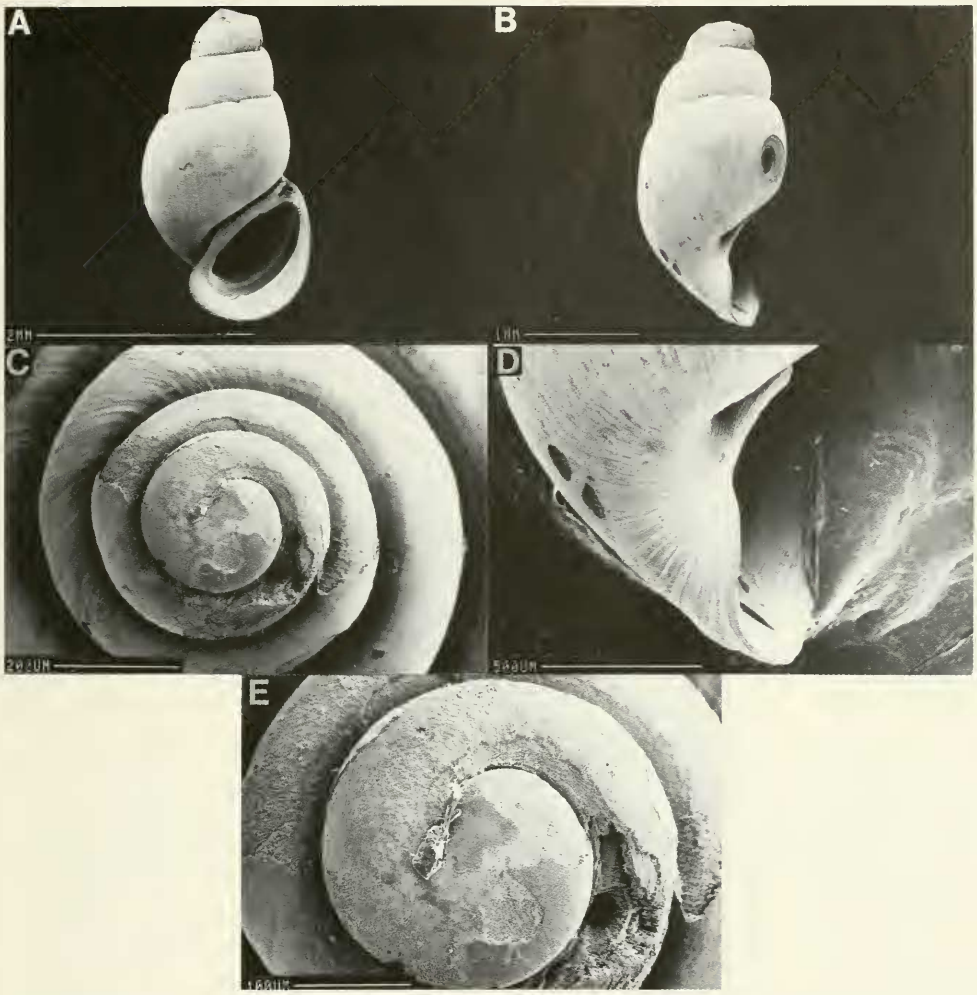

FIG. 79. SEM photographs of shells of *Neotricula duplicata* from D85-79. B, D show the abapical lip deflection. C, E. Enlargements of apical whorls.

Paratypes. ANSP 373152, A12668; 373151, A12667; ZAMIP M0003; Figure 70E, G–I; Figure 78B–E.

Type Locality. Huang-sha-ping Village, Jiangnan Town, Anhua County, Yiyang Prefecture. 28°21′24″E, 110°15′11″N. Figure 1, site 4. Collection numbers D85-79, 5 October 1985, Davis, Hoagland & Chen; D87-2, 18 March 1987, Davis & Chen.

Etymology. Named for the duplication of anatomical research effort on specimens collected from this population in both 1985 and 1987, not realizing in 1987 that the population had been dissected and analyzed in 1985.

Habitat

Some 400 m from Zijiang River, a small stream flowed from a hill through rice fields. The stream was about 10 cm deep, 14 cm wide with a mud substratum. Snails were collected in the upper narrow shaded part of the stream from under stones. Associated molluscan fauna: *Gyraulus* sp.

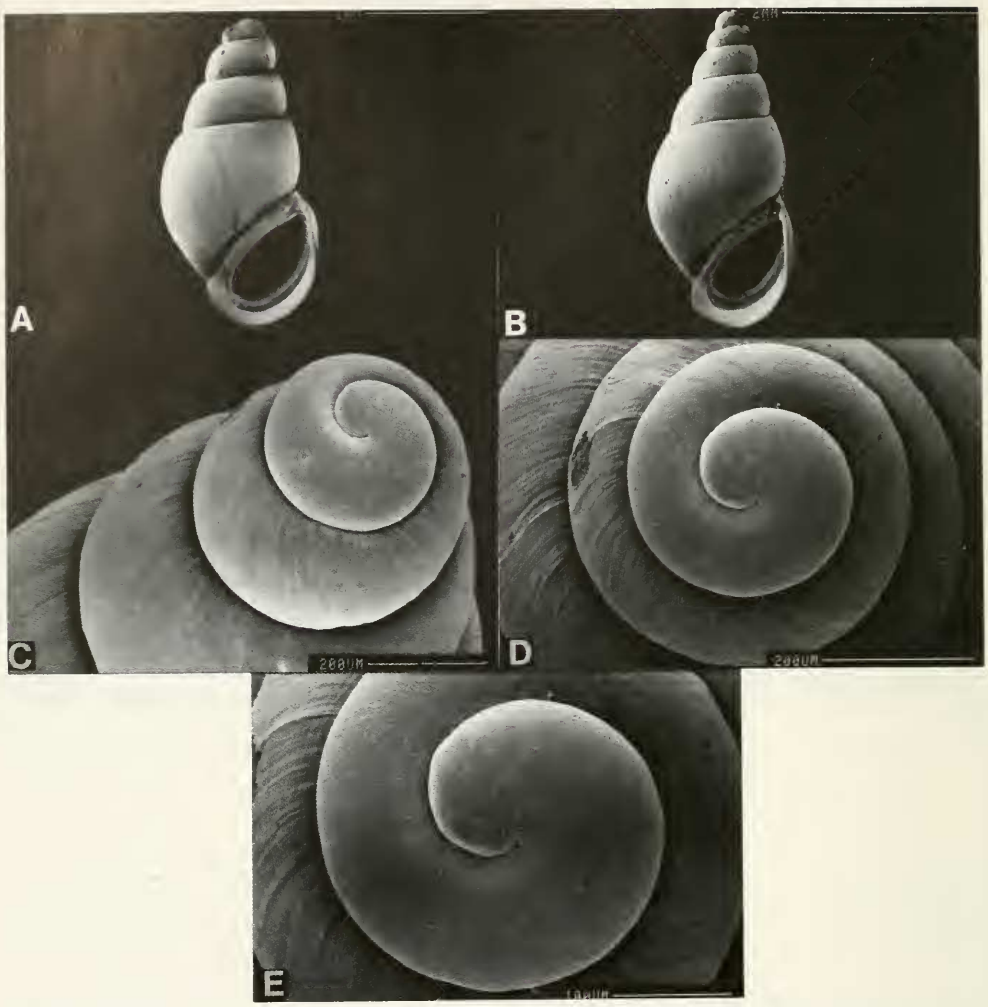

FIG. 80. SEM photographs of shells of *Neotricula duplicata* from D87-2. C–E. Enlargements of apical whorls.

Description

Shell. Shells are illustrated in Figures 70E–I, 78A–E, 79, 80. They are small, ovate-conic (Tables 39–41). Because most snails are eroded, it is difficult to analyze size classes based on whorl numbers. It is clear that there are two size classes of mature snails (Table 39); females are larger than males (Table 41). Additionally, there appear to be two size classes within each sex (Table 41). The size range based on uneroded shells is 2.72–3.88 mm. The aperture is pyriform. Adapically there is a strong apertural beak; there is no beak tubercle. There may or may not be an internal notch groove.

The whorls at the suture are smooth (not crenulated). There is an umbilical chink. SEM analysis reveals faint spiral microsculpture at the shoulders of the whorls after the second whorl (Fig. 80D, E).

The inner lip is straight to arched, narrowly separated from the body whorl, and uniformly thick. The adapical end of the aperture is only

TABLE 39. Measurements in mm of D85-79 shells of *Neotricula duplicata*. Mean ± standard deviation (range). e = eroded apical whorls; ( ) = number measured. Sex unknown.

	Holotype	Paratypes	
	large class	large class	small class
No. Whorls	4e	3e–4e (3)	3e–5e (5)
Length (L)	3.44	3.03±0.06 (3.00–3.10)	2.87±0.10e (2.72–3.00)
Width (W)	1.72	1.57±0.10 (1.50–1.68)	1.46±0.04 (1.44–1.48)
L last three whorls	3.12	2.91±0.16 (2.80–3.10)	2.67±0.06 (2.56–2.72)
L body whorl	2.24	2.12±0.14 (2.04–2.28)	1.94±0.02 (1.92–2.96)
L penultimate whorl	0.52	0.45±0.02 (0.44–0.52)	0.47±0.02 (0.44–0.48)
W penultimate whorl	1.10	0.99±0.07 (0.92–1.06)	0.97±0.02 (0.96–1.00)
W 3rd whorl	0.76	0.66±0.05 (0.60–0.70)	0.65±0.02 (0.64–0.68)
L aperture	1.60	1.51±0.12 (1.44–1.64)	1.36±0.04 (1.32–1.40)
W aperture	1.08	0.95±0.08 (0.88–1.04)	0.86±0.04 (0.80–0.88)
x	0.48	0.48±0.07 (0.40–0.52)	0.44±0.06 (0.36–0.52)
y	0.20	0.15±0.06 (0.08–0.16)	0.15±0.04 (0.10–0.20)

TABLE 40 Measurements in mm of paratype shells of *Neotricula duplicata* from D87-2. Mean ± standard deviation (range). e = eroded apical whorls; ( ) = number measured. Sex unknown.

No. Whorls	5e	5.5 (3)	6.0 (2)
Length (L) of eroded shell	3.44		
Length of uneroded shells		2.89±0.20 (2.72–3.12)	3.53 (3.46,3.60)
Width (W)	1.60	1.37±0.09 (1.32–1.48)	1.61 (1.60,1.62)
L last three whorls	2.92	2.59±0.15 (2.48–2.76)	3.10 (3.00,3.20)
L body whorl	2.08	1.87±0.08 (1.80–1.96)	2.18 (2.08,2.28)
L penultimate whorl	0.56	0.45±0.03 (0.42–0.48)	0.54 (0.52,0.56)
W penultimate whorl	1.06	0.91±0.05 (0.88–0.96)	1.10 (1.08,1.12)
W 3rd whorl	0.72	0.62±0.05 (0.58–0.68)	0.72 No variation
L aperture	1.52	1.33±0.09 (1.28–1.44)	1.52 (1.44,1.60)
W aperture	1.00	0.85±0.06 (0.84–0.92)	0.96 No variation
x	0.52	0.37±0.05 (0.32–0.40)	0.42 (0.40,0.44)
y	0.16	0.10±0.02 (0.08–0.12)	0.14 (0.12,0.16)

TABLE 41. Measurements (mm) of shells of *Neotricula duplicata* from both collections where animals were used for dissections. Mean ± standard deviation (range). All except two shells were eroded, therefore lengths are less than for entire specimens. e = eroded. *, probably a male. ( ) = number measured.

	Females			Males		
No. Whorls	2e–5e (3)	5.5 (1)	6.0 (1)	4e–5e (2)	5.0(1)*	5.5 (2)
Length (L) of eroded shells	3.31±0.45e (2.80–3.68)			3.22 (3.12, 3.32)		
Length of uneroded shells		3.60	3.88		2.88	3.12 No var.
Width (W)	1.77±0.08 (1.68–1.84)	1.76	1.76	1.57 (1.56, 1.58)	1.48	1.56 No var.
L last three whorls	3.24 (N = 2) No var.	3.20	3.36	2.88 (2.76, 3.00)	2.62	2.76 (2.72, 2.80)
L body whorl	2.36±0.08 (2.28–2.44)	2.36	2.36	2.10 (2.08, 2.12)	1.96	1.96 (1.92, 2.00)
L penultimate whorl	0.69±0.34 (0.48–1.08)	0.52	0.62	0.49 (0.42, 0.56)	0.40	0.46 (0.44, 0.48)
W penultimate whorl	1.12±0.04 (1.08–1.16)	1.12	1.16	1.05 (1.02, 1.08)	0.96	1.01 (1.00, 1.02)
W 3rd whorl	0.64 (N = 2) (0.56, 0.72)	0.78	0.82	2.88 (2.76, 3.00)	2.62	2.76 (2.72, 2.80)
L aperture	1.60±0.06 (1.56–1.68)	1.60	1.64	1.46 (1.42, 1.48)	1.32	1.38 (1.36, 1.40)
W aperture	1.07±0.08 (0.88–0.92)	1.08	1.06	0.92 No var.	0.88	0.94 (0.92, 0.96)

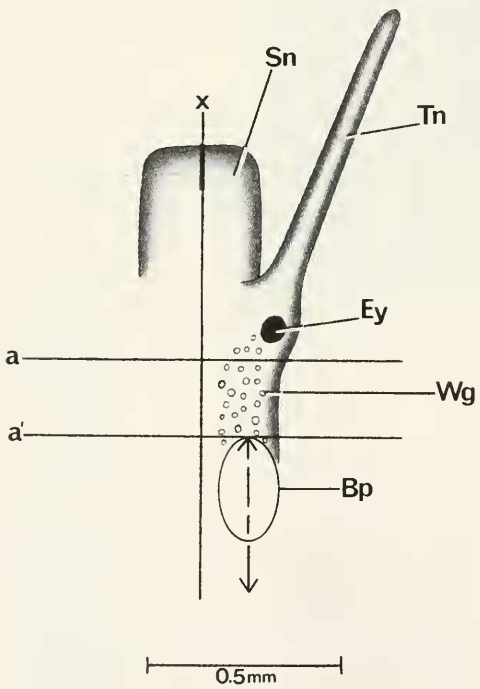

FIG. 81. Head of a male *Neotricula duplicata* from D85-72 showing the relationship of the base of the penis (Bp) to the mid-line of the snout-neck (x).

slightly separated from the body whorl. There is no apertural sinus. In side view, the outer lip is straight; the outer lip is slightly scooped forward. In side view, the inner lip has a strong deflection angle, some 140°. There is no varix. The abapical lip just beyond the base of the shell 0.48 ± 0.07 mm; the abapical lip has a spout.

SEM examinations of the apical whorls (Figs. 79C–E; 80C–E) show that the tip of the apical whorl is smooth, but that just beyond the tip the shell is minutely wrinkled. Coarse growth lines begin just before 1.75 whorls.

External features. The head is dark grey to black. There may or may not be white granules close to the eyes extending posteriorly back along the neck (Wg, Fig. 81). When granules occur, they do not form a dense lunate mass or "eyebrow."

Opercula from both collections are shown in Figures 82, 83. They are elongate-ovoid and are composed of discernable flaky layers. The muscular attachment pad (Fig. 82B, D) is pronounced and wide (66% width of the operculum).

Mantle cavity. Mantle cavity organs are shown in Figure 84; not all gill filaments are

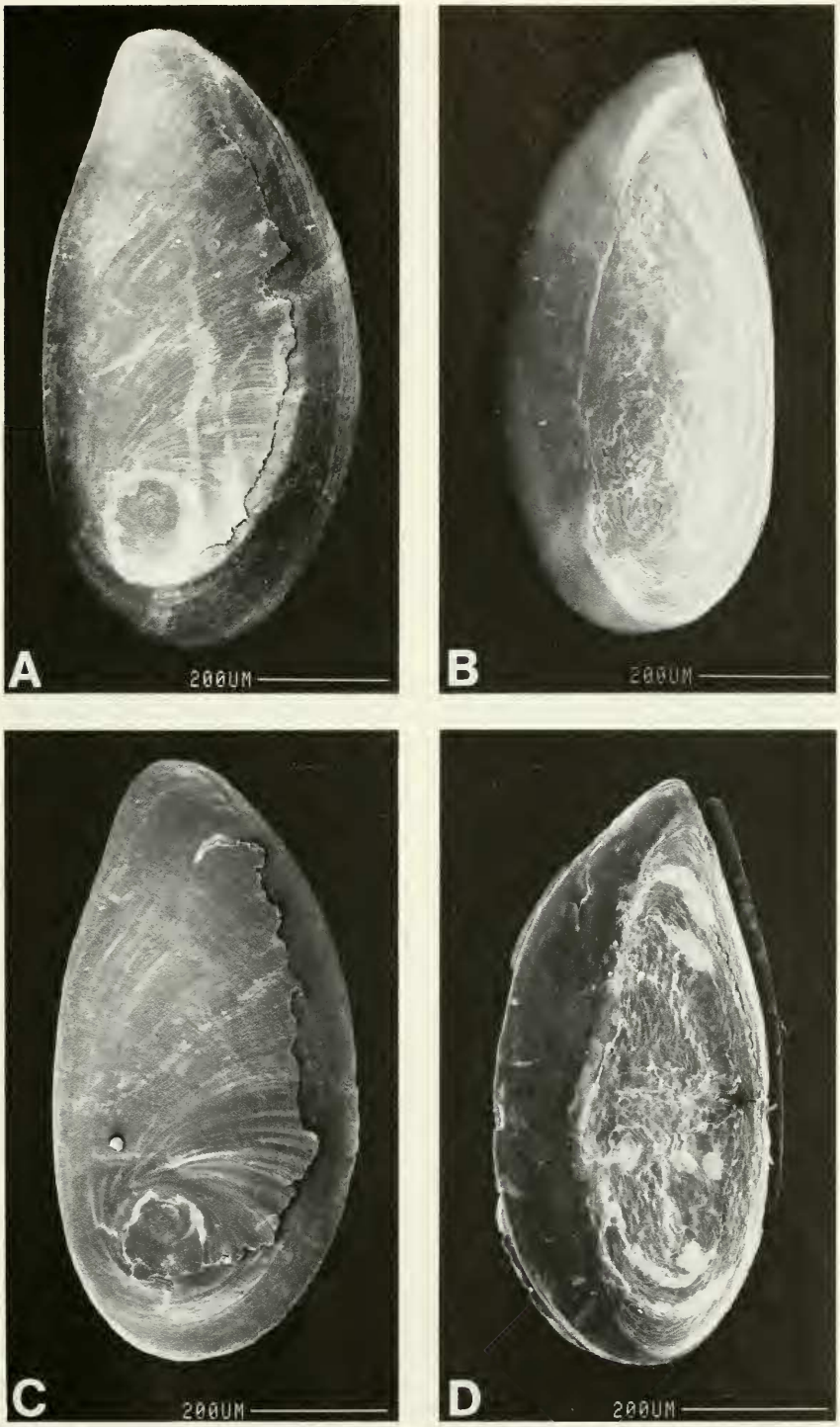

FIG. 82. Opercula of *Neotricula duplicata* from D85-79. A, C. Outer surface; B, D. Inner surface. Note the external loose, flaky layer (A, C, D).

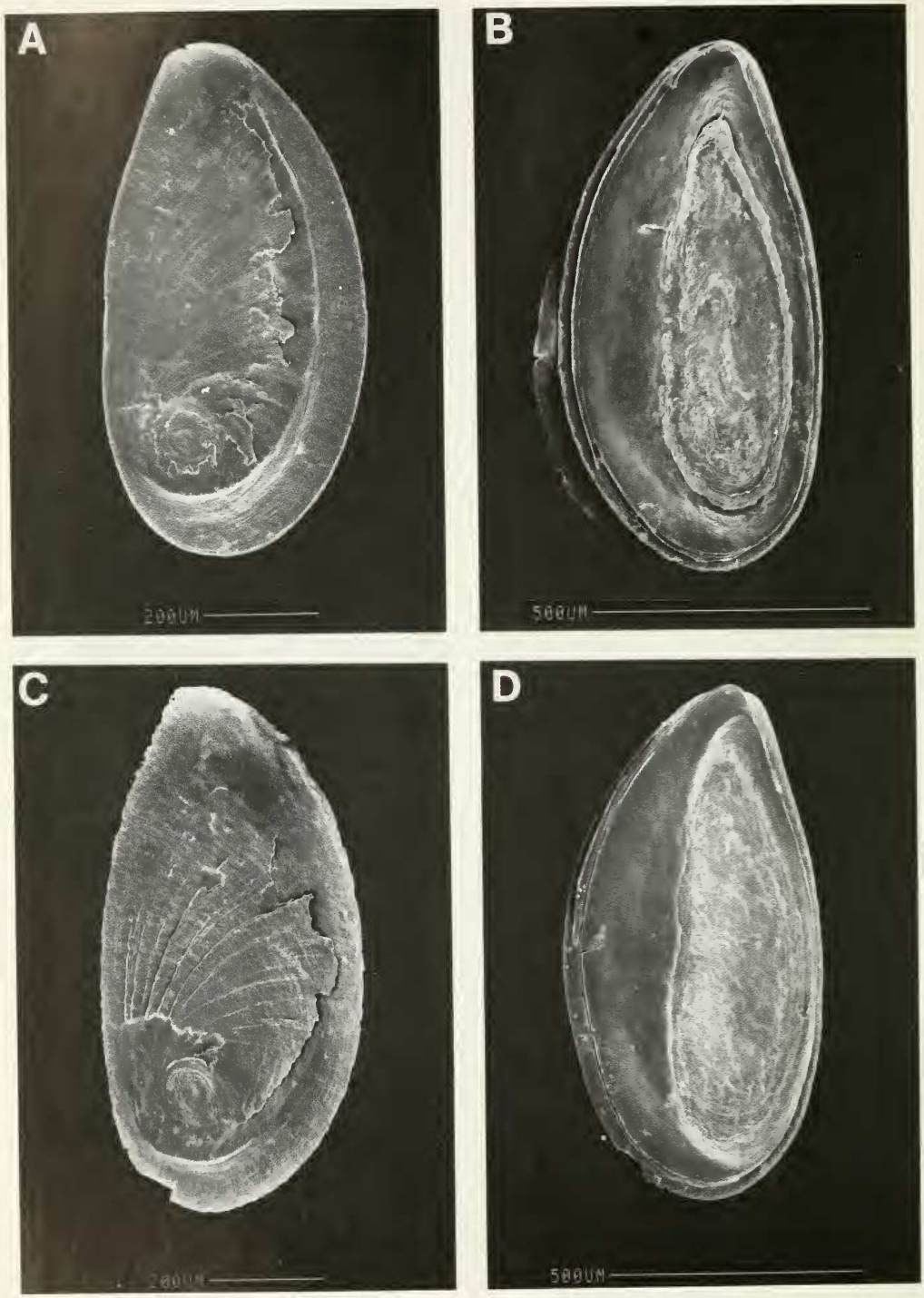

FIG. 83. Opercula of *Neotricula duplicata* from D87-2.

TABLE 42. Lengths (mm) or counts of non-neural organs of *Neotricula duplicata*. Mean ± standard deviation (range). For D87-2 snails, N = 5 for females, N = 4 for males; for D85-79 snails, N = 5 for females, N = 3 for males unless stated otherwise.

	Females		Males	
	D87-2	D85-79	D87-2	D5-79
Body	4.99±0.45 (4.46–5.70)	4.90±0.51 (4.20–5.46)	4.43±0.14 (4.30–4.56)	4.31±0.02 (4.30–4.34)
Digestive gland	1.95±0.46 (1.30–2.50)	2.03±0.20 (1.74–2.30)	2.02±0.14 (1.86–2.20)	1.92±0.14 (1.76–2.00)
Gonad	0.61±0.13 (0.48–0.74) N = 4	0.75±0.05 (0.70–0.80)	1.50±0.38 (1.20–2.10)	1.23 N = 2 (1.16, 1.30)
Total pallial oviduct (= TPO)	1.70±0.20 (1.50–1.90) N = 3	2.04±0.34 (1.78–2.50) N = 4	—	—
Bursa copulatrix (= Bu)	0.47±0.12 (0.30–0.60) N = 4	0.48±0.05 (0.44–0.56)	—	—
Duct of bursa	0.17±0.06 (0.10–0.20) N = 3	0.10 No var. N = 2	—	—
Bu ÷ TPO	0.32±0.12 (0.20–0.43) N = 3	0.23±0.04 (0.18–0.30)	—	—
Seminal receptacle	0.21±0.07 (0.16–0.30)	0.25±0.05 (0.18–0.26)	—	—
Duct of seminal receptacle	0.06 No var. N = 2	0.06 N = 1	—	—
Mantle cavity	1.51±0.18 (1.26–1.70)	1.48±0.07 (1.40–1.56) N = 4	1.33±0.04 (1.30–1.38)	1.35±0.19 (1.14–1.52)
Ctenidium (= CT)	1.27±0.19 (1.00–1.50)	1.28±0.09 (1.20–1.36) N = 4	1.07±0.09 (1.00–1.20)	1.15±0.19 (0.94–1.30)
Osphradium (= OS)	0.37±0.13 (0.20–0.48)	0.37±0.03 (0.34–0.40) N = 3	0.35±0.06 (0.28–0.36)	0.36±0.13 (0.24–0.50)
No. gill filaments	19.3±1.7 (17–21)	18.0±1.4 (16–19) N = 4	17.0±1.2 (16–18)	23.6±7.1 (16–30)
OS ÷ CT	0.30±0.11 (0.17–0.44)	0.29±0.04 (0.23–0.28) N = 3	0.33±0.07 (0.23–0.40)	0.32±0.10 (0.20–0.38)
Gf_1	0.20±0.09 (0.12–0.34) N = 8	0.28±0.05 (0.24–0.36) N = 4	—	—
Gf_2	0.24±0.07 (0.20–0.30) N = 8	0.23±0.03 (0.20–0.26) N = 4	—	—
Total Gf	0.46±0.08 (0.32–0.56) N = 8	0.50±0.05 (0.44–0.50) N = 4	—	—
$Gf_2 \div Gf_1 + Gf_2$	0.43±0.15 (0.25–0.63)	0.54±0.07 (0.48–0.64) N = 4	—	—
Prostate	—	—	0.85±0.13 (0.70–1.00)	0.87±0.06 (0.80–0.90)
Seminal vesicle	—	—	0.53±0.22 (0.20–0.70)	0.45±0.09 (0.40–0.56)
Penis	—	—	1.16±0.27 (0.90–1.54)	1.51±0.22 (1.36–1.76)

illustrated. Measurements and counts are given in Table 42. The osphradium is approximately mid-gill; it is short (ratio of 0.29). The shape of the osphradium is lunate, not oval. The number of gills ranges from 17 to 30. Gill filament section Gf_2 is normal; the length of the longer gill filaments is 0.46 to 0.50 mm long. The shape of the gill leaflet in side view is moderate to high domed. There is no circular patch of white or yellowish granules just

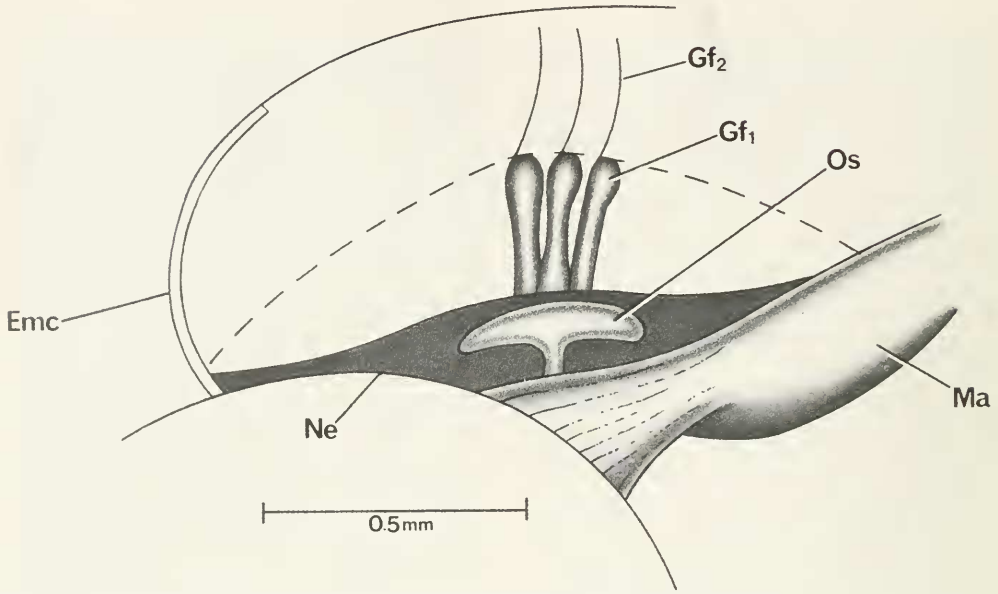

FIG. 84. Mantle cavity organs of *Neotricula duplicata* from D89-79. Dashed line is the trajectory for measuring length of gill and mantle cavity. Only three central gill filaments are illustrated.

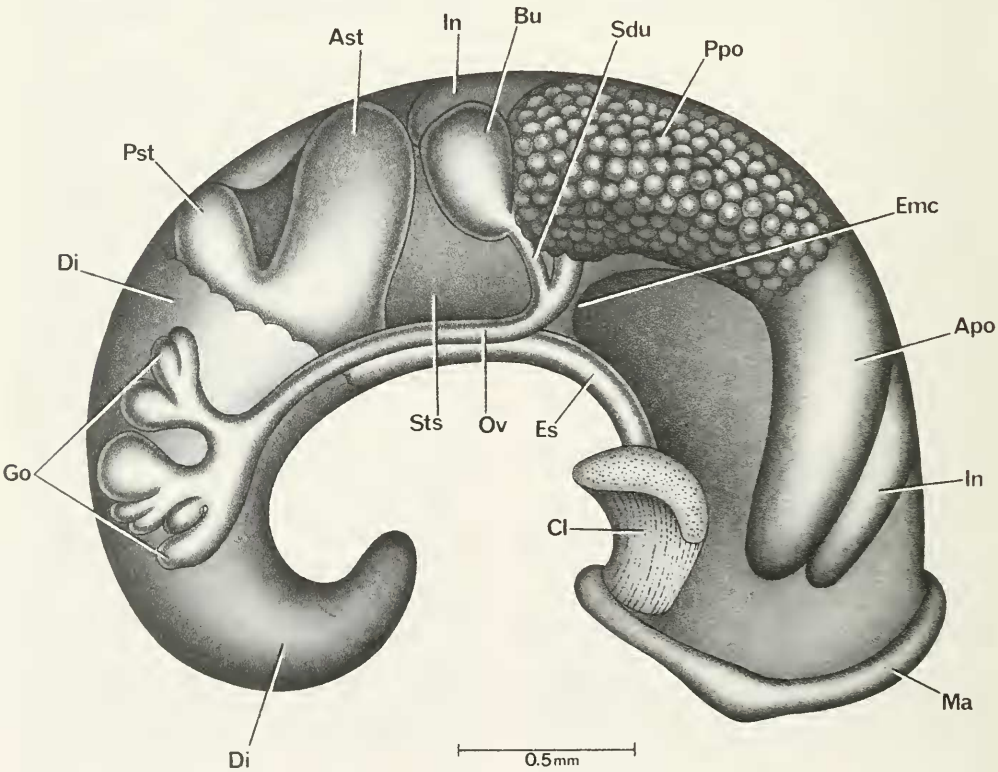

FIG. 85. Uncoiled female *Neotricula duplicata* with head and kidney tissue removed; from D85-79.

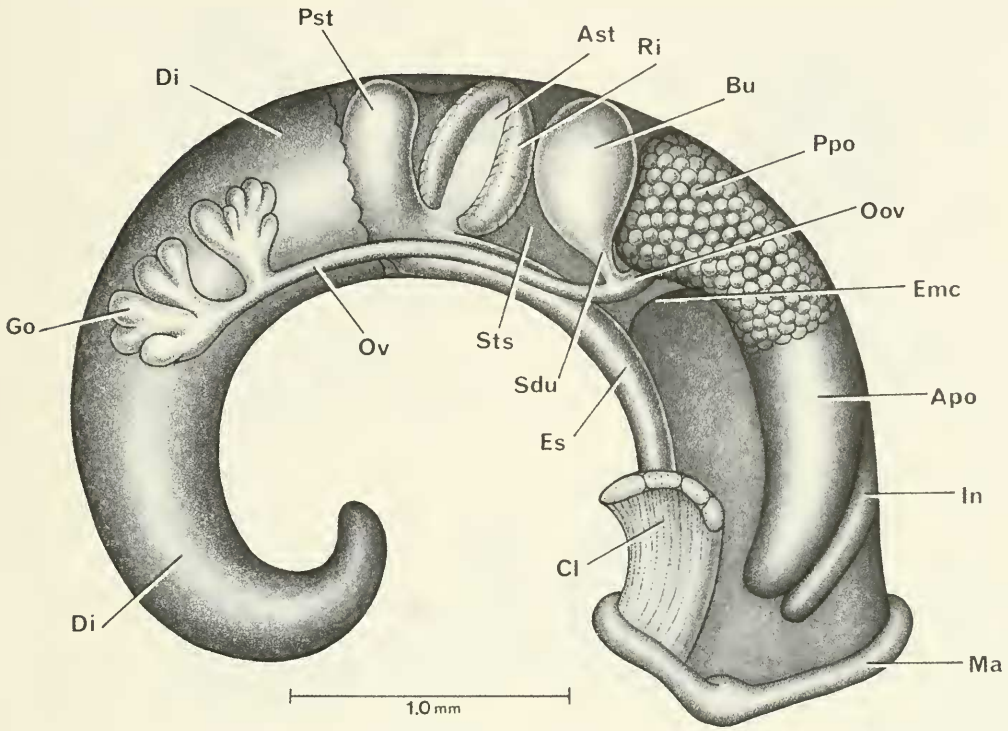

FIG. 86. Uncoiled female *Neotricula duplicata* with head and kidney tissue removed from D87-2.

anterior to the osphradium next to the neck-mantle collar (Ma) juncture.

Female reproductive system. The bodies of uncoiled females without head or kidney tissue are shown in Figures 85, 86. Organ measurements are given in Table 42. Important features are: (1) The gonad is posterior to the stomach; it is relatively short and of few lobes. (2) The albumen gland (Ppo) is of normal length. (3) The bursa copulatrix (Bu) is clearly visible posterior to the albumen gland; the bursa is small and round to oval. (4) The oviduct runs from the gonad to the albumen gland without coiling. (5) The bursa copulatrix complex of organs is shown in Figures 87, 88. Figure 87A is positioned exactly as in Figures 85, 86. The spermathecal duct (Sd) opens into the posterior mantle cavity; it is short and swollen in most specimens. (6) The seminal receptacle (Sr) arises from the dorsal surface at the juncture of the duct of the bursa and the spermathecal duct. (7) The duct of the seminal receptacle (Dsr) slowly increases in diameter to form a club-shaped (not spherical) storage sac that lies dorsal to the bursa copulatrix. In some specimens, it is clear that the seminal receptacle is a U-shaped continuation of the duct of the bursa and that the spermathecal duct attaches at the bottom of the "U" (Fig. 88C). (8) The sperm duct (Sdu) arises from the duct of the bursa on the ventral side just posterior to the duct of the seminal receptacle.

Male reproductive system. The posterior section of an uncoiled male with kidney tissue removed is shown in Figure 89. It is the same in specimens from both D85 and D87 collections. The outline of the gonad (Go) is shown (dashed line) but most of the lobes of the gonad are removed to show the seminal vesicle (Sv) coiled dorsal to the gonad. Measurements of organs are given in Table 42. Important features are: (1) The gonad overlaps the posterior part of the posterior chamber of the stomach (Pst). (2) The prostate (Pr) overlaps the posterior end of the mantle cavity (Emc) and covers the style sac. (3) The seminal vesicle, while coiling dorsal to the gonad, does not extend over the stomach. (4) The anterior vas deferens leaves the prostate (Pr) close to

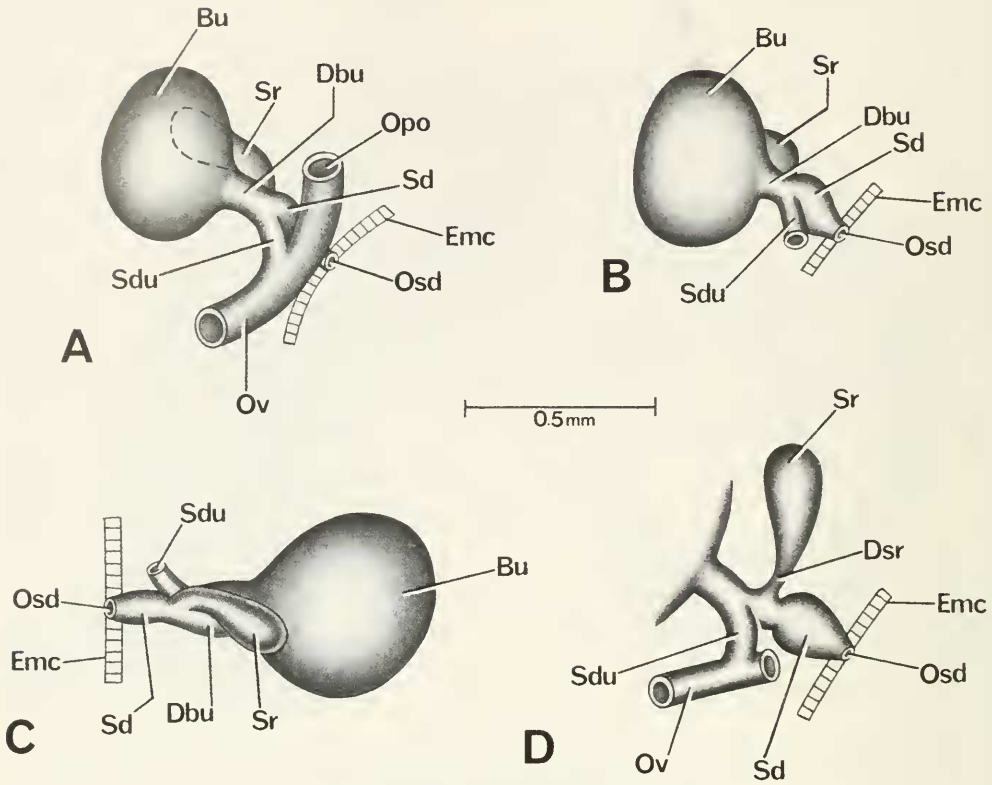

FIG. 87. Details and variation of bursa copulatrix complex of organs of *Neotricula duplicata* from D85-79. Figure A is in same orientation as in Figures 85 and 86. B. Swelling of spermathecal duct (Sd) seen in most individuals. C. Bursa complex seen in B flipped over 180° so that Emc is to left; this view shows juncture of duct of the bursa (Dbu), seminal receptacle (Sr) and spermathecal duct (Sd). D. As in A, but with oviduct (Ov) pulled to left to show the juncture of Dsr and Sd with duct of bursa.

TABLE 43. Radular statistics for *Neotricula duplicata*. Mean ± standard deviation (range). In mm except for the width of the central tooth in μm. N = number counted.

	D85-77	D87-2
Shell length (not eroded)	3.20±0.26 (2.84–3.60) N = 8	3.43±0.21 (4.44–5.20)
Radula length	0.55±0.04 (0.66–0.60) N = 11	0.57±0.04 (0.52–0.62) N = 10
Radula width	0.08±0.004 (0.072–0.088) N = 11	0.08±0.006 (0.078–0.092) N = 10
Total rows of teeth	70.4±4.1 (61–74) N = 8	60.1±8.0 (46–69) N = 10
No. rows of teeth forming	9.0±2.1 (7–13) N = 8	10.3±3.3 (6–15) N = 10
Central tooth width	15.5±0.8 (14.6–16.8) N = 9	17.1±1.5 (15.8–19.0) N = 7

the posterior end of the mantle cavity (Emc). (5) The penis is simple, with a small evertible papilla (Fig. 90B). In some specimens, the papilla is withdrawn and cannot be seen (living tissue, fresh microscope mount). In others, only the tip of the papilla can be seen being

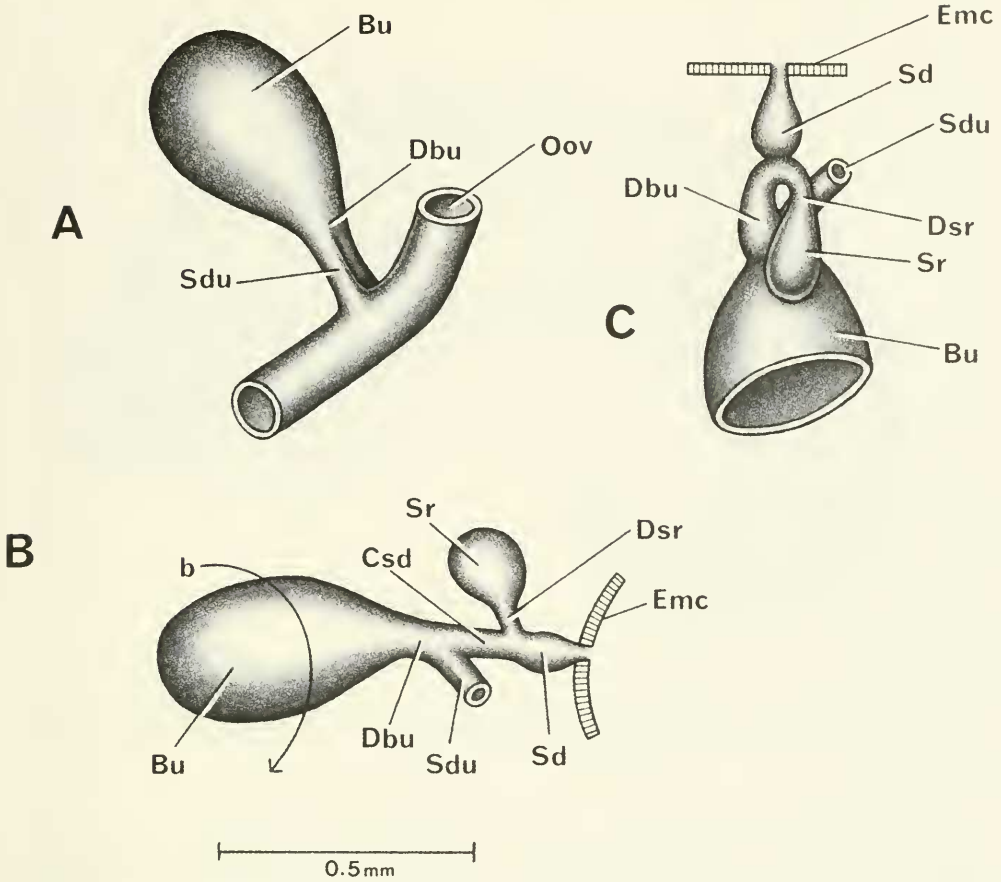

FIG. 88. Details and variation of bursa copulatrix complex of organs of *Neotricula duplicata* from D87-2. Figure A is in same orientation as in Figures 85 and 86. B–C. Variation in configuration of seminal receptacle (Sr). B. Bursa complex rotated in the direction of arrow to show interconnections of Dbu, Csd, Sr and Sd. C. Dorsal side of bursa complex to show that duct of bursa (Dbu) makes a U-shaped bend into duct of seminal receptacle (Dsr). Swollen short spermathecal duct (Sd) enters bottom of U-shaped bend. Note: Common sperm duct (Csd) is that portion of duct extending from duct of bursa between Sdu and Sd. Duct of bursa is defined in all papers as that duct extending from bursa copulatrix (Bu) anteriorly to point where another sperm duct connects to it, e.g. the Sdu.

pushed out and then withdrawn. (6) The base of the penis (Bp, Figs. 81, 90A) is oriented on the neck in diverse ways. The angle of the long axis of attachment varies from parallel to the mid-line of the snout-neck (x) through 90°. The base may overlap the mid-line or be to the right of mid-line. (7) No ejaculatory duct is seen in the base of the penis or in the neck.

Digestive system. The digestive gland is posterior to the stomach in both sexes. However, in some males of the D87-2 collection both digestive gland and gonad covered the posterior chamber of the stomach.

Radular statistics are given in Tables 43 and 44. The most commonly encountered formula in the D85-79 collection was:

$\frac{2\text{-}1\text{-}2}{2(3)\text{-}(3)2}$; 3-1[2]-3(2); 12-15; 11-14;

in the D87 2 collection it was:

$\frac{3(2)\text{-}1\text{-}(2)3}{3(2)\text{-}(2)3}$; 3(4)-1-3; 12-14; 11-13.

SEM photographs of radulae from snails of both collections are given in Figures 91–94 No significant differences occur between the

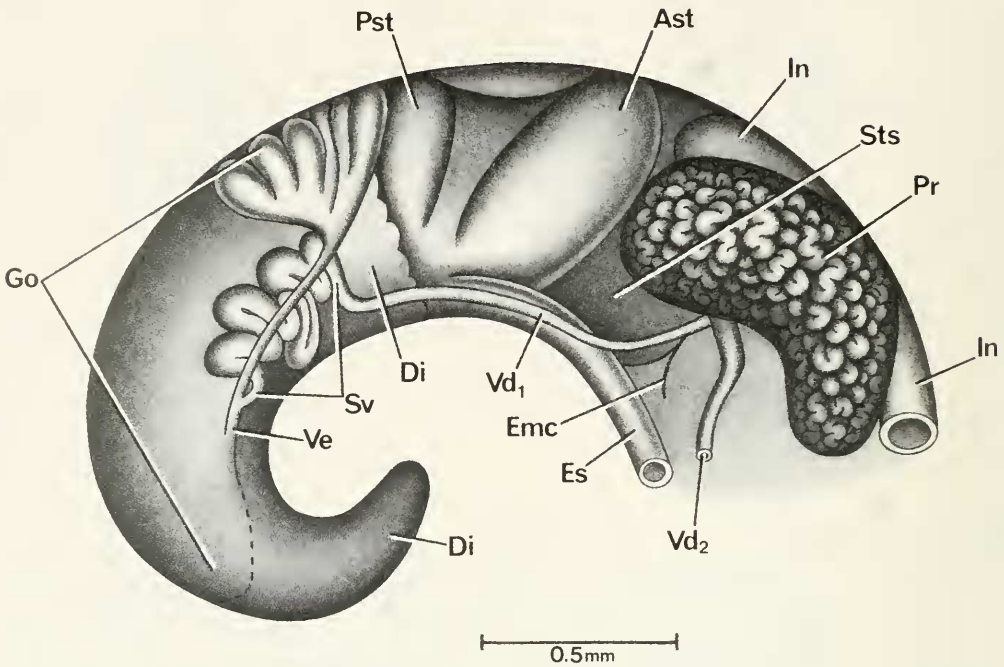

FIG. 89. Uncoiled male of *Neotricula duplicata* from D85-79. Anterior part of mantle cavity omitted. Posterior lobes of the gonad (Go) removed to show coiled seminal vesicle (Sv) dorsal to gonad. Dashed line indicates extent of gonad.

snails of the two collections; the tooth morphologies are the same and are typical of the generalized triculine type. Of note is the split or fork in the dominant central cusp of the lateral tooth (i.e. the "1" of the 3-1-3) (Fig. 91C, 92C, D, 93G, 94C).

The stomach has a noteworthy character. The anterior chamber of the stomach (Ast, Fig. 95) has at the anterior and posterior edges prominent yellow ridges (Yri).

Nervous system. Measurements of neural structures are given in Table 45. The RPG ratio indicates a moderately concentrated dorsal aspect of the nerve ring.

Remarks

These detailed anatomical studies of a single population collected two years apart provide a unique opportunity to assess (1) how well methods provide an adequate assessment of qualitative and quantitative characterstokes. The 1987 study is a control for the 1985 study, particularly as it was not remembered in 1987 that the 1985 assessment had been made. (2) Variation due to sampling (in part) and actual quantitative changes that could have occurred in two years. This is the first time that we have obtained an indication of the amount of variation that might be expected in such a study. This is of considerable help in assessing how much difference may actually exist when comparing two populations, each studied only once, e.g. between *N. cristella* and *N. dianmenensis* of this monograph.

Overall, there was excellent agreement in qualitative anatomy when comparing the two year classes. There was significant variation in cusp counts between year classes, particularly involving the marginal teeth. More variation occurred in central tooth cusp numbers in the 1987 year class.

Conchologically, *N. duplicata* is most similar to *N. dianmenensis*, *N. lilii*, and *Tricula gredleri* (Figs. 153, 154). Differences from *N. dianmenensis* are given on page 234. *Neotricula duplicata* differs from *T. gredleri* in three characters (10%). The former has spiral microsculpture lacking in the latter (char. 6). The former has an abapical spout lacking in the

TABLE 44. Cusp formulae for the radular teeth of *Neotricula duplicata* with the percent of radulae in which a given formula was found at least once.

Central Teeth (N = 10)		Lateral Teeth		Inner Marginal Teeth		Outer Marginal Teeth	
			D85-79				
2-1-2 / 3-3	70%	3-1[2]-3	100%	9	—	9	10%
2-1-2 / 2-2	30%	3-1[2]-2	50%	10	10%	10	20%
2-1-2 / 3-2	30%	4-1[2]-3	30%	11	20%	11	60%
2-1-2 / 2-3	20%	2-1[2]-3	20%	12	50%	12	70%
3-1-3 / 2-2	10%			13	100%	13	60%
3-1-2 / 2-2	10%			14	90%	14	40%
				15	50%	15	—
				16	30%	16	—
				17	20%	17	—
				$\bar{X}$* = 13.6±1.5		12.0±1.1	
				N = 108		120	
			D87-2				
3-1-3 / 3-3	60%	3-1[2]-3	100%	11	—	11	40%
2-1-2 / 3-3	50%	4-1[2]-3	40%	12	70%	12	90%
2-1-2 / 2-3	40%	3-1[2]-4	30%	13	80%	13	30%
3-1-3 / 2-2	30%	2-1[2]-3	10%	14	60%	14	20%
2-1-2 / 3-2	20%	3-1[2]-2	10%	15	20%	15	—
2-1-2 / 2-2	10%			$\bar{X}$ = 12.9±0.7		12.1±1.3	
				N = 100		N = 100	
3-1-3 / 2-3	10%						
3-1-2 / 3-3	10%						
2-1-2 / 3-2	10%						
2-1-3 / 3-3	10%						

*Mean ± standard deviation of cusp number for all teeth counted.

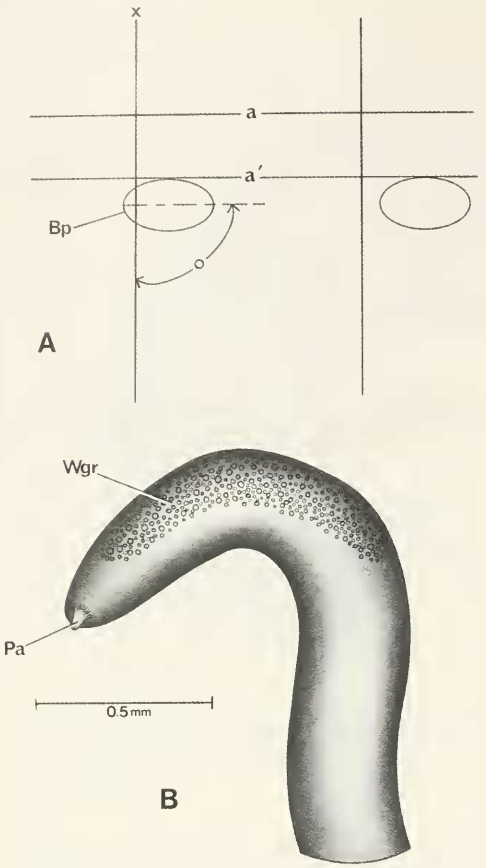

FIG. 90. A. The position of base of the penis of *Neotricula duplicata* relative to the snout-neck mid-line (x). B. Penis.

latter (char. 12). The latter has an adapical beak tubercle lacking in the former (char. 24). Anatomical differences are considerable, those used to define the genera among others (Fig. 157).

Conchologically, *N. duplicata* differs from *N. lilii* by having a wrinkled protoconch, not a smooth one (char. 8); having an adapical beak instead of a notch (char. 9); having a straight to arched inner lip, not a sinuate one (char. 13); having a thick inner lip, not a thin one (char. 19); by lacking a slight varix found in the latter (char. 23); and by lacking an adapical outer lip angle seen in the latter (char. 25). Anatomically, these species differ in nine characters (19%) (Figs. 157, 158). The differences are: The former has an elongated oval operculum with two or more layers (chars. 2, 3); the latter has an ovate operculum with one layer. The opercular attachment pad is very wide in the former, wide in the latter (char. 4). Gill filament section Gf_2 is of medium length in the former, long in the latter (char. 8). The bursa shape is ovoid in the former, round in the latter (char. 15). The spermathecal duct is short in the former, long in the latter (char. 19). The spermathecal duct runs directly anterior from the duct of the bursa to the mantle cavity in the former; it slants away at an angle in the latter (char. 20). The vas deferens bends away from the prostate at the posterior end of the mantle cavity in the former, at mid-prostate in the latter (char. 31). *Neotricula lilii* has very many rows of teeth on the radula; *N. duplicata* has many (char. 42).

***Neotricula lilii* Chen & Davis, sp. nov.**

Holotype. ZAMIP-M0002, Figure 70J.

Paratypes. ANSP 373138, A12654, Figure 70 K, L Figure 96A-D.

Type Locality. Chang Wang Village, Chuanxing Town, Lingxian County, Zhuzhou Prefecture. 26°17′18″N, 113°41′3″E. Figure 1, Site 2.

Etymology. Named for Dr. Li Li, Zhuzhou Prefectural Epidemic station, who collected this species.

Habitat

The assigned field collection number was D85-74. Snails came from a mountain stream 550 m above sea level. The stream was 10 to 15 cm deep, with small rocks, leaves and mud. There was low vegetation beside the stream.

Description

Shell. The shells are small, ovate-conic, with 5.5 to 6.0 whorls (Figs. 60A–B, 70J–L, 96A–B). Measurements are given in Tables 46, 47. Limited data suggest that females are larger than males (Table 47) with the lengths of the last three whorls of females ranging from 2.98–3.28; those for males, 2.72–2.80. The aperture is pyriform. Adapically there is a wide apertural notch; there is no beak tubercle.

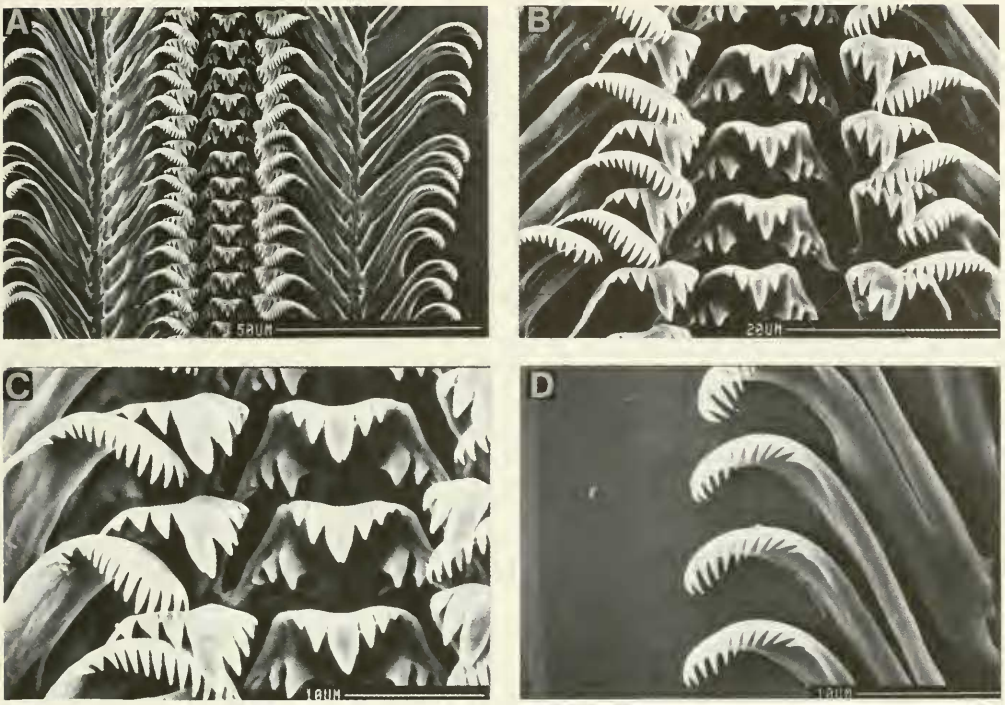

FIG. 91. Radula of *Neotricula duplicata* from D85-79. Centrals, laterals and inner marginals featured in B, C. D. Outer marginals.

TABLE 45. Lengths (mm) of neural structures of *Neotricula duplicata*. Mean ± standard deviation (range). * = neural elements measured to calculate the RPG ratio. N = number measured.

	D85-79 (N = 4)	D87-2 (N = 5)
Cerebral ganglion	0.26±0.03 (0.22–0.30)	0.24±0.03 (0.24–0.26)
Cerebral commissure	0.05±0.02 (0.02–0.06)	0.04±0.01 (0.03–0.06)
Pleural ganglion		
Right (1)*	0.14±0.03 (0.10–0.16)	0.13±0.02 (0.10–0.16)
Left	0.12±0.03 (0.08–0.14)	0.12±0.01 (0.10–0.12)
Pleuro-supraesophageal connective (2)*	0.14±0.04 (0.10–0.18)	0.11±0.02 (0.10–0.14)
Pleuro-subesophageal connective	0.06±0.05 (0.00–0.10)	0.06±0.02 (0.03–0.08) N = 4
Supraesophageal ganglion (3)*	0.13±0.02 (0.10–0.14)	0.12±0.02 (0.10–0.14)
Subesophageal ganglion	0.11±0.02 (0.10–0.12)	0.11±0.01 (0.10–0.12) N = 4
Osphradio-mantle nerve	0.08±0.01 (0.06–0.08)	0.08±0.04 (0.00–0.12)
RPG ratio (2 ÷ 1+2+3)*	0.34±0.08 (0.26–0.45)	0.31±0.03 (0.28–0.35)

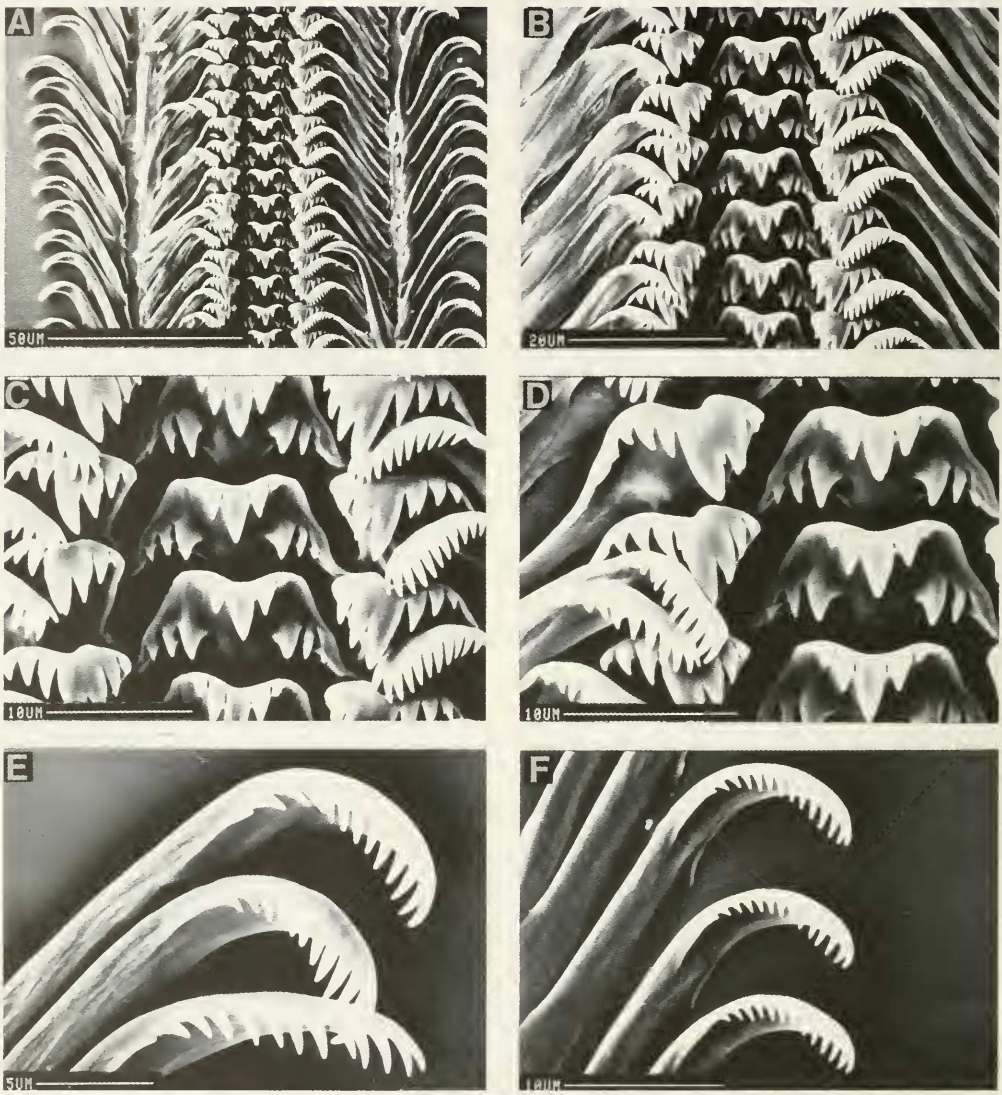

FIG. 92. Radula of *Neotricula duplicata* from D85-79. Centrals, laterals and inner marginals featured in B–D. E, F. Outer marginals.

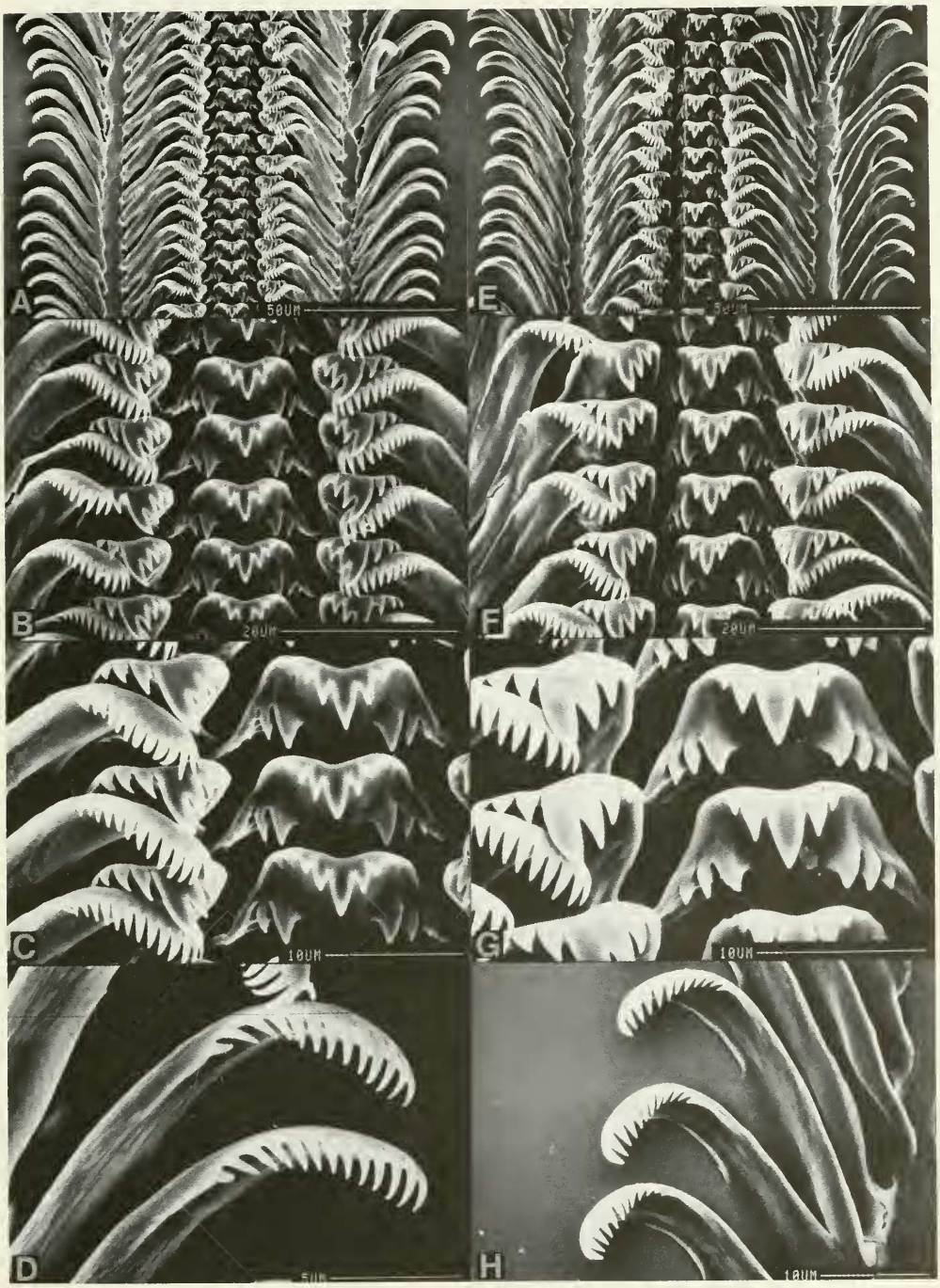

FIG. 93. Radula of *Neotricula duplicata* from D87-2. Centrals, laterals and inner marginals featured in B, C, E, G. D, H = outer marginals. A–D = males; E–H = females.

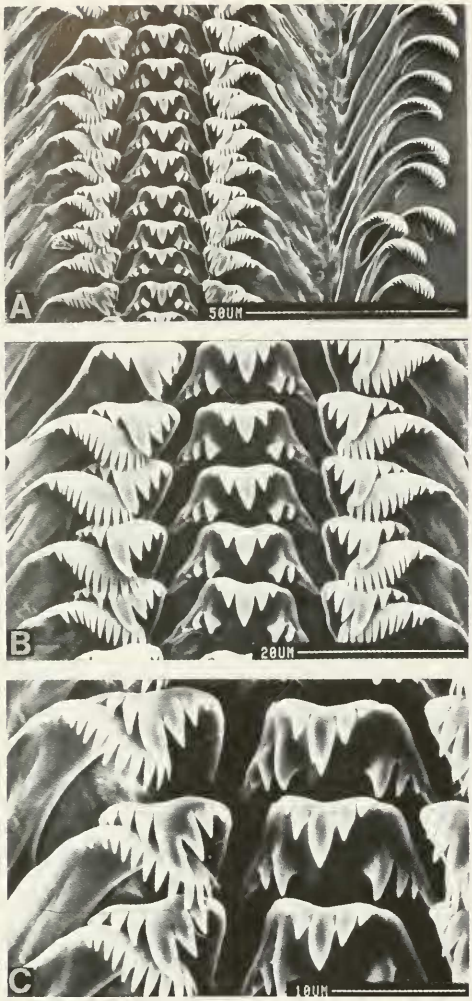

FIG. 94. Radula of female *Neotricula duplicata* from D87-2.

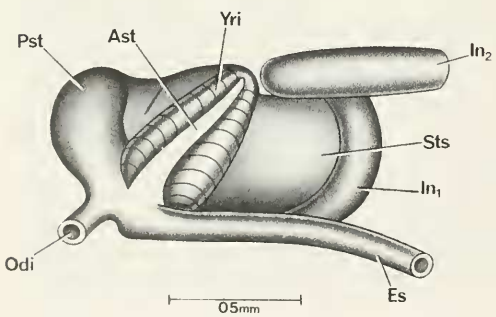

FIG. 95. Ventral aspect of the stomach of *Neotricula duplicata* in same orientation as in Figures 85, 86.

There is no internal notch groove. There is a pronounced adapical outer lip angle.

The whorls at the sutures are smooth (not crenulated). There is an umbilicus. SEM analysis reveals faint spiral microsculpture at the shoulders of the whorls after 1.75 whorls (Fig. 96A, C).

The inner lip is slightly sinuate and clearly separated from the body whorl in most specimens; it is uniformly thickened. In some (< 20%), the adapical inner lip is fused to the body whorl. The adapical end of the aperture is only slightly separated from the body wall. An apertural sinus is apparent examining the outer lip in side view. In side view, the outer lip, abapical to the sinus, is straight. The outer lip is slightly scooped forward. In side view, the inner lip has a strong deflection angle. There is a slight varix. There is an abapical spout. The abapical lip projects beyond the base of the shell 0.50 ± 0.05. SEM examination of the shell reveals that the apical whorl is smooth. (Fig. 96D).

External features. The head is grey. There are no granules about the eyes and no "eyebrow." The operculum is corneous and paucispiral. The inner lip edge is straight abapically and slightly sinuate towards the apertural beak end (adapically). The muscle attachment callus is pronounced and narrow, only 40% of the operculum width. A porous, regularly pitted surface of the callus was found in most specimens (75%) (Fig. 96E–H).

Mantle cavity. Measurements and counts of mantle cavity structures are given in Table 48. The ovoid osphradium is mid-gill; it is short. There are 20–24 gill filaments. Gf_2 is long. The length of the longest filament is 0.51 mm. The larger gill filaments are moderately domed. There is no spherical patch of white granules anterior to the osphradium where the mantle collar joins the neck.

Female reproductive system. The body of an uncoiled female without head or kidney tissue is shown in Figure 97. Organ measurements are given in Table 48. Important features are: (1) The gonad (Go) is posterior to the stomach; it is short and consists of few groups or bundles of lobes. (2) The bursa copulatrix (Bu) is spherical and prominent posterior to the albumen gland (Ppo). (3) The bursa is short. (4) The albumen gland is standard (= normal) length. (5) The bursa copulatrix complex of organs is shown in Figure 98A, B in the same orientation as in Figure 97. The nar-

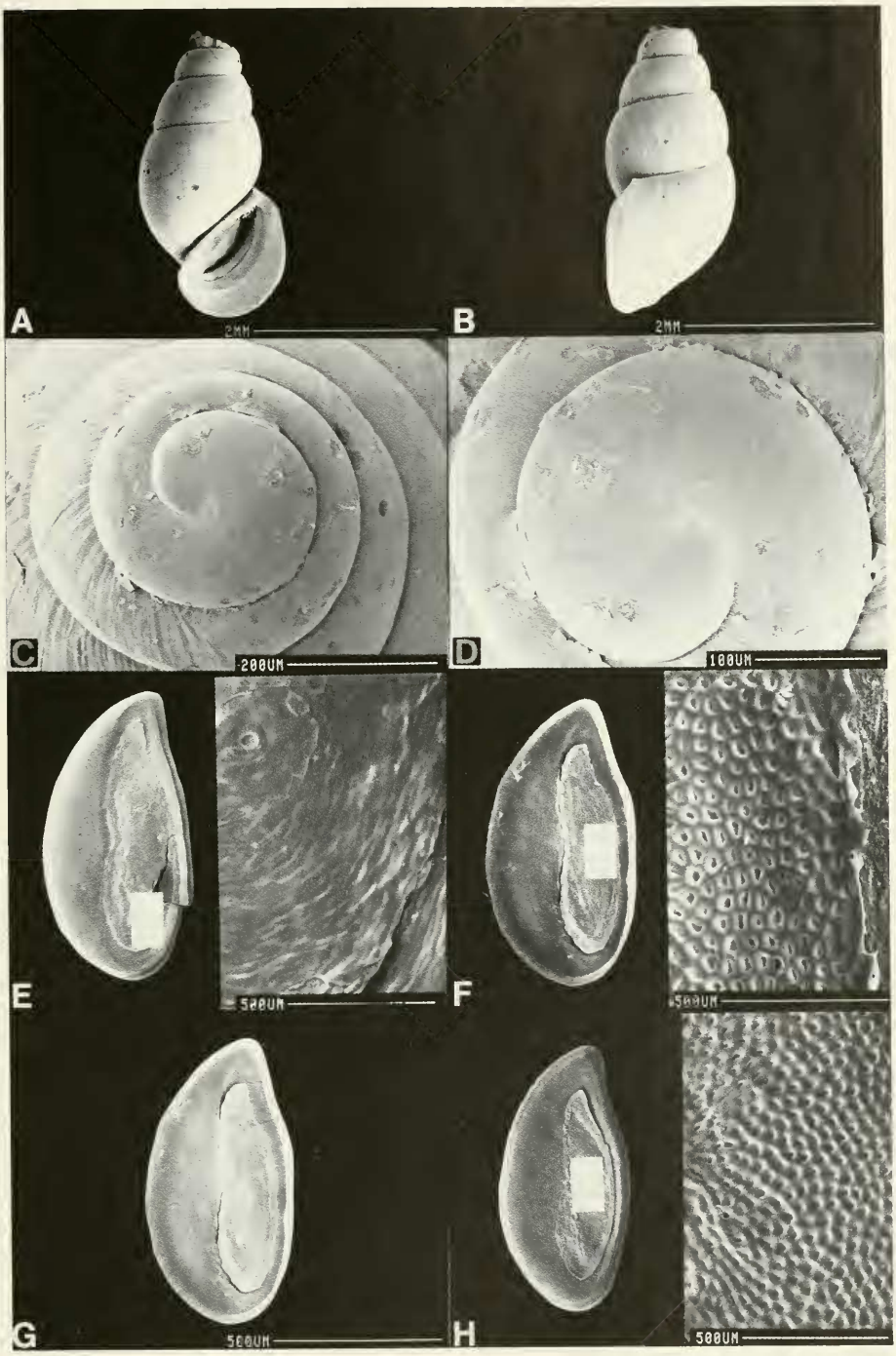

FIG. 96. SEM photographs of shells and operculum of *Neotricula lilii*. C, D. Enlargements of apical whorls. E–H. Inner surfaces of four opercula; insets provide enlargements of attachment pads to reveal microstucture.

TABLE 46. Shell measurements (mm) for the types of *Neotricula lilii*. Mean ± standard deviation (range). e = eroded apical whorls. N = number measured.

		Paratypes	
	Holotype	Larger (N = 1)	Smaller (N = 4)
No. Whorls	5.5	4e	4e to 5.5
Length (L)	3.20	3.20	2.98±0.18 (2.76–3.20)
Width (W)	1.52	1.68	1.51±0.10 (1.38–1.62)
L last three whorls	2.76	3.00	2.70±0.11 (2.54–2.80)
L body whorl	1.96	2.20	1.90±0.09 (1.76–1.96)
L penultimate whorl	0.48	0.48	0.49±0.02 (0.48–0.52)
W penultimate whorl	0.98	1.12	1.03±0.05 (0.96–1.08)
W 3rd whorl	0.72	0.80	0.72±0.04 (0.68–0.76)
L aperture	1.40	1.60	1.39±0.10 (1.24–1.48)
W aperture	0.92	1.04	0.93±0.06 (0.86–1.00)
x	0.52	0.56	0.50±0.05 (0.44–0.56)
y	0.12	0.20	0.15±0.04 (0.12–0.20)

TABLE 47. Shell measurements (mm) for *Neotricula lilii* used for anatomical work. Mean ± standard deviation (range). e = eroded apical whorls. N = number measured.

	Females		Males
	Larger Size Class (N = 3)	Small Size Class (N = 1)	(N = 3)
No. Whorls	4e–6.0	5.75	3e–4e
Length (L)	3.43±0.19 (3.20–3.56)	3.12	2.89±0.12 (2.76–3.00)
Width (W)	1.63±0.08 (1.56–1.72)	1.48	1.47±0.06 (1.40–1.52)
L last three whorls	3.11±0.15 (2.98–3.28)	2.72	2.76±0.04 (2.72–2.80)
L body whorl	2.21±0.12 (2.08–2.28)	1.92	1.95±0.06 (1.88–2.00)
L penultimate whorl	0.55±0.04 (0.52–0.60)	0.48	0.49±0.04 (0.44–0.52)
W penultimate whorl	1.13±0.06 (1.08–1.20)	1.00	1.03±0.04 (1.00–1.08)
W 3rd whorl	—	—	—
L aperture	1.59±0.10 (1.48–1.68)	1.32	1.35±0.08 (1.28–1.44)
W aperture	0.99±0.02 (0.96–1.00)	0.96	0.89±0.02 (0.88–0.92)
x	0.52±0.06 (0.44–0.56)	0.52	0.45±0.02 (0.44–0.48)

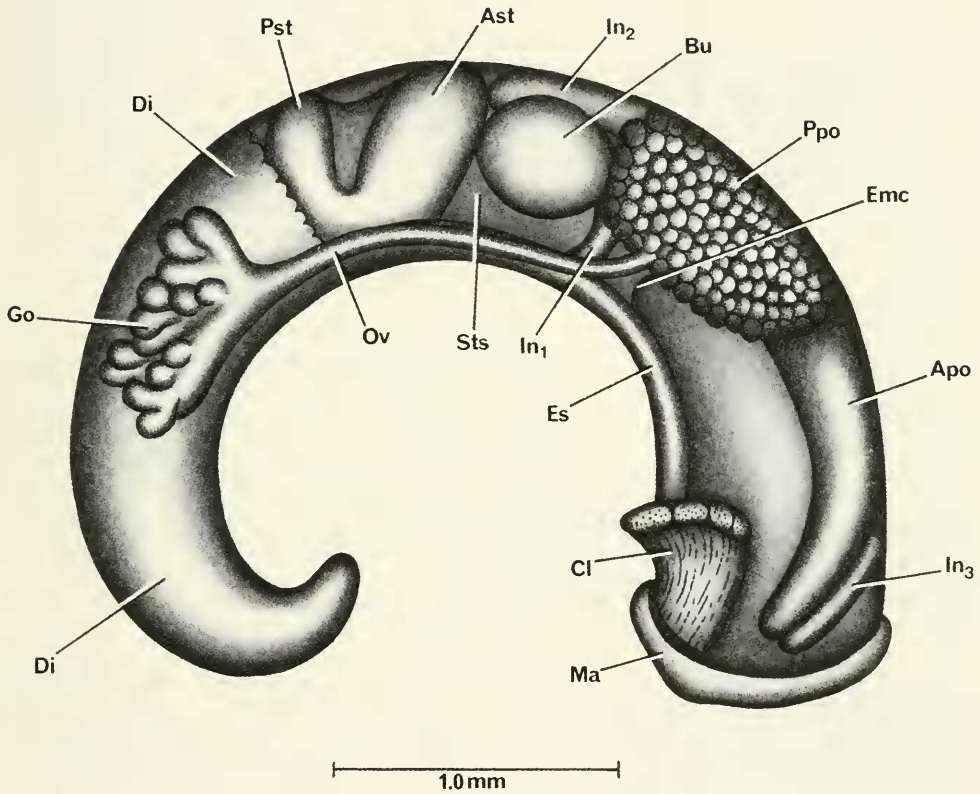

FIG. 97. Uncoiled female *Neotricula lilii* with head and kidney tissue removed.

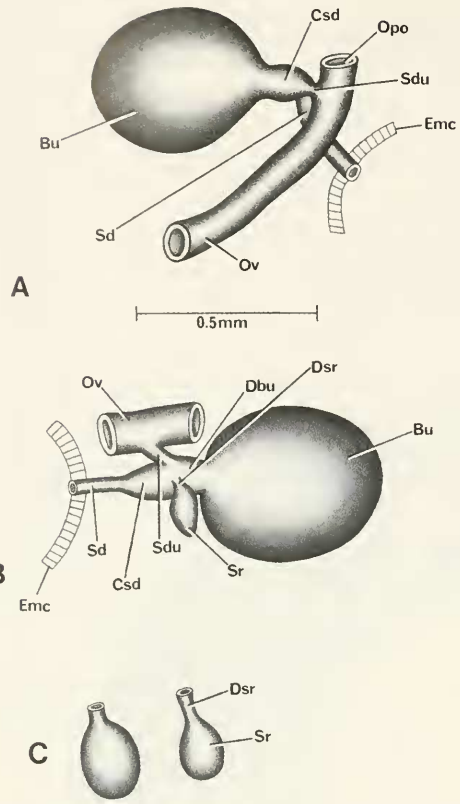

FIG. 98. Details and variation of bursa copulatrix complex of organs of *Neotricula lilii*. Figure A is in same orientation as in Figure 97. B. Bursa flipped over to show place where seminal receptacle (Sr) enters common sperm duct (Csd). C. Variation in size and shape of seminal receptacle.

row spermathecal duct dilates to form the common sperm duct (Csd) from which opens the sperm duct (Sdu) and the seminal receptacle (Sr) (Fig. 98 B). (6) The sperm duct is very short and to the left of the common sperm duct. (7) The seminal receptacle arises some 45° from the opening of the sperm duct; it arises from the right dorso-lateral side of the sperm duct. (8) The seminal receptacle varies in shape from elliptical to sub-spherical (Fig. 98C); it has a very short duct (Dsr). (9) The duct of the bursa (from the bursa to openings of Dsr and Sdu) is extremely short. (10) The distance from the posterior end of the mantle cavity (Emc) to the bursa is short, only 0.16 mm to 0.32 mm. The spermathecal duct—common sperm duct run straight posteriorly from the end of the mantle cavity to the bursa.

Male reproductive system. A section of an uncoiled male without kidney tissue is shown in Figure 99. The anterior gonadal lobes are removed to show the seminal vesicle (Sv). Organ measurements are given in Table 48. Important features are: (1) The gonad (Go) slightly overlaps the posterior chamber of the stomach. (2) The seminal vesicle (Sv) arises from the vas efferens (Ve) at mid-gonad to slightly posterior to mid-gonad. (3) The prostate (Pr) overlaps the posterior end of the mantle cavity and covers half the style sac (Sts). (4) The anterior vas deferens (Vd_2) diverges from the prostate slightly anterior to the posterior end of the the mantle cavity. (5) The penis is simple with a papilla (Pa) that everts (Fig. 100B). There is a massive concentration of white granules along the anterior convex edge. (6) The penis arises to the right of the snout-neck mid-line (Fig. 100A). The long axis of the penial base (Bp) is swollen at its base increasing the diameter from 0.14 mm to 0.22 mm. (7) No ejaculatory duct is seen in the penial base or neck.

Digestive system. The digestive gland is posterior to the stomachs of both males and females. Radular statistics are given in Tables 49 and 50. The radula is illustrated in Figures 101, 102. The central tooth is the generalized triculine type (Fig. 101B, E). The dominant cusp of the lateral tooth (the "1" of the 3-1-3) is almost always bifurcated (Fig. 101). The most commonly encountered cusp formula is

$$\frac{3(2)\text{-}1\text{-}(2)3}{2\text{-}2};\ 3\text{-}[2]\text{-}3(4);\ 13\text{-}15;\ 12\text{-}14.$$

Nervous system. It is standard triculine. Measurements are given in Table 51. The RPG ratio of 0.44 indicates that the dorsal nerve ring is moderately concentrated.

Remarks

Conchologically, *N. lilii* is most similar to *N. duplicata* and *N. dianmenensis* (Figs. 153–155). The comparison of these three species is given in the remarks section for the two previously treated species. Anatomically, *N. lilii* is most similar to *N. cristella*, a species that has a very different shell (Figs. 154, 156–158). There are five differences (Tables 80, 81) (10%): *N. lilii* has an operculum with a single layer whereas the operculum of *N. cristella*'s has two or more layers (char. 3). The former

TABLE 48. Lengths (mm) or counts of non-neural organs and structures of *Neotricula lilii*. N = number of snails used. Mean ± standard deviation (range).

	Females (N = 4)	Males (N = 3)
Body	4.96±0.82 (3.92–5.86)	4.27±0.08 (4.64–4.80)
Gonad	0.80±0.12 (0.70–0.96)	1.42±0.07 (1.36–1.50)
Digestive gland	2.03±0.23 (1.80–2.30)	2.13±0.19 (2.00–2.34)
Posterior pallial oviduct (= albumen gland)	1.00±0.08 (0.96–1.10) N = 3	—
Anterior pallial oviduct (= capsule gland)	1.14±0.16 (0.96–1.26) N = 3	—
Total pallial oviduct = OV	2.15±0.22 (1.92–2.36) N = 3	—
Bursa copulatrix = BU	0.52±0.04 (0.50–0.56) N = 3	—
Duct of BU	0.10 (N = 1)	—
BU ÷ OV	0.24±0.02 (0.23–0.26)	—
Seminal receptacle	0.19±0.02 (0.16–0.20)	—
Duct of seminal receptacle	0.04±0.02 (0.02–0.06)	—
Mantle cavity	1.54±0.20 (1.20–1.56)	1.37±0.07 (1.30–1.44)
Gill (G)	1.19±0.15 (1.0–1.36)	1.22±0.07 (1.16–1.30)
Osphradium (OS)	0.32±0.05 (0.28–0.38)	0.38±0.02 (0.36–0.40)
OS ÷ G	0.27±0.07 (0.22–0.38)	0.31±0.02 (0.28–0.33)
No. of filaments	21.8±1.7 (20–24)	21.4±0.6 (21–22)
Gf_2	0.32±0.03 (0.28–0.36) N = 6	Males & Females
Gf_1	0.19±0.03 (0.16–0.20) N = 6	Males & Females
Total Gf = TGF	0.51±0.05 (0.46–0.58) N = 6	Males & Females
Gf_2 ÷ TGF	0.63±0.04 (0.58–0.69) N = 6	Males & Females
Prostate	—	1.02±0.13 (0.90–1.16)
Seminal vesicle	—	1.00±0.20 (0.80–1.20)
Penis	—	1.15±0.01 (1.50–1.52)

TABLE 49. Radular statistics for *Neotricula lilii*. Mean ± standard deviation (range). N = 4. In mm except for width of central tooth in μm.

Shell length	3.00±0.17 (2.80–3.16)
Radular length	0.58±0.01 (0.57–0.60)
Radular width	0.08 (0.072–0.080)
Total rows of teeth	87 (84, 90) (N = 2)
No. rows of teeth forming	19 (16, 22) (N = 2)
Central tooth width	17.2 (16.2–17.9) N = 3

has a moderate number of gill filaments whilst the latter has few (char. 6). The male gonad overlaps the stomach of the former; it is posterior to the stomach in the latter (char. 27). The anterior vas deferens leaves the prostate at mid-prostate in the former; from the prostate at the posterior end of the mantle cavity in the latter (char. 31). The penial tip of the former has a papilla; that of the latter a long penial filament.

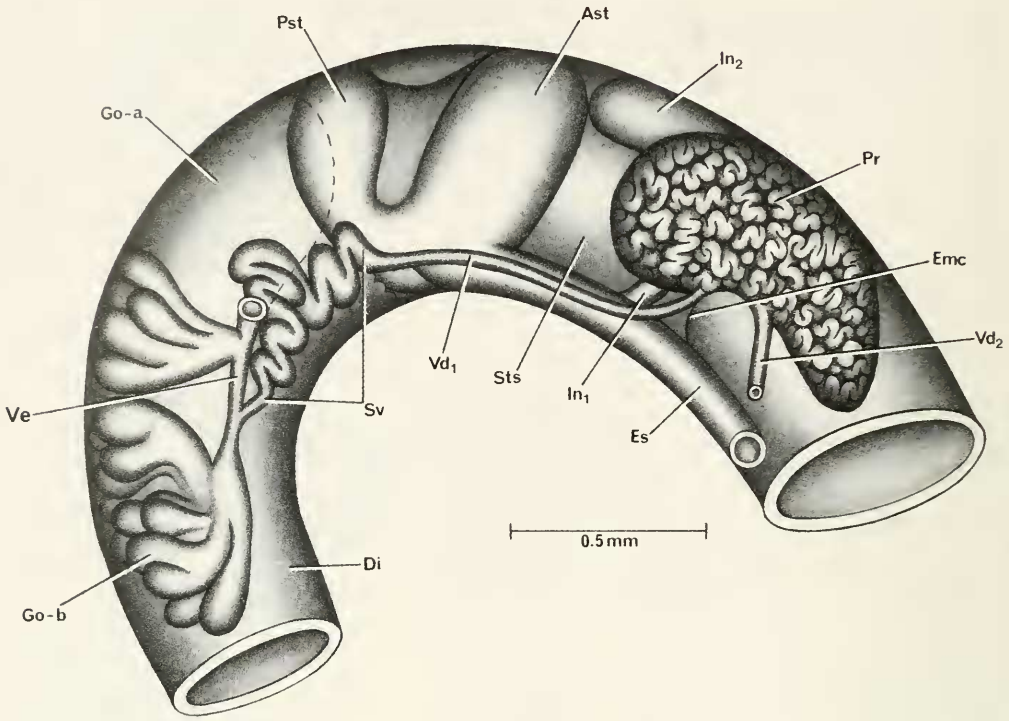

FIG. 99. Uncoiled male of *Neotricula lilii* without head or kidney tissue. Anterior part of mantle cavity omitted as is posterior end of digestive gland.

TABLE 50. Cusp formulae for the radular teeth of *Neotricula lilii* with the percent of the three radulae in which a given formula was found at least once.

Central Teeth		Lateral Teeth		Inner Marginal Teeth		Outer Marginal Teeth
$\frac{3\text{-}1\text{-}3}{2\text{-}2}$	66%	3-1[2]-3	100%	12	—	33%
$\frac{2\text{-}1\text{-}2}{2\text{-}2}$	33%	3-1-3	66%	13	100%	66%
$\frac{3\text{-}1\text{-}3}{2\text{-}3}$	33%	4-1[2]-3	33%	14	100%	100%
		3-1-4	33%	15	66%	33%
				16	33%	—
				$\bar{X}$ * 14.2±0.9 N = 30		13.8±1.0 N = 30

*Mean ± standard deviation of cusp number for all teeth counted.

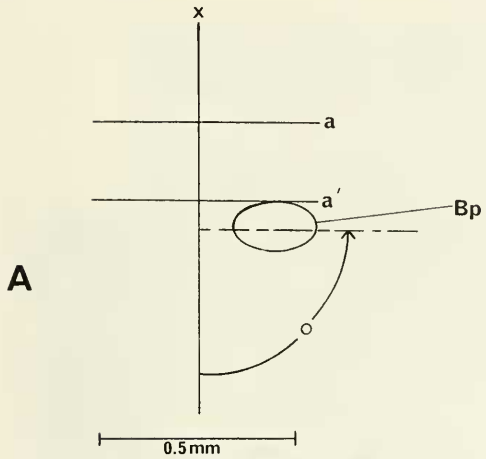

FIG. 100. A. Relationship of base of the penis of *Neotricula lilii* to mid-line of snout-neck (x) and to posterior end of eye lobes (a). B. Penis.

Neotricula minutoides (Gredler, 1885)

Paralectotypes. SMF 4155; pl. 4, fig. 1, in Yen, 1939.

Type locality. "Aus Quellen bei Hensan"; Heng-shan-hsien, Hunan (Yen, 1939). Near site 1, fig. 1 (Hengshan)

Synonymy. Bithynia minutoides Gredler, 1885
Hydrobia minutoides (Gredler, 1887)
Tricula minutoides, Yen, 1939
Neotricula minutoides, this paper

Habitat

Specimens collected for this paper came from Tong Meng Village, Xikou town, Cili County, Changde Prefecture; 29°13′58″N, 110°44′12″E; Figure 1 site 8. The field collection number was D85-83 on 7 October 1985. Specimens were collected from Tong meng village, Xikou Tow, Cili County, Changde Prefecture; 29°13′58″N, 110°44′12″E; Figure 1 site 8. The assigned collection number was D85-83. The habitat was a small perrenial stream 15–25 cm wide and 5–10 cm deep at an altitude of 550 m above sea level. The stream was shaded; the flow was slow. The bottom of the stream was paved with small stones in mud. The water was clean and cool. The sides of the stream had weeds and short shrubery.

TABLE 51. Lengths of neural structures of *Neotricula lilii.* Mean ± standard deviation (range). N = 4. * = neural elements measured to calculate the RPG ratio.

Cerebral ganglion	0.25±0.01 (0.24–0.26)
Cerebral commissure	0.09±0.05 (0.04–0.16)
Pleural ganglion	
Right (1)*	0.11±0.01 (0.10–0.12)
Left	0.10 (N = 3) No var.
Pleuro-supraesophageal connective (2)*	0.17±0.03 (0.12–0.18)
Pleuro-subesophageal connective	0.08±0.03 (0.04–0.10) N = 3
Supraesophageal ganglion (3)*	0.11±0.03 (0.10–0.14)
Subesophageal ganglion	0.08±0.04 (0.10–0.12) N = 3
Osphradio-mantle nerve	0.02 (0, 0.04) N = 2
RPG ratio* = 2 ÷ 1+2+3	0.44±0.08 (0.33–0.50)

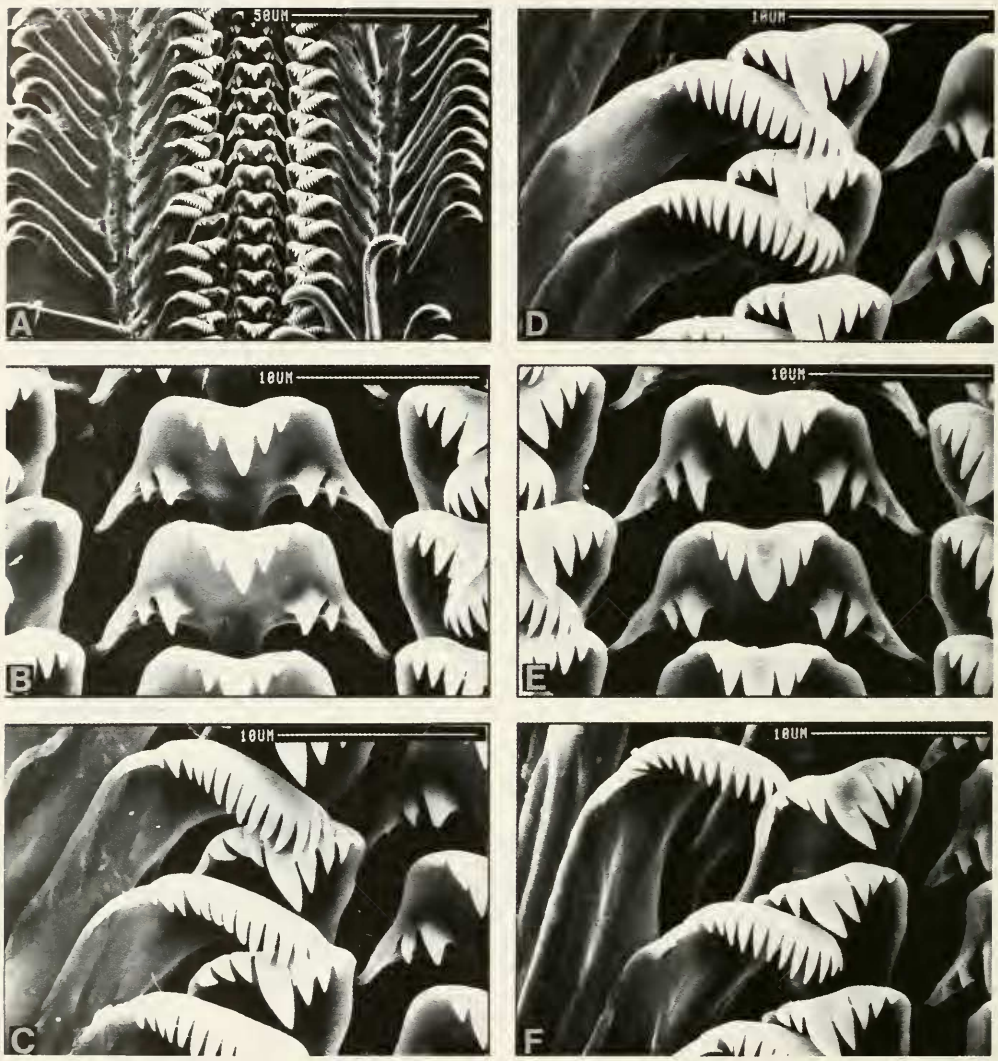

FIG. 101. Radula of *Neotricula lilii*. A. Segment of radula. B, E. Central teeth. C, D, F. Lateral and inner marginal teeth.

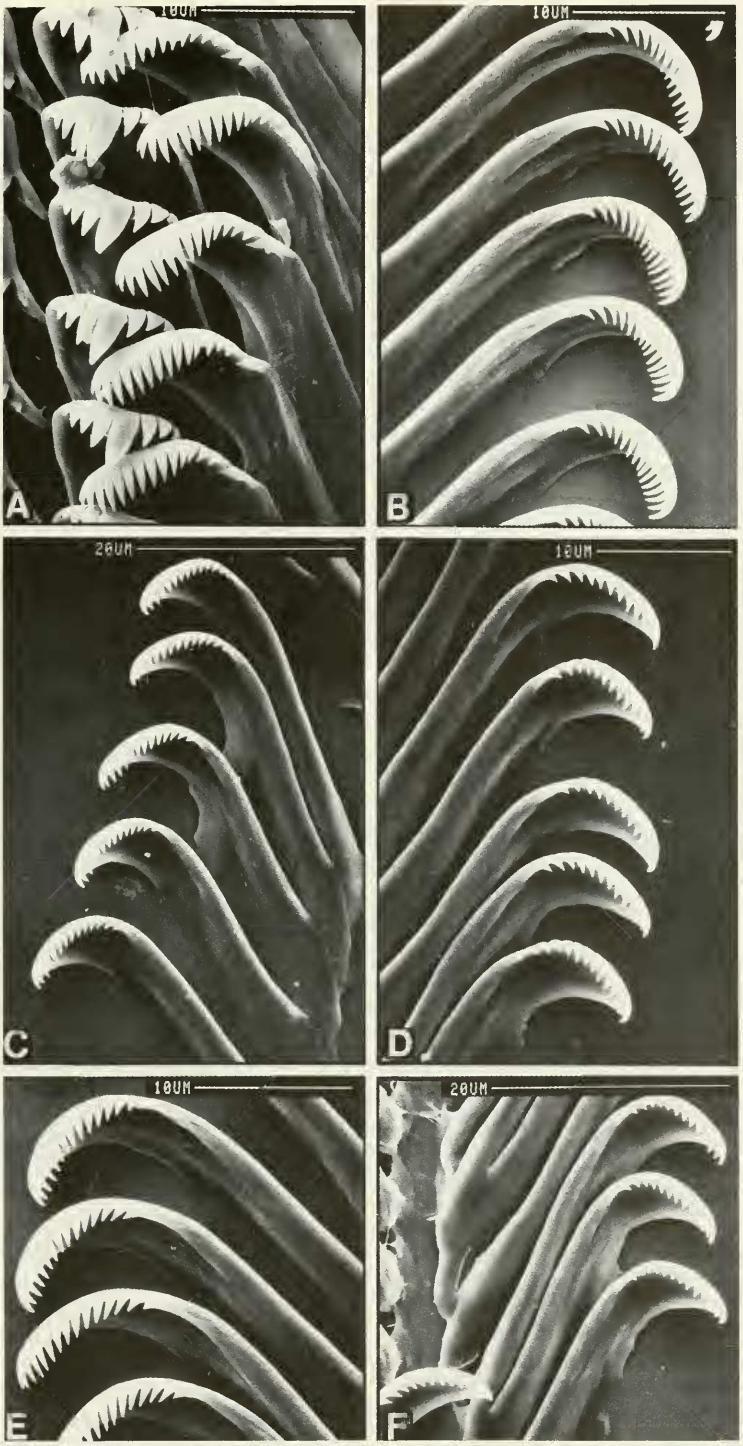

FIG. 102. Radula of *Neotricula lilii*. A. Right lateral and inner marginal teeth. B–F. Outer marginal teeth; B, D, F = right; C, E = left outer marginal teeth.

TABLE 52. Shell measurements (mm) of *Neotricula minutoides*. Mean ± standard deviation (range). N = 5; all shells 5.5 whorls.

Length (L)	3.41±0.20 (3.14–3.60)
Width (W)	1.68±0.09 (1.60–1.80)
L last three whorls	3.07±0.18 (2.84–3.28)
L body whorl	2.28±0.15 (2.12–2.48)
L penultimate whorl	0.50±0.04 (0.44–0.56)
W penultimate whorl	1.09±0.05 (1.04–1.16)
W 3rd whorl	0.72±0.03 (0.68–0.76)
L aperture	1.53±0.13 (1.40–1.70)
W aperture	1.02±0.07 (0.96–1.12)
x	0.44±0.05 (0.40–0.52)
y	0.18±0.05 (0.12–0.24)

Depository

Specimens are deposited in ZAMIP, M0006; ANSP, 373136, A12652.

Description

Shells. The shells are small, ovate-conic with 5.5 whorls (Figs. 60C–G, 103A–E). Lengths range from 3.14–3.60 mm (Table 52). The aperture is pyriform. Adapically there is no notch or beak, nor is there an internal notch groove. There is no adapical outer lip angle.

The whorls at the suture are smooth (not crenulated). There is a pronounced umbilicus. SEM analysis reveals faint traces of spiral microsculpture on the adapical part of the whorls of the teleoconch.

The inner lip is thick and arched. It is clearly separated from the body whorl by a narrow gap. The adapical apertural lip is pulled away from the body whorl but the interspace is filled with shell layers (as is the inner side of the inner lip). There is no apertural sinus. In side view, the outer lip is straight and slightly scooped forward. In side view, the inner lip is straight. There are no apertural teeth or notches, no varix, no spout. The abapical lip projects beyond the base of the shell 0.44 ± 0.05 mm.

As seen with SEM, the protoconch is minutely wrinkled (Fig. 103C–E). Growth lines begin on the teleconch at 2.0 whorls.

External Features. The head is dark grey, with few or no white granules about the eyes. The operculum is corneous and paucispiral (Fig. 103F). It appears to grow in layers. The internal attachment pad is prominent, some 49% the width of the operculum.

Mantle cavity. Mantle cavity structures are typically triculine. Organ measurements are given in Table 53. The osphradium is located mid-gill; it is small. Only one gill filament was measured; it was 0.58 mm long. For this filament Gf_2 was long.

Female reproductive system. An uncoiled female without head and with kidney tissue removed is shown in Figure 104. Measurements of organs are given in Table 53. Important features are: (1) The gonad is posterior to the stomach, is small, and consists of one or two bundles of lobes. (2) The bursa copulatrix (Bu) is round, small and situated directly posterior to the albumen gland (Ppo). It is not occluded by the posterior part of the albumen gland. (3) The albumen gland is short. (4) The bursa copulatrix complex of organs is shown in Figure 105. The orientation of organs in Figure 105A is the same as that in Figure 104. The bursa (Bu) is short. (5) The seminal receptacle (Sr) is spherical; it may or may not have a duct. In either case, it opens into the base of the duct of the bursa where the latter runs into the spermathecal duct (Sd) and also receives the sperm duct (Sdu). This opening for the seminal receptacle is on the dorso-lateral side of the bursa complex (Fig. 105C). (6) When there is a discernable duct of the seminal receptacle, it is extremely short, about 0.02 mm. (7) The spermathecal duct is short and swollen; it is nearly a straight, as well as a direct continuation of the duct of the bursa; it opens into the posterior end of the mantle cavity (Emc).

Male reproductive system. The posterior half of an uncoiled male with kidney tissue removed is shown in Figure 106. Measurements of organs are given in Table 53. Important features are: (1) The gonad (Go) is posterior to the stomach. It consists of several bundles of lobes (removed in Figure 106 to reveal the seminal vesicle) arising from the vas efferens. (2) The prostate (Pr) overlaps the posterior end of the mantle cavity (Emc.) (3) The seminal vesicle (Sv) arises from mid-vas efferens. (4) The seminal vesicle forms a small knot of ducts dorsal to the gonad; it does not continue onto the stomach. (5) The anterior vas deferens (Vd_2) leaves the prostate near the posterior end of the mantle cavity (Emc). (6) The penis (Figure 107B) is simple, slender and differs from that of any other Hunan species by being highly extensible. (7) The penis has no papilla nor was an ejaculatory duct found at the base of the penis or in the neck. (8) The orientation of the base of the penis on the neck is shown in Figure 107A. It slightly overlaps the snout-neck mid-line; it is

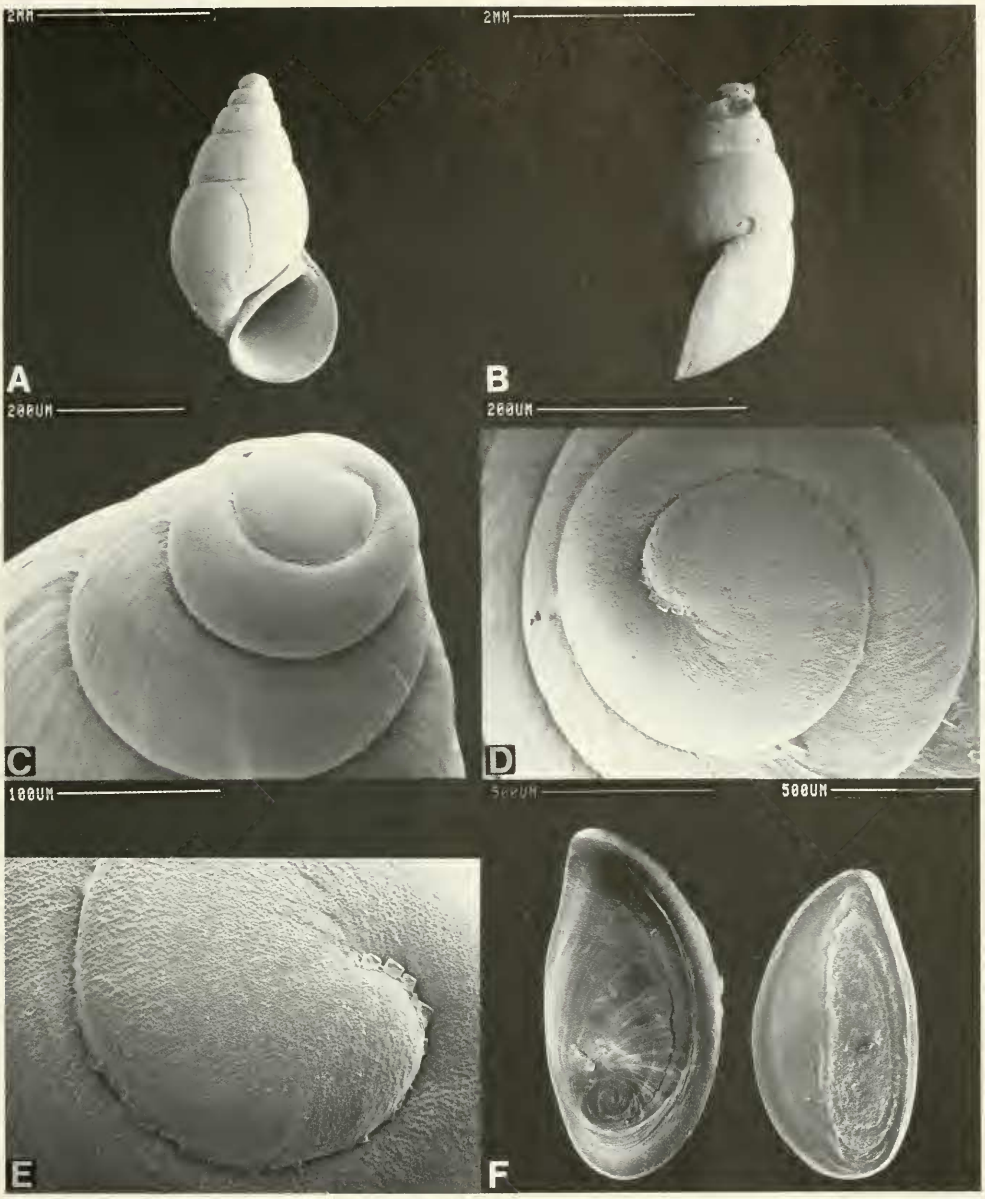

FIG. 103. SEM photographs of shells and opercula of *Neotricula minutoides*. Note in B that the outer lip is slanted. C–E. Details of protoconch and in C, beginning teleconch. F. Opercula with outer surface (left) and inner surface (right).

orientated at an angle of 40° to the snout-neck mid-line (x).

Digestive system. The digestive gland covers the posterior chamber of the stomach of both sexes. Radular statistics are given in Tables 54 and 55. There are 56.4 ± 4.8 rows of teeth along a radula of 0.51 mm length. The most frequently encountered formula is

$$\frac{(2)3\text{-}1\text{-}3(2)}{2\text{-}2};\ 2 \text{ to } 4\text{-}[2]\text{-}2(3);\ 12\text{-}14;\ 11\text{-}14.$$

TABLE 53. Lengths (mm) or counts of non-neural organs and structures of *Neotricula minutoides*. N = number of snails used. Mean ± standard deviation (range).

	Females (N = 5)	Males (N = 1)
Body	5.02±0.13 (4.90–5.16)	4.40
Gonad	0.83±0.15 (0.70–1.00)	1.28
Digestive gland	2.10±0.28 (1.80–2.36)	1.90
Posterior pallial oviduct (= albumen gland)	0.80 (0.60, 1.00) N = 2	—
Anterior pallial oviduct (= capsule gland)	1.28 (1.16, 1.40) N = 2	—
Total pallial oviduct = OV	2.02±0.34 (1.76–2.40)	—
Bursa copulatrix = BU	0.55±0.14 (0.40–0.66)	—
Duct of BU	—	—
BU ÷ OV	0.28±0.10 (0.17–0.35)	—
Seminal receptacle	0.10 (no var.) N = 2	—
Duct of Seminal receptacle	—	—
Mantle cavity	1.56 (1.36, 1.76) N = 2	1.40
Gill (G)	1.40 (1.20, 1.60) N = 2	1.24
Osphradium (OS)	0.41 (0.36, 0.46) N = 2	0.44
OS ÷ G	0.29 (0.29, 0.30) N = 2	0.35
No. of filaments	17 (13, 21) N = 2	18
Gf_2	0.36 N = 1	—
Gf_1	0.22 N = 1	—
Total Gf = TGF	0.58 N = 1	—
Gf_2 ÷ TGF	0.62 N = 1	—
Buccal mass	0.57 N = 1	—
Prostate	—	1.10
Seminal vesicle	—	0.48
Penis	—	2.60

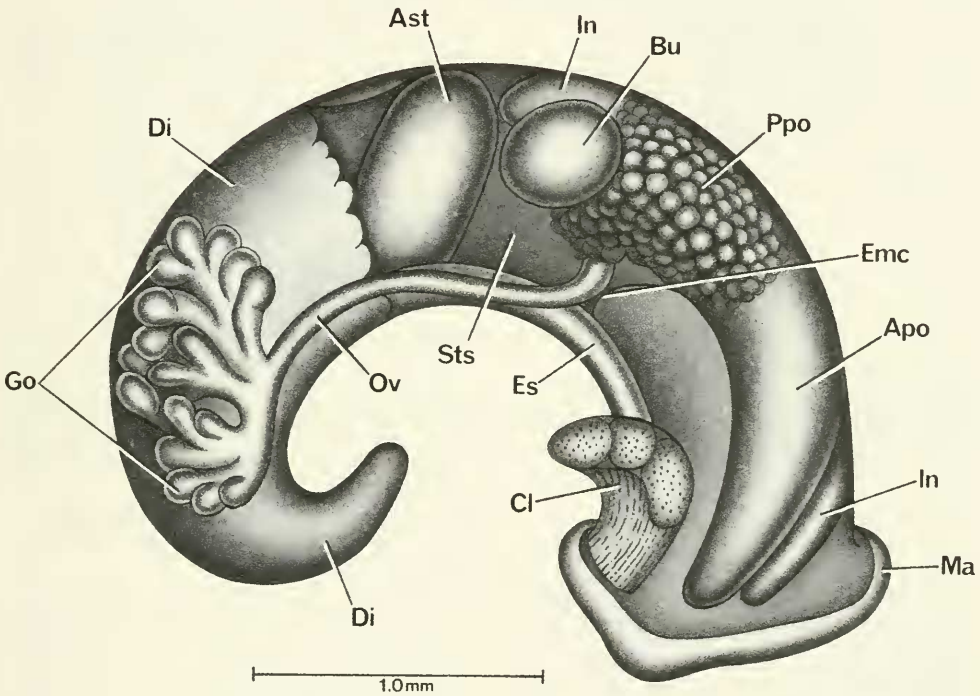

FIG. 104. Uncoiled female *Neotricula minutoides* with head and kidney tissue removed.

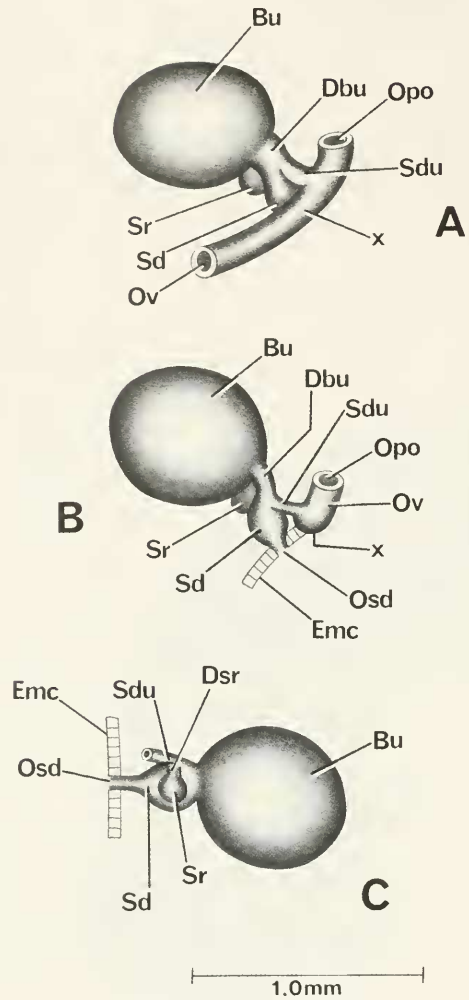

FIG. 105. Details and variation of the bursa copulatrix complex of organs of *Neotricula minutoides*. Figure A is in the same orientation as in Figure 104. B. Section of oviduct cut away at "x" to show continuation of duct of bursa (Dbu) into spermathecal duct (Sd) with latter opening (Osd) into posterior end of mantle cavity. C. Bursa complex flipped over to show relationships of seminal receptacle to sperm duct (Sdu), spermathecal duct (Sd) and duct of bursa.

The radula is shown in Figure 108. A pronounced bifurcation of the blade of the primary cusp of the lateral tooth may be found (Fig. 108C, D, E). Otherwise tooth morphologies are standard triculine.

TABLE 54. Radular statistics for *Neotricula minutoides*. Mean ± standard deviation (range). N = number used. In mm except for width of central tooth in μm.

	Females (N = 6)
Shell length	3.67±0.30 (3.40–4.00)
Radular length	0.51±0.06 (0.44–0.57)
Total rows of teeth	56.4±4.8 (50–60) N = 7
No. rows of teeth forming	10.9±6.3 (5–21) N = 8
Central tooth width	15.1±1.1 (13.4–16.8) N = 13

Nervous system. Measurements are given in Table 56. The RPG ratio is 0.45; the dorsal nerve ring is thus moderately concentrated.

Remarks

Conchologically, this species most closely resembles *Tricula bambooensis* (Figs. 153–155). *Neotricula minutoides* has a proportionally much wider shell (compare illustrations here with Davis et al., 1986: fig. 20A–E). Additionally, the outer lip of the former, in side view, is scooped forward; it is parallel with the axis of coiling in the latter (char. 15). The adapical aperture of the former is fused to the body whorl; it is slightly separated from the body whorl in the latter (char. 21). The aperture of the former is pyriform; it is oval in the latter (char. 3).

The most prominent anatomical differences are those that separate the two genera.

TRICULINI Davis, 1979

Type genus. Tricula Benson, 1843

Diagnosis. Those genera of Triculinae in which the spermathecal duct enters the pericardium. The oviduct makes a 360° closed twist. In the plesiomorphic state, the seminal receptacle arises from the oviduct; in the derived state, the seminal receptacle is lost and its function taken over by derived structures attaching to the oviduct-spermathecal duct juncture. There is no sperm duct.

Genera assigned. Delavaya, *Fenouilia*, *Lacunopsis*, *Lithoglyphopsis*, *Tricula*. (N=5).

Lithoglyphopsis Thiele, 1928

Type species. Lithoglyphus modestus Gredler, 1886 [1887]

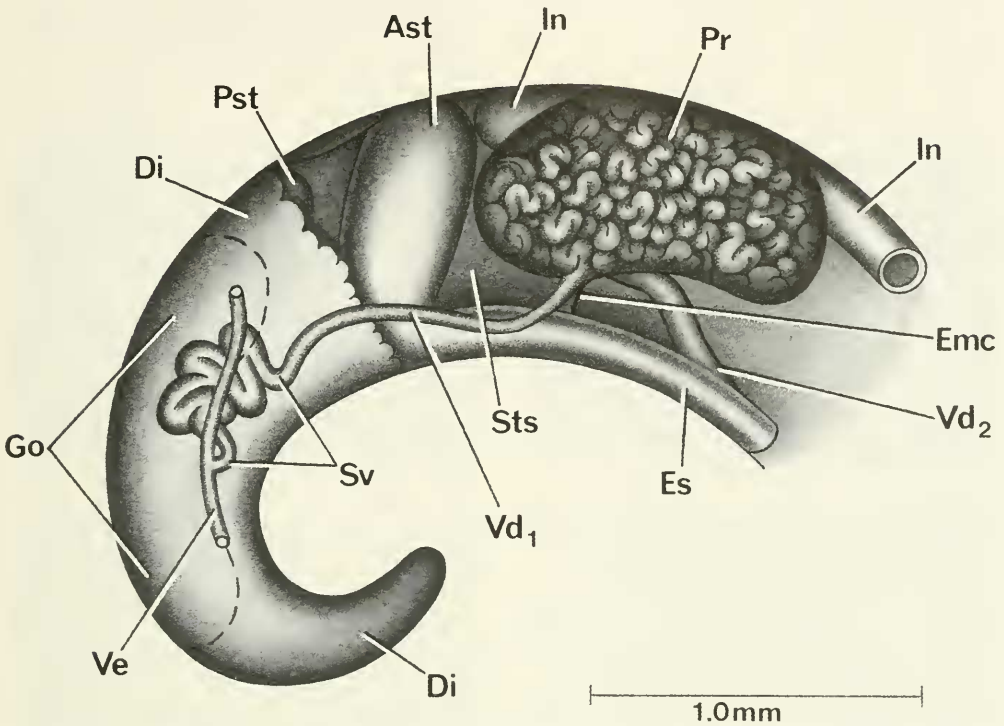

FIG. 106. Uncoiled male of *Neotricula minutoides* without head or kidney tissue. Anterior part of mantle cavity omitted. Outline of gonad (Go) represented by a dashed line; lobes of gonad removed to show knot of tubes of seminal vesicle (Sv).

TABLE 55. Cusp formulae for the radular teeth of *Neotricula minutoides* with the percent of radulae in which a given formula was found at least once. N = 7 radulae. [ ] indicates one cusp support with a split blade.

Central Teeth		Lateral Teeth		Inner Marginal Teeth		Outer Marginal Teeth	
3-1-3 / 2-2	71%	3-[2]-2	57%	11	29%	11	100%
2-1-2 / 2-2	57%	2-[2]-3	29%	12	71%	12	71%
3-1-3 / 3-2	29%	4-1-3	29%	13	86%	13	71%
		4-[2]-3	29%	14	71%	14	43%
3-1-3 / 2-3	14%	3-1-2	14%	$\bar{X}$ * = 12.5±1.9		12.1±1.6	
2-1-3 / 2-2	14%	3-1-3	14%	N = 64		N = 64	
		4-[2]-2	14%				

*Mean ± standard deviation of cusp number for all teeth counted. N = number of teeth counted on 7 radulae.

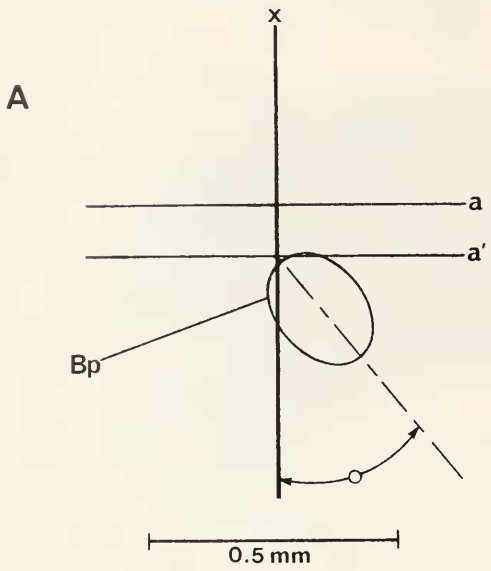

FIG. 107. A. Relationship of base of the penis of *Neotricula minutoides* to mid-line of the snout-neck (x) and to posterior end of the eye lobes (a). B. Penis.

TABLE 56. Lengths (mm) of neural structures of *Neotricula minutoides.* Mean ± standard deviation (range). N = number used = 2. * = neural elements measured to calculate the RPG ratio.

Cerebral ganglion	0.28 (0.26, 0.30)
Cerebral commissure	0.06 (0.5, 0.6)
Pleural ganglion Right (1)*	0.13 (0.12, 0.14)
Left	0.11 (0.10, 0.12)
Pleuro-supraesophageal connective (2)*	0.20 (no var.)
Pleuro-subesophageal connective	0.07 (0.04, 0.10)
Supraesophageal ganglion (3)*	0.11 (0.10, 0.12)
Subesophageal ganglion	0.11 (0.10, 0.12)
Osphradio-mantle nerve	0.05 (0.04, 0.06)
RPG ratio* = 2 ÷ 1+2+3	0.45 (no var.)

Lithoglyphopsis modesta (Gredler)

Types. Paralectotypes SMF 4214a. Figure 109A = specimen figured by Yen (1939). Figure 109B-D = additional type specimens.

Type locality. See above

Synonymy. Lithoglyphus modestus Gredler, 1886
Lithoglyphopsis modesta, Thiele, 1928
Lithoglyphopsis modesta, Wenz, 1939: 580, Figure 1581
Lithoglyphopsis, *modestus* Yen, 1939: 43, pl. 4, Figure 7.

Habitat

The type locality is today known as Baisha, Hengshan County from the Xiangjiang River; 25°58′22″N, 112°45′55″E, Figure 1, locality 9. Snails were collected by diving to obtain stones from the river bottom at a depth of about 2.0–2.5 m. Collected by Chen and Wu in 1986, collection number 86-B, ANSP 373144, A12660, ZAMIP M00054.

The locality from which snails were used for most of the dissections was Anhua town, Anhua County, Zijiang River; 28°23′46″N, 111°,12′41″E, Figure 1, locality 10. The collection number was D87-1, by Davis, Chen and Xing on 16 March 1987, ANSP 373150, A12666. Snails were collected 1.6 km upstream from the town boat landing. Collections came from the shores of a small island in the middle of the river. Water flows through a stone breakwater at the upstream end of the

Type locality. Hen-Kiou-fee bis Pe-shang (Gredler, 1886), = Heng-dshou-fu bis Pe-shang, Hunan (Yen, 1939).

Designation. By Thiele, 1928

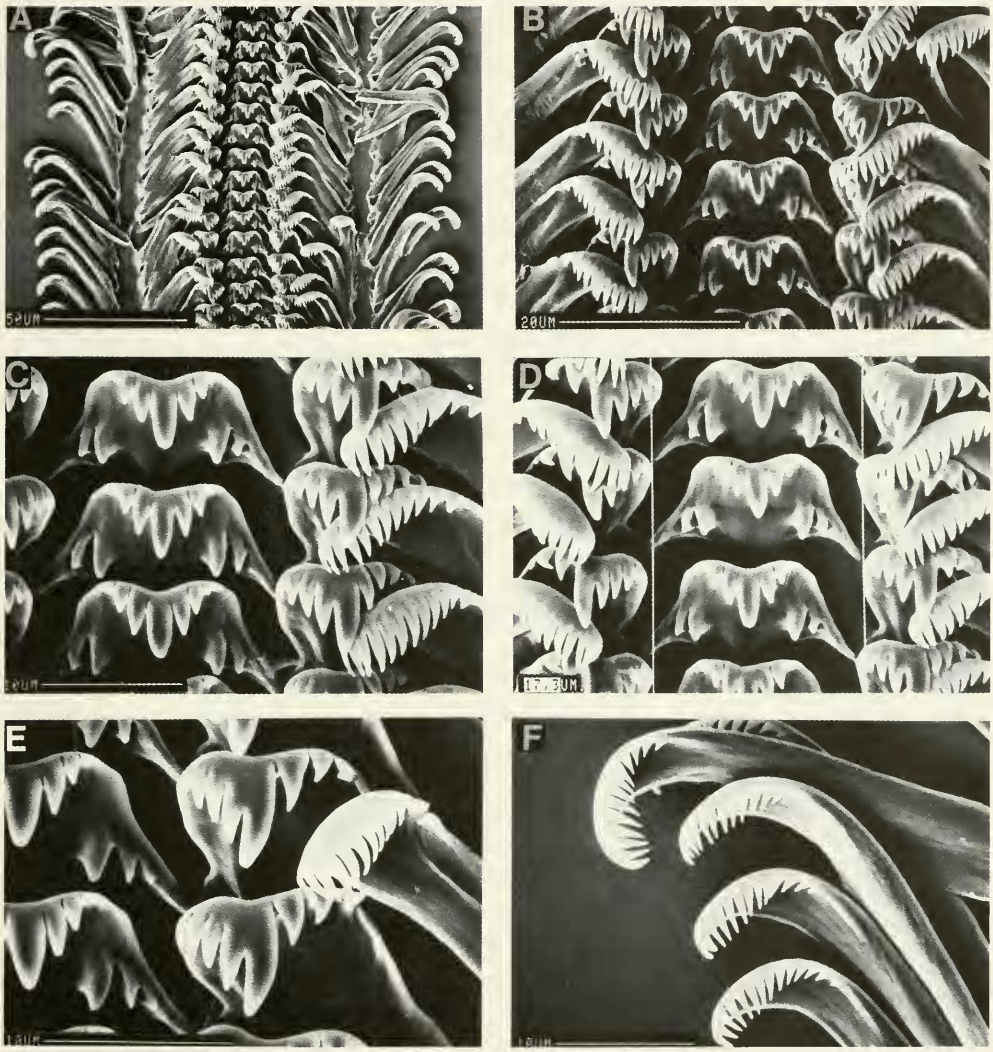

FIG. 108. Radula of *Neotricula minutoides*. A. Section of radula. B–E. Central, lateral and inner marginal teeth. F. Outer marginal teeth.

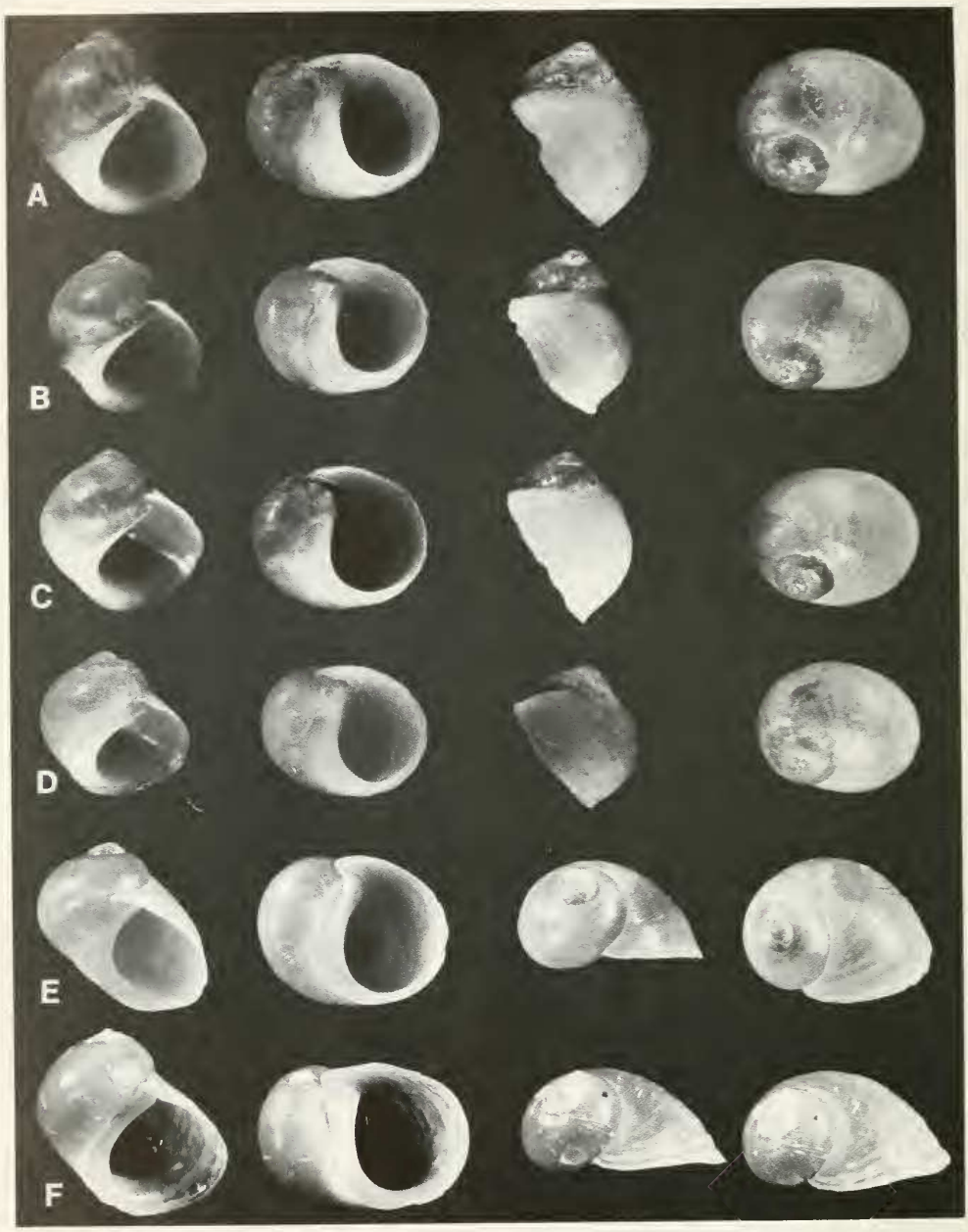

FIG. 109. Shells of *Lithoglyphopsis modesta*. A–D, paralectotypes, SMF; A. specimen figured by Yen (1939). E, F. Specimens from Anhua, D87-1. A = 4.56 mm long; other shells printed at same scale.

TABLE 57. Shell measurements (mm) of Anhua and Baisha populations of *Lithoglyphopsis modesta*. Mean ± standard deviation (range). N = numbered measured.

	Anhua		Baisha	
	Female (N = 5)	Male (N = 6)	Female (N = 5)	Male (N = 5)
No. Whorls	3.0–3.5	3.0–3.5	3.0–4.0	3.5–4.0
Length (L)	5.18±0.04 (4.58–5.57)	5.10±0.60 (4.16–5.66) N = 5	4.53±0.27 (4.16–4.91)	4.46±0.31 (4.15–4.90)
Width (W)	4.87±0.33 (4.74–4.99)	4.68±0.42 (3.91–5.16)	4.49±0.23 (4.24–4.83)	4.58±0.32 (4.23–4.98)
L body whorl	4.91±0.40 (4.37–5.41)	4.76±0.54 (3.91–5.24)	4.27±0.22 (4.07–4.65)	4.19±0.32 (3.90–4.65)
L penultimate whorl	0.15±0.04 (0.08–0.17)	0.21– No. var.	0.20±0.05 (0.17–0.25)	0.252– No. var.
W penultimate whorl	1.12±0.15 (0.99–1.33)	1.06±0.10 (0.99–1.25) N = 5	1.00±0.09 (0.91–1.04)	1.04±0.11 (0.91–1.16)
W 3rd whorl	0.44±0.04 (0.42–0.50) N = 3	0.42±0.06 (0.33–0.50) N = 4	0.44±0.04 (0.42–0.50)	0.46±0.50 (0.42–0.50)
L aperture	4.43±0.19 (4.16–4.66)	4.20±0.31 (3.66–4.58)	4.05±0.17 (3.90–4.07)	4.03±0.20 (3.90–4.32)
W aperture	3.62±0.23 (3.24–3.83)	3.52±0.31 (3.00–3.83)	3.29±0.15 (3.15–3.49)	3.32±0.30) (3.07–3.74)
L crescent	2.31±0.19 (2.08–2.50)	2.25±0.35 (1.83–2.58)	2.04±0.19 (1.83–2.32)	2.20±0.35 (1.83–2.57)
W crescent	0.42±0.06 (0.33–0.50)	0.35±0.06 (0.25–0.42)	0.38±0.09 (0.25–0.50)	0.58±0.17 (0.49–0.83)
W columellar plate	0.73±0.06 (0.67–0.83)	0.77±0.17 (0.50–1.00)	0.68±0.07 (0.58–0.75)	0.72±0.08 (0.66–0.83)
L "A"	5.53±0.25 (5.16–5.74)	5.26±0.44 (4.58–5.66)	4.95±0.22 (4.73–5.23)	5.08±0.30 (4.81–5.48)
W "A"	4.20±0.27 (3.91–4.58)	4.08±0.33 (3.58–4.49)	3.64±0.22 (3.49–3.94)	3.74±0.26 (3.49–4.07)

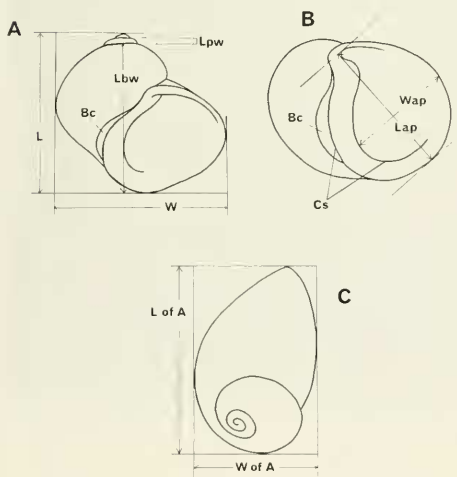

FIG. 110. Illustration to show three shell orientations for measurements.

island. Snails were collected from the bottom surface of stones along the protected inner edge of the breakwater where there was an expansive shallow water area some 30 cm deep and with emergent vegetation. Associated fauna included: *Stenothyra hunanensis*, *Semisulcospira* sp, a species of Viviparidae, a planorbid, and *Radix* sp.

Description

Shells. Shells measurements are given in Table 57 for the two populations. Shells are illustrated in Figures 109–113. How measurements are made for these globose shells is given in Figure 110. Shells are medium to long in length. They are nearly round in outline with the apex to base alignment as in Figure 110C; they are globose and smooth. The shell is dominated by the body-whorl.

FIG. 111. Shells of *Lithoglyphopsis modesta* from Anhua (D87-1) A–C; "*L.*" *liliputinus*, D; and *Guoia viridulus*, paralectotypes, E, F. Shell A is 4.72 mm long; other shells printed at same scale.

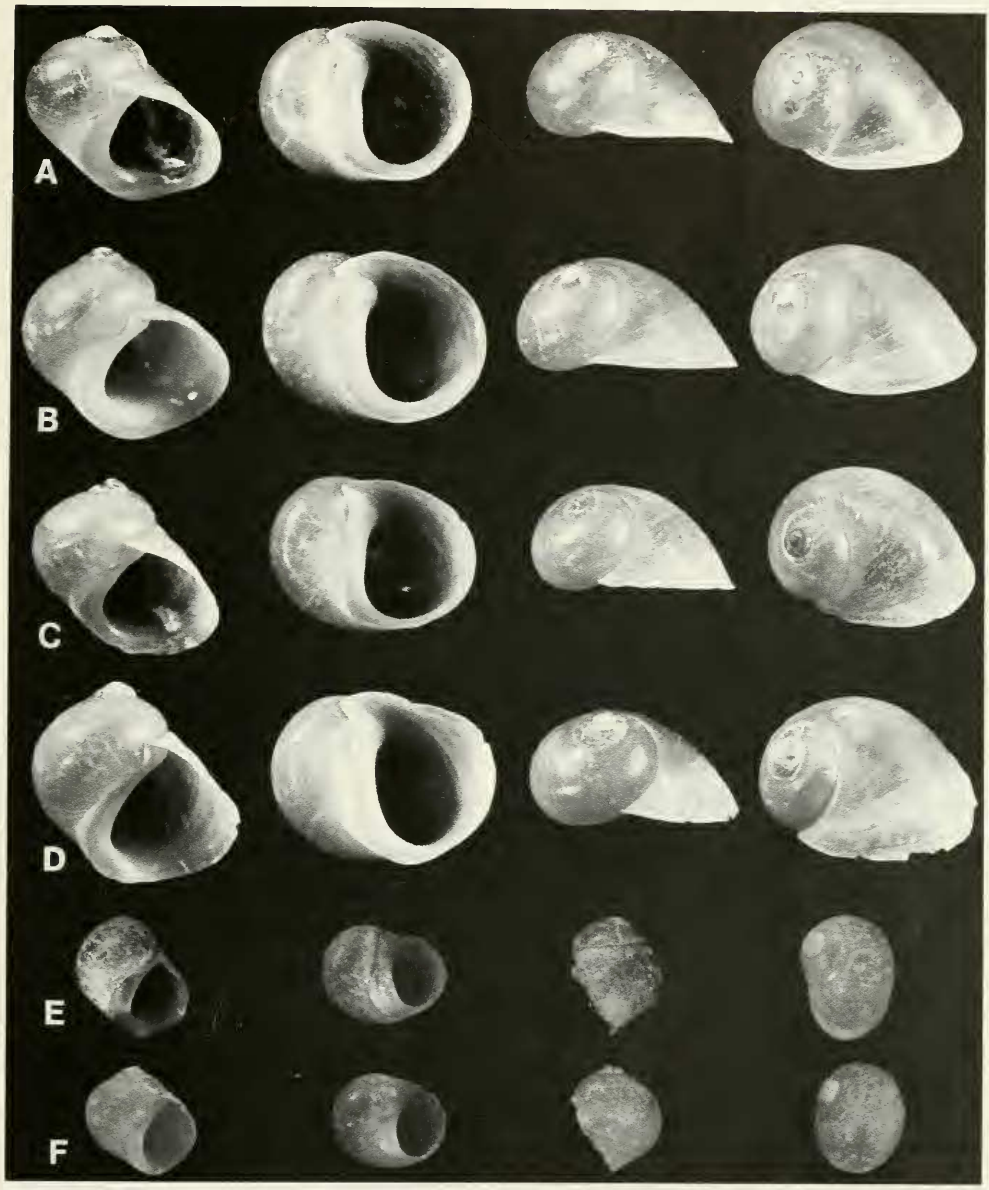

FIG. 112. Shells of *Lithoglyphopsis modesta* from Baisha (86-B), A–D. A, B = males; C, D = females. "*L.*" *liliputinus*, E, F. A = 4.72 mm; other shells printed to same scale.

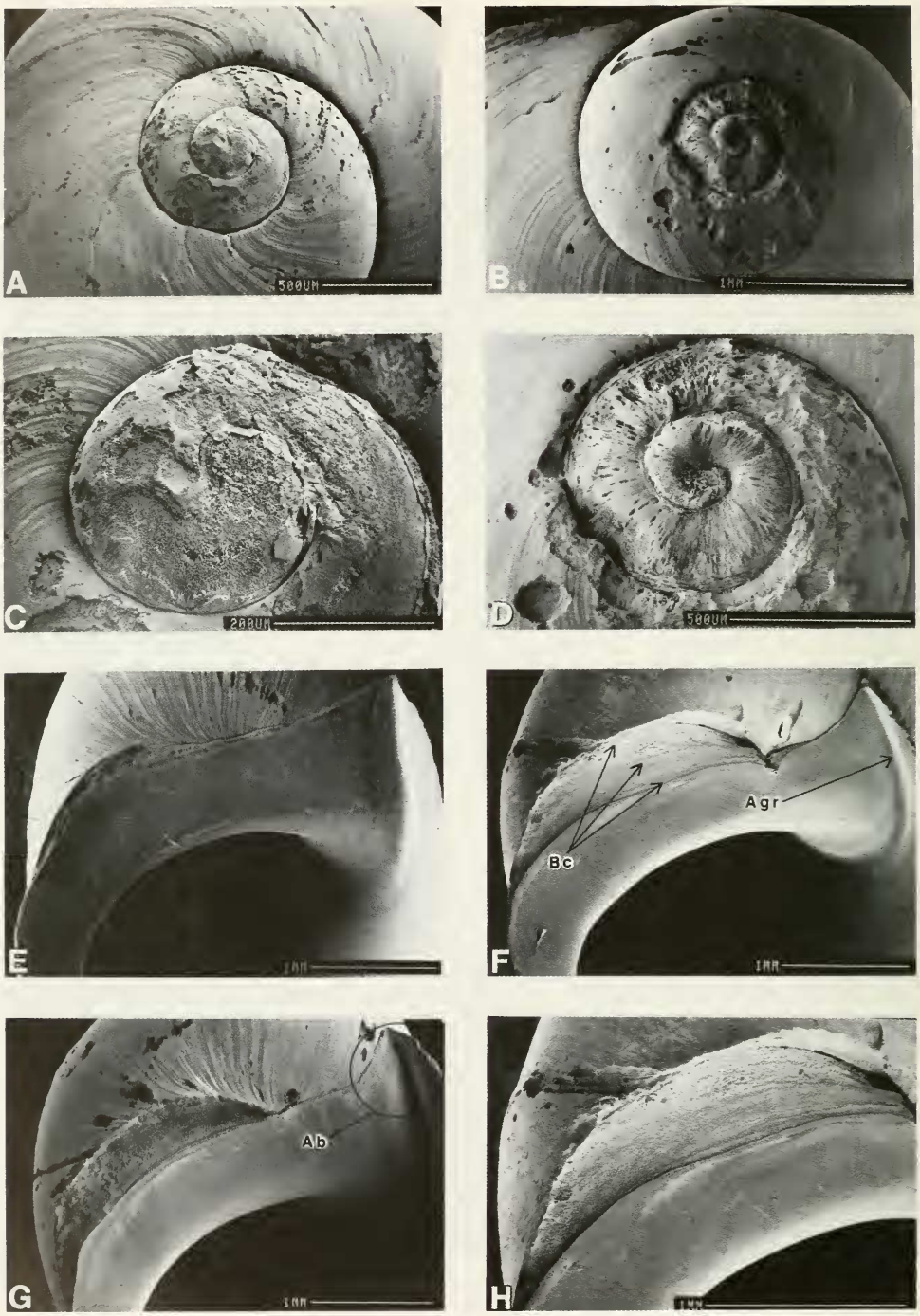

FIG. 113. SEM photographs of shells of *Lithoglyphopsis modesta*. A–C. Enlargements of apical whorls. Spiral microsculpture is seen on second and third whorls. E–H. Enlargement of apertural areas showing basal crescent (Bc), apertural beak (Ab), and beak or adapical apertural groove (Agr).

TABLE 58. Lengths (mm) or counts of non-neural organs and structures of *Lithoglyphopsis modesta*. Mean ± standard deviation (range). N = number of snails used. *See text for discussion of pallial oviduct length.

	Females	Males (N = 2)
Body	7.52±1.52 (4.96–9.40) N = 6	7.85 (7.50, 8.20)
Digestive gland	3.01±0.60 (2.16–4.0) N = 6	3.65 (3.10, 4.20)
Gonad	1.96±0.21 (1.10–2.20) N = 6	3.35 (2.70, 4.00)
Posterior pallial oviduct (= albumen gland)	1.43±0.06 (1.40–1.50) N = 6	—
Anterior pallial oviduct (= capsule gland)	2.89 N = 1	—
Total pallial oviduct = PO	4.23±0.33 (3.70–4.60)	—
Bursa copulatrix	0.87 (0.80, 0.94) N = 2	—
Duct of bursa	0.31±0.09 (0.22–0.40) N = 3	—
Bu ÷ PO	0.22 (0.18–0.25) N = 2	—
Seminal receptacle	0.19 (0.18, 0.20) N = 2	—
Duct of seminal receptacle	0.33±0.04 (0.30–0.38) N = 3	—
Buccal mass	1.60±0.13 (1.50–1.78) N = 4	—
Mantle cavity	4.57±0.26 (4.28–4.86) N = 5	4.08 (3.96, 4.20)
Osphradium = Os	1.94±0.22 (1.76–2.30)	1.15 (1.0, 1.30)
Gill = G	4.20±0.26 (4.28–4.86)	3.70 (3.60, 3.80)
Os ÷ G	0.47±0.05 (0.39–0.48)	0.31 (0.26, 0.36)
No. filaments	39±2 (38–41) N = 4	41 no variation
Gf_2	0.43±0.19 (0.20–0.80) N = 16	male + female
Gf_1	1.04±0.14 (0.70–1.30) N = 16	male + female
Total Gf = TGF	1.48±0.21 (1.06–1.90) N = 15	male + female
Gf_2 ÷ TGF	0.29±0.12 (0.13–0.41) N = 16	male + female
Prostate	—	2.52 (1.84, 3.20)
Seminal vesicle	—	1.60 no variation
Penis	—	3.67 (3.60, 3.74)

TABLE 59. Radula statistics for *Lithoglyphopsis modesta.* Mean ± standard deviation (range). In mm except for the width of the central tooth in μm. N = number measured.

	Females (N = 10)	Males (N = 7)
	Anhua Population (D87–1)	
Greatest shell dimension	4.92±0.47 (4.00–5.36)	4.91±0.26 (4.44–5.20)
Radular length	2.52±0.20 (2.26–2.90)	2.44±0.16 (2.20–2.66)
Radular width	0.23±0.02 (0.20–0.27)	0.23±0.01 (0.22–0.24)
Total rows of teeth	69±5 (62–77)	66±3 (61–70)
No. rows of teeth forming	31±4 (25–36)	25±5 (19–32)
Central tooth width	55±4 (48–58)	55±1 (54–56)
	Baisha Population (1986)	
Greatest shell dimension	4.79±0.25 (4.60–5.16)	4.77±0.32 (4.28–5.12)
Radular length	2.60±0.36 (2.10–2.96)	2.78±0.13 (2.10–3.00)
Radular width	0.21±0.01 (0.20–0.22)	0.21±0.01 (0.20–0.22)
Total rows of teeth	66±8 (55–77)	74±3 (71–80)
No. rows of teeth forming	34±7 (23–40)	37±2 (35–39)
Central tooth width	51±5 (48–60)	49±2 (48–52)

TABLE 60. Cusp formulae or the radular teeth of *Lithoglyphopsis modesta* with the percent of radulae in which a given formula was found at least once. N = number used and/or counted.

Central Teeth		Lateral Teeth		Inner Marginal Teeth		Outer Marginal Teeth	
				Anhua Population (N = 10)			
1/2-2	60%	0-1-3	80%	6	30%	6	20%
1/3-3	50%	2-1-0	70%	7	90%	7	90%
1/3-2	40%	3-1-0	60%	8	90%	8	70%
1/2-3	10%	0-1-2	40%	9	30%	9	20%
		4-1-0	10%	10	0	10	10%
				$\bar{X}^*$ = 7.4±0.8 N = 100		7.5±0.9	
				Baisha Population (N = 3)			
1/2-2	67%	0-1-3	100%	5	—	5	33%
		2-1-0	67%	6	33%	6	100%
1/2-3	67%	0-1-2	67%	7	67%	7	100%
1/3-2	33%	3-1-0	33%	8	67%	8	33%
				$\bar{X}^*$ = 7.40±0.9 N = 30		6.3±0.6	

*Mean ± standard deviation of cusp number for all teeth counted.

TABLE 61. Dimensions of neural structures from five individuals of *Lithoglyphopsis modesta*. Mean ± standard deviation (range). In mm; L = length. * = neural elements measured to calculate the RPG ratio.

Cerebral ganglion L	0.55±0.07	(0.46–0.64)
Pleural ganglion L		
Right (1)*	0.26±0.04	(0.20–0.30)
Left	0.18±0.02	(0.16–0.20)
Cerebral commissure L	0.30±0.07	(0.20–0.38)
Pleuro-supraesophageal connective L (2)*	0.19±0.03	(0.16–0.24)
Pleuro-subesophageal connective L	0.02	(n variation)
Supraesophageal ganglion L (3)*	0.29±0.03	(0.24–0.32)
Subesophageal ganglion L	0.20±0.03	(0.18–0.24)
Osphradio-mantle nerve L	0.27±0.08	(0.20–0.30)
Pedal commissure L	0.23±0.11	(0.10–0.30)
RPG ratio* (2 ÷ 1+2+3)	0.26±0.03	(0.23–0.30)

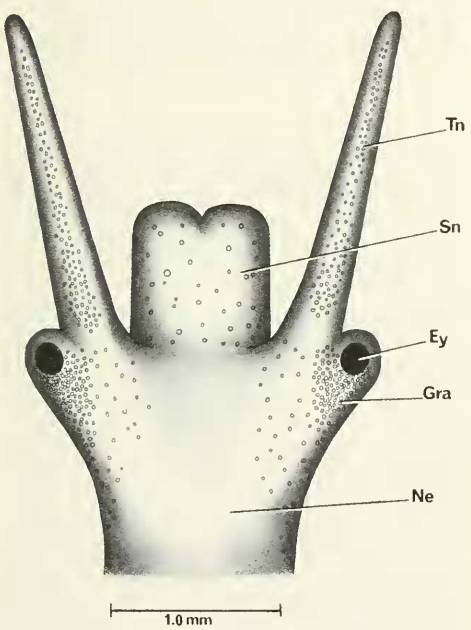

FIG. 114. Head of *Lithoglyphopsis modesta* from a snail collected from D87-1.

The apex is a protruding nipple, a scant 7 to 8% of the overall shell length. In side view, with axis of coiling vertical, the outer lip is straight and slanted back (to the right) 35° to the axis of coiling (Fig. 109, column 3). The shell length (L) is always with the axis of coiling vertical. Greatest overall length (L of A) is with the shell resting on the aperture (Fig. 110C). The aperture is measured by tilting the axis of coiling so that the plane of the aperture is horizontal (Lap, Fig. 110B). There is a wide columellar shelf 0.32 to 0.36 mm wide (Cs, Fig. 110B); the edge at the aperture is straight to slightly arched. There is a pronounced crescent-shaped ridge to the left of the columellar shelf with a somewhat depressed concavity, the basal crescent (Bc), between the ridge and the columella. The peristome is complete. There is no umbilicus. The adapical end of the aperture is produced into a beak-like projection (Ab, Fig. 113G). The aperture shape is round to broadly pyriform. The apex of some individuals may have a reddish color; the cleaned shell is horn yellow.

The SEM pictures of varied aspects of the shell are shown in Figure 113. The apical whorls are shown in Figure 113A–D. They are invariably eroded. Spiral microsculpture is evident (Fig. 113A, B, D). Figure 113E–H shows variation in the size of the basal crescent (Bc). The apertural beak (Ab) is featured in Figure 113F–G showing the groove (Agr) running inside it.

External features. The head is shown in Figure 114; it is broad and squat; there are pronounced bulging eye lobes at the base of each tentacle. In these character-states the head is similar to those of *Fenouilia* and *La-*

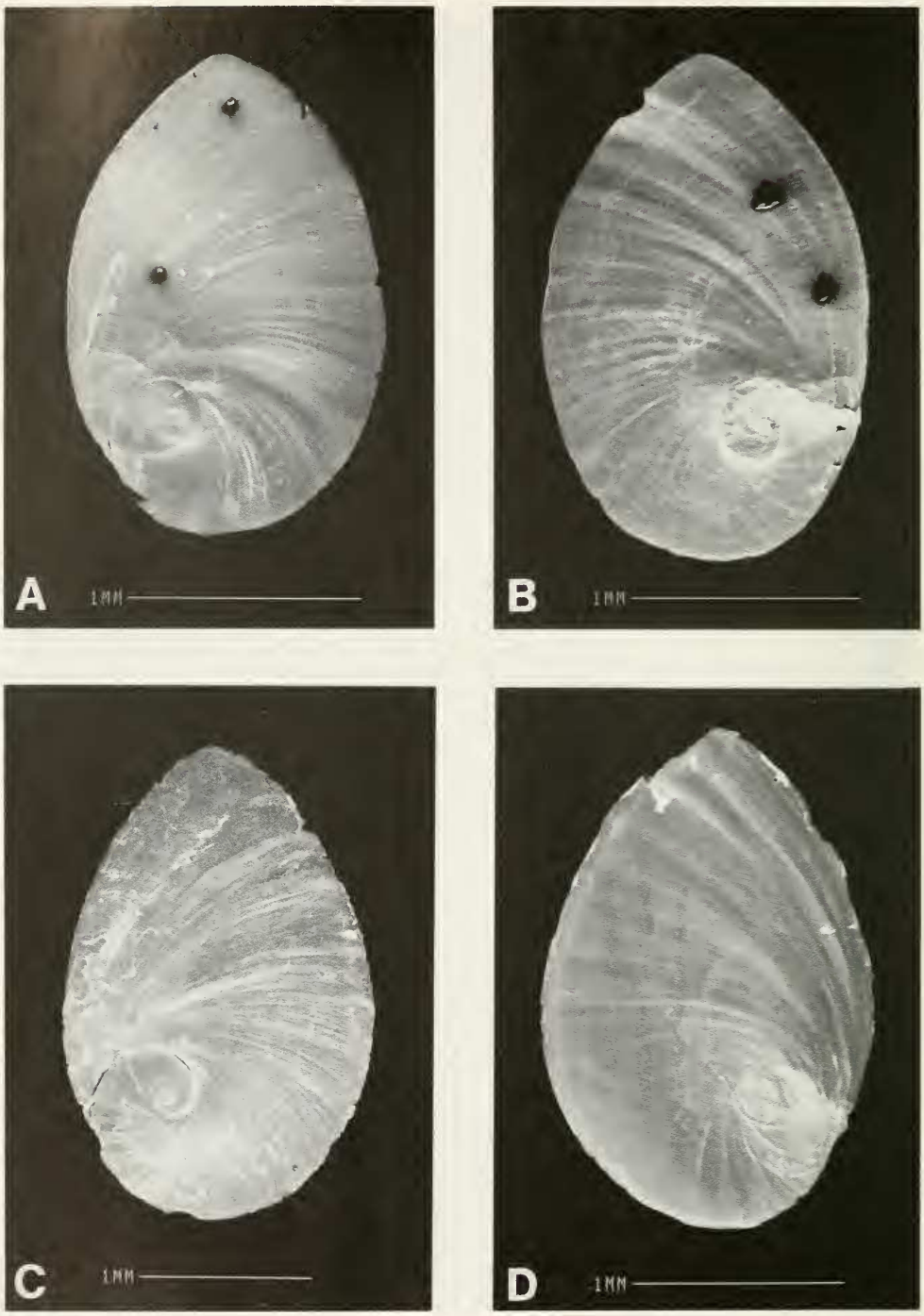

FIG. 115. Opercula of *Lithoglyphopsis modesta*. A, B from Baisha snails; C, D from Anhua snails. A, C. External surfaces; B, D. Internal surfaces.

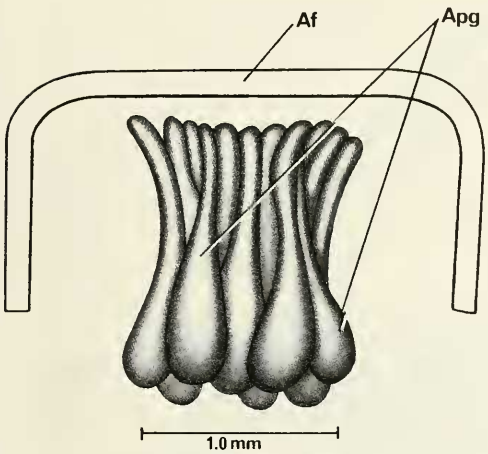

FIG. 116. Masses of anterior pedal glands (Apg) in anterior foot seen through dorsal surface.

cunopsis. The granules shown on the head vary in color from bright lemon yellow to light yellow to white. There is a pronounced omniphoric groove; no suprapedal fold. The operculum is shown in Figure 115; it is regularly ovate, corneous, paucispiral without discernable internal pad; without ridges. The attachment area is barely distinguishable.

Opening the anterior foot dorsally and removing the buccal mass and supporting muscle bands, one sees a mass of tubular anterior pedal glands (Figure 116). These come up as a bunch over the elongated pedal commissure.

Mantle cavity. The reflected mantle is shown in Figure 117A. The mantle cavity is typical for those of species of Triculini in which the spermathecal duct (Sd) enters the pericardium and the pericardium (Pe) swells out into the mantle cavity. Organ measurements and statistics are given in Table 58.

The osphradium (Os) is long; the posterior end may be considerably narrowed (Figs. 117, 119C). Variation in osphradial shape is shown in Figure 119C. The terminal gill filament Gf_2 is short, that is the ratio is 0.29 ± 0.12 (Table 58). The length of the longest filaments is 1.48 ± 0.21 mm. In lateral view the filament is pleated and Gf_2 has a pronounced dome (Fig. 117B).

The pericardium bulges out into the mantle cavity and the opening into the pericardium for sperm entry is clearly observable (Ope, Fig. 117A). The mantle cavity organs and arrangement is typical of the taxa of the *Tricula* clade of Triculini.

Female reproductive system. The body of an uncoiled female without head and with kidney tissue removed is shown in Figure 118. Measurements of the relevant organ systems are given in Table 58. Important features to note are: (1) The body is squat and fat as would be expected from shell shape. (2) The dorsal surface is densely pigmented with melanin. (3) The posterior pallial oviduct (Ppo) makes a pronounced bend over the style sac. (4) The gonad covers the stomach. (5) The sperm enter the system at the rear of the mantle cavity through the pericardium (Ope, Fig. 117A). The pericardium swells out into the mantle cavity. The spermathecal duct (Sd) is a short tube running from the pericardium to the swollen section of the oviduct (Fig. 119A). (6) The oviduct makes a tight twist or coil dorsal to the bursa copulatrix. (7) The seminal receptacle (Dsr) arises from the oviduct posterior to the duct of the bursa (Dbu, Fig. 119A). (8) The bursa complex is dorsal to the posterior pallial oviduct (= albumen gland). (9) The oviduct opens into the pallial oviduct close to the posterior end of the mantle cavity, i.e. not into the posterior end of the pallial oviduct. (10) The bursa is short. (11) The albumen gland length is short if the albumen gland is measured from the posterior edge on the stomach thereby not including the bend over the style sac (ratio of 0.35 ± 0.02). However, measuring along the bend the actual length (functional length) averages 1.83 mm and this divided by that pallial oviduct length averages 0.45 ± 0.03, i.e. the functional length is standard.

Character-states 5–7 are the same as those found in *Tricula*, *Fenouilia*, and *Delavaya*.

Male reproductive system. The body of an uncoiled male is shown in Figure 120 without head and with kidney tissue removed. Measurements of relevant organs are given in Table 58. Important features are: (1) The gonad consists of moderately large lobes draining into a vas efferens (Ve). (2) The posterior vas deferens arises from the vas efferens at mid-gonad or slightly posterior to mid-gonad and

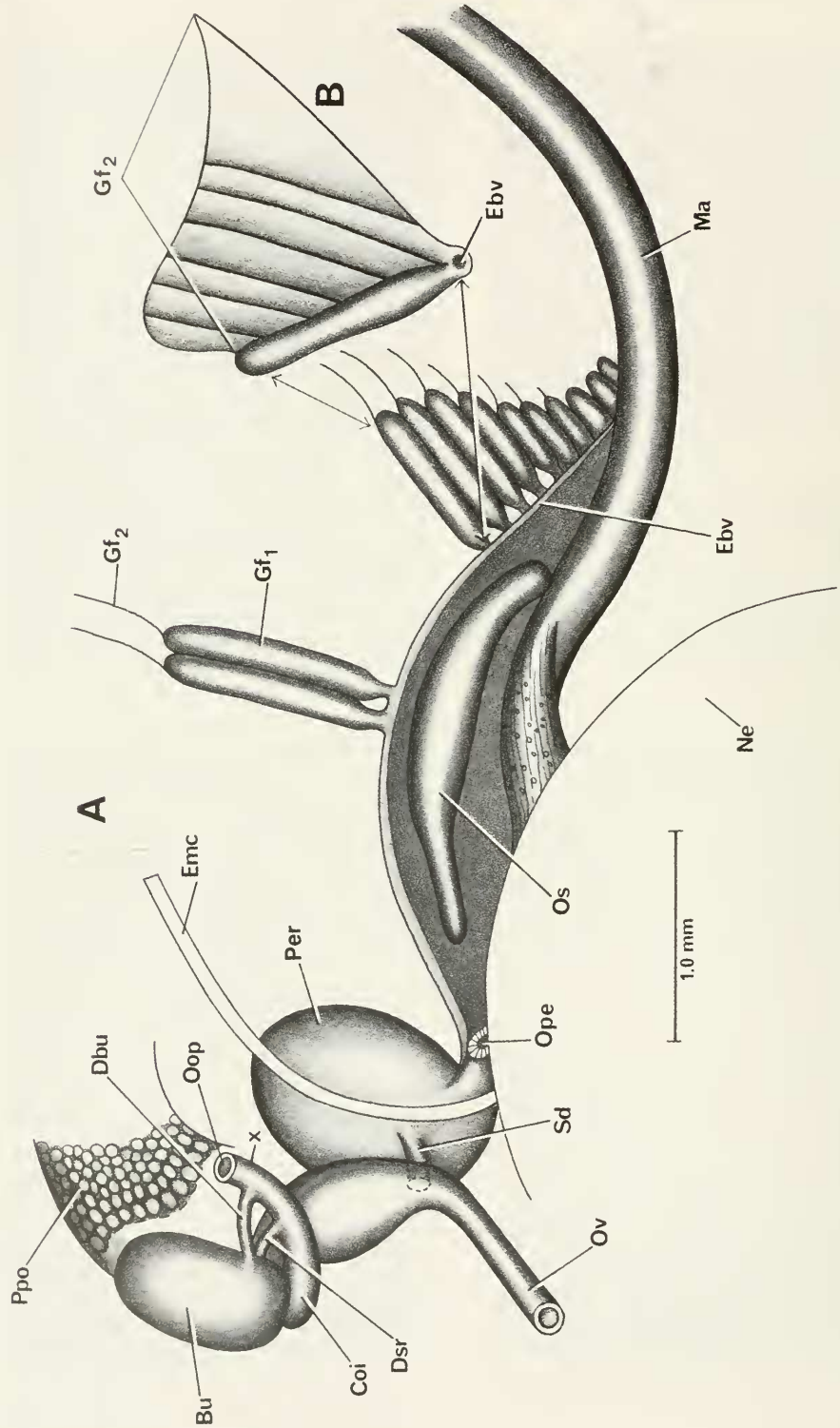

FIG. 117. Cut and reflected mantle (A) showing mantle cavity structures and their relationship to posterior end of mantle cavity (Emc), pericardium (Pe) and bursa copulatrix (Bu) complex of organs. Not all gill filaments (Gf_2 & Gf_1) are shown. B. A single gill filament.

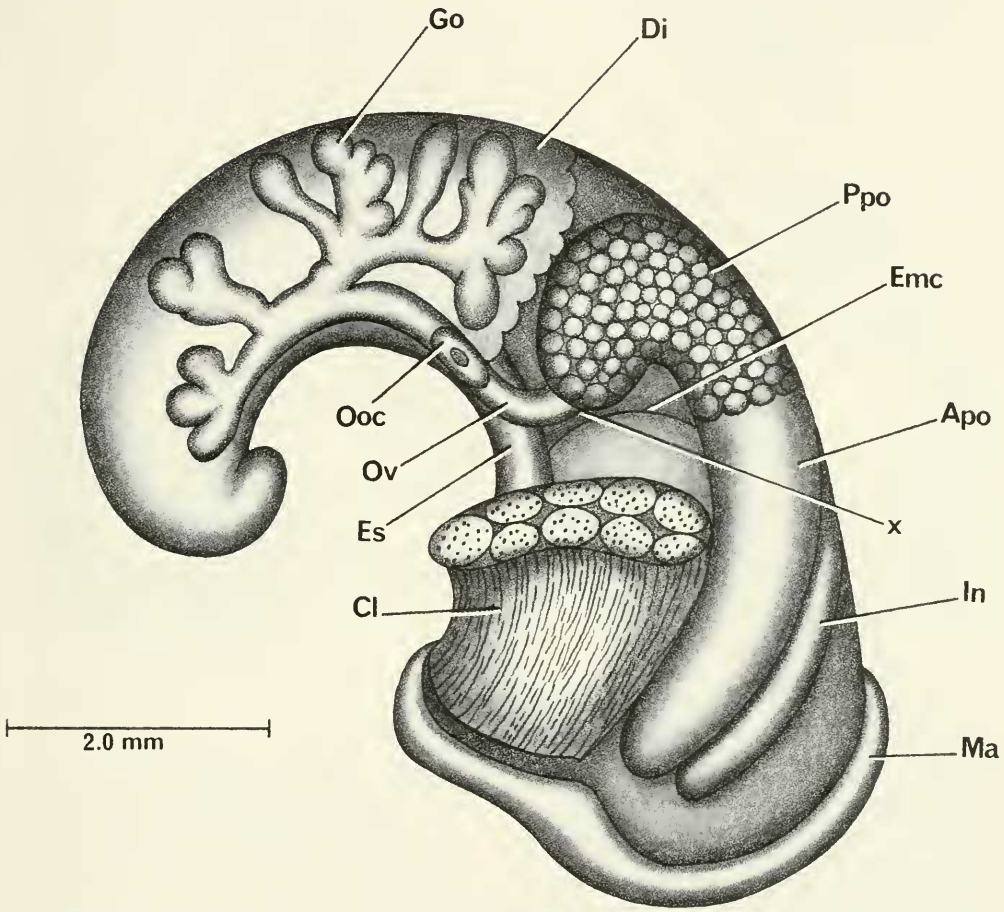

FIG. 118. Uncoiled female *Lithoglyphopsis modesta* with head and kidney tissue removed.

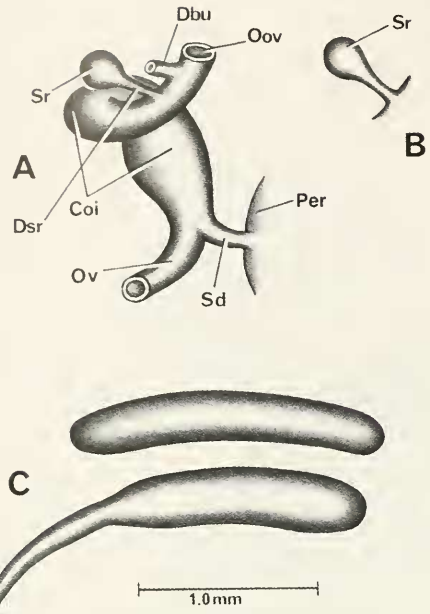

FIG. 119. Bursa copulatrix complex of organs; A, B. Variation in shape of the *osphradium*, C; refer also to Os, Figure 117A. In Figure A, organs are in the same orientation as in Figures 117 and 118. However, here the bursa copulatrix is cut away to show the oviduct coil (Coi) and the seminal receptacle (Sr) where it attaches to oviduct. B. Variation in the shape of seminal receptacle.

forms a loosely coiled seminal vesicle (Sv) visible to the left side of the gonad. (3) The gonad covers the stomach (is ventro-lateral to it). (4) The prostate is comparatively massive, covering the style sac and part of the anterior chamber of the stomach. (5) The penis is simple, without lobes (Fig. 121B). The anterior end is extremely slender, that is, a long penial filament (Pf). There is no papilla. (6) There is a slender muscular ejaculatory duct (Ej) beneath the base of the penis in the neck. (7) The shaft of the penis arises to the right of the snout-neck mid-line (x, Fig. 121A at an angle of 30° ± 10°).

Digestive system. The digestive gland covers the posterior chamber and most of the anterior chamber of the stomach (Figs. 118, 120) in males and females. The buccal mass and salivary glands are shown in Figure 122A. The paired salivary glands (Sg) are massive and run posteriorly over the nerve ring. The radular sac (Rs) is extremely elongate and coils up dorsally along the buccal mass (Bm) between the buccal mass and the right cerebral ganglion (Rcg, Fig. 122B).

The radula is shown in Figure 123. Teeth counts and statistics are given in Tables 59 and 60. Diagnostic features are (1) the large, singular triangular anterior cusp of the central tooth, (2) the massive basal cusps on the face of the central tooth, and (3) the massive dominant cusp on the lateral tooth.

The stomach (Fig. 124) has a relatively slender posterior chamber (Pst) that is slanted from ventral to dorsal along its whole length and is buried dorsal to the digestive gland. The digestive gland covers part of the anterior chamber (Ast) as does the prostate. There is no caecal appendix.

Nervous system. There are several noteworthy features of the nervous system (Fig. 122B). (1) The RPG ratio has a mean of 0.26 (Table 61); the pleuro-supraesopheageal connective is short. (2) The cerebral commissure is elongate (exceeds 0.12 mm). (3) The cerebral ganglion have melanin splotches (Fig. 122B). (4) The pedal commissure is elongate (exceeds 0.12 mm). (5) The osphradio-mantle nerve is elongate (exceeds 0.12 mm).

Remarks

Lithoglyphopsis modesta could only be confused with various species of *Lacunopsis* on the basis of shell. Anatomically they differ as the latter has several accessory seminal receptacles; the generalized seminal receptacle is lost.

Liu et al. (1980) described *Lithoglyphopsis ovatus*, *L. grandis*, *Lacunopsis yunnanensis* and *L. auris* as new species from Yunnan, China. On the basis of the shell illustrations given, and in the absence of anatomical data, it is not possible to ascertain generic status or discuss relationships. *Lacunopsis yunnanensis* has a shell with a pronounced keel. That together with the central tooth morphology given indicates a possibility that a species of *Fenouilia* is involved.

The shells of *Lythoglyphopsis liliputanus* (Gredler, 1881) look like a miniature *L. modesta* (Figs. 111D, 112E, F). Nothing is known

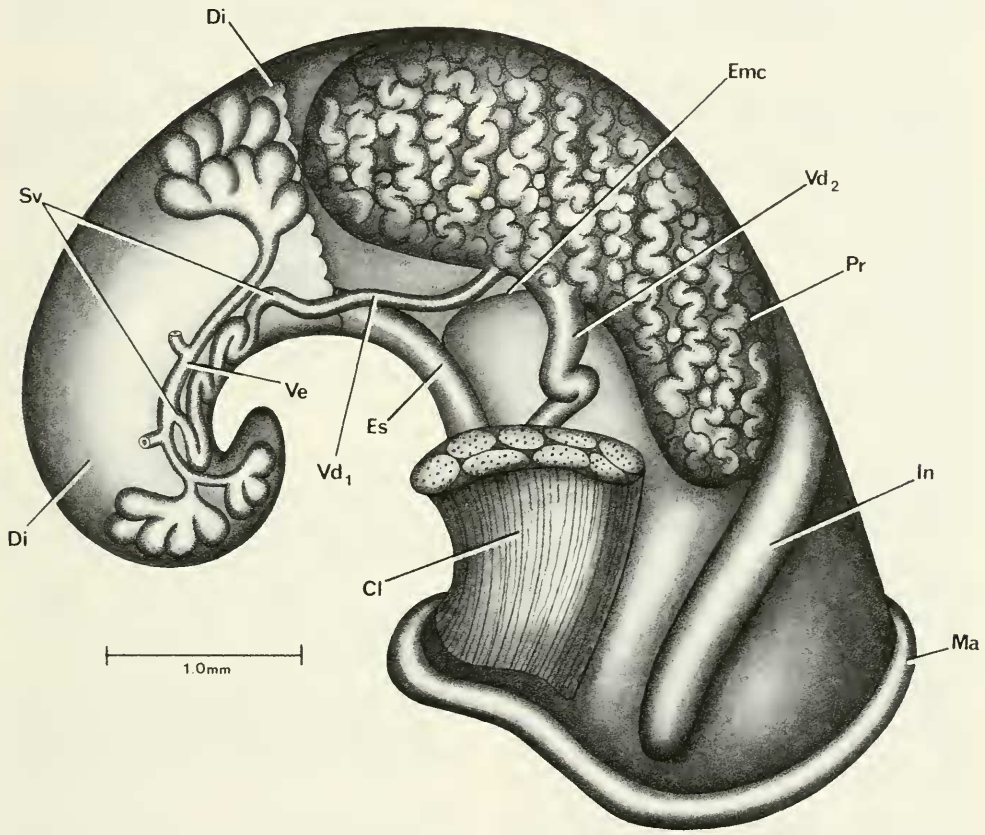

FIG. 120. Uncoiled male *Lithoglyphopsis modesta* without head and with kidney tissue removed. Two bundles of gonadal lobes were cut away.

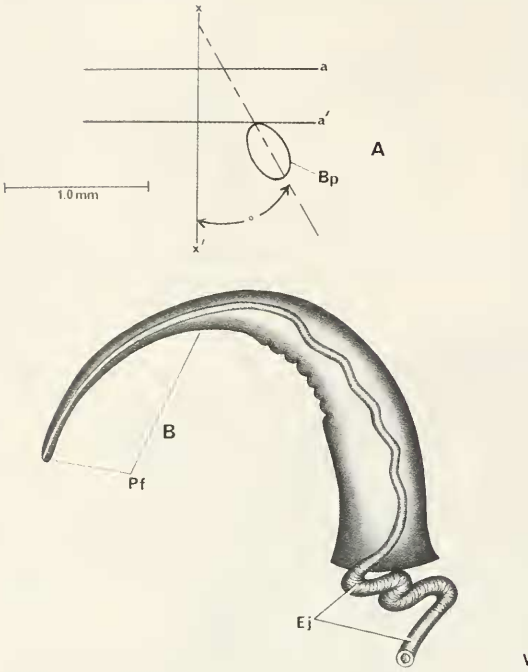

FIG. 121. A. Relationship of base of penis (Bp) of *Lithoglyphopsis modesta* to snout-neck mid-line (x). B. Penis

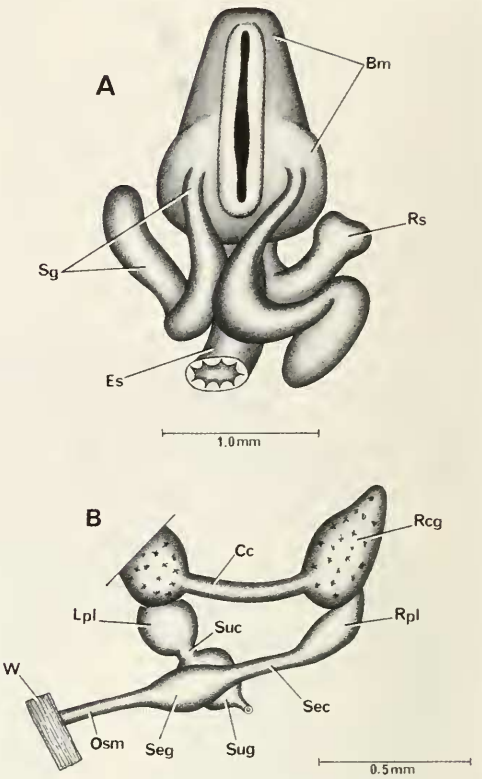

FIG. 122. A. Dorsal aspect of the buccal mass of *Lithoglyphopsis modesta*. B. Dorsal aspect of nerve ring.

of this species except for the shells. The type locality is Lien-dshou-ho in Kwangtung [= Guangdong Province], immediately south of Hunan (Yen, 1939). The lectotype and paralectotypes are in the Bozen Museum, No. 109 (Zilch, 1974).

It is probable that there are additional species of *Lythoglyphopsis*. The closest relationship of *L. modesta* to any other Triculinae thus far studied is with *Fenouilia kreitneri* (see Davis et al. 1983). Both species have a fat body, thus fitting a shell shape that is globose or rather trochoid. The shells are quite different. *Lythoglyphopsis modesta* has a globose-conic shell where as *Fenouilia* has a trochoid to trochoid-ovate shape. The shell of the former is smooth, that of the latter has keels. The characters of the head are the same. The female reproductive system is virtually the same except for two substantive differences. One is the very short spermathecal duct of the former bridging the oviduct to the pericardium where the oviduct turns towards the bursa complex. The spermathecal duct is elongated in the latter. The other is the bending around of the posterior pallial oviduct thus covering the bursa complex of organs (in the former). In the latter, the pallial oviduct does not bend; the bursa is posterior to the pallial oviduct. The male reproductive system is the same in both taxa with one substantive difference; the penis of the former has a long penial filament lacking in the latter. The radular sac is extremely elongated and coils up dorsally along the buccal mass; it is short, that is, generalized in length in the latter (as also in *Lacunopsis*). The cerebral commissure of the former, is over double that of the latter. The gill filaments are different. In the former they are of moderate length with a short section of Gf_2 clearly seen. In the later, the gill filament Gf_1 is elongated; Gf_2 is not visible with the mantle reflected.

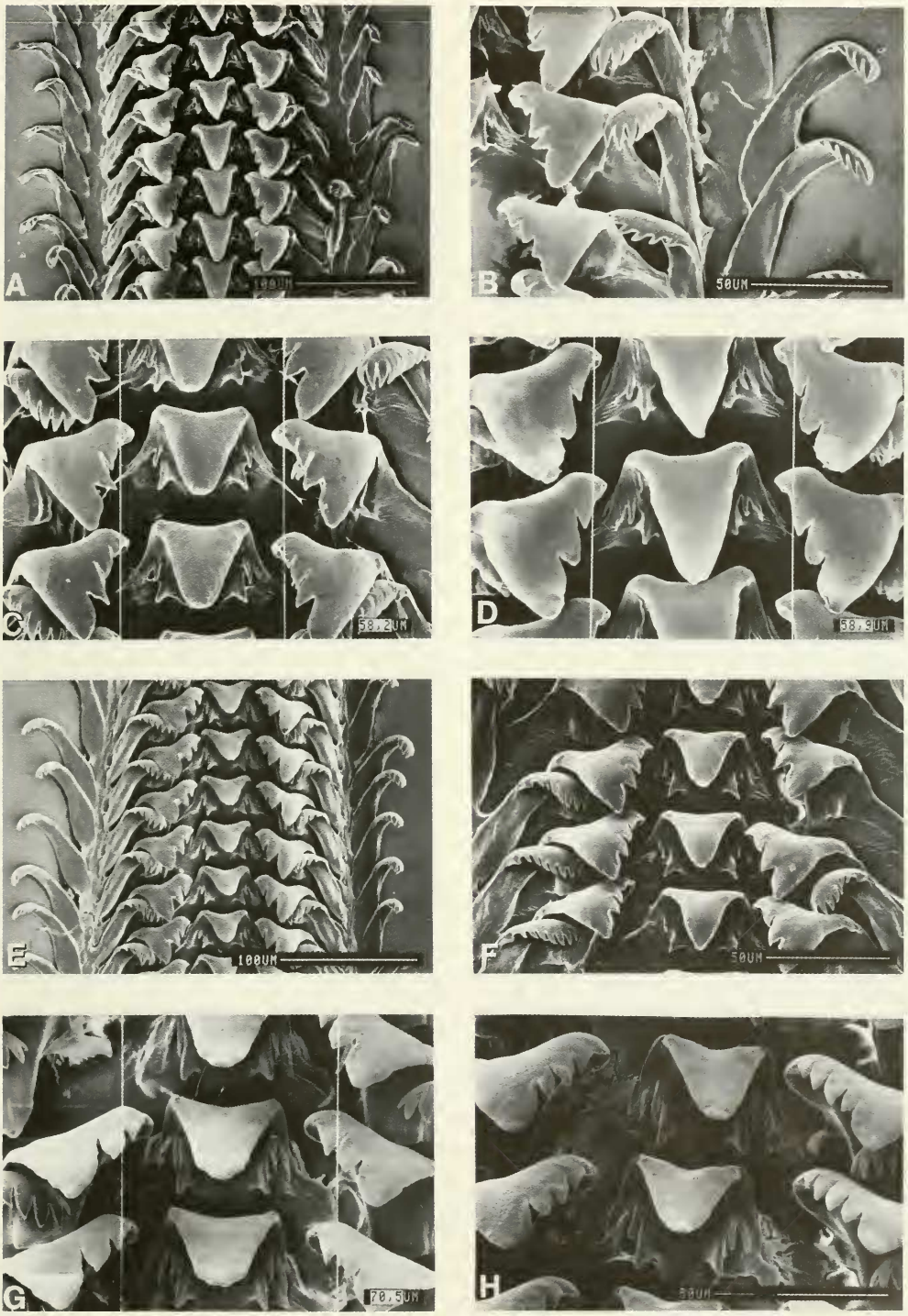

FIG. 123. Radula of *Lithoglyphopsis modesta*. A, E segments of radula. C, D, G, H. Central and lateral teeth. B, E, F. Lateral, inner and outer marginal teeth.

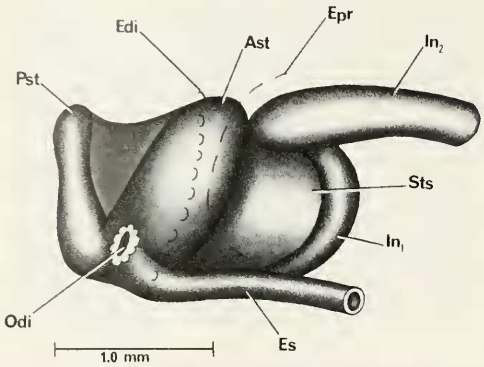

FIG. 124. Ventral aspect of the stomach of *Lithoglyphopsis modesta*.

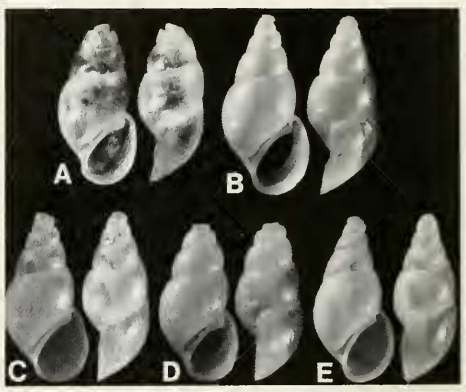

FIG. 125. Shells of *Tricula gredleri*. Figure A is 3.2 mm long; other shells are printed at same scale.

However, given this series of differences between the two taxa, without more data for more species, it is not possible to define generic limits clearly.

Tricula Benson, 1843

Type Species. *Tricula montana* Benson, 1843: 465

Type locality. Bhimtal, N. India

Designation. By monotypy

Assigned species. Based on anatomical study; type species and Chinese species only. *T. montana* Benson, 1843; *T. bambooensis* Davis & Zheng, 1986 (in Davis et al., 1986b); *T. bollingi* Davis, 1968; *T. gregoriana* Annandale, 1924; *T. hudiequanensis* Davis & Guo, 1986 (in Davis et al., 1986b); *T. ludongbini* Davis & Guo, 1986; *T. xianfengensis* Davis & Guo, 1986; *T. xiaolongmenensis* Davis & Guo, 1986. *T. gredleri* Kang, 1986; *T. maxidens* Chen & Davis, sp. nov; *T. odonta* Liu, Zhang & Wang, 1983a. N = 11.

Diagnosis. Shells small to medium, ovate-conic. Central tooth as in *Neotricula*. The oviduct makes a tight 360° twist dorsal to the bursa. The spermathecal duct enters the pericardium; the spermathecal duct starts as a wide duct when diverging from the oviduct and narrows to a slender duct at the pericardium. The duct of the seminal receptacle arises from the oviduct, from the base of the duct of the bursa, or from the duct of the bursa. The duct of the bursa runs undiminished in diameter into the oviduct close to the opening of the oviduct into the albumen gland. Some species of *Tricula* have a pericardial bursa (Davis et al., 1986b: 515, fig. 40). The type species has a pericardial bursa (Davis et al., 1986a: 434, fig. 6A).

Tricula gredleri Kang, 1986

Syntypes. Hubei Medical College, Department of Parasitology, Wuhan City, Hubei Province, People's Republic of China. Figured in Kang (1986: pl.1, fig. 2). Holotype not segregated in Kang's collection. SMF 305653–305654

Type locality. Maluxi, "(28°56′N, 109°92′E)", Orientalis Commune, Guzhang County, Hunan Province. Collected 18 Oct. 1983.

Etymology. Named for Vincent Gredler, the German malacologist who first described Chinese *Tricula* from Hunan Province.

Habitat

Specimens studied for this paper were collected from a small stream at Yantuo Village, Xiaoguanping Town, Guzhang County, Xiangxi Prefecture; 28°42′7″N, 110°0′37″E (Fig. 1, site 12), 20 May 1987, Li Chi-Jian. The habitat was 700 m at the edge of the stream shaded by short shrubs. The name of the stream is You Shui He (he = small stream). The field number is D87-3.

Depository

Specimens are catalogued into the collections of ZAMIP, M0008; ANSP 373141, A12657.

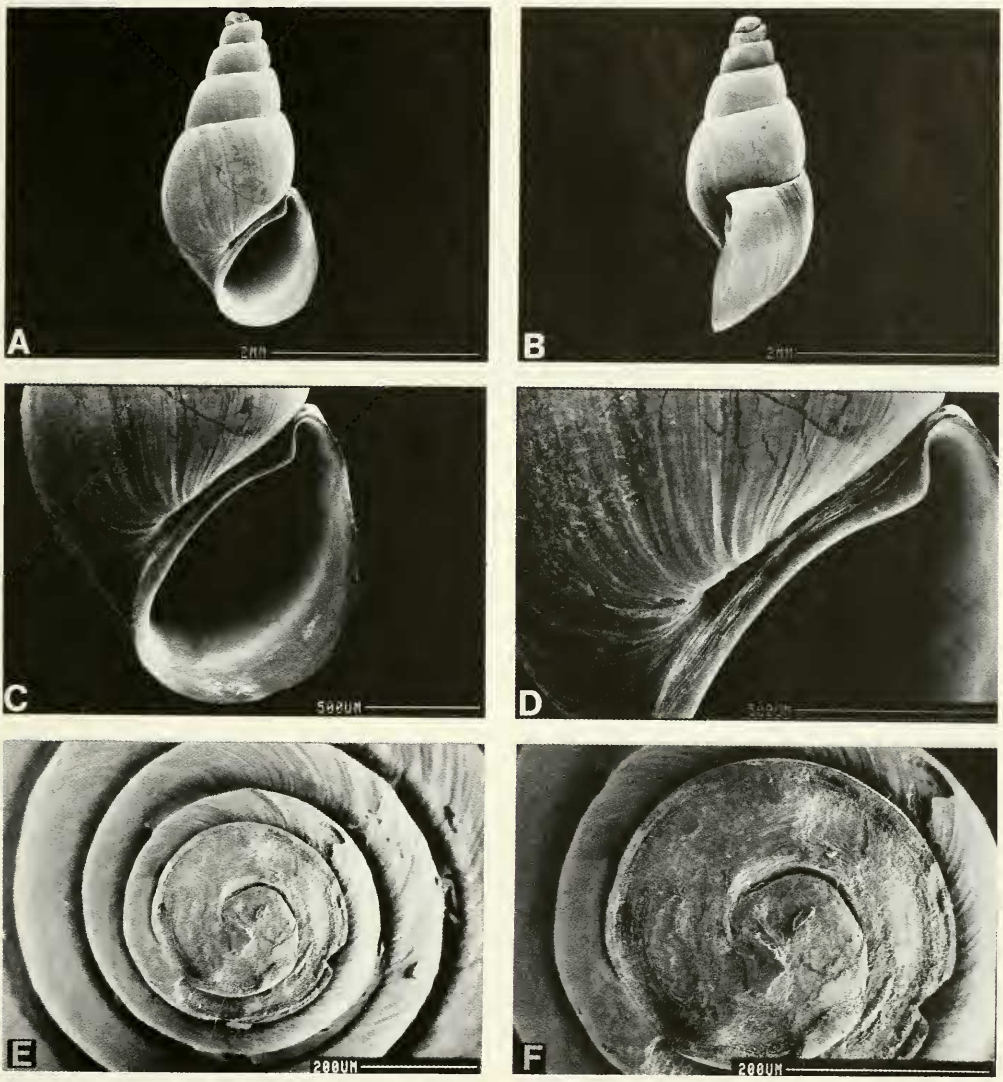

FIG. 126. SEM photographs of shells of *Tricula gredleri*. A, B. Whole shells of mature individuals; C–D. Magnified view of the aperture showing small but deep umbilicus and pronounced apertural notch. E, F. Eroded protoconchs; teleoconch begins at 1.75 whorls.

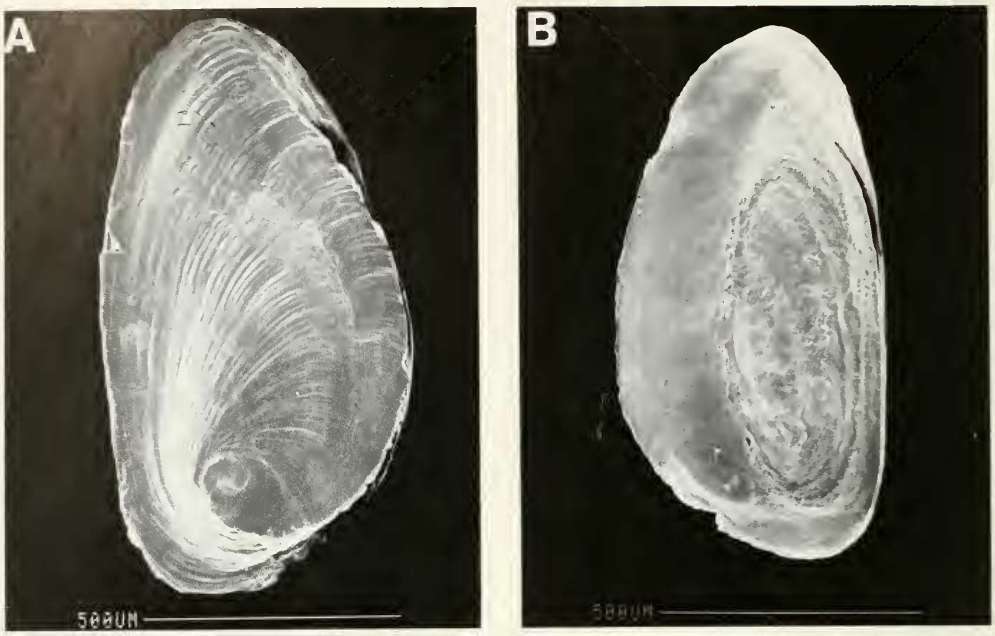

FIG. 127. Opercula of *Tricula gredleri*. Outer surface at left (A); inner surface to the right (B).

Description

Shell. Shells are small, ovate-conic, and smooth (Figs. 125, 126). Virtually all shells are eroded at the apices so that a true understanding of length is not possible. Lengths do exceed 3.30 mm (Table 62). The aperture is pyriform. Adapically there is a pronounced apertural beak with beak tubercle. There is no internal notch groove. There is no adapical outer lip angle.

The whorls at the suture are smooth (not crenulated). There is an umbilical chink. The inner lip is straight abapical to the beak tubercle; it is separated from the body whorl. Adapically shell material may be layered between the lip and the body whorl to the point of fusion. The inner lip is uniformly thin. An apertural sinus is seen when the outer lip is seen in side view. Abapical to the sinus the lip is straight to slightly scooped forward. In side view, the inner lip is straight; there is no spout, no varix.

The abapical lip projects beyond the base of the shell 0.38 ± 0.02 mm.

External features. The head is translucent; there is no deposition of melanin pigment. There are no white or yellow granules about the eyes. The operculum (Fig. 127) is corneous and paucispiral. It is unique in being especially thickened abapically and sitting cap-like on the foot. The attachment pad is prominent, some 56% the width of the operculum.

Mantle cavity. Mantle cavity organs are shown in Figure 128. Organ measurements and counts are given in Table 63. The osphradium is positioned slightly anterior to mid-gill; it is elliptical and short. There are 13 to 19 gill filaments with both Gf_1 and Gf_2 elements prominent. The longest gill filaments are 0.48 ± 0.09 mm long. Gill filament section Gf_2 is long. In side view, the largest gill filaments are moderately domed.

The portal for sperm entry into the pericardium (Ope) is shown. The pericardium (Pe) is considerably swollen and there is an enormous pericardial bursa (Pbu) pushing the lining of the mantle cavity far forward into the mantle cavity.

Female reproductive system. An uncoiled female without head and with kidney tissue removed is shown in Figure 129. Measurements of organs are given in Table 63. Important features are: (1) The gonad is posterior to the stomach. It is small and consists

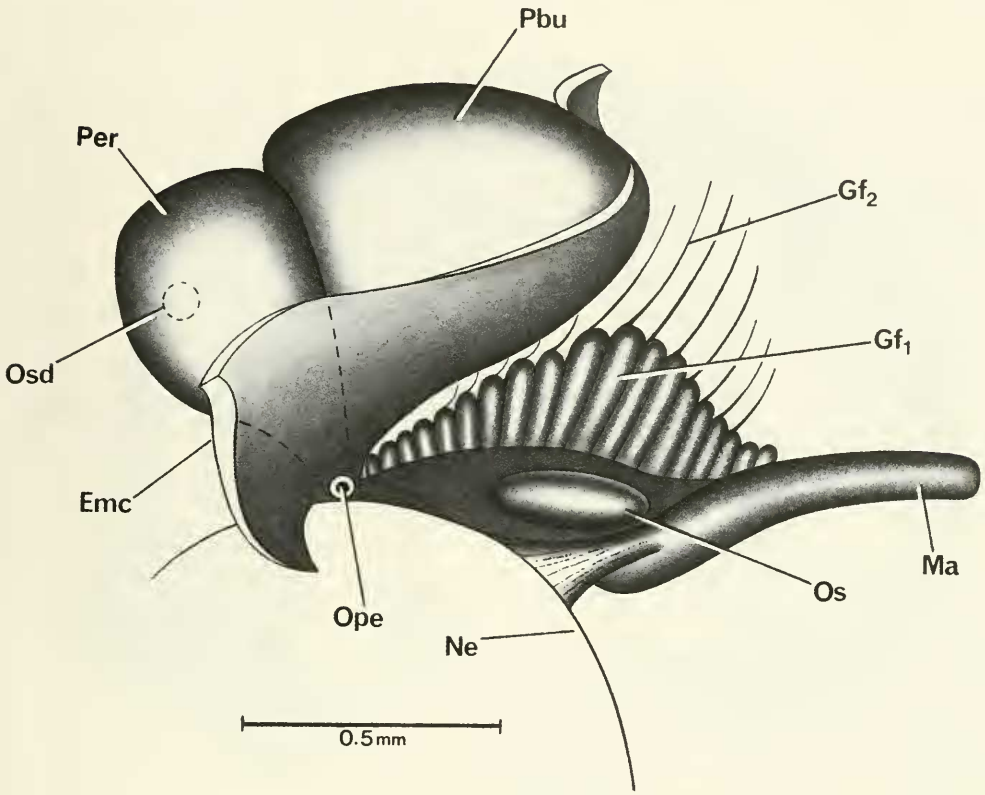

FIG. 128. Mantle cavity of *Tricula gredleri* showing the enormous pericardial bursa (Pbu) bulging into mantle cavity.

TABLE 62. Shell measurements (mm) of *Tricula gredleri* syntypes and of shells of snails used for dissections. All shells that had eroded apices = e. Mean ± standard deviation (range). N = number measured. M = male, F = female.

	Syntypes (N = 2)		For Anatomy (N = 5)
	1.	2.	
No. Whorls	4e	5e	3e–4e
Length (L)	3.08e	3.12e	3.16 (4e,M); 3.32 (4e,F)
Width (W)	1.40	1.36	1.52±0.11 (1.36–1.64)
L last three whorls	2.80	2.76	3.01±0.11 (2.84–3.16)
L body whorl	2.04	2.08	2.20±0.11 (2.12–2.36)
L penultimate whorl	0.44	0.40	0.54±0.02 (0.52–0.56)
W penultimate whorl	0.92	0.96	1.06±0.05 (1.00–1.12)
W 3rd whorl	0.64	0.60	0.71±0.04 (0.68–0.76)
L aperture	1.48	1.48	1.50±0.08 (1.40–1.56)
W aperture	0.80	0.88	0.99±0.05 (0.92–1.04)
x			0.38±0.02 (0.36–0.40)
y			0.18±0.06 (0.10–0.24)

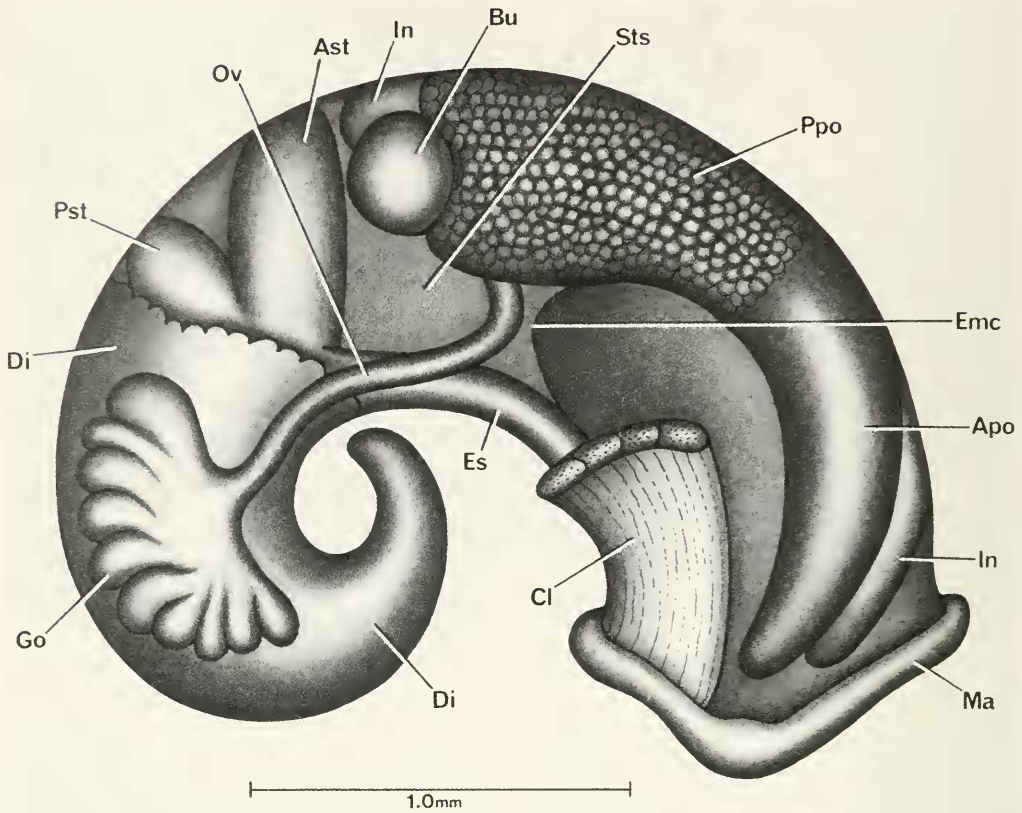

FIG. 129. Uncoiled female *Tricula gredleri* with head and kidney tissue removed.

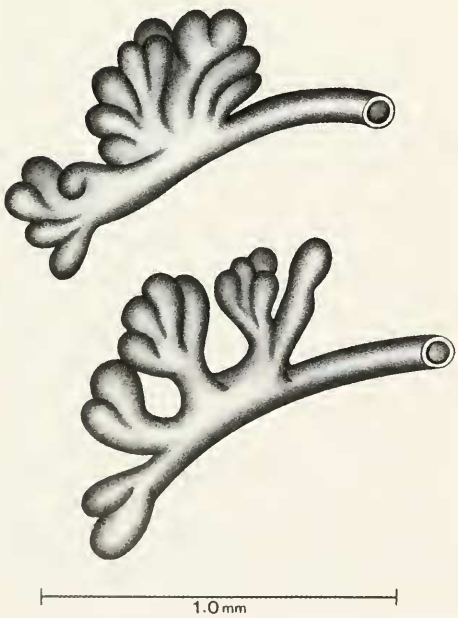

FIG. 130. Variation in gonad structure of female *Tricula gredleri*.

of one to four bundles of lobes Figures 129, 130. (2) The bursa copulatrix (Bu) is round to sub-triangular, minute, and clearly visible posterior to the albumen gland (Ppo). (3) The albumen gland is of normal size. (4) The bursa copulatrix complex of organs is shown in Figures 131, 132. In Figure 131 the orientation of the bursa complex is the same as in Figure 129. The 360° twist of the oviduct (Ov) and the duct of the bursa arising from the oviduct are seen in Figure 131; these two character-states are seen in all genera of the tribe Triculini. (5) The species is unique in having such an enlarged pericardial bursa (Pbu). (6) In Figure 132A and B, it is shown that the duct of the seminal receptacle arises from the oviduct slightly posterior to the opening of the duct of the bursa either slightly offset dorsolaterally, or directly in line with the opening of the duct of the bursa (Fig. 132 C). (7) The seminal receptacle (Sr) is a small sphere. (8) There is no spermathecal duct, or, at best, a minute one; the oviduct appears, in gross dissection, to be fused to the pericardium (Sdo,

TABLE 63. Lengths (mm) or counts of non-neural organs and structures of *Tricula gredleri*. N = number of snails used. Mean ± standard deviation (range).

	Females (N = 5)	Males (N = 2)
Body	4.96±0.45 (4.30–5.44)	4.80 (4.60, 5.00)
Gonad	0.85±0.11 (0.70–1.00)	2.60 (2.40, 2.80)
Digestive gland	2.17±0.32 (1.70–2.50)	1.97 (1.92, 2.02)
Posterior pallial oviduct (= albumen gland)	1.05±0.19 (0.80–1.20) N = 4	—
Anterior pallial oviduct (= capsule gland)	1.13±0.15 (1.00–1.30) N = 4	—
Total pallial oviduct = OV	2.14±0.17 (2.00–2.40)	—
Bursa copulatrix = BU	0.31±0.01 (0.31–0.32)	—
Duct of BU	0.17±0.01 (0.16–0.18) N = 3	—
BU ÷ OV	0.14±0.01 (0.13–0.16)	—
Seminal receptacle	0.17±0.01 (0.16–0.18) N = 4	—
Duct of seminal receptacle	0.08±0.02 (0.06–0.10) N = 4	—
Mantle cavity	1.42±0.13 (1.30–1.60)	1.55 (1.50, 1.60)
Gill (G)	1.07±0.17 (1.30–1.60)	1.11 (1.10, 1.12)
Osphradium (OS)	0.35±0.08 (0.30–0.46) N = 4	0.31 (0.24, 0.38)
Os ÷ G	0.35±0.09 (0.25–0.46) N = 4	.28 (0.22, 0.34)
No. of filaments	16.8±2.3 (13–19)	16.0 (No var.)
Buccal mass	0.58±0.09 (0.50–0.68)	—
Gf_2	0.26±0.06* (0.20–0.36) N = 6	—
Gf_1	0.22±0.08* (0.18–0.26) N = 6	—
Total Gf = TGF	0.48±0.09* (0.38–0.62) N = 6	—
Gf_2 ÷ TGF	0.54±0.03* (0.50–0.58) N = 6	—
Prostate	—	0.93 (0.86, 1.00)
Seminal vesicle	—	0.70 (0.60, 0.80)
Penis	—	2.60 (2.00, 3.20)

*males and females

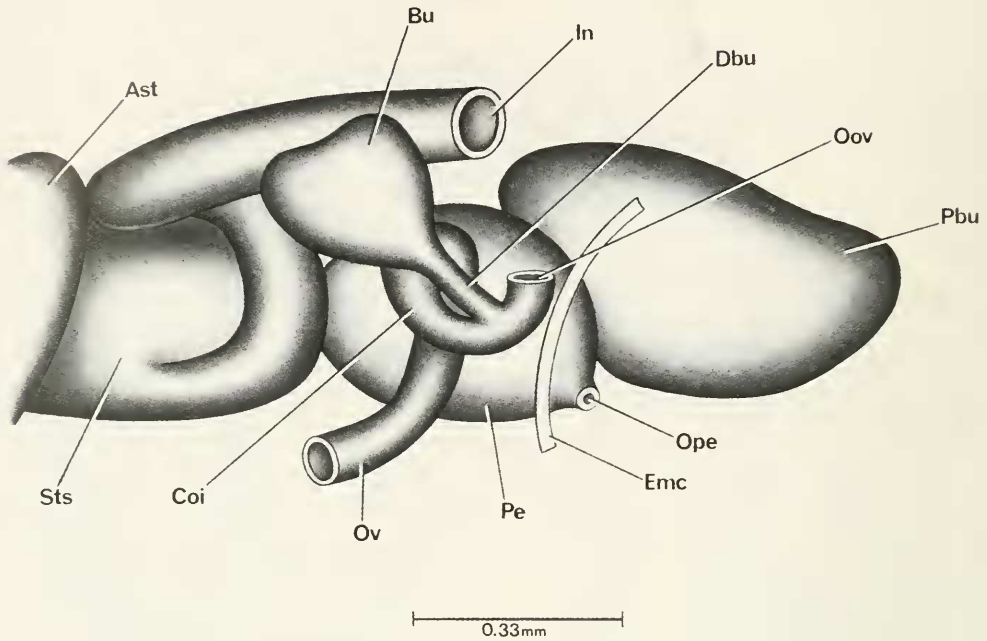

FIG. 131. Details and variation of bursa copulatrix complex of organs relative to style sac (Sts), pericardium (Pe) and posterior end of mantle cavity (Emc).

TABLE 64. Radular statistics for *Tricula gredleri*. Mean ± standard deviation (range). N = number used. In mm except for width of central tooth in μm.

	Females (N = 3)	Males (N = 4)
Shell length	3.41±0.17	3.30
	(3.28–3.60)	(3.10, 3.40) N = 2
Radular length	0.49±0.10	0.51±0.03
	(0.39–0.60)	(0.47–0.54)
Radular width	0.07±0.002	0.07±0.01
	(0.072–0.076)	(0.060–0.072)
Total rows of teeth	56±4.4	63.4±4.2
	(53–61)	(61–70)
No. rows of teeth forming	16.0±2.0	16.3±1.5
	(14–18)	(15–18)
Central tooth width	13.7±1.0	15.1±1.4
	(12.8–15.0) N = 8	(13.1–17.1) N = 17

Fig. 132B). (9) Sperm enter the female system from the mantle cavity into the pericardium hence to the oviduct.

Male reproductive system. An uncoiled male without head and with kidney tissue removed is shown in Figure 133. Two bundles of gonadal lobes are cut away to show the seminal vesicle (Sv). Measurements are given in Table 63. Important features are: (1) The gonad fills the digestive gland (Di) and covers the posterior and anterior chambers of the stomach. (2) The prostate (Pr) overlaps the posterior end of the mantle cavity (Emc). (3) The seminal vesicle (Sv) arises from the vas efferens (Ve) about mid-gonad. (4) The seminal

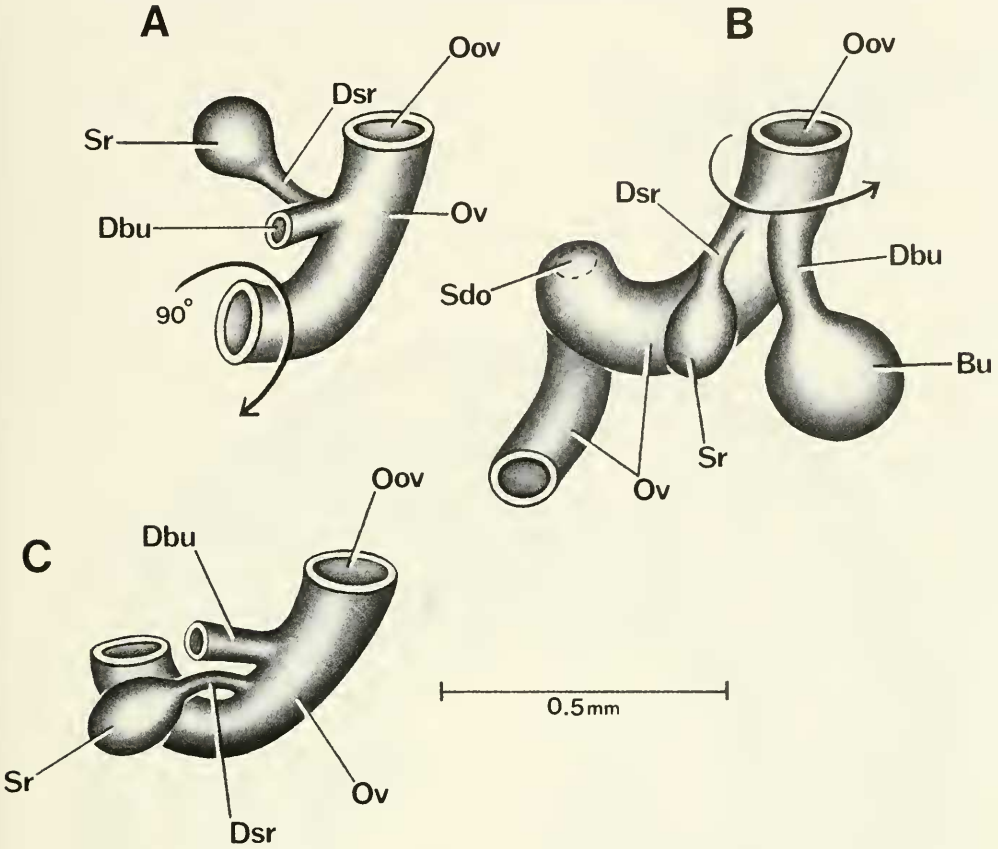

FIG. 132. Details and variation of bursa copulatrix complex of organs of *Tricula gredleri*. A. Compared with Figure 131, bursa copulatrix cut off and duct system rotated 90° to show position of seminal receptacle (Sr) and its duct (Dsr). Complex in A is further rotated in B to show where duct of seminal receptacle (Dsr) opens into oviduct (Ov). C. Section of oviduct oriented as in Figure 131 showing a variation in position of opening of duct of seminal receptacle into oviduct, the usual *Tricula* position.

TABLE 65. Cusp formulae for the radular teeth of *Tricula gredleri* with the percent of the seven radulae in which a given formula was found at least once.

Central Teeth		Lateral Teeth		Inner Marginal Teeth		Outer Marginal Teeth	
$\frac{3\text{-}1\text{-}3}{2\text{-}2}$	71%	2-[2]-3	86%	8	29%	8	14%
$\frac{3\text{-}1\text{-}3}{3\text{-}3}$	14%	3-[2]-2	86%	9	57%	9	71%
$\frac{3\text{-}1\text{-}2}{2\text{-}2}$	14%	2-[2]-4	43%	10	71%	10	57%
$\frac{2\text{-}1\text{-}2}{2\text{-}2}$	14%	4-[2]-2	14%	11	57%	11	71%
$\frac{4\text{-}1\text{-}3}{3\text{-}2}$	14%						
				$\bar{X}$ * = 9.69±2.01 N = 70		9.0±3.1 N = 70	

*Mean ± standard deviation of cusp number for all teeth counted.
[ ] = blade bifurcates thus resembling two cusps.

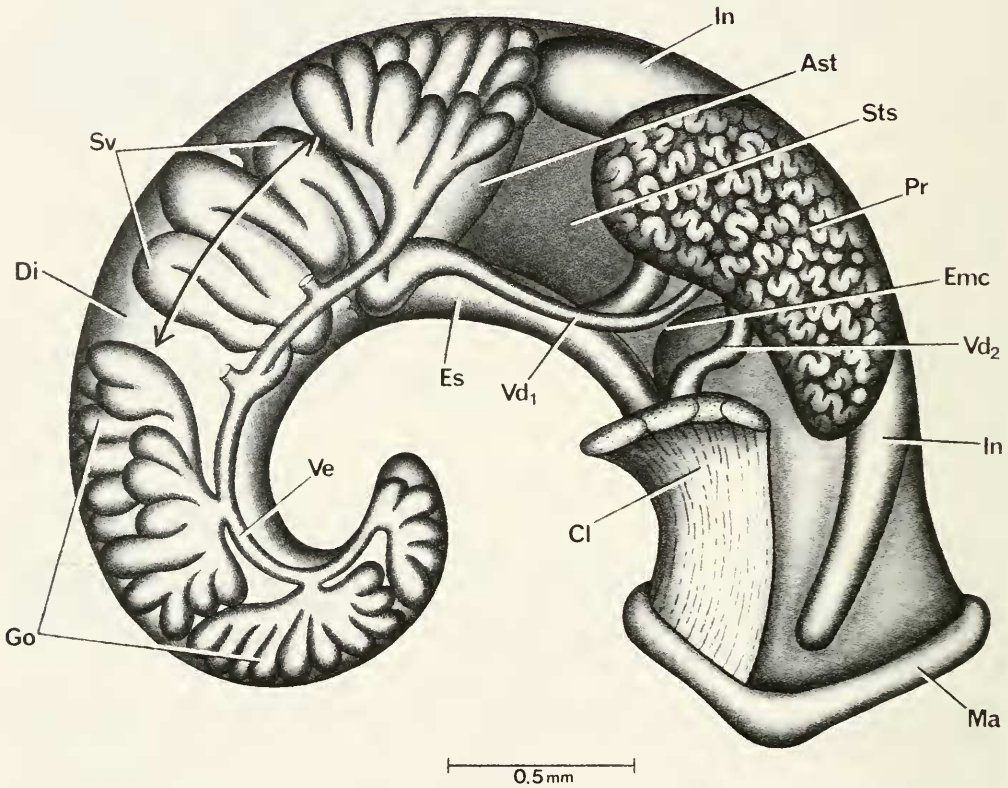

FIG. 133. Uncoiled male of *Tricula gredleri* without head or kidney tissue. Two sections of gonadal lobes removed to reveal seminal vesicle coiled dorsal to gonad.

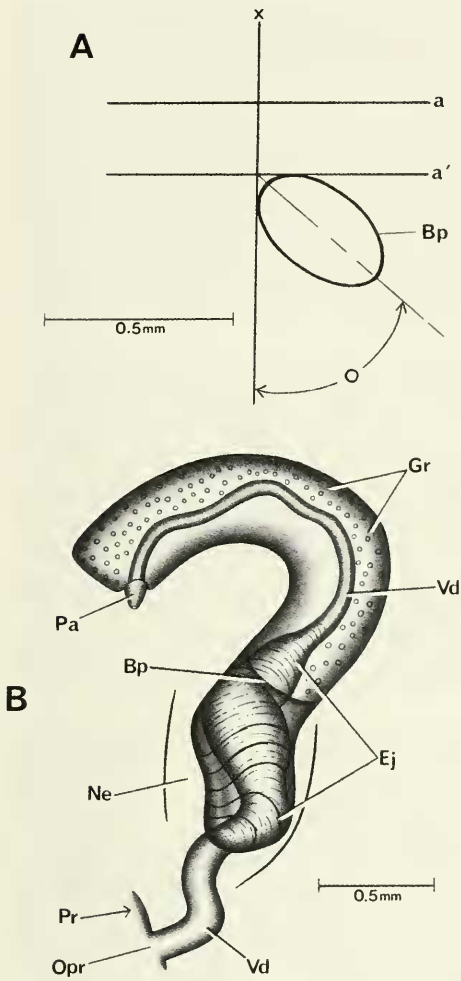

FIG. 134. A. Relationship of base of penis of *Tricula gredleri* to mid-line of snout-neck (x) and to posterior end of eye lobes (a). B. Penis.

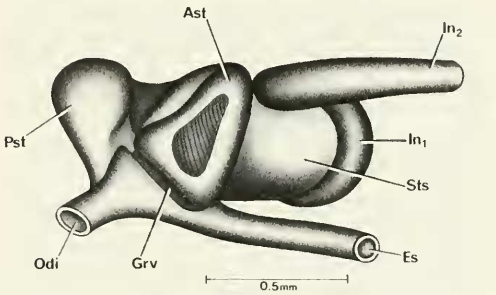

FIG. 135. Stomach of *Tricula gredleri* oriented exactly as in Figures 129, 131, and 133.

TABLE 66. Lengths of neural structures of *Tricula gredleri*. Mean ± standard deviation (range). N = number used = 5. * - neural elements measured to obtain the RPG ratio.

Cerebral ganglion	0.24±0.02 (0.22–0.26)
Cerebral commissare	0.04±0.02 (0.02–0.06)
Pleural ganglion	
Right (1)*	0.12±0.02 (0.10–0.14)
Left	0.12±0.02 (0.10–0.14)
Pleuro-supraesophageal connective (2)*	0.14±0.02 (0.12–0.16)
Pleuro-subesophageal connective	0.14±0.03 (0.10–0.16)
Supraesophageal ganglion (3)*	0.12±0.02 (0.10–0.14)
Subesophageal ganglion	0.12±0.02 (0.10–0.14)
Osphradio-mantle nerve	0.07±0.03 (0.04–0.12)
RPG ratio* = 2 ÷ 1+2+3	0.37±0.04 (0.33–0.41)

vesicle coils dorsal to the gonad from mid-gonad anterior to cover the posterior chamber of the stomach. (5) The anterior vas deferens (Vd_2) leaves the prostate near the posterior end of the mantle cavity (Emc). (6) The penis is unique among triculine taxa (Figure 134B). The anterior end is blunt with a protudable papilla (Pa) emerging from the edge of the square penial tip at the concave side of the penis. (7) The ejaculatory duct is massive and extends as a wide muscular duct from the base of the penis along the dorsal aspect of the neck to the end of the neck. (8) The orientation of the base of the penis to the snout-neck mid-line is shown in Figure 134A. It is to the right of the mid-line ("x"), and at an angle of 45°–50° to it.

Digestive system. The digestive gland is posterior to the stomach of both sexes. The stomach is shown in Figure 135. Two features of note are: (1) there is a groove (Gr) or crease between the anterior chamber of the stomach (Ast) and the section of stomach receiving the esophagus (Es) and duct of the digestive gland (Odi). (2) The anterior chamber (Ast) is yellow with a centrally positioned grey area.

Radular statistics are given in Tables 64 and 65. There appears to be sexual dimorphism in the number of rows of teeth on the

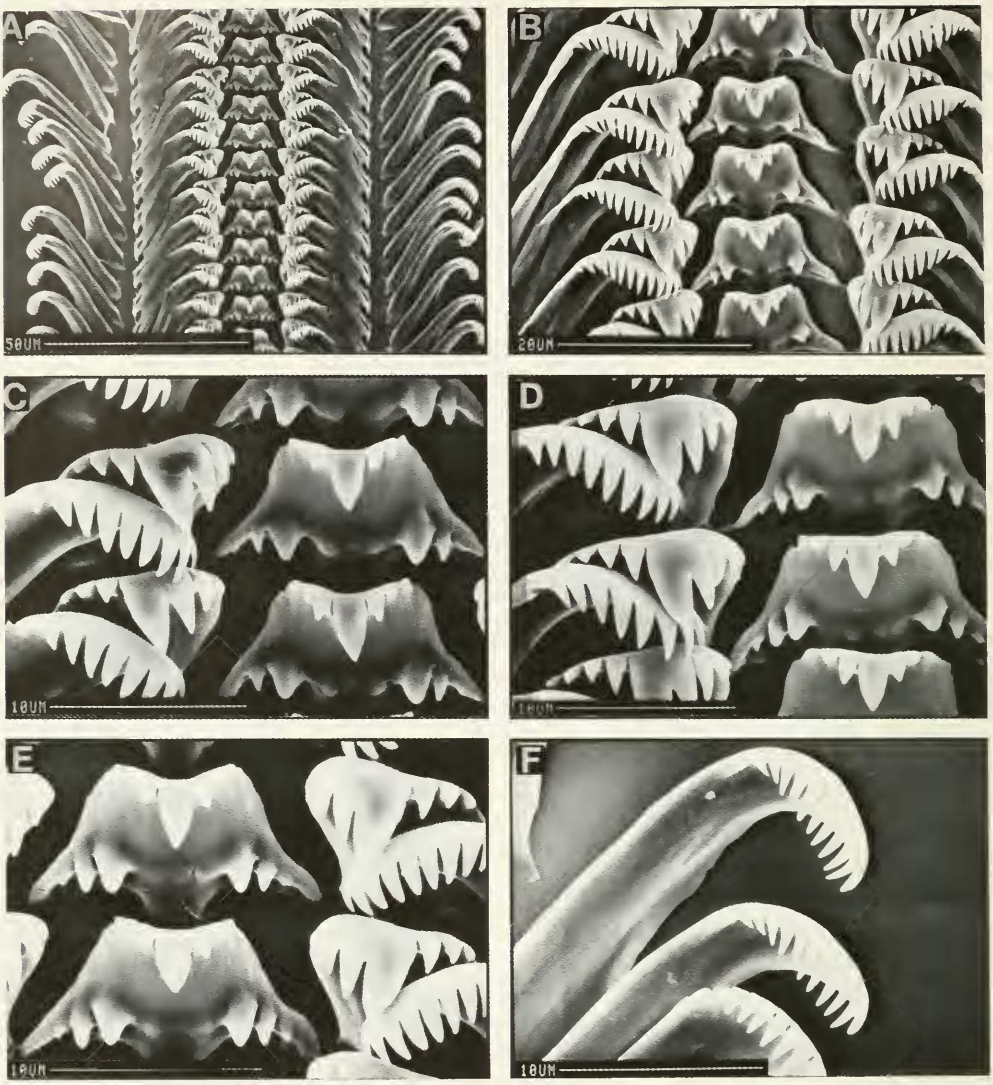

FIG. 136. Radula of *Tricula gredleri*. A. Section of radular ribbon. B-E. Central, lateral and inner marginal teeth. F. Outer marginal teeth. Note pronounced bifurcation of the blade of the major cusp of lateral tooth (especially in Figs. C–E).

radular ribbon; males have more (61 to 70 on a radula 3.30 mm long). However, the sample size is small. The most frequently encountered formula is

$$\frac{3\text{-}1\text{-}3}{(3)2\text{-}2(3)};\ 2(3)\text{-}[2]\text{-}2(3);\ 9\text{-}11;\ 9\text{-}11.$$

SEM photographs of radulae are shown in Figure 136. The dominant cusp of the lateral tooth (Fig. 136B–E) has a blade that bifurcates. Otherwise the tooth morphologies are standard triculine.

Nervous system. Measurements are given in Table 66. The RPG ratio of 0.37 indicates that the dorsal nerve ring is moderately concentrated. The pleuro-subesophagal connective of this species is unusual for its length, equal to that of the pleuro-supraesophageal connective.

Remarks

Conchologically, *Tricula gredleri* is most similar to *N. duplicata* (Figs. 153–155). Conchological comparison with *N. duplicata* is given in the remarks section for that species. Anatomically, *T. gredleri* has the generic-level character-states that serve to differentiate it from *N. duplicata.*

Tricula gredleri has seven *unique* anatomical character-states (Tables 80, 81). The operculum is cap-like, not a flat sheet (char. 2). The oviduct is fused to the pericardium; there is no discernable length of spermathecal duct (chars. 19,20). The penial opening of this species arises form the concave edge of a blunt tip (char. 34). The anterior chamber of the stomach is lemon yellow (char. 40). The pleuro-subesophageal connective is long (char. 48).

Tricula gredleri belongs to the species group within *Tricula* that has a pericardial bursa *T. montana*, *T. gredleri*, *T. gregoriana* and *T. maxidens.* Its closest relationship anatomically is with *T. odonta.*

Tricula maxidens Chen & Davis, sp. nov.

Holotype. ZAMIP, M0009, Figure 137A.

Paratypes. ANSP 373140, A12656, Figure 137B–E.

Type locality. Yantuo Village, Xiaoguanping Town, Guzhang County, Xiangxi Prefecture; 28°42′7″N, 110°0′37″E. Figure 1, site 12.

Etymology. contraction from the Latin maximum (the greatest) and dens (tooth).

Habitat

These snails were collected in sympatry with *Tricula gredleri* and *Akiyoshia chinensis* from a small mountain stream at an altitude of 700 m. The field number assigned was D87-3.

Description

Shell. Shells are small, smooth, and cylindrical-conic (Figs. 137A–E; 138A–D, F). They mature at 5.5 whorls with the largest size class ranging in length from 2.08–2.24 mm (Table 67). The sutures are deep and the whorls are slightly convex. Cleaned shells are glassy; there is no umbilicus. The aperture is semi-circular with the inner lip a flat-straight edge. The inner lip is fused to the body whorl. The outer lip in side view, is straight, without notch or sinuation. With the outer lip down and 90° to the horizontal, the inner lip is seen in side view with a slight angulation. The most prominent feature is the relatively gigantic columellar tooth seen in the aperture (Fig. 138B) that continues inside the shell wrapping the columella adapically. SEM analyses of the apical whorls indicates that they are minutely malleated to smooth (Fig. 138D, F).

External Features. The head is devoid of melanin pigment. There are no white or yellow granules or glands around the eyes. The operculum (Fig. 138E) is corneous, paucispiral and kidney-bean shaped. The embayment on the columellar side corresponds to the large tooth on the columella. The attachment pad is narrow (33% of operculum width) and moderately prominent.

Mantle cavity. Mantle cavity organs are shown in Figure 139A. Organ measurements and counts are given in Table 68. The osphradium (Os) is mid-gill, and long. There are 10 to 15 well developed gill filaments. The longest gill filament are 0.27 ± 0.01 mm long. The Gf_2 part of the gill is long. Sperm enter the pericardium at the rear of the mantle cavity (Ope). The pericardium (Pe) is moderately swollen and bulges out into the mantle cavity. A discrete but small and delicate pericardial bursa (Fig. 139D) was seen in two individuals, it measured 0.30 x 0.14 mm.

Female reproductive system. An uncoiled female without head and with kidney tissue removed is shown in Figure 140. Measurements of organs are given in Table 68. Important features are: (1) The gonad (Go) is posterior to the stomach; it is small and with bundles of lobes. (2) The bursa copulatrix is round and small; half the bursa is dorsal to the posterior end of the albumen gland (Ppo). (3) The albumen gland is of standard length. (4) The bursa copulatrix complex of organs is shown in Figure 139. The orientation in Figure 139A is the same as that in Figure 140. The bursa copulatrix (Bu) is short. (5) The seminal receptacle (Sr) is spherical; it has a short duct (Dsr) opening into the right ventro-lateral edge of the oviduct (Ov) just posterior to the opening of the duct of the bursa (Dbu) into the oviduct. (6) The spermathecal duct (Sd) is moderately long; it runs to open into the pericardium (Pe). (7) The pericardium is swollen with sperm and distends into the posterior mantle cavity. In some specimens, a minute

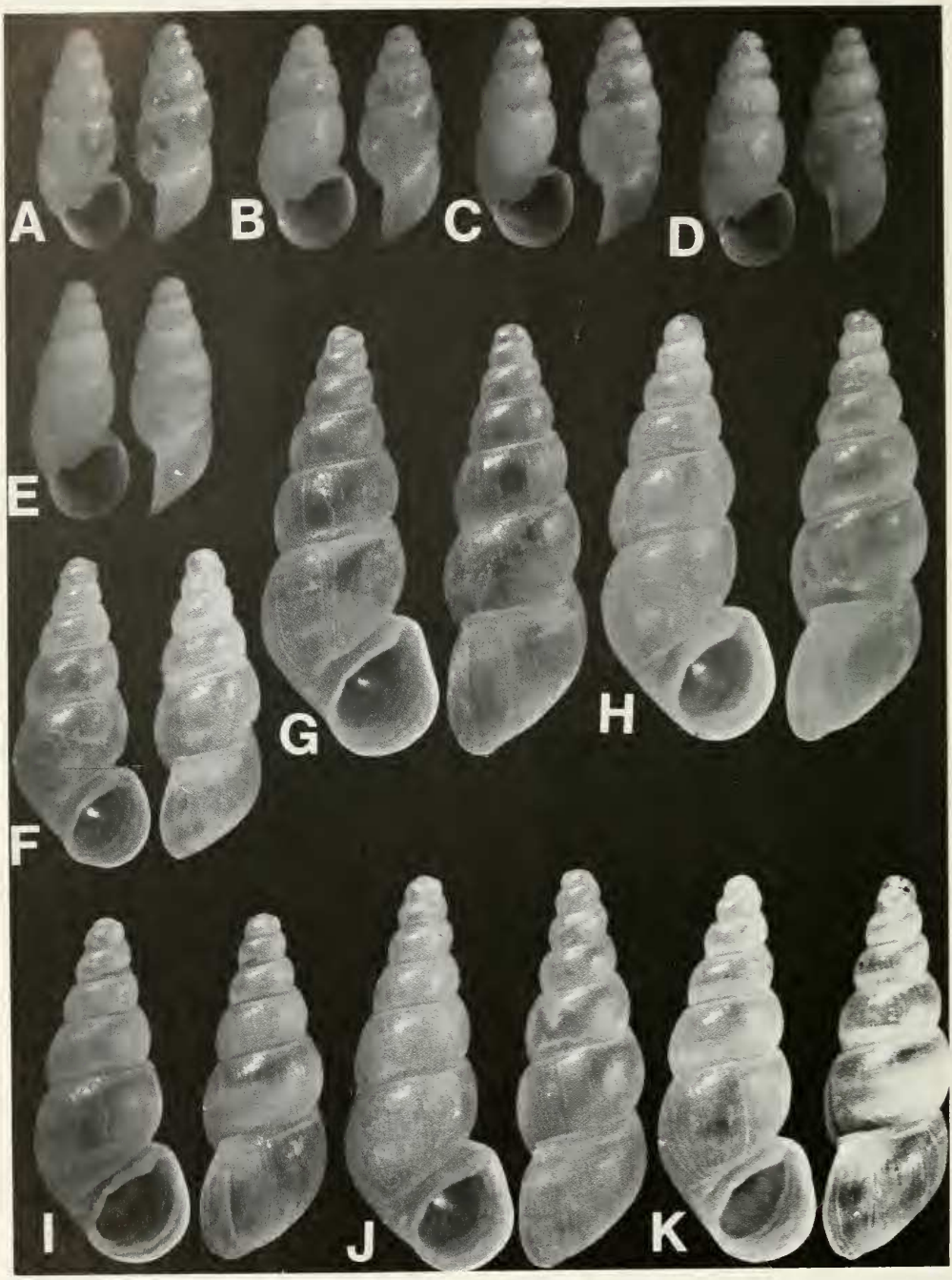

FIG. 137. Shells of *Tricula maxidens*, A–E; *Tricula odonta*, F–K. A. Holotype; B–E. Paratypes. Length of A = 1.94 mm; other shells printed to same scale.

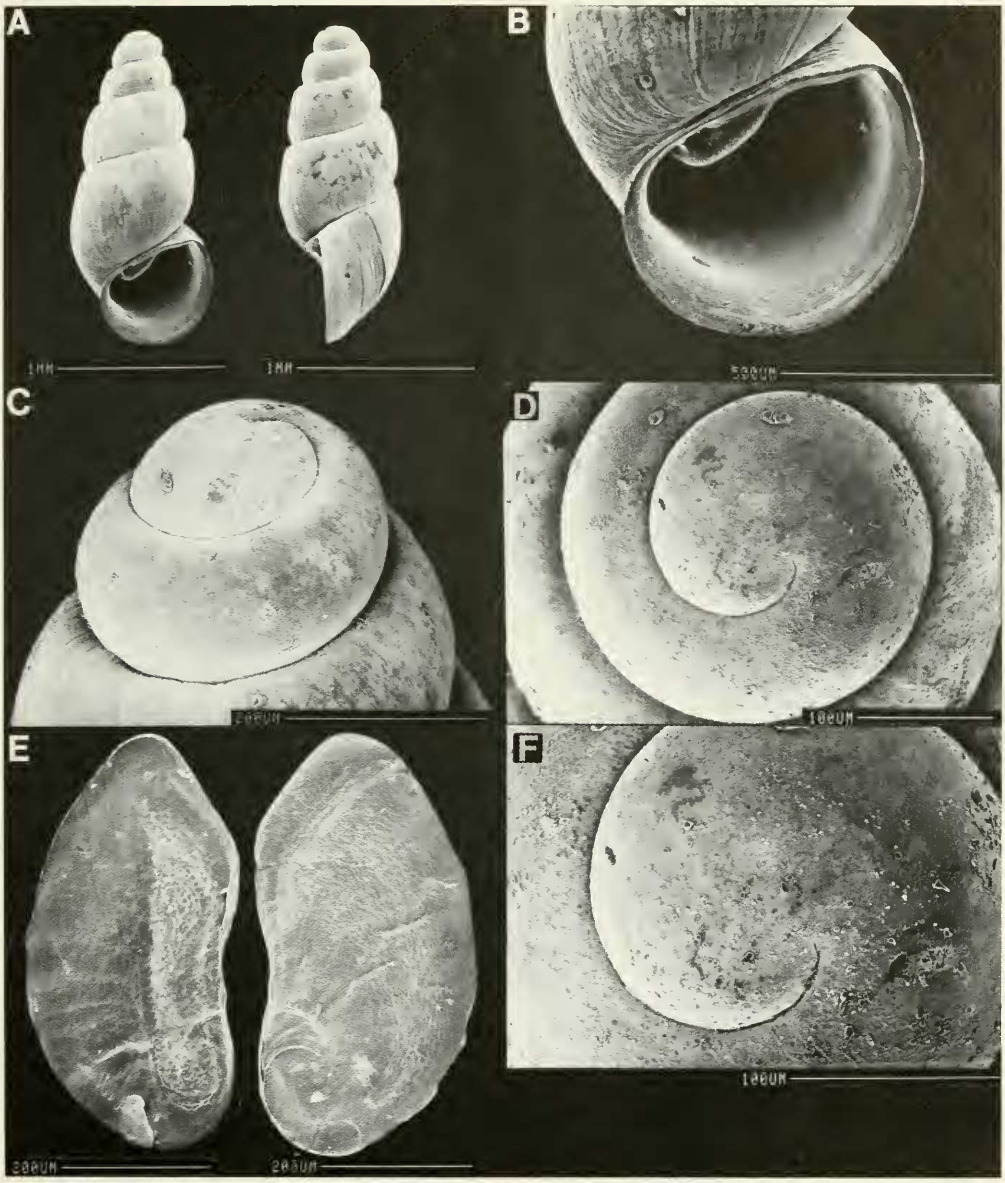

FIG. 138. SEM photographs of shells and opercula of *Tricula maxidens*. A. Shells of mature individuals. Note straight outer lip (right photo) and prominent columellar tooth. B. Enlargement of aperture showing columellar tooth. C, D, F. Protoconch. Although encrusted, protoconch is seen to be vaguely malleated. E. Opercula: right operculum shows outer surface with paucispiral growth line; left operculum shows inner surface with narrow attachment pad.

TABLE 67. Shell measurements (mm) of *Tricula maxidens*. Mean ± standard deviation (range). b = broken apical whorls. N = number measured.

		Paratypes	
	Holotype	Large class (N = 5)	Small Class (N = 3)
No. Whorls	5.5	5.5	5.5
Length (L)	1.94	2.17±0.06 (2.08–2.24)	1.97±0.06 (1.92–2.04)
Width (W)	0.86	0.92±0.03 (0.90–0.96)	0.82±0.03 (0.80–0.86)
L last three whorls	1.82	1.95±0.03 (1.92–2.00)	1.73±0.08 (1.68–1.82)
L body whorl	1.24	1.34±0.04 (1.28–1.36)	1.16±0.10 (1.08–1.28)
L penultimate whorl	0.40	0.40±0.03 (0.36–0.44)	0.35±0.02 (0.32–0.36)
W penultimate whorl	0.68	0.71±0.01 (0.70–0.72)	0.62±0.02 (0.60–0.64)
W 3rd whorl	0.48	0.50±0.01 (0.48–0.52)	0.46±0.02 (0.44–0.48)
L aperture	0.76	0.86±0.02 (0.84–0.90)	0.73±0.06 (0.68–0.80)
W aperture	0.58	0.62±0.02 (0.60–0.64)	0.55±0.05 (0.52–0.60)
x	0.30	0.34±0.02 (0.32–0.36)	0.32 no variation
y	0.08	0.08±0.01 (0.06–0.10)	0.07±0.03 (0.04–0.10)

pericardial bursa was observed (Fig. 139D, Pbu).

Male reproductive system. An uncoiled male with head and kidney tissue removed is shown in Figure 141. Lengths of non-neural organs are given in Table 68. Important features are: (1) The gonad (Go) covers the posterior chamber of the stomach and most of anterior chamber (Ast). (2) The prostate (Pr) is relatively massive and overlaps the posterior end of the mantle cavity (Emc); it covers half the style sac. (3) The vas deferens arises from mid-gonad to slightly anterior to mid-gonad (Fig. 142). (4) The seminal vesicle forms a short coil of tubes dorsal to the gonad and posterior to the stomach. (5) The anterior vas deferens (Vd_2) leaves the prostate slightly posterior to the anterior end of the prostate (Fig. 141). (6) The penis is simple, without papilla; it is slender (Fig. 143B). (7) There is a pronounced ejaculatory duct (Ej) in the base of the penis. (8) The orientation of the long axis of the penial base (Bp) to the snout-neck mid-line (x) is shown in Fig. 143A. The penial base is to the right of the mid-line and at an angle of 40°.

Digestive system. The digestive gland is posterior to the stomach in both sexes. Radular statistics are given in Tables 69 and 70. There are 59.8 ± 6.4 rows of teeth along a radula of 0.29 ± 0.04 mm (= equivalent of 207 teeth per mm). The most frequently encountered formula is

$$\frac{3\text{-}1\text{-}3}{2\text{-}2};\ 3(4)\text{-}1\text{-}4;\ 12\text{–}14;\ 13\text{–}14.$$

The radula is shown in Figure 144; radula morphology is of the generalized *Tricula* type. The central anterior cusp of the central tooth is long and dagger-like. The dominant cusp of the lateral tooth is slender and dagger-like.

The stomach (Fig. 145) is the usual type but with a diagnostic grey streak (Gs) running across the ventral surface of the anterior chamber (Ast).

Nervous system. Measurements not taken.

Remarks

Conchologically, among species of Triculinae, *T. maxidens* is unique and clearly separated from all other species (Figs. 153–155). Unique character-states (Tables 2, 76) are the cylindrical-conic shape (char. 2) and the massive tooth nearly filling the aperture (char. 16). The columella within the body whorl has

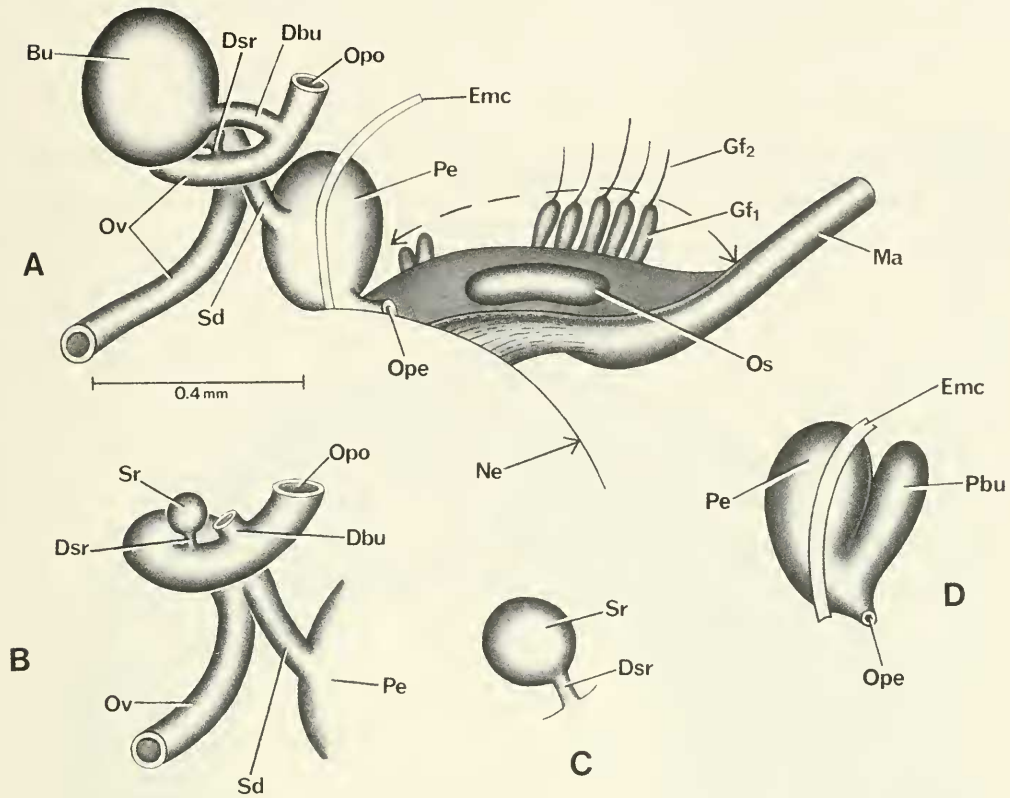

FIG. 139. Details and variation of bursa copulatrix of organs of *Tricula maxidens*. Figs. A and B in the same orientation as in Figure 140. C. Enlarged seminal receptacle. D. Pericardium with minute pericardial bursa (Pbu).

a raised spiral keel. The shell seems more similar to *Pseudobythinella* than to *Tricula*.

Anatomically, this species is most closely allied phenetically to *T. xiaolongmenensis* (Figs. 156–158). It differs from that species in 11 character-states (26%); see Tables 80, 81. Some of these differences are: In *T. maxidens* the bursa is covered by the albumen gland; in *T. xiaolongmenensis* the bursa is posterior to the albumen gland (char. 14). In the former, the duct of the seminal receptacle arises from the inside edge of the oviduct; it arises from the outside edge in the latter (char. 24). The former has a slight pericardial bursa; the latter has no pericardial bursa (char. 25). The radula is short in the former, of medium length in the latter (char. 41). The central anterior cusp of the central tooth is long and dagger-like in the former, the standard type in the latter (char. 44).

Tricula odonta Liu, Zhang & Wang, 1983a

Holotype. SX 788104 (= IZAS; Beijing, People's Republic of China). Figure 1.

Type locality Shangnan, Shaanxi Province. 24 October 1978

Distribution. Shangnan, Shangxian, Zhenping, Tongguan, Ningqiang and Yuanqu of Shanxi Province; Xingshan and Wufeng of Hubei Province; Henan Province

TABLE 68. Lengths (mm) or counts of non-neural organs and structures of *Tricula maxidens*. N = number of snails used. Mean ± standard deviation (range).

	Females (N = 5)	Males (N = 2)
Body	3.30±0.33 (2.90–3.68)	3.24 (3.22, 3.26)
Gonad	0.47±0.09 (0.36–0.60)	1.31 (0.90, 1.72)
Digestive gland	1.32±0.19 (1.00–1.48)	1.41 (1.40, 1.42)
Posterior pallial oviduct (= albumen gland)	0.58±0.11 (0.54–0.70) N = 3	—
Anterior pallial oviduct (= capsule gland)	0.67±0.15 0.50–0.80) N = 3	—
Total pallial oviduct = OV	1.23±0.23 (1.00–.150)	—
Bursa copulatrix = BU	0.24±0.05 (0.22–0.30)	—
Duct of BU	0.09±0.01 (0.08–0.10) N = 4	—
BU ÷ OV	0.20±0.06 (0.16–0.30)	—
Seminal receptacle	0.07±0.01 (0.06–0.08) N = 3	—
Duct of seminal receptacle	0.02 N=1	—
Mantle cavity	0.81±0.08 (0.74–0.90) N = 3	0.82 N = 1
Gill (G)	0.66±0.13 (0.54–0.80) N = 3	0.70 N = 1
Osphradium (OS)	0.28 (0.24, 0.32) N = 2	0.26 N = 1
OS ÷ G	0.39 (0.38, 0.40) N = 2	0.37 N = 1
No. filaments	12.7±2.5 (10–15)	14 N = 1
Gf_2	0.17±0.01 (0.16–0.18)	—
Gf_1	0.11±0.01 (0.10–0.12)	—
Total Gf = TGF	0.27±0.01	—
Gf_2 ÷ TGF	0.61±0.04 (0.57–0.64)	—
Prostate	—	0.75 (0.70, 0.80)
Seminal vesicle	—	0.65 (0.40, 0.90)
Penis	—	0.64 (0.52, 0.76)

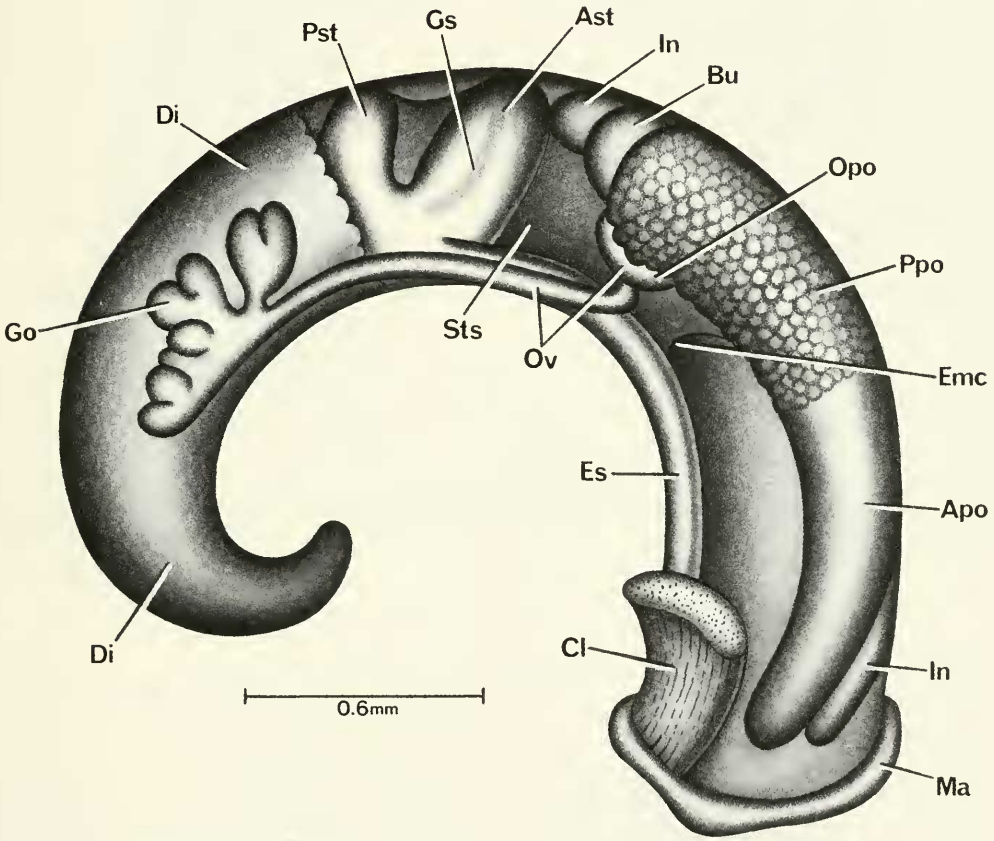

FIG. 140. Uncoiled female *Tricula maxidens* with head and kidney tissue removed.

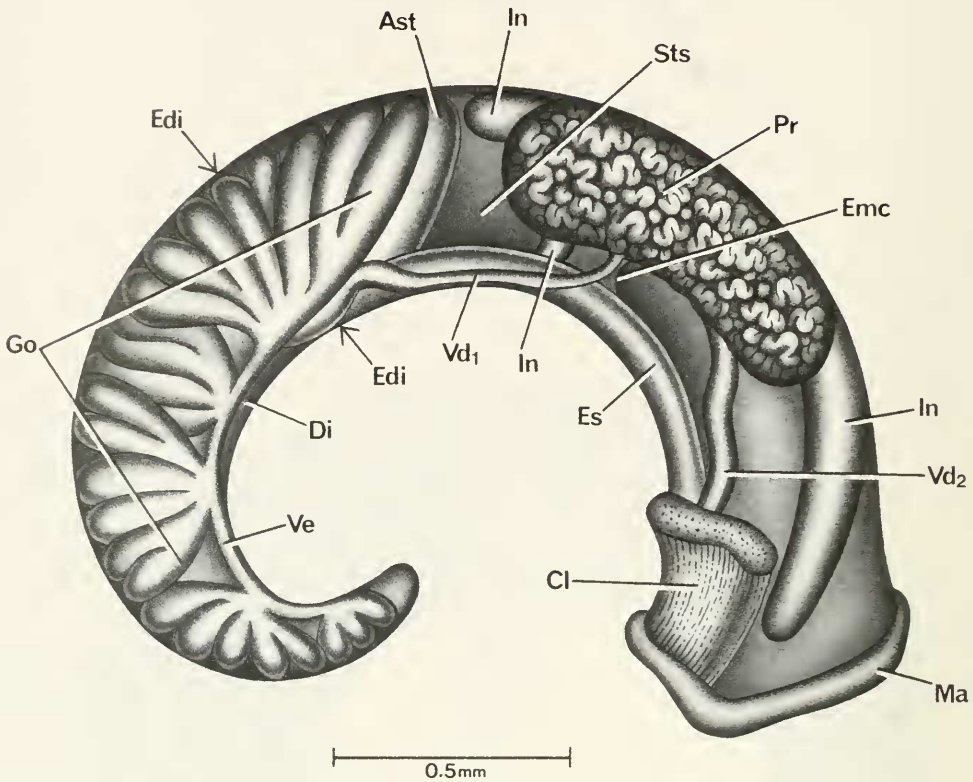

FIG. 141. Uncoiled male of *Tricula maxidens* without head or kidney tissue.

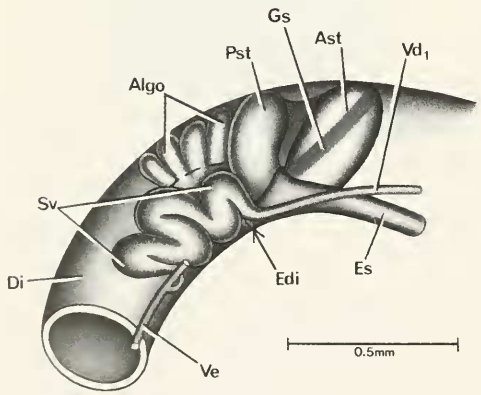

FIG. 142. A. Figure to show seminal vesicle (Sv) of *Tricula maxidens* in relationship to stomach. Most of gonad and vas efferens cut away.

TABLE 69. Radular statistics for *Tricula maxidens*. Mean ± standard deviation (range). N = number used. In mm except for width of central tooth in μm.

	Females (N = 4)
Shell length	2.19±0.08 (2.08–2.24)
Radular length	0.29±0.04 (0.240–0.204)
Radular width	0.03±0.01 (0.028–0.040)
Total rows of teeth	59.8±6.4 (55–69)
No. rows of teeth forming	11.3±1.5 (9–12)
Central tooth width (N = 18)	9.6±0.3 (9.0–10.1)

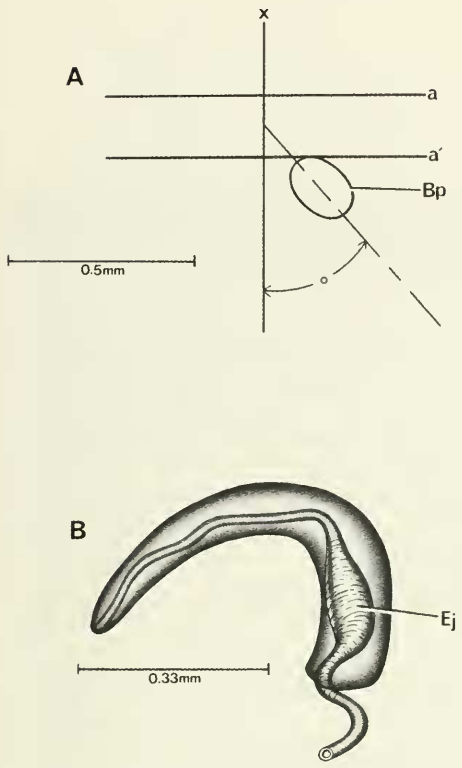

FIG. 143. *Tricula maxidens*: A. Relationship of base of penis to mid-line of snout-neck (x) and to posterior end of eye lobes (a). B. Penis.

Habitat

Material for this study was collected on 7 October 1985 from Shenglong Village, Sanhuokou Town, Cili County, Changde Prefecture; 29°38′35″N, 110°39′12″E; Figure 1, site 7. The field collection number assigned was D85-82. Specimens came from a small stream flowing to the Lishui River. The collector was Dr. Liu Wen Jian of Cili County Public Health Station.

Depository

Specimens for this study were deposited in ZAMIP, M0005; ANSP, 368773, A12145.

Description

Shell. Shell measurements are given in Table 71; See Figures 137F–K, 146. Mature males and females are primarily 7.0 whorls; relatively few are 6.0 or 6.5 whorls (Table 71). Only one specimen of 7.5 whorls was ever seen (within the size range of 7.0 whorls snails of Table 71). Shells are medium sized with a length range of 3.76 to 4.36 mm for shells of 7.0 whorls (the dominant size class). Shells are ovate-turretted. The whorls are slightly convex; the sutures are deep. The peristome is complete; the inner lip is widely separated from the body whorl along its entire length (0.08 ± 0.02 mm, range 0.06–0.10;

TABLE 70. Cusp formulae for the radular teeth of *Tricula maxidens* with the percent of the seven radulae in which a given formula was found at least once.

Central Teeth		Lateral Teeth		Inner Marginal Teeth		Outer Marginal Teeth	
3-1-3 / 2-2	100%	3-1-4	75%	12	75%	12	25%
		4-1-4	75%	13	100%	13	75%
4-1-4 / 2-2	25%	2-1-3	25%	14	100%	14	100%
4-1-3 / 2-2	25%	5-1-4	25%	15	25%	15	25%
				16	25%	16	25%
3-1-4 / 2-2	25%						
2-1-3 / 2-2	25%			$\bar{X}$ * = 13.4±0.9 N = 40		13.9±0.9 N = 40	
3-1-3 / 2-3	25%						

* Mean ± standard deviation of cusp number for all teeth counted.

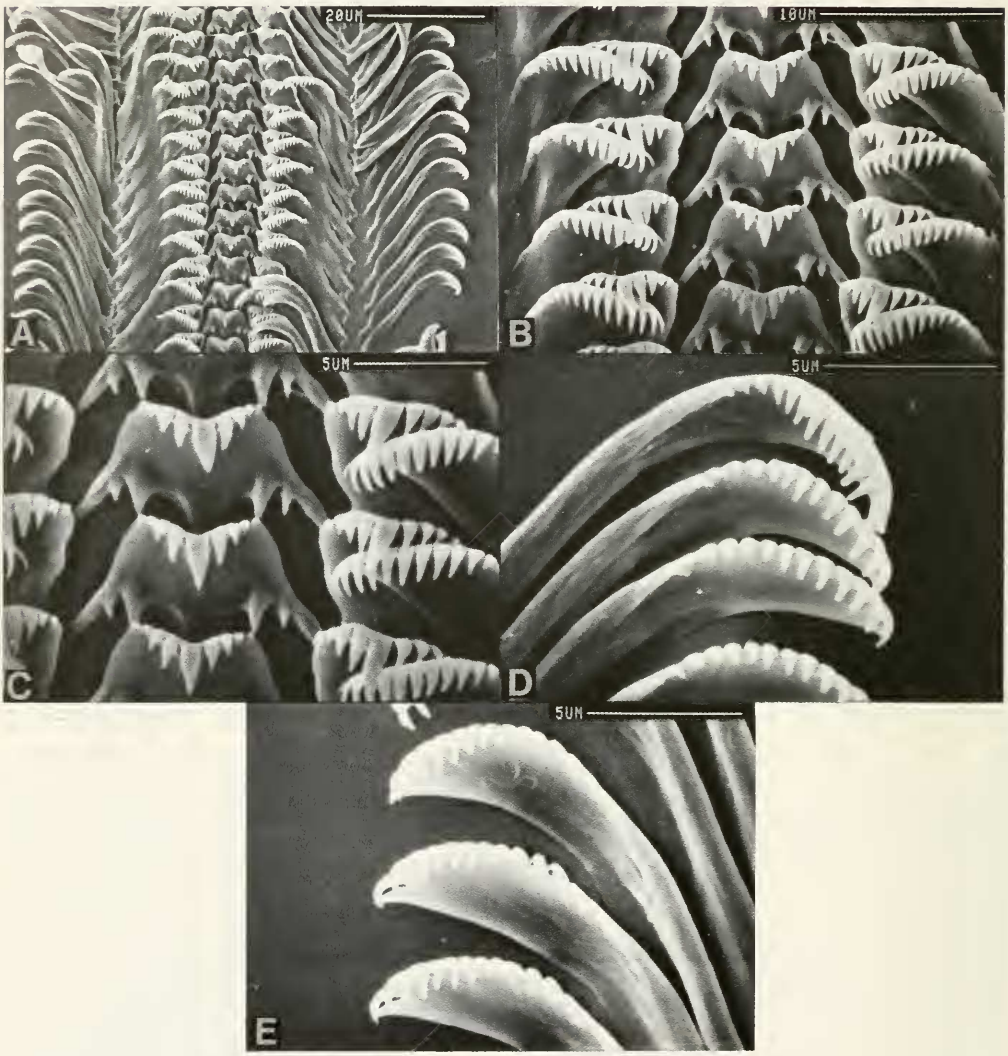

FIG. 144. Radula of *Tricula maxidens*. A. Part of radular ribbon. B, C. Central, lateral and inner marginal teeth. D, E. Outer marginal teeth.

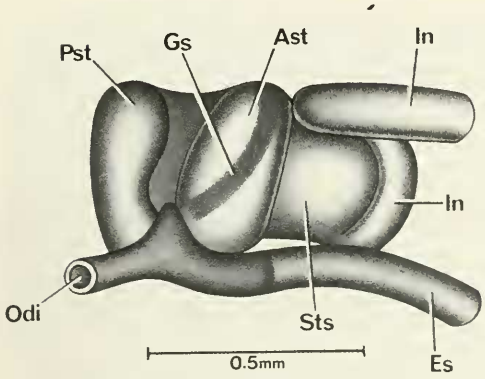

FIG. 145. Stomach of *Tricula maxidens*.

N = 5). The aperture is pyriform. The adapical end of the inner lip has a tooth-like swelling; this, plus the thickening of the outer lip opposite the swelling, enclose an adapical notch. Mid-columella there is a marked indentation. Although the inner lip is separated from the body whorl, there is no umbilicus in some individuals; there is one in some. Facing the aperture of the shell the adapical outer lip may be sinuate (16%); in side view, the outer lip is scooped forward (83%) or straight (17%). When the outer lip is scooped forward there is an adapical sinuation or notch. There is no basal post (see Davis et al., 1986). The cleaned shell is glistening, glassy.

The nuclear whorls (Fig. 146) have a rough, wrinkled surface. There are 1.5 nuclear whorls. The roughened surface may not be discerned at magnifications less than 200 or 300X. The aperture has six diagnostic features: (1) There is an adapical notch or beak bounded by (2) a thickening or node on the inner lip; (3) The inner lip has an angulation located some 60% of the length of the inner lip abapically from the adapical end of the aperture. The inner lip is thickened noticeably from the fulcrum of the angle to the apertural notch. (4) There is an indentation at the fulcrum of the angle. Abapical to the fulcrum of the angle the inner lip edge is thin. (5) In side view, the adapical end of the outer lip is slightly sinuate, the remaining lip is straight. (6) With the outer lip down, 90° to the horizontal, the inner lip has a slight sinuation that corresponds to a slight trough seen on the abapical end of the inner lip in apertural view.

External features. The head of this species is dark gray. No cluster of white granules or glands about the eyes were observed.

The operculum is corneous. The typical paucispiral growth line is not seen; the nucleus is prominent (Fig. 147E–G). The operculum has an odd irregular shape reflecting

TABLE 71. Shell measurements (mm) of mixed males and females of *Tricula odonta*. Mean ± standard deviation (range). N = number measured.

No. specimens (N)	N = 7	N = 2	N = 1
No. Whorls	7.0	6.5	6.0
Length (L)	4.09±0.22	3.40	3.00
	(3.76–4.36)	(3.32, 3.48)	—
Width (W)	1.52 ±0.10	1.40	1.28
	(1.48–1.60) N = 5	—	—
L body whorl	2.09±0.09	1.86	—
	(1.96–2.24)	(1.84, 1.88)	—
L penultimate	0.69±0.06	0.58	0.56
whorl	(1.16–1.26) N = 5	(1.02, 1.08)	—
W penultimate	1.20±0.05	1.06	0.98
whorl	(1.16–1.26) N = 5	(1.02, 1.08)	—
L last three whorls	3.25±0.17	2.78	2.48
	(3.04–3.48)	(1.71, 2.84)	—
L apertue	1.34±0.05	1.20	1.04
	(1.28–1.40) N = 5	—	—
W aperture	0.89±0.02	0.85	0.76
	(0.88–0.92) N = 5	(0.84, 0.86)	—
x	0.37±0.08		
	(0.28–0.48) N = 4		
y	0.19±0.07		
	(0.12–0.28) N = 4		

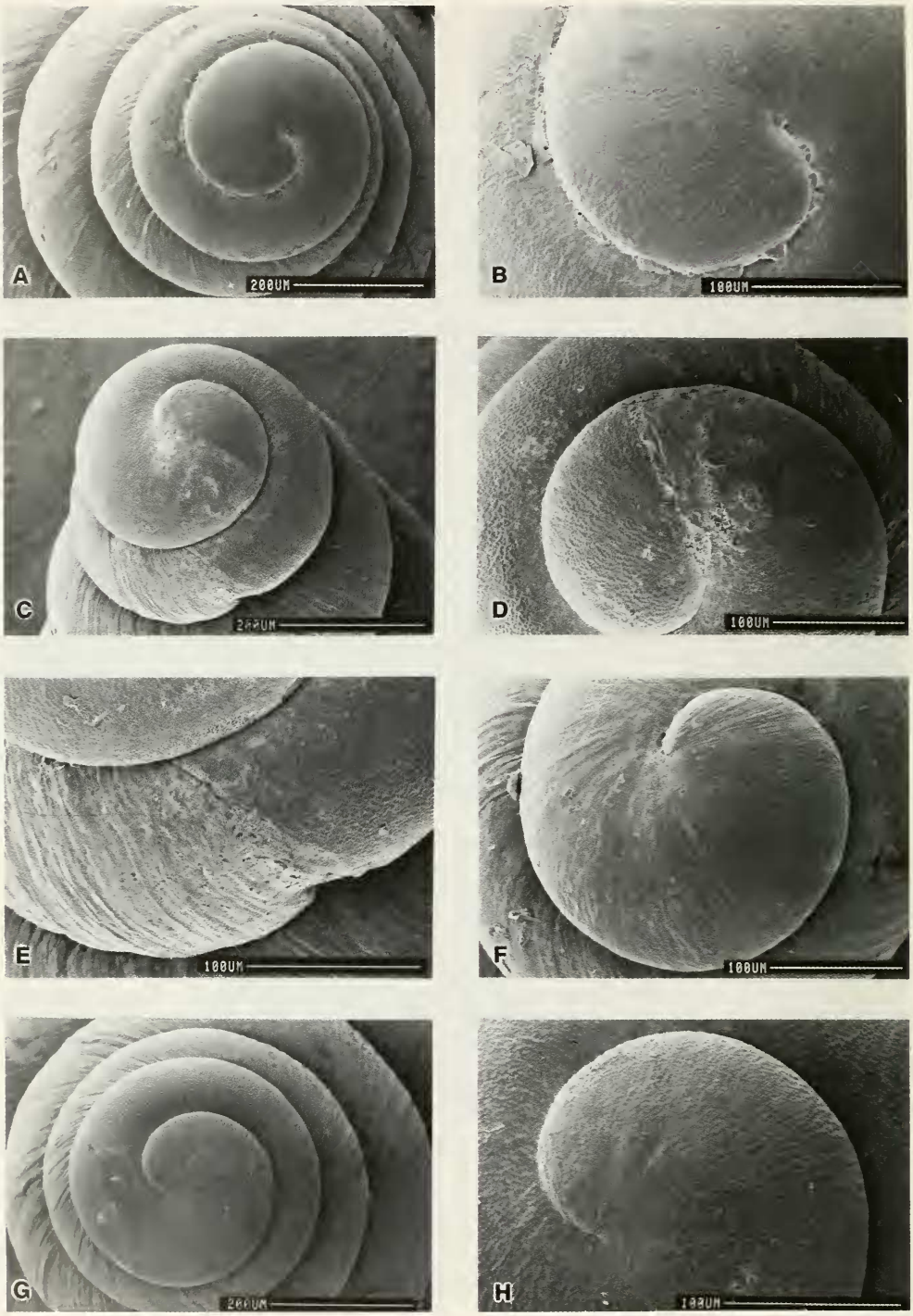

FIG. 146. SEM photos of shell apical whorls of *Tricula odonta*. Teleoconch begins at about 1.50 to 2.0 whorls (A, C, G). The protoconch is heavily wrinkled (B, D, F, H).

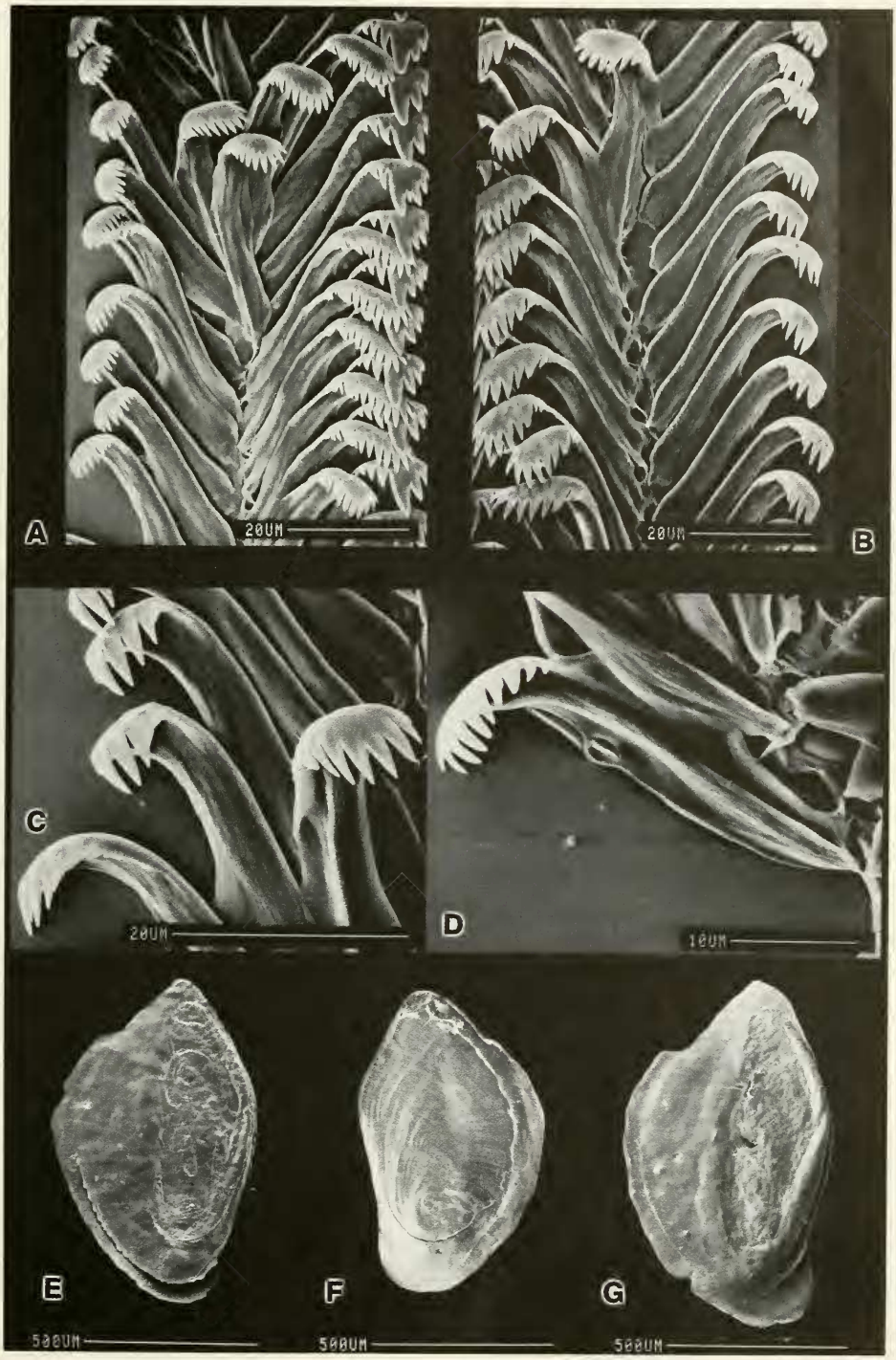

FIG. 147. Radula (A–D) and opercula (E–G) of *Tricula odonta*. A. Left lateral, inner and outer marginal teeth. B–D. Marginal teeth. E, G. Inner surfaces. Note irregular shape of opercula and thickened ridge along columellar edge of operculum in G. F. Outer surface. All three opercula show the double layers (see text).

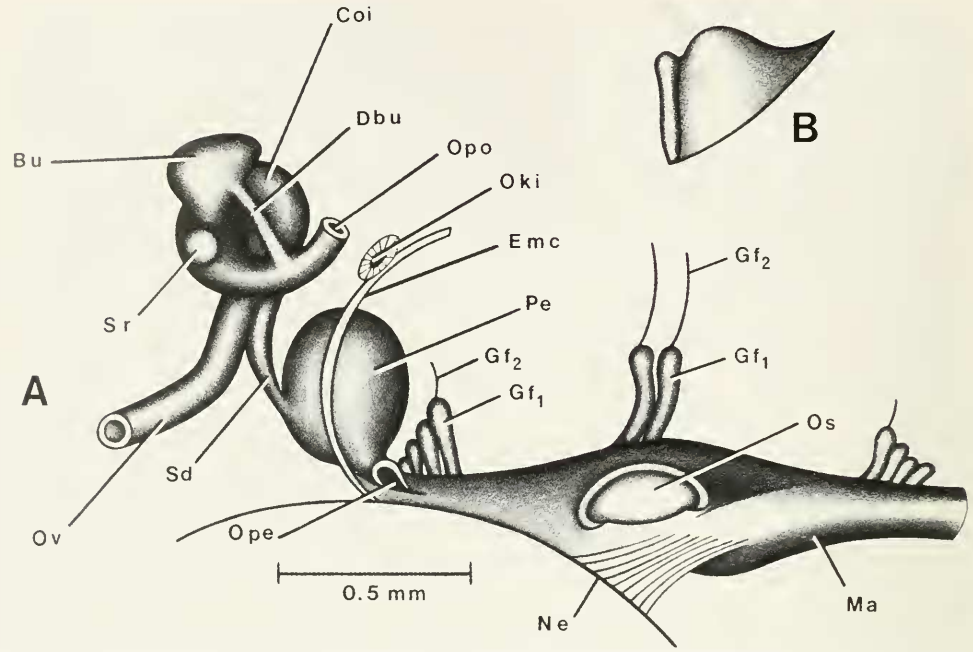

FIG. 148. Details and variation of bursa copulatrix complex of organs and mantle cavity structures of *Tricula odonta*. A in same orientation as in Figure 149. Not all gill filaments shown. B. Single gill filament.

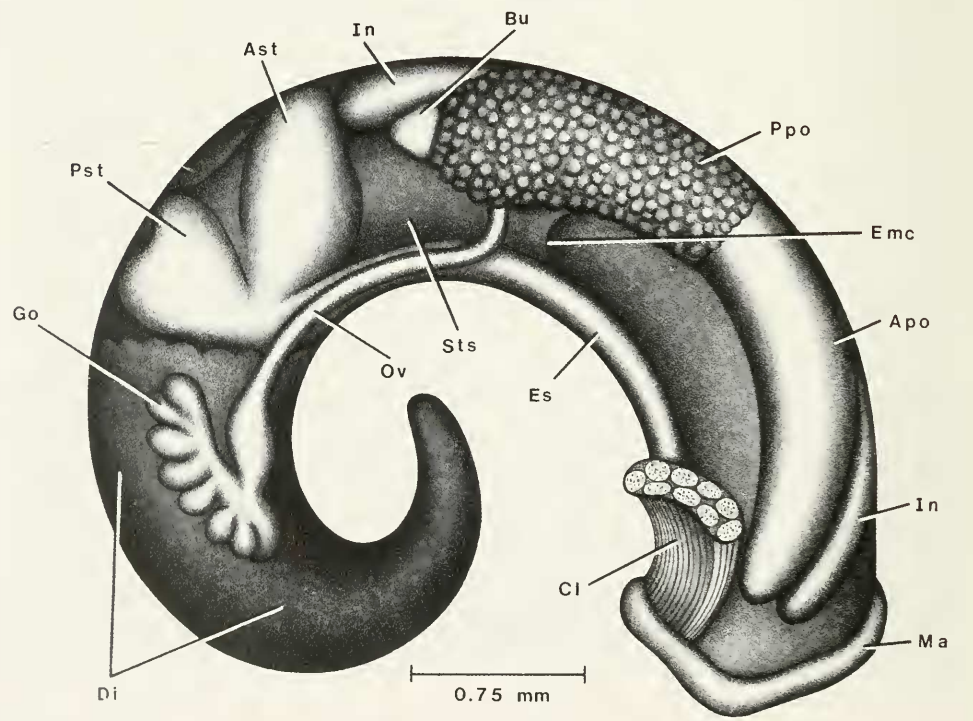

FIG. 149. Uncoiled female *Tricula odonta* with head and kidney tissue removed.

TABLE 72. Lengths (mm) or counts of non-neural organs and structures of *Tricula odonta*. Mean ± standard deviation (range). N = number measured.

	Females (N = 3)	Males (N = 2)
Body	5.83±0.36 (5.60–6.24)	4.74 (4.7, 4.78)
Gonad	0.74±0.15 (0.60–0.90)	1.55 (1.50, 1.60)
Digestive gland	2.45±0.19 (2.24–2.60)	2.04 (2.00, 2.08)
Mantle cavity	1.83±0.15 (1.80–2.00)	1.53 (1.50, 1.60)
Osphradium	0.34±0.05 (0.30–0.40)	0.33 (0.30, 0.36)
Ctenidium = Gill	1.63±0.15 (1.50–1.80)	1.38 (1.36, 1.40)
OS ÷ G	0.21±0.04 (0.17–0.25)	0.24 (0.22, 0.26)
Gill filament No.	29.7±1.5 (28–31)	25.5 (24, 27)
Buccal mass (males + females; N = 3)	0.57±0.06 (0.50–0.62)	—
Posterior pallial oviduct (= albumen gland)	0.92 (0.64, 1.20) N = 2	—
Anterior pallial oviduct (= capsule gland)	1.12 (1.0, 1.24) (N = 2)	—
Total pallial oviduct = OV	2.04 (1.64, 2.44) N = 2	—
Bursa copulatrix = BU	0.28±0.03 (0.24–0.30)	—
Duct of BU	0.21±0.04 (0.16–0.24)	—
BU ÷ OV	0.14	
Seminal receptacle	0.11±0.03 (0.08–0.14)	—
Gf_2	0.26±0.02* (0.24–0.28)	—
Gf_1	0.23±0.02* (0.20–0.24)	—
Total Gf = TGF	0.49±0.01* (0.48–0.50)	—
Gf_2 ÷ TGF	0.53±0.04* (0.50–0.58)	
Prostate	—	0.75 (0.70, 0.80)
Seminal vesicle	—	0.66 N = 1
Penis	—	1.62 (1.40, 1.84)

*males and females

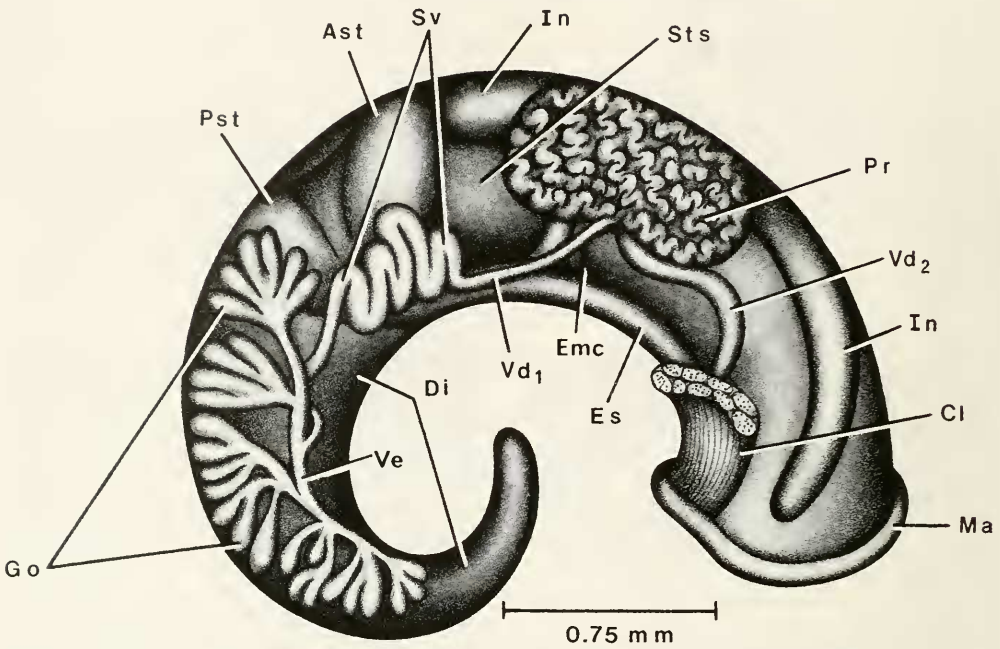

FIG. 150. Uncoiled male of *Tricula odonta* without head or kidney tissue.

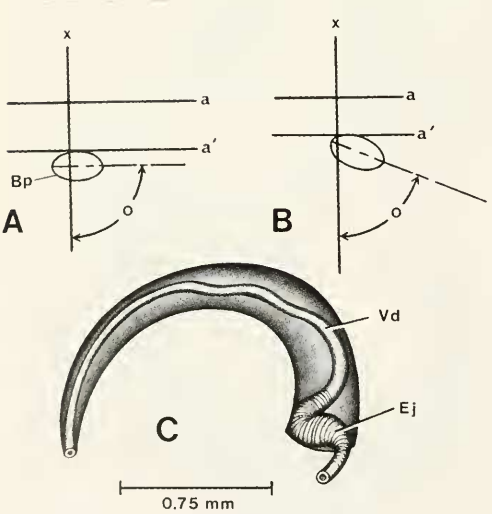

FIG. 151. A, B. Relationship of base of penis to mid-line of snout-neck (x) and to posterior end of eye lobes (a) of *Tricula odonta*; C. Penis.

TABLE 73. Radular statistics for males and females of *Tricula odonta*. Mean ± standard deviation (range). N = 5. In mm except for width of central tooth in μm.

Shell length:	No shell measurements; radulae came from heads of snails used in dissections.
Radular length	0.54±0.04 (0.52–0.62)
Radular width	0.08±0.004 (0.08–0.09)
Total rows of teeth	61.3±4.4 (56–69)
No. rows of teeth forming	7±1.7 (5–10)
Central tooth width	19.8±2.9 (18.1–23.6)

the pyriform shape of the aperture and the mid-inner lip indentation. It is particularly narrow at the abapical end, not broadly or regularly rounded as in those species with an oval operculum. The operculum consists of two layers that are readily separated if the oper-

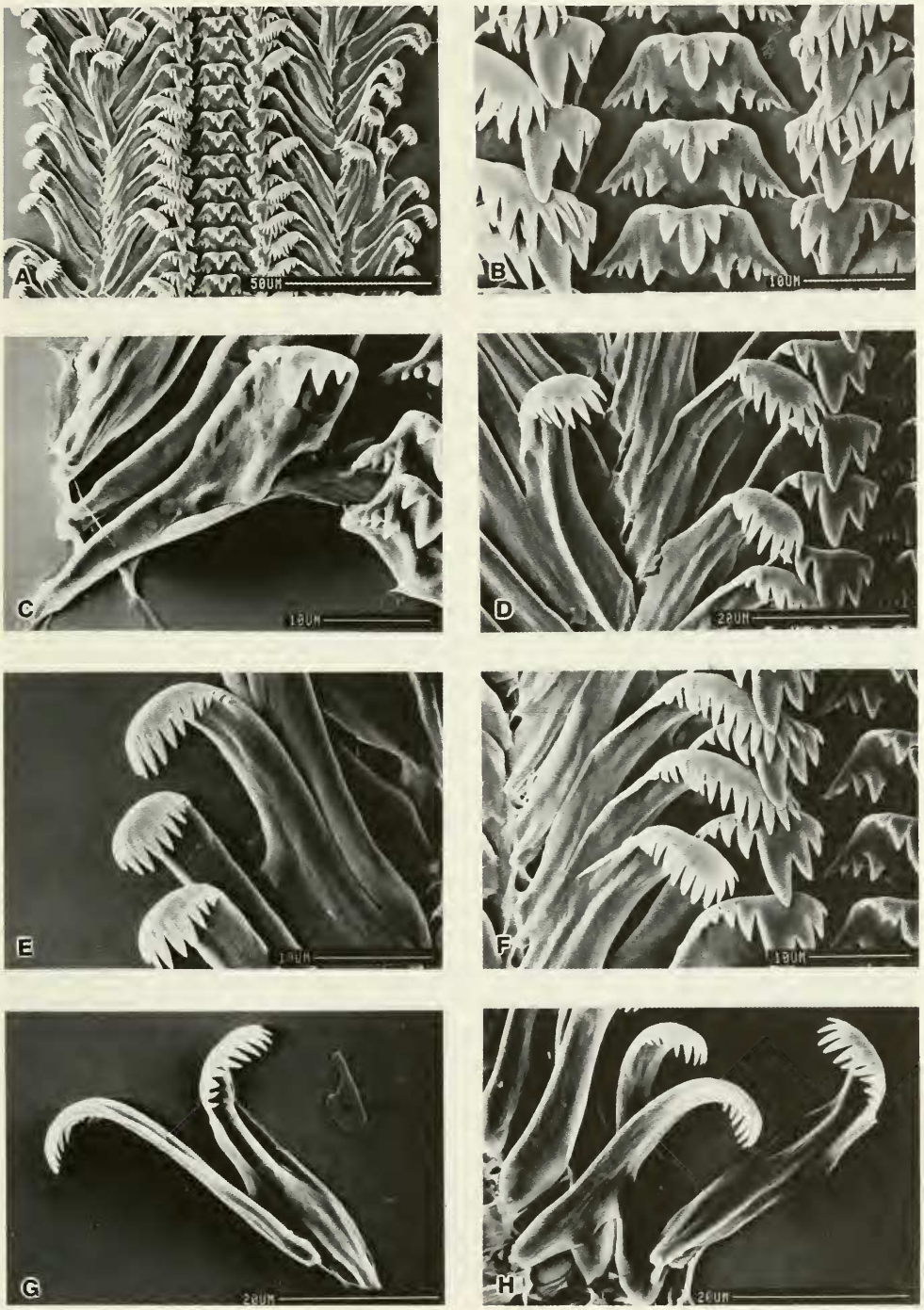

FIG. 152. Radula of *Tricula odonta*. A. Part of a radular ribbon. B. Central tooth. C. Left lateral tooth. D, F. Left lateral and marginal teeth. Note pronounced bifurcation of the major cusp of lateral tooth. E, G, H. Marginal teeth.

TABLE 74. Cusp formulae for the radular teeth of *Tricula odonta* with the percent of the radulae in which a given formula was found at least once. N = number of radulae used.

Central Teeth N = 6		Lateral Teeth N = 6		Inner Marginal Teeth (N = 3)		Outer Marginal Teeth (N = 4)	
3-1-3 / 3-3	50%	2-1[2]-3	83%	7	—	7	25%
		3-1-3	33%	8	—	8	50%
3-1-3 / 2-2	33%						
		2-1-2	17%	9	33%	9	25%
2-1-2 / 3-3	33%						
		1-1[2]-2	17%	10	66%	10	50%
				11	33%	11	25%
2-1-2 / 4-4	17%						
				12	66%	12	50%
3-1-3 / 4-4	17%						
				13	66%	13	25%
				14	33%	14	25%
						15	25%
				$\bar{X}$ * = 11.5±1.6 N = 30		9.2±1.7 N = 40	

*Mean ± standard deviation of cusp number for all teeth counted.

TABLE 75. Lengths of neural structures of four individuals of *Tricula odonta*. Mean ± standard deviation (range). * = neural elements measured to attain the RPG ratio.

Cerebral ganglion	0.24±0.03 (0.20−0.26)
Cerebral commissure	0.03±0.02 (0.02−0.06)
Pleural ganglion	
Right (1)*	0.12±0.02 (0.10−0.14)
Left	0.12±0.02 (0.10−0.14)
Pleuro-supraesophageal connective (2)*	0.20±0.07 (0.12−0.24)
Pleuro-subesophageal connective	0.05±0.04 (0.02−0.10)
Supraesophageal ganglion (3)*	0.12±0.01 0.10−0.12)
Subesophageal ganglion	0.09±0.03 (0.06−0.12)
Osphradio-mantle nerve	0.05±0.02 (0.02−0.06)
RPG ratio* = 2 ÷ 1+2+3	0.45±0.10 (0.32−0.55)

culum is left too long in dilute Clorox used for digesting and clearing away tissue fused to the operculum There is an inner thickened ridge on the columellar side. The attachment callus is 54.5 ± 3.5% of the width of the operculum; it is prominent and much thickened in some specimens.

Mantle cavity. Measurements and counts of mantle cavity structures are given in Table 72. See Figure 148A. The osphradium is short (mean ratio 0.22 ± 0.04; N = 5). The position of the osphradium is approximately mid-gill (Fig. 148A). The slender aspect of the gill filament (Gf_2) is long (mean ratio 0.53 ± 0.04; N = 3). The length of the longest gill filament is 0.49 ± 0.01 mm long (N = 3). The shape of the filaments is shown in Figure 148B. It is high domed.

Female reproductive system. The body of an uncoiled female with head and kidney tissue removed is illustrated (Fig. 149). Measurements of the relevant organs are given in Table 72. Diagnostic features are: (1) The gonad is posterior to the stomach. (2) The bursa copulatrix (Bu) is posterior to the pallial oviduct (Ppo) at mid-ventrolateral surface as shown. (3) The bursa copulatrix complex of organs is the same as seen in T. *bollingi* (Davis, 1968) in that the oviduct makes a tight loop (twist of 360°) dorsal to the bursa (Fig. 148A). (4) The seminal receptacle is spherical, posterior to the duct of the bursa (Dbu) and fused to the surface of the oviduct on the mid-ventral surface, not from the inner curvature as seen in other species. (5) The spermathecal duct enters the pericardium; the

pericardium is swollen with sperm. (6) Sperm enter the pericardium at the posterior end of the mantle cavity (Ope, Fig. 148A) (7) The bursa copulatrix is minute (mean ratio, 0.15 ± 0.04; N = 3). (8) The length of the posterior pallial oviduct is standard.

Male reproductive system. The body of an uncoiled male with head and kidney tissue removed is shown (Fig. 150). Lengths of relevant organs are given in Table 72. Important features are: (1) The gonad either overlaps the posterior chamber of the stomach or is posterior to the stomach. (2) The prostate overlaps the posterior end of the mantle cavity and covers the anterior half of the style sac. (3) The vas deferens arises from mid-vas efferens to slightly anterior to mid-gonad. (4) The seminal vesicle coils on the stomach; in some individuals, the posterior vas deferens was not swollen to form the seminal vesicle (presumable immature, just pre-sperm production individual). (5) The anterior vas deferens (Vd_2) leaves the prostate slightly anterior to mid-prostate. (6) The penis is simple, without papilla (Fig. 151C). The opening of the vas deferens is comparatively large and pronounced. (7) The base of the penis is 0.18 ± 0.03 mm posterior to the eye-lobes (Fig. 151A, B). Variation in the position of the base of the penis to the snout-neck mid-line (x) is shown in Figure 151 A, B. A part of the penial base is to the left of the mid-line. The long axis of the penial base varies from 65° to 90° to the snout-neck mid-line. (8) There is a large ejaculatory duct (Ej) in the base of the penis (Fig. 151C).

Digestive System. The digestive gland is posterior to the stomach. Radular statistics are given in Tables 73 and 74. Radular morphology is the generalized *Tricula* type (Figs. 147A–D, 152). There are 61 rows of teeth per radula length of 0.54 mm. The major cusp of the lateral teeth is massive and split thus giving the appearance of being two cusps. The most commonly encountered formula is

$$\frac{3(2)\text{-}1\text{-}(2)3;}{3(2)\text{-}(2)3}\ \ 2(3)\text{-}[2]\text{-}3;\ 9\text{-}14;\ 7\text{-}14.$$

Nervous System. Lengths of neural structures are given in Table 75. The RPG ratio of 0.45 shows the dorsal nerve ring to be moderately concentrated.

Remarks

Conchologically, aside from *Neotricula aperta*, *T. odonta* has the most distinctive shell (Fig. 153) in that it attains 7.0 whorls (Tables 2, 76) (char. 29). It has a beak tubercle (char. 24) as do two other species: *Tricula gredleri* and *N. dianmenensis*. The adapical aperture is widely separated from the body whorl as is seen in *N. cristella* (char. 21). The inner lip is widely separated from the body whorl as it is in *N. cristella* (char. 20). A unique state, the inner lip is differentially thickened (char. 19). Another unique state, the inner lip has a notch (char. 17). Among species of *Tricula*, only this species of those thus far studied, has an abapical apertural spout (char. 12), an angled inner lip (char. 13), and an abapical lip deflection angle. (char. 18).

Anatomically, *Tricula odonta* stands apart from other species of *Tricula* (Tables 80, 81), but is most similar to *T. xianfengensis* (Figs. 156–158). *Tricula odonta* differs from the latter in 17 characters (37%). Most notable are the difference in operculum shape that reflects differences in shell apertural shape (char. 2), the differences in Gf_2 length (char. 8), female gonad length (char. 12) and seminal receptacle duct length (char. 23). *Tricula odonta* has a large ejaculatory duct; the latter does not have an ejaculatory duct (chars. 36, 37). The radula of the former is of medium length, of the latter, long (char. 41). The dorsal nerve ring is moderately concentrated in the former, elongated in the latter (char. 42).

MULTIVARIATE RELATIONSHIPS

Shells

The 29 shell characters scored are given in Table 2, the actual scores in Table 76. All species of *Tricula* and *Neotricula,* as well as other species having shells resembling those of *Tricula* or *Neotricula* and for which anatomical data are available, were included. The sources for data for species not treated in this paper are listed in Appendix I. The phenogram based on UPGMA treatment of distance coefficients is given in Figure 153. Distance coefficients were used because the cophenetic correlation (phenogram to orignal matrix) was r = 0.928 for distances; r = 0.725 using similarities.

It is clear that one cannot sort species to genus on the basis of shell characters. Additionally, of the 21 species, four (19%) could not be clearly distinguished on the basis of the shell characters used; *Tricula bollingi* phenotypes 1 and 3 clustered with *T. ludongbini*,

TABLE 76. Scoring of 44 OTUs for 29 shell characters listed in Table 2. Shells from the same population of some species varied for some characters. Such a species was divided into as many as three OTUs, e.g. xin-1, xin-2, xin-3. All species for which there were adequate anatomical data were used. Abbreviations are : ape, *N. aperta;* bur, *N. burchi;* cri, *N. cristella;* dia, *N. dianmenenensis;* dup, *N. duplicata;* lil, *N. lilii;* min, *N. minutoides;* bam, *T. bambooensis;* boll, *T. bollingi;* grd, *T. gredleri;* grg, *T. gregoriana;* hud, *T. hudiequanensis;* lud, *T. ludongbini;* max, *T. maxidens;* mon, *T. montana;* odn, *T. odonta;* xin, *T. xianfengensis;* xia, *T. xiaolongmensis;* chi, *G. chinensis;* jin, *J. jinghongensis;* niz, *W. niuzhuangensis.*

	Neotricula													*Tricula* (N = 11)								
	1	2	3	4	5	6	7	8	9	10	11	12	13	14	15	16	17	18	19	20	21	22
	ape	bur-1	bur-2	cri-1	cri-2	dia-1	dia-2	dup-1	dup-2	lil-1	lil-2	min-1	min-2	bam-1	bam-2	bol-1	bol-2	bol-3	grd-1	grd-2	grg-1	grg-2
1	1	0	0	0	0	0	0	0	0	0	0	0	0	0	0	0	0	0	0	0	1	1
2	4	1	1	0	0	0	0	0	0	0	0	0	0	0	1	0	0	0	0	0	0	0
3	1	0	0	0	0	2	2	1	1	1	1	1	1	0	0	0	1	0	1	1	1	1
4	0	0	1	0	0	2	2	1	1	2	2	2	2	2	2	0	1	2	1	1	1	2
5	0	1	1	0	0	0	0	0	0	0	0	0	0	0	0	0	0	0	0	0	0	0
6	0	1	1	1	1	1	1	1	1	1	1	0	1	0	0	0	0	0	0	0	0	0
7	0	0	0	0	0	0	0	0	0	0	0	0	0	0	0	0	0	0	0	0	0	0
8	2	0	0	1	1	0	0	1	1	0	0	1	1	1	2	3	3	3	1	1	0	0
9	2	0	0	1	1	2	2	2	2	1	1	0	0	0	0	0	0	0	2	2	0	1
10	1	0	0	0	0	0	0	1	0	0	0	0	0	0	0	0	0	0	0	0	0	0
11	0	0	0	0	0	1	1	0	0	1	1	0	0	0	0	0	0	0	1	1	0	0
12	0	1	0	0	0	1	1	1	1	1	1	0	0	0	0	0	0	0	0	0	0	0
13	1	1	1	1	1	3	3	0	1	2	2	1	1	1	1	1	1	1	0	0	1	1
14	0	1	1	1	1	1	1	0	0	0	0	0	0	0	0	0	1	0	0	0	1	1
15	2	1	1	0	0	0	1	1	1	1	1	1	1	2	2	0	1	0	0	1	0	0
16	0	0	0	0	0	0	0	0	0	0	0	0	0	0	0	0	0	0	0	0	0	0
17	0	0	0	0	0	0	0	0	0	0	0	0	0	0	0	0	0	0	0	0	0	0
18	0	0	0	1	0	1	1	1	1	1	1	0	0	0	0	0	0	0	0	0	0	0
19	0	0	0	0	0	0	0	1	1	0	0	1	1	1	1	0	0	0	1	1	0	0
20	0	0	0	3	3	1	0	2	2	2	1	2	2	2	2	0	1	0	2	2	0	0
21	0	0	0	2	2	0	1	1	1	0	1	0	0	1	1	0	1	0	1	1	0	0
22	0	0	0	0	0	0	0	0	0	0	0	0	0	0	0	0	0	0	0	0	0	0
23	0	0	0	1	1	0	0	0	0	1	1	0	0	0	1	0	0	0	0	0	0	0
24	0	0	0	0	0	1	1	0	0	0	0	0	0	0	0	0	0	0	1	1	0	0
25	0	0	0	0	0	0	0	0	0	1	1	0	0	0	0	0	0	0	0	0	0	0
26	1	0	0	0	0	0	0	0	0	0	0	0	0	0	0	0	0	0	0	0	0	0
27	1	0	0	0	0	0	0	0	0	0	0	0	0	0	0	0	0	0	0	0	0	0
28	0	0	0	0	0	0	0	0	0	0	0	0	0	0	0	0	0	0	0	0	0	0
29	0	0	0	0	0	0	0	0	0	0	0	0	0	0	0	0	0	0	0	0	0	0

whereas phenotype 2 clustered with *T. xiaolongmenensis* phenotype 1. *Tricula xiaolongmenensis* phenotype 2 did not have close affinity to any other species in the upper half of the phenogram. *Tricula montana* phenotype 3 clustered with *T. gregoriana*, not with phenotypes 1 and 2 of *Tricula montana*. *Tricula xianfengensis* phenotype 2 did not have close affinity with any other species in the upper half of the phenogram. While most shells can be classified readily on the basis of the characters used (exact measurements and whorl numbers would allow further discrimination), four of the 44 OTUs (only 9%) do not cleanly segregate with their other conspecific OTUs.

It is useful to compare the phenogram with a plot of the Prim Network (Minimum Spanning Tree [MST]) (Fig. 154) based on the distance coefficients (drawn to scale of actual pathway distances). The two are useful in assessing those species most closely resembling a species of immediate concern. For example, what species might be conchologically confused with *Tricula gredleri*? An examination of Figures 153 and 154 indicates that *N. duplicata* is the most closely allied phenetically. The several differences are then readily found in Tables 2 and 76. With MST, only two OTUs of different species do not link with other conspecific OTUs (i.e. *T. montana* phenotype 3; *T. bollingi* phenotype 2). Thus, only 5% of the OTUs do not segregate cleanly. Table 77 provides a ranking of species by a

TABLE 76. (Continued)

	Tricula (N = 11)				*Tricula*												*Gamma-tricula*		*Jinhongia*		*Wucon-chona*	
	23	24	25	26	27	28	28	30	31	32	33	34	35	36	37	38	39	40	41	42	43	44
	hud-1	hud-2	lud-1	lud-2	max-1	max-2	mon-1	mon-2	mon-3	odn-1	odn-2	xin-1	xin-2	xin-3	xio-1	xio-2	chi-1	chi-2	jin-1	jin-2	niz-1	niz-2
1	1	1	0	0	0	0	0	0	0	1	1	1	2	1	0	0	0	0	0	0	0	0
2	0	1	0	0	3	3	1	2	1	1	1	0	1	2	1	1	0	0	0	1	0	0
3	0	0	0	0	0	0	0	1	1	1	1	0	0	0	1	1	0	0	0	0	1	1
4	1	2	2	2	0	0	0	1	2	2	2	1	1	1	0	1	1	2	0	1	0	1
5	0	0	0	0	0	0	0	0	0	0	0	0	0	0	0	0	1	1	1	1	0	0
6	0	0	0	0	0	0	0	0	0	0	0	0	0	0	0	0	0	1	1	1	1	1
7	0	0	0	0	0	2	0	0	0	0	0	0	0	0	0	0	0	0	1	1	0	0
8	1	2	1	2	0	0	0	0	0	1	1	2	2	2	2	2	0	0	0	1	0	1
9	0	0	0	0	0	0	0	0	0	1	1	0	1	0	0	1	0	0	0	0	1	1
10	0	0	0	0	0	0	0	0	0	0	0	0	0	0	0	0	0	0	0	0	0	0
11	0	0	0	0	0	0	0	0	0	1	1	0	0	0	0	0	0	0	0	0	0	0
12	0	0	0	0	0	0	0	0	0	1	1	0	0	0	0	0	0	0	1	1	0	0
13	1	1	1	1	0	0	0	1	0	3	3	0	0	0	0	0	1	1	1	1	2	2
14	1	1	0	0	0	0	0	0	1	0	0	0	0	1	1	0	1	1	1	0	0	0
15	1	1	0	1	0	0	0	1	0	0	1	0	0	0	0	0	0	1	1	1	0	1
16	0	0	0	0	1	1	0	0	0	0	0	0	0	0	0	0	0	0	0	0	0	0
17	0	0	0	0	0	0	0	0	0	1	1	0	0	0	0	0	0	0	0	0	0	0
18	0	0	0	0	0	0	0	0	0	1	1	0	0	0	0	0	0	0	0	1	1	1
19	1	1	0	0	0	0	0	0	0	2	2	0	0	0	0	0	1	1	0	0	0	0
20	2	2	0	0	0	0	0	0	0	3	3	0	0	0	0	0	2	2	0	0	0	0
21	1	1	1	1	1	1	1	1	1	2	2	0	0	0	1	1	1	1	0	0	0	0
22	0	0	0	0	2	2	0	0	0	0	0	0	0	0	1	1	0	0	0	0	2	2
23	0	0	0	0	0	0	0	0	0	0	0	0	0	0	0	1	1	1	0	1	0	0
24	0	0	0	0	0	0	0	0	0	1	1	0	0	0	0	0	0	0	0	0	0	0
25	0	0	0	0	0	0	0	0	0	0	0	0	1	0	0	0	1	1	0	0	0	0
26	0	0	0	0	0	0	0	0	0	0	0	0	0	0	0	0	0	0	0	0	0	0
27	0	0	0	0	0	0	0	0	0	0	0	0	0	0	0	0	0	0	0	1	0	0
28	0	0	0	0	0	0	0	0	0	0	0	0	0	0	0	0	0	0	1	1	0	0
29	0	0	0	0	0	0	0	0	0	1	1	0	0	0	0	0	0	0	0	0	0	0

TABLE 77. Ranking species on a consistency index for shell characters. The index = 1.0−[number of character state differences between phenotypes in a population ÷ 29 characters]. Numbers in ( ) = number of phenotypes.

N. aperta (1)	1.0	*T. ludongbini* (2)	0.93
N. cristella (2)	0.97	*N. dianmenensis* (2)	0.90
N. minima (2)	0.97	*T. bambooensis* (2)	0.90
T. gredleri (2)	0.97	*T. hudiequanensis* (2)	0.90
T. maxidens (2)	0.97	*G. chinensis* (2)	0.90
T. odonta (2)	0.97	*W. niuzhuangensis* (2)	0.90
N. burchi (2)	0.93	*T. xiaolongmenensis* (2)	0.86
N. duplicata (2)	0.93	*T. xianfengensis* (3)	0.83
N. lilii (2)	0.93	*T. bollingi* (3)	0.79
T. gregoriana (2)	0.93	*T. montana* (3)	0.79
		J. jinhongensis (2)	0.76

consistency index based on the character-state differences between OTUs of the same species (1.0 = no differences). This table helps clarify the problems of why *T. montana* and *T. bollingi* do not cleanly link with conspecific OTUs (i.e. three classes of phenotype varying over six character-states).

Principal Component Analysis (PCA) was done. There are ten components that account for 84.6% of the vaiance (Table 78). The first three components account for only 45% of the variance. Factor loading of characters for the first ten PCs are given in Appendix II. Ordination diagrams are not provided because: (1)

TABLE 78. Principal component analysis of shell data: First ten principal components are listed with the percentage of variance loading on each component.

Components	Eigenvalue	Percent	Cumulative
1	6.16870	21.27	21.27
2	3.56713	12.30	33.57
3	3.27486	11.29	44.86
4	2.59528	8.45	53.81
5	2.45005	8.45	62.26
6	1.76301	6.08	68.34
7	1.38014	4.76	73.10
8	1.30153	4.49	77.59
9	1.10735	3.82	81.41
10	0.93280	3.22	84.62

most taxa cluster too close together at the center of the plots; (2) the MST results (Fig. 155) are much less satisfactory than those given in Figure 154; there are 14 mismatches of phenotypes (i.e. 32%). Three dimensional scaling produced even less acceptable results.

PCA analysis is useful in demonstrating the utility of shell characters used for discriminating among species. The first component (Table 79) is not one of size but involves ten apertural characters that are most useful in distinguishing among species. As examples: (1) only four species (*N. dianmenensis*, *N. lilii*, *T. gredleri*, *T. odonta*) have a pronounced adapical apertural sinus; (2) only three species have an adapical apertural beak tubercle (*T. dianmenensis*, *T. gredleri*, *T. odonta*); (3) only *T. odonta* has a mid-lip inner lip notch and a shell of 7.0 whorls.

The second component is defined on the basis of seven components that include sculpture, size, varix formation, and shell base characters. The third component involves three (shape, columellar and apertural groove) characters, while the fourth is defined by four characters, with teeth and internal keels as well as sculpture and outer lip orientation.

The *Neotricula duplicata* cluster of five taxa (*N. duplicata*, *N. lilii*, *N. odonta*, *N. dianmenensis*, *N. gredleri*), best seen in Figures 153 and 154, have four to seven of the following seven character states: an outer lip sinus, adapertural beak or notch, abapical spout, a beak tubercle, a thickened inner lip, the inner lip completely separated from the body whorl, and an angled or sinuate inner lip.

All species of *Neotricula* thus far examined, except the alpha race of *N. aperta*, have spiral microsculpture on the shoulders of the teleoconch whorls; not so for species of *Tricula*. *Neotricula aperta* is unique for its globoseconic shape, wide columellar shelf, and keel on the base of the body whorl bordering the wide columellar shelf. Only *T. maxidens* has a cylindrical-conic shell and a large columellar tooth clearly visible in the aperture. Only *J. jinghongensis* has spiral microsculpture at the base of the body whorl and a basal post. Only *T. xiaolongmenensis* has a domed tooth on the *columella* inside the body whorl. Only *W. niuzhuangensis* has a spiral keel on the columella inside the body whorl that does not extend basally so as to be seen as a tooth in the aperture (in contrast to *T. maxidens*). Only three species have crenulated whorls at the suture: *N. burchi*, *G. chinensis*, *J. jinghongensis*.

Anatomy

Thirty OTUs were scored for 48 character states (Tables 80, 81). A UPGMA phenogram based on distance coefficient is given (Fig. 156). Distances were used as the cophenetic correlation because r = 0.960 is superior to that using similarity coefficients (r = 0.865). In this phenetic treatment, species do not group neatly into well-defined generic clusters. However, by eliminating characters with missing data and using the Prim Network (MST) (Fig. 157), well-defined generic groupings resulted.

In the PCA analysis, ten components were extracted before eigenvalues dropped below 1.0; these components accounted for 89.8% of the variance (Table 82). Factor loadings of characters on each of the ten components are given in Appendix III. Ordination on the first two PC axes is given (Fig. 158) with OTUs connected by the MST based on the original distance matrix (with characters involving missing data removed) (Fig. 157). The spe-

TABLE 79. Shell characters highly correlated on each of nine principal components. * = also loads ≥ 0.440 on another axis.

Characters	Loading	COMPONENTS I. APERTURAL/WHORLS
11	−0.849	sinus—adaptical aperture
24	−0.733	beak tubercle—adaptical aperture
13	−0.715	inner lip shape
18	−0.696	lip deflection angle
17	−0.665	notch, inner lip
29	−0.665	shell has 7.0 whorls
12	−0.653	abapical spout
20	−0.636	inner lip separated from body whorl
19	−0.632	inner lip thickness
9	−0.606	adapical notch, beak
3	−0.582	apertural shape
		II. SIZE, SCULTPURE, VARIX, SHELL BASE
6	+0.812	spiral microsculpture
5	+0.653	whorl at suture crenulated
28	+0.596	basal post
12*	+0.497	abapical spout
1	−0.461	size
8	−0.461	protoconch sculpture
23	+0.458	varix
		III. SHAPE, KEEL, COLUMELLAR SHELF: *N. APERTA* AXIS
26	+0.810	keel at external base of shell
27	+0.751	columellar shelf
10	+0.728	inner adapical apertural groove
2	+0.645	shape
		IV. STRUCTURE ON COLUMBELLA INSIDE OR OUTSIDE SHELL; OUTER LIP
16	−0.715	inner lip tooth
7	−0.611	spiral sculpture at shell base
22	−0.585	internal columellar keel
15	+0.443	outer lip scooped forward
		V. APERTURE, WHORL CRENULATION
3*	+0.574	apertural shape
5*	−0.499	crenulated suture
19*	−0.459	inner lip thickened
9*	+0.450	adaptical apertural notch, beak
		VI. VARIX, LIP SEPARATION
23*	−0.553	varix
21	−0.496	adaptical aperture separated from body whorl
20*	−0.444	inner lip separated from body whorl
		VII. LIP ANGLE, SIZE
25	−0.696	lip angle
1*	−0.570	aize
		VIII. LIP SINUATION
14	+0.734	lip sinuation
		IX. PROTOCONCH SCULPTURE
8*	−0.494	protoconch sculpture

cies fall cleanly into generic clusters on the ordination diagram. Through use of Figures 157 and 158, it is clear which species pairs are most similar anatomically; e.g., *Tricula montana* is most similar to *T. gregoriana*.

The ordination diagram and an assessment of anatomical characters with high loadings on each of the ten principal components are useful for assessing OTU relationships. The first and second components clearly separate genera (Table 83). Characters 17, 18, 24, 21 clearly serve to separate generic clusters. Species with the 360° open oviduct circle complex of organs with the spermathecal duct entering the pericardium are to the left upper and lower quadrants. Species that have lost

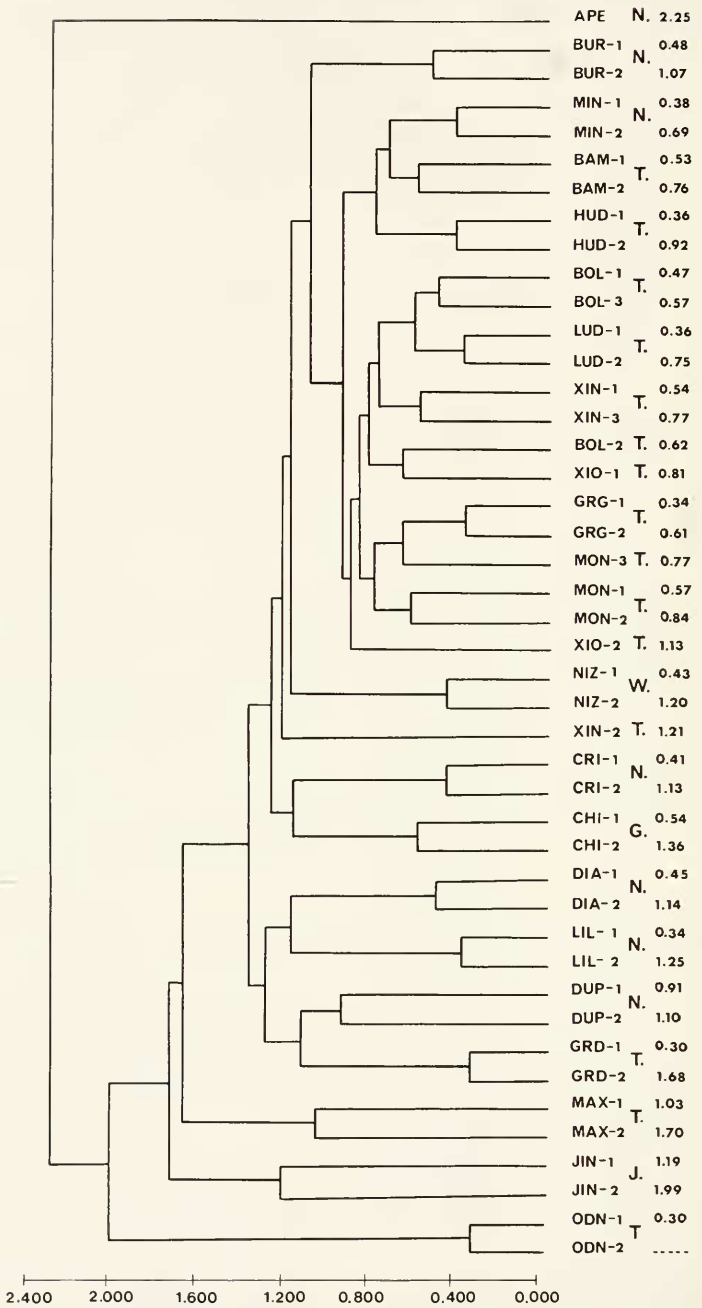

FIG. 153. Phenogram based on UPGMA treatment of distance coefficients involving shell characters from phenotypes (1–3) of 21 species (Tables 76, 77). G, *Gammatricula*; J, *Jinhongia*; N, *Neotricula*; T, *Tricula*; W, *Wuconchona*. APE, *N. aperta*; BUR, *N. burchi*; BAM, *T. bambooensis*; BOL, *T. bollingi*; CRI, *N. cristella*; CHI, *G. chinensis*; DIA, *N. dianmenensis*; DUP, *N. duplicata*; GRD, *T. gredleri*; GRG, *T. gregoriana*; HUD, *T. hudiequanensis*; JIN, *J. jinhongensis*; LIL, *N. lilii*; LUD, *T. ludongbini*; MAX, *T. maxidens*; MIN, *N. minutoides*; MON, *T. montana*; NIZ, *W. niuzhuangensis*; ODN, *T. odonta*; XIO, *T. xiaolongmenensis*; XIN, *T. xianfengensis*.

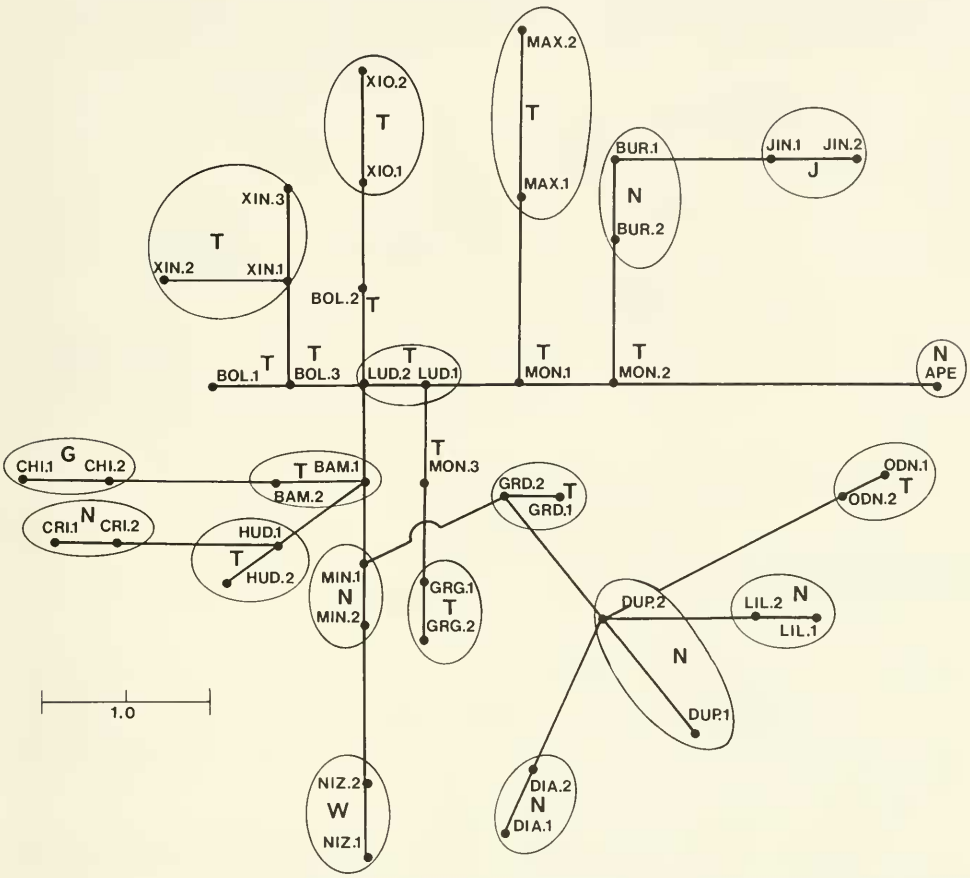

FIG. 154. Minimum spanning tree (MST) based on distance coefficients involving shell characters treated in Tables 2 and 76. The tree is drawn to scale using inter-taxon distances. See caption for Figure 153 for defining abbreviations.

the seminal recepatacle and have the spermathecal duct opening into the mantle cavity are in the upper right quadrant.

While major groupings along the 1st component are established by the four highly correlated characters given above, species placements are dictated by the 14 other characters with loadings ≤ 0.678. *Tricula gredleri* is far to the left because of character 37; it alone, of all the OTUs, has a massive ejaculatory duct. *Wuconchona niuzhuangensis* is far to the right because it shares with *Gammatricula chinensis* character states for characters 21 and 35; the function of the seminal receptacle is moved to the inside of the oviduct, and the concave edge of the penis has a white muscular zone. *Wuconchona* is displaced to the right of *Gammatricula* due to characters 17, 28, and 29. *Wuconchona* is unique in having a discrete U-shaped bend of the oviduct, a very short male gonad, and no vas efferens.

Distribution along the second principal component is due to the interaction of 12 characters. *Tricula gredleri*, *Neotricula dianmenensis*, and *N. minutoides* are at the bottom of the ordination diagram because of characters 2, 19, 20, 34, and 40. Unique to *T. gredleri* are operculum shape, fusion of the oviduct to the pericardium, the lemon color of

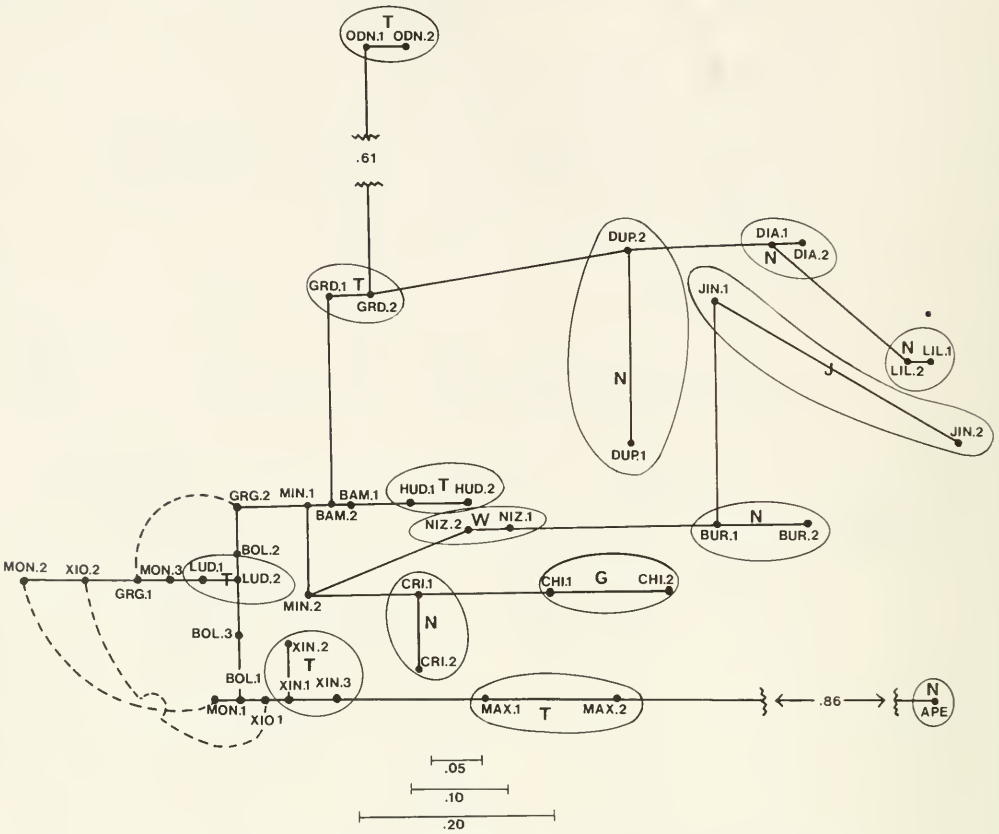

FIG. 155. MST based on shell distance coefficients following PCA analysis. Abbreviations are defined in caption for Figure 153. See text for details.

the anterior chamber of the stomach, and the position of the penial opening. *Neotricula dianmenensis* and *N. minutoides* have few rows of teeth per radula. *Tricula minutoids* has a highly extensible penis. *Jinhongia*, *Wuconchona* and *Gammatricula* are at the top because of the loss of the seminal receptacle (and duct).

Comparing Figures 156–158, it is seen which species are most similar anatomically and the affect of intrapopulation variation on distance measures. Linkages at a value $\leq$ 0.40 (distance coefficients) clearly involve population variation. Linkages $\geq$ 0.67 involve discrete species.

There are species clusters of phenetically closely related species. The biggest cluster, one that has the least distances among species, involves the *Tricula bollingi* complex: *T. bollingi*, *T. bambooensis*, *T. hudiequanensis* and *T. ludongbini*. These species occur in Yunnan, China. Within this complex, *T. hudiequanensis* is unique in that it has a scatter of a few white glands about the eyes (char. 1). The attachment pad of the operculum is very wide (char. 4). The shell is most similar to that of *T. bambooensis* (Figs. 153–155). However, there is a 12.5% difference between *T. hudiequanensis* and *T. bambooensis* (chars. 1, 4, 6, 8, 14, 37). Within the *T. bollingi* complex, *T. bollingi* is unique in that the female gonad is posterior to the stomach (char. 11), the radula is of medium length, not short (char. 41), and the radula has a moderate number of rows of teeth, not few (char. 42). The shell of *T. bollingi* is most similar to that of *T. ludongbini*.

A closely allied species pair involves *T. montana* from India and *T. gregoriana* from

TABLE 80. Anatomical characters and character-states (n = 48) showing one or more differences among 20 species belonging to the genera *Tricula* or *Neotricula*, or where the shells indicate affinity to these two genera.

	External Features (N = 5, 10%)
1. Glands about the eyes	no glands (0), scatter of a few glands (1), dense concentration of glands (2)
2. Operculum shape:	ovate (0), mid-columellar indentation (1), elongate-oval (2), irregular shape (3), cap-like (4)
3. Operculum:	single layer (0), two or more layers (1)
4. Operculum attachment pad:	wide (0), narrow (1), very wide (2)
5. Operculum; thick internal ridge:	none (0), has (1)
	Mantle Cavity (N = 5, 10%)
6. Gill filament number:	few (0), moderate (1), many (2)
7. Gill filament shape:	flat (0), moderate dome (1), high domed (2)
8. Gf_2 length:	long (0), medium (1), short (2)
9. Osphradium length:	long (0), short (1)
10. Circular grandular mass anterior to osphradium:	none (0), has (1)
	Female Reproductive System (N = 16, 33%)
11. Gonad:	behind stomach (0), overlaps stomach (1)
12. Gonad:	long (0), short (1), very short (2)
13. Bursa:	short (0), long (1), minute (2)
14. Bursa:	posterior to pallial oviduct [Ppo] (0), covered wholly or considerably by Ppo (1), ventral to Ppo (2), postero-lateral to Ppo (3)
15. Bursa:	round (0), triangular to subtriangular (1), ovoid (2)
16. Bursa; duct:	≥ 0.04 mm long (0), none (1)
17. Oviduct at bursa:	makes 360° tight twist (0), runs to Ppo without twist or bend (1), no twist but has discrete bend (2)
18. Spermathecal duct:	enters pricardium (0), enters mantle cavity (1)
19. Spermathecal duct:	long (0), short (1), none, fused to pericardium (2)
20. Spermathecal duct:	slants at an angle from duct of bursa or oviduct to mantle cavity, or at an angle from anterior-posterior axis (0), runs directly anterior from duct of bursa to mantle cavity (1), none, oviduct fused to pericardium (2)
21. Seminal receptacle:	arises from oviduct or duct of bursa (0), lost, function removed to inside swelling between duct of bursa and spermathecal duct (1), lost, function removed to inside oviduct (2)
22. Seminal receptacle duct:	U-shaped continuation of duct of bursa (0), arises from oviduct (1), from juncture of duct of bursa and oviduct (2), from duct or bursa (3), lost (4)
23. Seminal receptacle duct:	≥ 0.02 mm long (0), very short to ductless (1), seminal receptacle and duct lost (2)
24. Seminal receptacle arises from:	inside edg of oviduct in coil (0), outside edge of oviduct coil (1), from duct of bursa (2), seminal receptacle lost (3)
25. Pericardial bursa:	none (0), slight (1), large (2), extremely enlarged (3)
26. Albumen bland:	normal (0), short (1)
	Male Reproductive System (N = 11, 23%)
27. Gonad:	posterior to stomach (0), overlaps stomach (1)
28. Gonad:	long (0), short (1)
29. Vas efferens:	has (0), does not have (1)
30. Seminal vesicle:	coils posterior to stomach (0), coils also on stomach (1), coils only on stomach (2)
31. Vas deferens—2:	leaves prostate at Emc (0), leaves prostate at mid-prostate (1)
32. Penial tip:	no papilla (0), has papilla (1), long penial filament (2)
33. Penis:	normal (0), highly extensible (1)
34. Penial opening:	center of penial tip (0), from concave edge of blunt penial tip (1)

(*continued*)

TABLE 80. (Continued).

	External Features (N = 5, 10%)
35. Penis:	no white muscular zone on concave edge (0), has such zone (1)
36. Ejaculatory duct:	none (0), in base of penis (1), extends from penial base into the neck (2), only in neck (3)
37. Ejaculatory duct:	none (0), slight (1), large/prominent (2), massive (3)
	Digestive System (N = 9, 19%)
38. Digestive bland:	posterior to stomach (0), covers Pst (1)
39. Anterior chamber of stomach [Ast]:	no streak (0), with grey-melanin streak (1)
40. Ast lemon yellow color:	no (0), yes (1)
41. Radula:	short (0), medium length (1), long (2), very long (3)
42. Radula:	no. rows teeth: few (0), moderate no. (1), many (2)
43. Radula central tooth:	has paired swellings at posterior face of tooth between innermost basal cusps (1), lacks (0)
44. Radula central tooth:	central cusp: generalized type (0), long and dagger-like (1)
45. Lateral tooth major cusp:	1 (0), 1 [2] = (1)
46. Lateral tooth major cusp:	normal (0), displaced towards outer edge (1)
47. RPG ratio:	moderately concentrated (0), elongated (1), concentrated (2)
48. Length pleuro-subesophageal connective:	usual (0), none (1), long (2)

Yunnan, China. They are similar anatomically (Fig. 157) and conchologically (Figs. 153, 154). They differ in seven anatomical characters (15%).

PHYLOGENETIC RELATIONSHIPS

Phylogenies involving 19 genera of the three tribes of Triculinae were recently published (Davis et al. 1990; Davis & Kang, 1990; Davis, 1992). To these are now added the two additional genera (*Guoia*, *Lithoglyphopsis*), additions made possible because of this study. In this analysis, only one genus of the Jullieniini is used (outgroup), and the 13 genera grouped in the Triculini and Pachydrobiini. The characters and character-states used are listed in Table 84. There are 17 characters listed under synapomorphies, an additional 14 as autapomorphies. Scores are tabulated in Table 85. The result of the Hennig-86 analysis was 20 equally parsimonious trees with a length of 37, a consistency index of 86 and an ri (retention index; Farris, 1989) index of 91. Four of the trees and the Nelsen consensus tree are given (Figs. 159–163). All show the separation of the three tribes with the same genera assigned to each of the tribes. The only difference among the 20 trees for genera of the Triculini was the tricotomy of *Fenouilia*, *Lacunopsis*, *Lithoglyphopsis* or, alternatively, the divergence of *Fenouilia* from *Lacunopsis* and *Lithoglyphopsis*. The separation ((*Fenouilia*) (*Lacunopsis*, *Lithoglyphopsis*)) is warranted as *Fenouilia* has a trochoid shell, and the other two genera have globose shells.

The greatest shifting about involves genera of the Pachydrobiini. The consensus tree reduces the shifting to produce a polycotomy for *Neotricula*, *Halewisia*, *Pachydrobia*, and *Jinhongia*. In all trees, *Gammatricula* and *Wuconchona* diverge from the same node separated from the node that supports the subcluster of ((*Robertsiella*) (*Guoia*-a, *Guoia*-b)).

A single tree resolves with the ordering of character-states involving (1) the position of the seminal receptacle and its duct, (2) the loss of the seminal receptacle and the direction of evolution of the location of the structures functionally replacing the seminal receptacle, and (3) an analysis of homoplasies (Fig. 164). The generalized position of the seminal receptacle is a branch off the oviduct posterior to the duct of the bursa and anterior to a coiling of the oviduct between the gonopericardial duct and the bursa copulatrix (outgroups *Hydrobia*, Hydrobiidae; *Pomatiopsis*, Pomatiopsinae: Pomatiopsini). This position is seen in the genera of the tribe Triculini. In the Triculini and Pachydrobiini, the position of

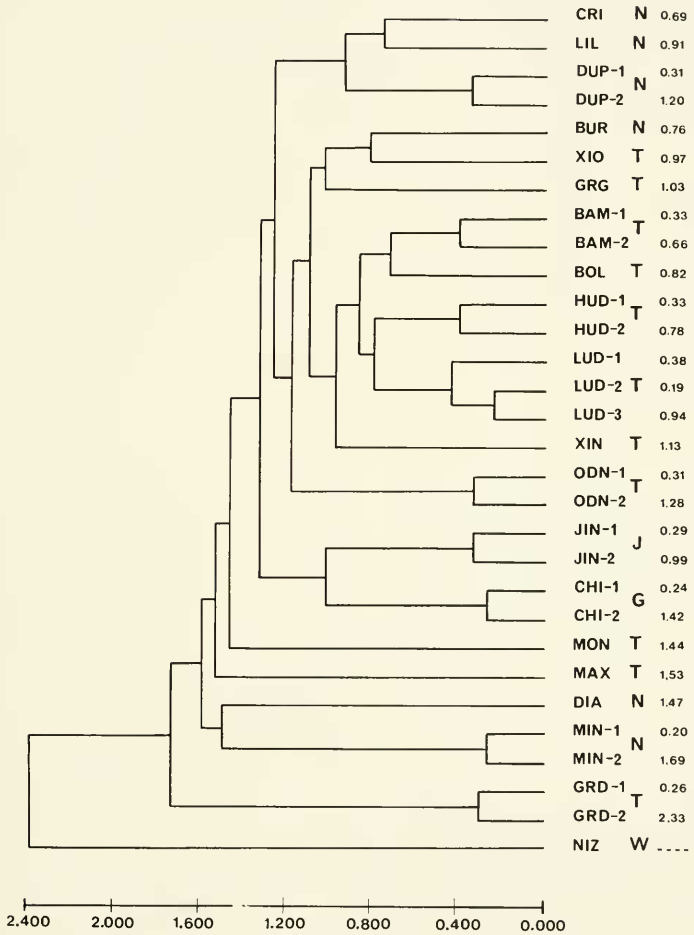

FIG. 156. Phenogram based an UPGMA treatment of distances based on all 48 anatomical characters from 1 to 2 phenotypes of 20 species. See Tables 80, 81. Abbreviations are defined in the caption for Figure 153.

TABLE 81. Scoring of 30 OTUs for 48 character-states listed in Table 80: bur-1, bur-2, etc. indicates that shells of *Neotricula burchi* exhibit more than one character-state for one or more characters. bur, *burchi*; cri, *cristella*; dia, *dianmenesis*; dup, *duplicata*; lil, *lilli*; min, *minutoides*; bam, *bambooensis*; bol, *bollingi*; grd, *gredleri*; grg, *gregoriana*; hud, *hudiequanensis*; lud, *ludongbini*; max, *maxidens*; mon, *montana*; odo, *odonta*; xian, *xianfengensis*; xio, *xiaolongmenensis*; chi, *chinensis*; jin, *jinhongensis*; niz, *niuzhuangensis*. NC = missing data.

	1 N.cri	2 N.dia	3 N.dup1	4 N.dup2	5 N.lil	6 N.min1	7 N.min2	8 N.bur	9 T.mon	10 T.bam1	11 Tbam2	12 Tboll	13 Tgred1	14 Tgred2	15 Tgreg
1	0	NC	0	1	0	0	1	2	1	0	0	0	0	0	2
2	0	2	2	2	0	0	0	0	0	0	0	0	4	4	0
3	1	1	1	1	0	1	1	0	0	0	0	0	0	0	0
4	0	0	2	2	0	0	0	NC	0	0	0	0	0	0	0
5	0	0	0	0	0	0	0	0	0	0	2	0	0	0	0
6	0	1	1	1	1	1	1	1	1	2	2	1	1	1	2
7	1	NC	1	2	1	NC	NC	NC	1	2	1	2	1	1	NC
8	0	1	1	1	0	0	0	NC	0	1	1	1	0	0	0
9	1	0	1	1	1	1	1	1	1	1	0	1	1	1	1
10	0	0	0	0	0	0	0	0	1	0	1	0	0	0	0
11	0	0	0	0	0	0	0	0	0	0	1	0	0	0	0
12	1	1	1	1	1	1	1	1	1	1	2	0	1	1	1
13	0	0	0	0	0	0	0	0	0	2	2	2	2	2	0
14	0	0	0	0	0	0	0	3	0	2	2	2	2	2	0
15	0	0	2	2	0	0	0	2	2	2	0	2	0	1	2
16	0	1	0	0	0	0	0	0	0	0	0	0	0	0	0
17	1	1	1	1	1	1	1	1	0	0	0	0	0	0	0
18	1	1	1	1	1	1	1	1	0	0	0	0	0	0	0
19	0	0	1	1	0	1	1	0	0	0	0	0	2	2	0
20	0	1	1	1	0	1	1	0	0	0	0	0	2	2	0
21	0	0	0	0	0	0	0	0	0	0	1	0	0	0	0
22	0	0	0	0	0	0	0	0	3	1	0	1	1	1	3
23	0	0	0	0	0	1	1	0	0	0	0	0	0	0	0
24	2	2	2	2	2	2	2	2	2	0	0	0	0	0	2
25	0	0	0	0	0	0	0	0	2	0	0	0	3	3	2
26	0	0	0	0	0	1	1	0	0	0	0	0	0	0	0
27	0	0	1	1	1	0	0	0	1	1	1	1	1	1	1
28	0	0	0	0	0	0	0	0	0	0	0	0	0	0	0
29	0	0	0	0	0	0	0	0	0	0	0	0	0	0	0
30	0	0	0	0	0	0	0	0	1	1	1	1	1	1	1
31	0	0	0	0	1	0	0	1	1	1	1	1	0	0	1
32	2	1	1	1	1	0	1	0	1	0	0	1	1	1	1
33	0	0	0	0	0	1	0	0	0	0	0	0	0	0	0
34	0	0	0	0	0	0	0	0	0	0	0	0	1	1	0
35	0	0	0	0	0	0	0	0	0	0	0	0	0	0	0
36	0	0	0	0	0	0	0	1	2	1	1	1	2	2	3
37	0	0	0	0	0	0	1	1	2	1	1	1	3	3	2
38	1	0	0	0	0	1	1	0	0	0	0	1	0	0	0
39	0	0	0	0	0	1	0	0	0	0	0	0	0	0	0
40	0	0	0	0	0	0	1	0	0	0	0	0	1	1	0
41	1	1	1	1	1	1	0	1	2	2	2	1	1	1	1
42	3	0	2	2	3	0	0	1	2	2	2	1	1	2	2
43	0	0	0	0	0	0	0	0	1	0	0	0	0	0	0
44	0	0	0	0	0	0	1	0	0	0	0	0	0	0	0
45	1	1	1	1	1	1	0	0	1	0	0	0	1	1	0
46	0	0	0	0	0	0	0	0	0	0	0	0	0	0	0
47	0	0	0	0	0	0	0	NC	0	0	0	0	0	0	0
48	0	0	0	0	0	0	0	NC	NC	0	0	0	2	2	0

TABLE 81. (Continued)

	16 Thud1	17 Thud2	18 Tlud1	19 Tlud2	20 Tlud3	21 Tmax	22 Todol	23 Todo20	24 Txian	25 Txiao	26 Jjin1	27 Jjin2	28 Wniz	29 Gchi1	30 Gchi2
1	1	1	0	0	0	0	0	3	1	2	1	1	2	1	1
2	0	0	0	0	0	1	3	1	0	0	0	0	2	0	0
3	0	0	1	1	1	0	1	0	1	0	1	1	0	1	1
4	2	2	0	0	0	1	0	1	2	1	0	0	2	0	0
5	0	0	0	0	0	0	1	2	0	0	0	0	1	0	0
6	1	1	2	2	2	0	2	2	2	1	1	1	0	1	1
7	2	2	2	2	2	NC	2	0	NC	NC	NC	NC	NC	0	1
8	0	0	0	0	0	0	0	1	1	0	1	1	0	0	0
9	1	1	1	1	1	0	1	0	1	1	1	1	1	1	1
10	0	0	0	0	0	0	0	0	0	0	0	0	1	0	0
11	1	1	1	1	1	0	0	1	1	NC	0	0	0	0	0
12	1	1	0	0	0	1	1	2	0	1	0	1	2	0	0
13	2	2	2	2	2	0	2	0	2	0	0	0	1	1	1
14	0	0	0	0	0	1	0	1	0	0	2	2	0	0	0
15	2	2	1	1	1	0	1	0	2	2	2	2	2	2	2
16	0	0	0	0	0	0	0	0	0	0	0	0	0	0	0
17	0	0	0	0	0	0	0	0	0	0	1	1	2	1	1
18	0	0	0	0	0	0	0	0	0	0	1	1	1	1	1
19	0	0	0	0	0	0	0	0	0	0	0	0	1	0	0
20	0	0	0	0	0	0	0	0	0	0	0	0	0	0	0
21	0	0	0	0	0	0	0	1	0	0	1	1	2	2	2
22	1	2	1	3	2	1	1	1	1	1	4	4	4	4	4
23	0	0	0	0	0	0	1	0	0	0	2	2	2	2	2
24	0	0	0	2	2	0	0	0	0	1	3	3	3	3	3
25	0	0	0	0	0	1	0	0	0	0	0	0	0	0	0
26	0	0	0	0	0	0	0	0	1	0	0	0	1	0	0
27	1	1	1	1	1	1	0	1	1	NC	1	1	0	0	0
28	0	0	0	0	0	0	0	0	0	0	0	0	1	0	0
29	0	0	0	0	0	0	0	0	0	0	0	0	1	0	0
30	1	1	1	1	1	0	2	2	1	0	0	0	1	0	0
31	1	1	1	1	1	1	0	0	1	1	1	1	1	1	1
32	1	1	0	0	0	0	0	0	0	0	1	1	2	1	1
33	0	0	0	0	0	0	0	0	0	0	0	0	0	0	0
34	0	0	0	0	0	0	0	0	0	0	0	0	0	0	0
35	0	0	0	0	0	0	0	0	0	0	0	0	1	1	1
36	1	3	1	2	3	1	1	1	0	1	1	1	0	1	1
37	2	2	2	2	2	2	2	2	0	1	2	2	0	1	1
38	0	0	0	0	0	1	0	0	0	0	1	1	1	0	0
39	0	0	0	0	0	1	0	0	0	0	0	0	0	0	0
40	0	0	0	0	0	0	0	0	0	0	0	0	0	0	0
41	3	3	2	2	2	0	1	1	2	1	1	1	1	1	1
42	2	2	2	2	2	2	2	2	2	2	2	2	2	2	2
43	0	0	0	0	0	0	0	0	0	0	0	0	0	0	0
44	0	0	0	0	0	1	0	0	0	0	1	1	0	0	0
45	0	0	0	0	0	0	1	1	0	0	0	0	0	0	0
46	0	0	0	0	0	0	0	0	0	0	0	0	1	0	0
47	0	0	0	0	0	NC	0	0	1	1	0	0	2	0	0
48	0	0	0	0	0	NC	0	0	0	2	0	0	1	0	0

the opening into the duct of the seminal receptacle shifts as follows: along the oviduct to the base of the duct of the bursa (one species of Tricula); → to stem off the duct of the bursa (one species of *Tricula*, nearly all *Neotricula*, *Halewisia*); → to stem off the sperm duct (*Pachydrobia*). The presumption is that no large scale rearangements of ducts were made in a single step. To obtain the uncoiled oviduct seen in *Neotricula* (contrast Triculini), first the duct of the seminal receptacle, then the spermathecal duct would have had to migrate along the oviduct to move onto the duct of the bursa. With this accomplished, the

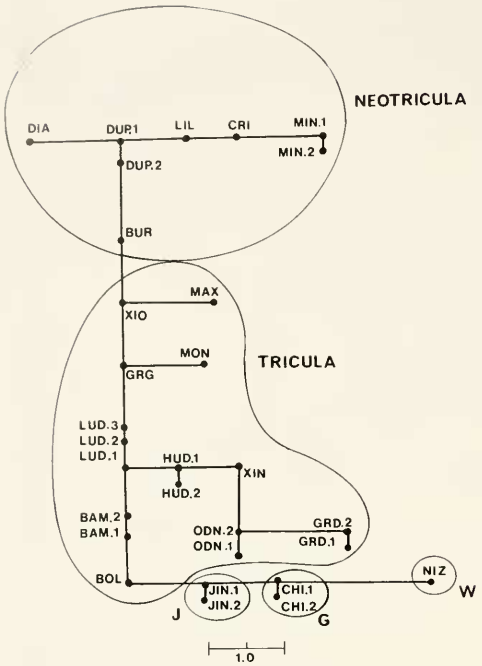

FIG. 157. MST based on distance coefficients involving all anatomical characters treated in Tables 80 and 81. The tree is drawn to scale using intertaxon distances. See caption for Figure 153 for defining abbreviations. Generic groupings have been circled.

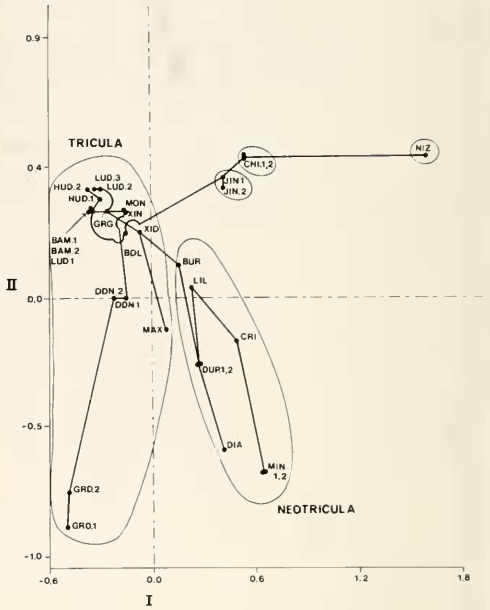

FIG. 158. Ordination diagram following PCA and MST seen in Figure 157. All characters scored in Table 81 as NC were removed in this analysis to permit the PCA treatment. The ordination is on the first two PCA axes. Generic groupings have been circled. See text for details. See caption for Figure 153 for defining abbreviations.

TABLE 82. Principal Component Analysis of anatomical data (matrix of 41 × 30). The first ten principal components are listed with the percentage of variance loading on each component.

Component	Eigenvalue	Percent	Cumulative
1	8.87575	21.65	21.65
2	6.86082	16.73	38.38
3	5.58656	13.63	52.01
4	3.54706	8.65	60.66
5	2.70292	6.59	67.25
6	2.60035	6.34	73.59
7	2.12427	5.18	78.77
8	1.83148	4.47	83.24
9	1.61804	3.95	87.19
10	1.05972	2.58	89.77

proximal section of the duct of the bursa (as seen in *Tricula*) would become the sperm duct, linking the new bursa complex to the oviduct to facilitate fertilization. In no case is a species of Pachydrobiini seen with the seminal receptacle arising from the oviduct! The most probable sequence is the move of the seminal receptacle from the oviduct to the duct of the bursa (situation seen in *Tricula* species b). Then the spermathecal duct mi-

TABLE 83. Characters with high loadings, that define each of ten components. **High loading on more than one axis (above).

Characters	Loadings	COMPONENT
		I. GENERIC ORGANIZERS*, N = 18
17*	+0.934	oviduct 360° circle
18*	+0.838	spermathecal duct enters pericardium
24*	+0.734	origin of seminal receptacle
27	−0.678	male gonad overlaps stomach
23	+0.658	seminal receptacle duct length
21*	+0.649	seminal receptacle lost
37	−0.644	ejaculatory duct prominence
36	−0.623	position of ejaculatory duct
6	−0.616	gill filament number
28	+0.610	male gonad length
29	+0.610	presence of vas efferens
46	+0.610	position of lateral tooth major cusp
35	+0.599	white muscular zone on penis
13	−0.580	bursa size
38	+0.579	digestive gland covers Pst
30	−0.546	poisition of seminal vesicle
41	−0.460	radula length
26	+0.519	albumen gland length
		II. SPERMATHECAL DUCT, RADULA, PENIS, STOMACH, N = 12
20	−0.871	orientation spermathecal duct
31	+0.847	where vas efferens leaves prostate
45	−0.784	major cusp of lateral tooth
19	−0.723	length spermathecal duct
15	+0.696	bursa shape
22	+0.665	configuration duct of seminal receptacle
2	−0.601	operculum shape
34	−0.575	position of penial opening
40	−0.575	color of Ast
42	+0.522	number of rows of teeth
39	−0.449	melanin streak on Ast
33	−0.471	penis highly extensible
		III. MALE REPRODUCTIVE, RADULA, OPERCULUM, STOMACH, N = 14
46**	+0.632	poisition major cusp lateral tooth
28**	+0.632	male gonad length
29**	+0.632	has/has not: vas efferens
2**	+0.596	operculum shape
40**	+0.589	Ast color
34**	+0.589	position penial opening
10	+0.573	gland mass anterior to osphradium
25	+0.570	pericardial bursa
19**	+0.514	length spermathecal duct
30**	+0.485	position serminal receptacle
5	+0.469	ridge on operculum
45**	+0.447	lateral tooth major cusp
3	−0.446	opercular layers
32	+0.446	penial tip
		IV. RADULA, OPERCULUM, REPRODUCTIVE, N = 5
44	−0.631	central cusp, central tooth
5**	+0.545	opercular ridge
30**	+0.529	position, seminal vesicle
14	−0.502	bursa position
26**	+0.470	albumen gland length
		V. OPERCULUM, FEMALE REPRODUCTIVE, MANTLE CAVITY, N = 4
3**	+0.646	opercular layers
12	−0.484	female gonad length

(*continued*)

TABLE 83. (Continued).

Characters	Loadings	COMPONENT
23**	+0.424	length duct seminal receptacle
10*	−0.421	gland mass anterior to osphradium
		VI. STOMACH, PENIS, FEMALE REPRODUCTIVE, N = 6
39**	+0.583	melanin streak on Ast
33**	+0.530	highly extensible penis
26**	+0.482	albumen bland length
38**	+0.475	digestive bland covers Pst
32**	−0.455	penis tip
16	−0.435	duct of bursa
		VII. CENTRAL TOOTH, OSPHRADIUM, OPERCULUM, N = 4
9	+0.617	osphradium length
43	+0.465	swelling on face of central tooth
5**	−0.443	opercular ridge
44*	−0.417	central cusp of central tooth
		VIII. CENTRAL TOOTH, N = 1
43**	−0.610	swellings on face of central tooth
		IX. BURSA, TEETH, N = 2
16**	−0.611	duct of bursa
42**	+0.523	rows of teeth: number
		X. BURSA, N = 1
14**	+0.538	position of bursa

grates along the oviduct to the duct of the bursa, with subsequent shift of the spermathecal duct from opening into the pericardium to opening into the posterior end of the mantle cavity next to the pericardium, and the uncoiling of the oviduct (as seen in *Neotricula* species of type a, and b). Subsequently, either the duct of the seminal receptacle migrates onto the sperm duct, or the point where the spermathecal duct joins the duct of the bursa moves distally towards the bursa leaving anterior to it that proximal piece of duct that once was the duct of the bursa, with the seminal receptacle attached to it (as seen in *Pachydrobia*). In this scenario, both *Halewisia* and *Pachydrobia* evolved from progenators resembling *Neotricula* species of type a (e.g. *N. aperta*, *N. cristella*). In *Halewisia* the spermathecal duct migrated to open into the bursa copulatrix. The shell is a derived type (Davis, 1979: 111). *Pachydrobia* has evolved a large first-order adaptive radiation (Davis, 1992) of greater than 14 species in which the shell has modified from the generalized *Tricula* type variously: larger, thick shells with thick lips; tendency to have pronounced macrosculpture (nodes, spines); tendency to shell assymetry.

There is parallel evolution in the Triculini and Pachydrobiini involving loss of the seminal receptacle and duct with new structures arising in different locations to accomodate the functions of the seminal receptacle. The solution to this loss is quite different in the two tribes, hence, no difficulty arises regarding correct tribal classification or assessment of intergeneric relationships. The tendency towards loss is minor in the Triculini, involving only one genus, *Lacunopsis*; it is major development in the Pachydrobiini involving the majority of genera (five of eight). In *Lacunopsis*, two or more accessary seminal receptacles arise to the exterior of the juncture of the oviduct and spermathecal duct. In the Pachydrobiini, solutions to the loss of the seminal receptacle are all within the relevant ducts (duct of the bursa, sperm duct, oviduct). The most parsimonious direction of evolution is as follows: the duct of the seminal receptacle is lost, the seminal receptacle becomes fused to the duct of the bursa close to or at the bursa (as in *N. dianmenensis*); → The seminal receptacle is replaced by an outpocketing within the encapsulated duct of the bursa (as in *Robertsiella*); → the sperm storage area shifts anteriorly to a swelling at the juncture of the duct of the bursa, spermathecal duct and sperm duct (as in *Jinhongia*); → the next shift is into the sperm duct (*Guoia*-a), and finally the oviduct (*Guoia*-b) → and farther posterior within the oviduct (*Wuconchona* and *Gammatricula*).

TABLE 84. Characters and character-states used for the cladistic analysis.

SYNAPOMORPHIES

1. Spermathecal duct opens to pericardium: (a) (0); (b) to posterior mantle cavity (1).
2. Oviduct makes: (a) a closed, tight 360° twist posterior to duct of the bursa (0); (b) an open 360° circle (1); (c) does not have the 360° twist or circle (2).
3. Sperm duct: (a) absent (0); (b) present and short (1); (c) present and elongated (2).
4. Spermathecal duct: (a) has primitive position between pericardium and oviduct as seen in *Pomatiopsis* (Pomatiopsinae) (0); (b) joins oviduct before oviduct twist (1); (c) joins oviduct 180° or more into oviduct circle (2); (d) joins duct of bursa, or common sperm duct (3); (e) joins bursa (4).
5. Seminal receptacle: (a) arises from primitive condition from oviduct posterior to the duct of the bursa (as in *Pomatiopsis*) (0); (b) from left side of the oviduct and pressed to the contour of the oviduct circle complex (1); (c) joins duct of bursa or common sperm duct (2); (d) joins the sperm duct (3); is lost; function replaced by: (e) an outpocketing of the encapsulated duct of the bursa (4); (f) an internal duct swelling at the juncture of bursa and spermathecal duct (5); (g) an outpocketing of sperm duct or swelling of sperm duct at juncture of sperm duct and oviduct (6); (h) within the oviduct (7); (i) two or more seminal receptacles arise from the oviduct (outside the duct) at the juncture of the oviduct with the spermathecal duct (8).
6. Duct of serminal receptacle(s): (a) short (0); (b) long (1); (c) lost due to fusion of the seminal receptacle to the duct of the bursa (2); (d) lost as the usual seminal receptacle is lost (3).
7. Gonad 1 or 2, or 3 finger-like tubes: (a) (0); (b) (1).
8. Vas deferens runs to style sac, turns posteriorly to form seminal vesicle: (a) (0); (b) (1).
9. Central tooth: (a) anterior cusps 5 or more (0); (b) only one large triangular blade (1)
10. Foot shape, power: (a) slender, weak (0); (b) wide, powerful (1)
11. Head shape: (a) standard (0); (b) wide, squat head; eyes in pronounced lobes (1)
12. Shell shape: (a) ovate-conic (0); (b) globose (1); (c) trochoid (2)
13. Shell size (a) small, thin (0); (b) increased length, thickness (1)
14. Penis with chitenous stylet: (a) (0); (b) (1).
15. Spermathecal duct with vaginal section: (a) (0); (b) (1).
16. Bursa copulatrix elongated relative to length of albumen gland: (a) (0); (b) (1).
17. Penis has a strongly developed muscular white zone at concave edge: (a) (0); (b) (1).

AUTAPOMORPHIES

Fenouilia

18. Gill filament section Gf_1 extremely elongated (1)

Lithoglyphopsis

19. Radular sac extremely elongated (1).
20. Posterior pallial oviduct bends 180° around (1).
21. Extremely long cerebral commissure (1).

Jinhongia

5f (above). Function of the seminal receptacle within an internal swelling at the juncture of the bursa and spermathecal duct (1).

Robertsiella

5e (above). Function of the seminal receptacle within a cavitation of the duct of the bursa (1).

22. Common sperm duct, duct of the bursa encapsulated (1).

Guoia

23. The penis has a glandular lobe (1).
24. The sperm duct is not only much elongated, it coils (1).

Wuconchona

25. The columella of the shell within the body whorl has a raised spiral ridge (1).
26. The spermathecal duct is short (1).
27. The male gonad is a wide sac, few lobes, floor of sac opens to a vas deferens, i.e. no vas efferens (1).
28. The dominant cusp of the lateral tooth is displaced towards the outside edge of the tooth (1).
29. The oviduct makes a U-shaped bend (1).

(*continued*)

TABLE 84. (Continued).

Gammatricula

30. The posterior half or third of the prostate is smooth (1).

Pachydrobia

31. The shell lip is especially thickened (1).
5d (above). The seminal receptacle arises from the sperm duct.

Halewisia

4e (above). The spermathecal duct joins the bursa copulatrix.

TABLE 85. Scoring 18 OTUs for synapomorphies listed in Table 84. Hub, *Hubendickia* (outgroup of Jullieniini); Tr-a, *Tricula* species a, Tr-b, species b; *Delavaya;* Fen, *Fenouilia; Lac, Lacunopsis;* Lit, *Lithoglyphopsis;* Ne-a, *Neotricula* species a, Ne-b, species b, Ne-c, species c; Hal, *Halewisia;* Pac, *Pachydrobia;* Gu-a, *Guoia* species a, Gu-b, species b; Rob, *Robertsiella;* Jin, *Jinhongia;* Wuc, *Wuconchona;* Gam, *Gammatricula.*

	1 Hub	2 Tr-a	3 Tr-b	4 Del	5 Fen	6 Lac	7 Lit	8 Ne-a	9 Ne-b	10 Ne-c	11 Hal	12 Pac	13 Gu-a	14 Gu-b	15 Rob	16 Jin	17 Wuc	18 Gam
1	0	0	0	0	0	0	0	1	1	1	1	1	1	1	1	1	1	1
2	1	0	0	0	0	0	0	2	2	2	2	2	2	2	2	2	2	2
3	0	0	0	0	0	0	0	1	1	1	2	1	2	2	1	1	0	1
4	2	1	1	1	1	1	1	3	3	3	4	3	3	3	3	3	0	3
5	1	0	2	0	0	8	0	2	2	2	2	3	6	7	4	5	7	7
6	1	0	0	0	0	0	0	0	1	2	1	1	3	3	3	3	3	3
7	1	0	0	0	0	0	0	0	0	0	0	0	0	0	0	0	0	0
8	1	0	0	0	0	0	0	0	0	0	0	0	0	0	0	0	0	0
9	0	0	0	1	1	1	1	0	0	0	0	0	0	0	0	0	0	0
10	0	0	0	0	1	1	1	0	0	0	0	0	0	0	0	0	0	0
11	0	0	0	0	1	1	1	0	0	0	0	0	0	0	0	0	0	0
12	0	0	0	0	2	1	1	0	0	0	0	0	0	0	0	0	0	0
13	0	0	0	1	1	1	1	0	0	0	0	1	0	0	0	0	0	0
14	0	0	0	0	0	0	0	0	0	0	0	0	1	1	1	0	0	0
15	0	0	0	0	0	0	0	0	0	0	0	0	1	1	1	0	0	0
16	0	0	0	0	0	0	0	1	0	0	1	0	0	0	0	0	1	1
17	0	0	0	0	0	0	0	0	0	0	0	0	0	0	0	0	1	1

There is clear-cut parallelism in the intraductal shifting of sperm storage. The *Robertsiella-Guoia* clade has highly derived character-states: the chitenous sheath on the penial papilla, the vaginal section of the spermathecal duct, the thick, straight and relatively short continuous duct running from the end of the mantle cavity into the bursa, and the loss of the seminal receptacle. The clade is relatively old within the 12 ± 4 million years in which the triculine macro adaptive radiation (Davis, 1992) has been evolving. The presence of *Robertsiella* in Malaysia and *Guoia* in Hunan, China, indicate both the age of the clade in and its origin in northern Burma or Yunnan, China. Three character-states involving the sperm storage location are found within this one clade: (1) within an outpocketing of the encapsulated duct of the bursa (*Robertsiella*), (2) within the sperm duct next to the oviduct (*Guoia*-a), (3) within the proximal oviduct (*Guoia*-b). The parallel situation is seen in the genera *Wuconchona* and *Gammatricula* that are found only (thus far) in southeastern China. In these genera, the simplified gonad, penial-characters (but lacking the chitenous penial stylet), and sperm storage in a more distal section of oviduct indicate a clade of derived taxa clearly divergent from the *Robertsiella-Guoia* clade.

Other parallelisms are simply partitioned and understood. In each second order radiation (Davis, 1980, 1992) there are trends for increasing size (seen in shell length), increasing complexity in sculpture (from smooth → ribs → reticulate sculpture, spiral cords, spines or nodes), and changes in shape (ovate-conic to turreted, globose, assymetry

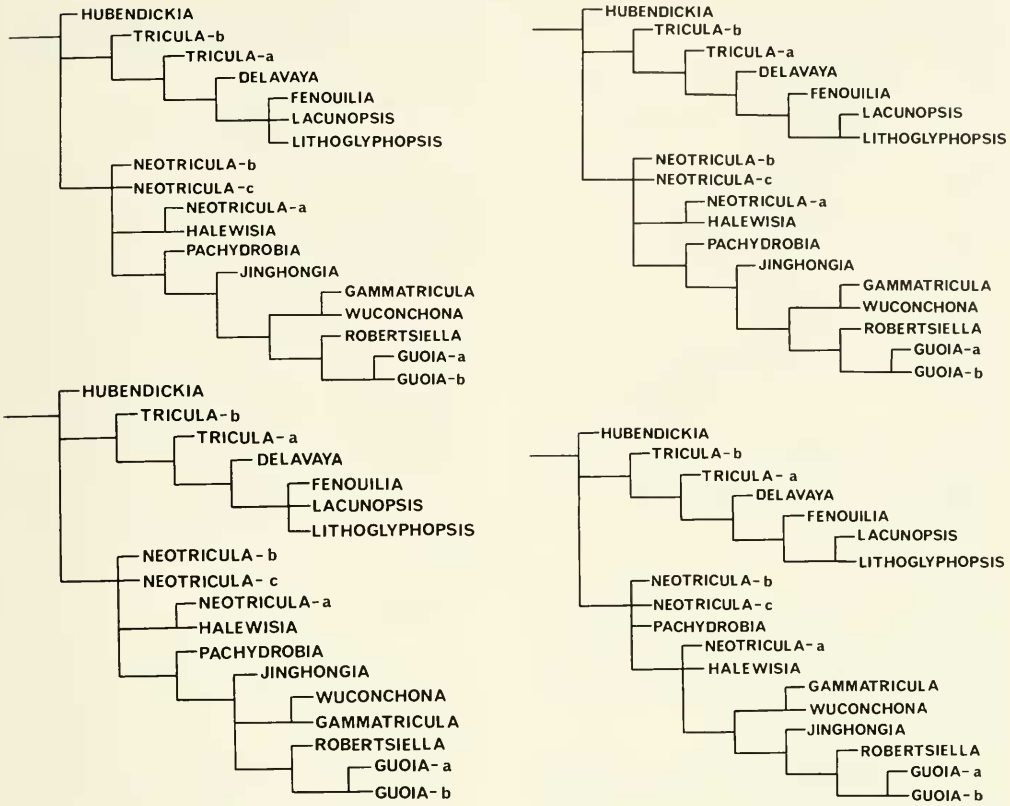

FIGS. 159–162 Four representatives of the 20 computer-generated cladograms following the Hennig-86 treatment of data given in Tables 85 and 86. See text for details.

(see Davis, 1979). The primitive small ovate-conic shell seen in *Tricula*, *Neotricula*, *Jinhongia* and *Gammatricula* is the basic platform from which splendid first order adaptive radiations arose, most with distinctive patterns of shell development (e.g. *Pachydrobia*, *Jullienia*, *Hubendickia*, *Lacunopsis*. However, while one can discern the shells of *Lacunopsis* from those of *Hubendickia* or *Pachydrobia*, there is convergence in the globose shell types such that the shell character-states of *Guoia*, *Lithoglyphopsis* and *Lacunopsis* merge. Fortunately, there is extreme anatomical divergence between *Guoia*, *Lacunopsis* and *Lithoglyphopsis*; accordingly these genera are readily classified in one or the other of the relevant second order radiations.

The length of the duct of the seminal receptacle increases with increasing anatomical complexity in the Jullieniini and Triculini. The trend is particularly pronounced in the Jullieniini (Davis, 1979; 1991). There is a parallel increase in the length of the sperm duct involving some derived genera of the Triculini and Pachydrobiini; it is particularly evident in *Guoia*.

OLD PROBLEMS RESOLVED

Two unsolved questions of a decade ago can now be answered. (1) What is *Lithoglyphopsis* and its relationship to *Lithoglyphopsis aperta* Temcharoen, 1971? (2) Given the impact of the Himalayan orogeny as a driving force of the spectacular triculine radiation, too few species of *Tricula* or species morphologically close to *Tricula* had been found a decade ago (Davis, 1980). There were numerous species of *Pachydrobia*, *Lacunopsis*, *Hubendickia*, etc. known a decade ago, but only three species of *Tricula*, *sensu* Davis,

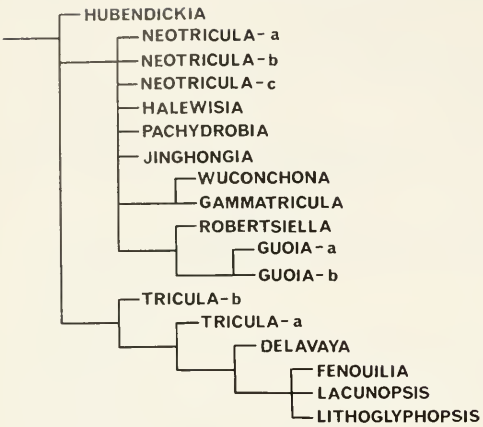

FIG. 163. The nelsen consensus tree resolving the 20 trees generated following the Hennig-88 treatment of data given in Tables 85 and 86.

1979, had been found in Southeast Asia. A few species from Burma had been described as *Tricula* on the basis of shells (reviewed in Davis, 1980). It was predicted that more would be found (Davis, 1980). How extensive was the *Tricula* radiation?

Concerning the first question, it is evident that *Lithoglyphopsis* is most closely related to *Fenouilia* and *Delavaya* anatomically and to *Lacunopsis* conchologically. *Lithoglyphopsis* is a derived genus in the tribe Triculini. *Lithoglyphopsis aperta*, the snail host for *Schistosoma mekongi*, is the type species for the genus *Neotricula* (Davis et al., 1986a). *Neotricula* is an anatomically generalized genus in the tribe Pachydrobiini. Thus, while *Lithoglyphopsis* and *Neotricula* are members of the same subfamily, they are highly divergent genera within the Triculinae.

The second issue is now resolved. With research initiated in Yunnan, China, in 1983 (Davis et al., 1986b) and with this and other ongoing research, it is clear that *Tricula, sensu* Davis, 1979, comprises an extremely large radiation primarily located in southern China. The concept of *Tricula sensu* Davis, 1979, has changed. The anatomical data support four genera with a *Tricula*-type shell: *Tricula*, *Neotricula*, *Gammatricula*, and *Jinhongia*. Anatomical data have been published for seven species of *Neotricula*, eleven species of *Tricula* and one each for *Jinhongia* and *Gammatricula*. These 20 species are one third of the estimated 60 species (conservative estimate) with *Tricula*-like shells that we think occur throughout southern China, Burma and northern Vietnam (Davis, 1992).

BIOGEOGRAPHY

Biogeography at a glance is provided in Figure 165. An area cladogram for river evolution is given with the number of species of each genus for which we have anatomical data listed for each region of river. Overall Triculinae biogeography has been reviewed recently (Davis, 1992). Only a few points need to be emphasized here. (1) Thus far, *Neotricula* has its greatest deployment in the mid to lower Yangtze River, whereas *Tricula* has more species in the upper Yangtze River. (2) The distribution of *Guoia*, *Robertsiella*, *Tricula* and *Neotricula* show that the major innovative anatomical developments in the Triculini and Pachydrobiini had occurred before the Yangtze-Mekong river drainages were completely separated.

(3) The tribes Triculini and the derivative Pachydrobiini dominate the Yangtze River drainage; no Jullieniini have been found, thus far, in the mid or lower Yangtze River drainages. Conversely, the Jullieniini dominate the Mekong River drainage with their greatest radiation in the lower Mekong River. (4) Only *Pacydrobia* of the Pachydrobiini and *Lacunopsis* of the Triculini have undergone explosive adaptive radiations (considering all genera of the Triculini and Pachydrobiini); this has occurred in the lower Mekong River. (5) The most derived anatomical character-states are found in the lower river systems.

(6) There are considerable ecological differences among tribes. With the exception of *Kunmingia* living in the shallow basin of a limestone spring, the other genera of the Jullieniini live in a large river environment. Considering the Triculini and Pachydrobiini, only *Lacunopsis*, *Lithoglyphopsis*, *Guoia*, *Halewisia* and *Pachydrobia* live in large rivers. *Fenouilia* lives on the bottom of a large lake, as did *Parapyrgula* (presumed extinct). *Tricula*, *Neotricula*, *Jinhongia* and *Gammatricula* live in upland shaded small streamlets of pure, cold water. Only *Neotricula aperta* has adjusted to living in a large river environment.

There are numerous species of *Neotricula* and *Tricula* in Hubei Province and provinces to the east, species that are in the process of being studied. We have seen at least one additional species of *Gammatricula*. The proven distribution of *Tricula* is from northern India to

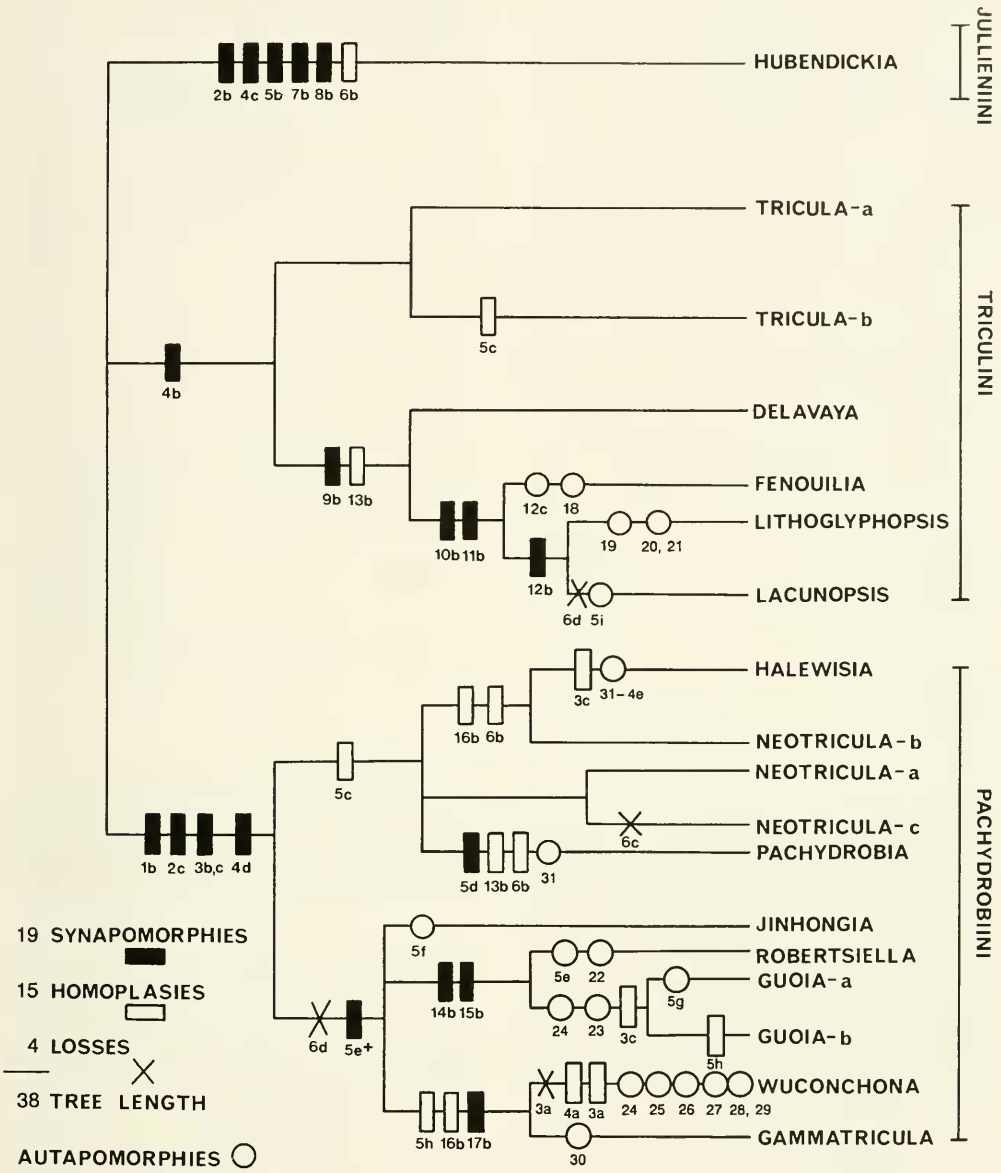

FIG. 164. The cladogram resulting from weighting one character in particular, the seminal receptacle, and the direction of evolution of character states with the primitive condition being 5a (= score 0) (see Table 85) (all Triculini except *Lacunopsis*); the shift of the duct of the seminal receptacle to the duct of the bursa (5c = score 2); the loss of the seminal receptacle, its function transferred into the duct of the bursa ($5e^+$ and 5e on the cladogram); the move within the duct system to the juncture of duct of the bursa, sperm duct and spermathecal duct (5f) → to the sperm duct (5g) → to the oviduct (5h). Parallelisms are accounted for; see text for details.

the East China Sea. As discussed in Davis (1992), there are numerous diverse Triculinae in Yunnan that have not yet been studied. It is highly probable that species of *Neotricula* will be found among them in the upper Yangtze River drainage. While this study has done

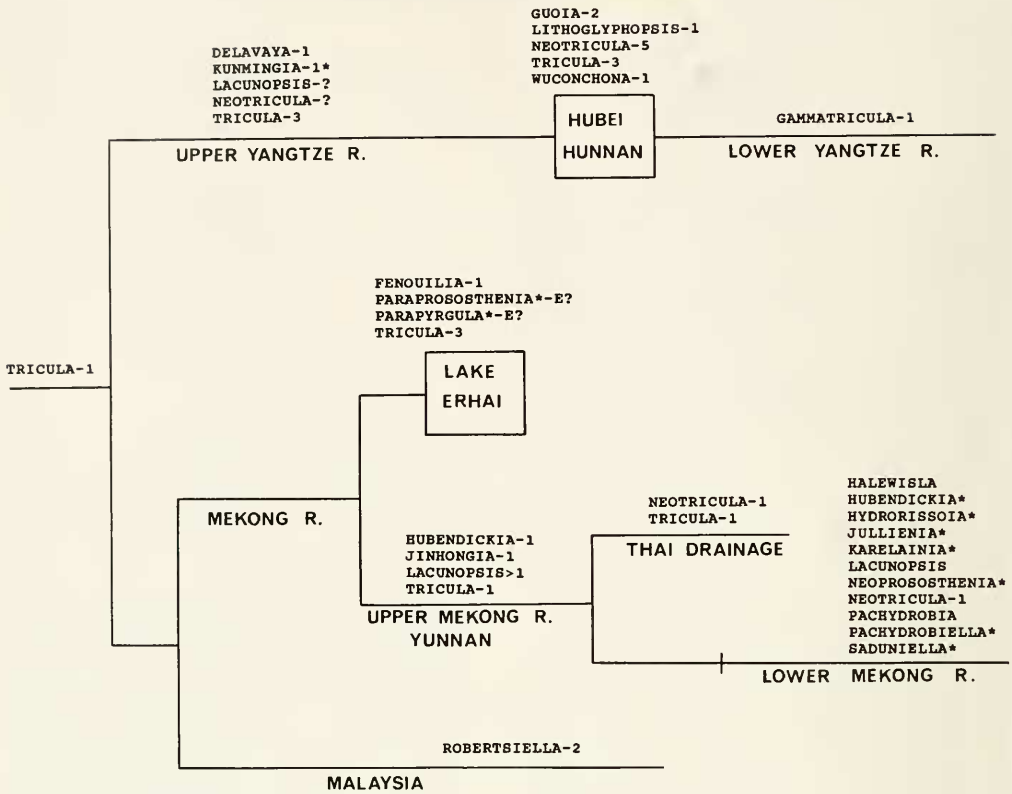

FIG. 165. An area cladogram for rivers showing the location of triculine genera. Those genera with the asterisk belong to the tribe Jullieniini. The question mark indicates the possibility that the genus might be found there. E? indicates probable extinction. With the exception of *Pachydrobia* and *Lacunopsis* in the lower Mekong River, each with more than ten species, the number of species of each genus of the Triculini and Pachydrobiini studied anatomically is given at each location along the drainage systems. *Tricula*-1 is *Tricula montana* of northern India. See text for further details.

much to reduce the probability that new genera of Triculinae will be found (we would expect one or two more, especially in Yunnan), there is considerably more to be learned concerning species of *Tricula* and *Neotricula* and their patterns of distribution.

ACKNOWLEDGEMENTS

Use of the facilities of Hunan Medical College and the Zhejiang Academy of Medical Sciences is gratefully acknowledged. The drawings were made by Davis with renderings by Elizabeth Carrossa and Susan Trammell. Scanning electron microscope work was done by Dr. Chen Cui-E and Caryl Hesterman. Photographs of the shells were taken and printed by Dr. Chen and Caryl Hesterman. Graphics were done by Susan Trammell. Dr. John Hendrickson is thanked for his help in executing the NTSYS programs. The work was supported by the National Natural Science Foundation of China award No. 3860607 to Dr. Chen, and N.I.H. award A1 11373 to Dr. Davis.

LITERATURE CITED

ANNANDALE, N., 1924, The molluscan hosts of the human blood fluke in China and Japan, and species liable to be confused with them. In E. C. FAUST, and H. E. MELENEY, Studies on schistosomiasis japonica. *American Journal of Hygiene Monographic Series*, No.3: 269–294, 1 pl.

BENSON, W. H., 1843, Description of *Camptoceras*, a new genus of the Lymnaeidae, allied to *Ancylus*, and of *Tricula*, a new type of form allied to *Melania*. *Calcutta Journal of Natural History*, 3(12): 465–468.

BRANDT, R. M., 1974, The non-marine aquatic Mollusca of Thailand. *Archiv für Molluskenkunde*, 105: 1–423.

CROSSE, H. & P. FISCHER, 1876, Mollusques fluviatiles, recueillis au Cambodge, par la Mission scientifique francaise de 1873. *Journal de Conchyliologie*, 24: 313–342, pls. 10–11.

DAVIS, G. M., 1967, The systematic relationship of *Pomatiopsis lapidaria* and *Oncomelania hupensis formosana* (Prosobranchia: Hydrobiidae). *Malacologia*, 6(1–2): 1–143.

DAVIS, G. M., 1968a, A systematic study of *Oncomelania hupensis chiui*. *Malacologia*, 7(1): 17–70.

DAVIS, G. M., 1968b, New *Tricula* from Thailand. *Archiv für Molluskenkunde*, 98: 291–317.

DAVIS, G. M., 1969a, Reproductive, neural and other anatomical aspects of *Oncomelania minima* (Prosobranchia: Hydrobiidae). *Venus, Japanese Journal of Malacology*, 28(1): 1–36.

DAVIS, G. M., 1969b, *Oncomelania* and the transmission of *Schistosoma japonicum*: a brief review. In HARINASUTA, C., ed., *Proceedings of the Fourth Asian seminar on parasitology and tropical medicine, schistosomiasis and other snail-transmitted helminthiasis*, 24–27 February, Manila. pp. 93–103.

DAVIS, G. M., 1979, The origin and evolution of the gastropod family Pomatiopsidae, with emphasis on the Mekong River Triculinae. *Monograph of the Academy of Natural Sciences of Philadelphia* No. 20: 1–120.

DAVIS, G. M., 1980, Snail hosts of Asian *Schistomosoma* infecting man: origin and coevolution. In J. I. BRUCE, et al., eds., *The Mekong schistosome, Malacological Review, Supplement* 2: 195–238.

DAVIS, G. M., 1981, Different modes of evolution and adaptive radiation in the Pomatiopsidae (Prosobranchia: Mesogastropoda). *Malacologia*, 21(1/2): 209–262.

DAVIS, G. M., 1992, Evolution of prosobranch snails transmitting Asian *Schistosoma*; coevolution with *Schistosoma*: a review. *Progress in Clinical Parasitology*, in press.

DAVIS, G. M. & P. CARNEY, 1973, Description of *Oncomelania hupenis lindoensis*, first intermediate host of *Schistosoma japonicum* in Sulawesi (Celebes). *Proceedings of the Academy of Natural Sciences of Philadelphia*, 124(1): 1–34.

DAVIS G. M. & G. GREER, 1980, A new genus and two new species of Triculinae (Gastropoda: Prosobranchia) and the transmission of a Malaysian mammalian *Schistosoma* sp. *Proceedings of the Academy of Natural Sciences of Philadelphia*, 132: 245–276.

DAVIS, G. M. & Z. B. KANG, 1990, The genus *Wuconchona* of China (Gastropoda: Pomatiopsidae: Triculinae): anatomy, systematics, cladistics, and transmission of *Schistosoma*. *Proceedings of the Academy of Natural Sciences of Philadelphia*, 142: 119–142.

DAVIS, G. M., C. E. CHEN, X. G. XING & C. WU, 1988, The Stenothyridae of China, No. 2: *Stenothyra hunanensis*. *Proceedings of the Academy of Natural Sciences of Philadelphia*, 140(2): 247–266.

DAVIS, G. M., V. KITIKOON & P. TEMCHAROEN, 1976, Monograph on "*Lithoglyphopsis*" *aperta*, the snail host of Mekong River schistosomiasis. *Malacologia*, 15(2): 241–287.

DAVIS, G. M., Y. H. KUO, K. E. HOAGLAND, P. L. CHEN, H. M. YANG, & D. J. CHEN, 1984, *Kunmingia*, a new genus of Triculinae from China: phenetic and cladistic relationships. *Proceedings of the Academiy of Natural Sciences of Philadelphia*, 136: 165–193.

DAVIS, G. M., Y. H. GUO, K. E. HOAGLAND, P. L. CHEN, L. C. ZHENG, H. M. YANG, D. J. CHEN & Y. F. ZHOU, 1986b, Anatomy and systematics of triculine (Prosobranchia: Pomatiopsidae: Triculinae) freshwater snails from Yunnan, China, with descriptions of new species. *Proceedings of the Academy of Natural Sciences of Philadelphia*, 138(2): 466–575.

DAVIS, G. M., Y. H. KUO, K. E. HOAGLAND, P. L. CHEN, H. M. YANG & D. J. CHEN, 1983, Advances in the Systematics of the Triculinae (Gastropoda: Prosobranchia): the genus *Fenouilia* of Yunnan, China. *Proceedings of the Academy of Natural Sciences of Philadelphia* 135: 177–199.

DAVIS, G. M., Y. H. KUO, K. E. HOAGLAND, P. L. CHEN, H. M. YANG & D. J. CHEN, 1985, *Erhaia*, a new genus and new species of Pomatiopsidae from China (Gastropoda: Rissoacea). *Proceedings of the Academy of Natural Sciences of Philadelphia*, 137: 48–78.

DAVIS, G. M., Y. Y. LIU & Y. G. CHEN, 1990, New Genus of Triculinae (Prosobranchia: Pomatiopsidae) from China: Phylogenetic Relationships. *Proceedings of the Academy of Natural Sciences of Philadelphia*, 142: 143–165.

DAVIS, G. M., N. V. S. RAO & K. E. HOAGLAND, 1986a, In search of *Tricula* (Gastropoda: Prosobranchia): *Tricula* defined, and a new genus described. *Proceedings of the Academy of Natural Sciences of Philadelphia*, 138(2): 426–442.

FARRIS, J. S., 1988, *Hennig 86, Version 1.5*. Stony Brook, N.Y. 18 pp.

FARRIS, J. S., 1989, The retention index and the rescaled consistency index. *Cladistics* 5: 412–419.

FENG, X. C., F. H. ZHOU & S. J. ZHANG, 1985, New discovery of first intermediate hosts of *Paragonimus skrjabini—Tricula gredleri* Kang sp. nov. and *Akiyoshia (Saganoa) odonta* Kang sp. nov. *Hunan Medicine*, 2(4): 65.

FENG, X. C., F. H. ZHOU & S. J. ZHANG, 1986, Discovery of new snails, first intermediate hosts, transmitting *Paragonimus* in Guzhang County. *Chinese Public Health*, 5(5): 38–39.

GREDLER, P. V., 1881, Zur Concylien-Fauna von China. III. Stück. *Jahrbücher der Deutschen Malakozoologischen Gesellschaft*, 8: 110–132.

GREDLER, P. V., 1885, Zur Concylien-Fauna von China. VIII. S.1–19. Selbstverlag, Bozen.

GREDLER, P. V., 1886, Zur Concylien-Fauna von China. IX. *Malakozoologische Blätter* (n.s.) 9: 1–20. Cassel.

GREDLER, P. V., 1887, Zur Conchylien-Fauna von China. XII. Stuck. *Nachrictsblatt der Deutschen Malakozoologische Gesellschaft*, No. 19 (11 u.12): 168–178.

GUO, Y. H. & J. R. GU, 1985, Studies on the intermediate host of *Schistosoma* and *Paragonimus*: 1. *Tricula jinhongensis*, a new species of *Tricula* from Yunnan Province. (Gastropoda: Hydrobiidae). *Acta Zootaxonomica Sinica*, 10(3): 250–252.

HERSHLER, R. & F. G. THOMPSON, 1988, Notes on morphology of *Amnicola limosa* (Say, 1817) (Gastropoda: Hydrobiidae) with comments on status of the subfamily Amnicolinae. *Malacological Review*, 21: 81–92.

IOGANZEN, B. G. & Y. A. STAROBOGATOV, 1982, A finding of a freshwater mollusk of the family Triculidae (Gastropoda: Prosobranchia) in Siberia. *Zoologichesky* Zhurnal, 61(8): 1141–1147.

KANG, Z. B., 1983a (Sept.), A new genus and three new speices of the family Hydrobiidae (Gastropoda: Prosobranchia) from Hubei Province, China. *Oceanologia et Limnologia Sinica*, 14(5): 499–505.

KANG, Z. B., 1983b (Nov.), Two new molluscan hosts for *Paragonimus skrjabini. Oceanologia et Limnologia Sinica*, 14(6): 536–541.

KANG, Z. B., 1985, Descriptions of a new species of *Bythinella* from China. *Acta Hydrobiologica Sinica*, 9(1): 84–88.

KANG, Z. B., 1986, Descriptions of eight new minute freshwater snails and a new and rare species of land snail from China (Prosobranchia: Pomatiopsidae, Hydrobiidae; Hydrocenidae). *Archiv für Molluskenkunde*, 117: 73–91.

KRUSKAL, J. B., 1964, Multidimensional scaling by optimizing goodness of fit to a nonmetric hypothesis. *Psychometrika*, 29: 1–27.

KURODA, T. & T. HABE, 1954, New aquatic gastropods from Japan. *Venus*, 18(2): 71–78.

KURODA, T. & T. HABE, 1957, Trolobiontic aquatic snails from Japan. *Venus*, 19: 183–196.

LIU, Y. Y., T. K. LOU, Y. X. WANG & W. Z. ZHANG, 1981, Subspecific differentiation of oncomelaniid snails. *Acta Zootaxonomica Sinica*, 6(3): 253–266

LIU, Y. Y., Y. X. WANG & W. Z. ZHANG, 1980, On new species and new records of freshwater snails of the family Hydrobiidae from Yunnan, China. *Acta Zootaxonomica Sinica*, 5(4): 358–368.

LIU, Y. Y. & W. Z. ZHANG, 1979, On new genus and species of freshwater snails harbouring cercariae of lung flukes from China. *Acta Zootaxonomica Sinica*, 4(2): 132–136.

LIU, Y. Y., W. Z. ZHANG & C. E. CHEN, 1982, *Pseudobythinella shimenensis*, sp. nov., a new aquatic *Paragonimus* cercariae carrying snail from Hunan Province. *Acta Zootaxonomica Sinica*, 7(3): 254–256.

LIU, Y. Y., W. Z. ZHANG, Y. X. WANG, C. E. CHEN & S. Z. CHEN, 1982, Discovery of *Akiyoshia* Kuroda et Habe (Hydrobiidae: Mollusca) from China with descriptions of two new species. *Acta Zootaxonomica Sinica*, 7(4): 364–367.

LIU, Y. Y., W. Z. ZHANG, & Y. X. WANG, 1983a, Studies on *Tricula* (Prosobranchia: Hydrobiidae) from China. *Acta Zootaxonomica Sinica*, 8(2): 135–139.

LIU, Y. Y., W. Z. ZHANG & Y. X. WANG, 1983b, Three new species of Hydrobiidae (Gastropoda: Prosobranchia) from China. *Acta Zootaxonomica Sinica*, 8(4): 366–369.

LOU, T. K., Y. Y. LIU, W. Z. ZHANG & Y. X. WANG, 1982, A discussion on the classification of *Oncomelania* (Mollusca). *Sinozoologica*, 2: 97–117.

MOELLENDORFF, O.F. VON, 1885, Diagnoses specierum novarum sinensium. *Nachrichtsblatt der deutschen Malakozoologischen Gesellschaft*, 11(u.12): 161–170.

MOELLENDORFF, O.F. VON, 1888, Materialien zur Fauna von China. *Malakozoologische Blätter* (n.f.) 10: 132–163, pl. 4.

ROHLF, F. J., J. KISHPAUGH & D. KIRK, 1972, *NT-SYS: Numerical taxonomy system of multivariate statistical programs.* Technical Report, State University of New York, Stony Brook, NY.

TEMCHAROEN, P., 1971, New aquatic mollusks from Laos. *Archiv. für Molluskenkunde*, 102: 91–109.

TRYON, G. W., 1862, Notes on American fresh water snails, with descriptions of two new species. *Proceedings of the Academy of Natural Sciences of Philadelphia*, 14: 451–452.

THIELE, J., 1928, Revision des systems der Hydrobiiden und Melaniiden. *Abteilung für Systematik, Ökologie und Geographie der Tiere*, 55: 351–402.

VOGE, M., D. BRUCKNER & J. I. BRUCE, 1978, *Schistosoma mekongi* sp. n. from man and animals, compared with four geographic strains of *Schistosoma japonicum. Journal of Parasitology*, 64(4): 577–584.

WENZ, W., 1939, Gastropoda, Part 3, Prosobranchia. Pp. 555–581 in O. H. SCHINDEWOLF, ed., *Handbuch der Paläozoologie*, Berlin (Borntraeger).

YEN, T. C., 1939, Die chinesischen Land-und Süsswasser—Gastropoden des Naturmuseums Senckenberg. *Abhandlungen der Senckenbergischen Naturforschenden Gesellschaft*, 444: 1–234.

ZILCH, A., 1974, Vinzenz Gredler und die Erforchung der Weichtiere Chinas durch Franzikaner aus Tirol. *Archiv für Molluskenkunde*, 104: 171–228.

Revised Ms. accepted 16 December 1991

APPENDIX 1. Sources of data for species of Triculinae used in the multivariate analyses (excluding species treated in this paper).

Neotricula aperta (Temcharoen, 1971): in Davis et al., 1976 [Type species of genus; designated in Davis et al., 1986a].
Neotricula burchi (Davis, 1968)
Tricula montana Benson, 1843: in Davis et al., 1986a [Type species of genus]
T. bambooensis Davis & Zheng, 1986: in Davis et al. 1986b
T. bollingi Davis, 1968
T. gregoriana Annandale, 1924: in Davis et al., 1986b
T. hudiequanensis Davis & Guo, 1986: in Davis et al., 1986b
T. ludongdini Davis & Guo, 1986: in Davis et al., 1986b
T. xianfengensis Davis & Guo, 1986: in Davis et al., 1986b
T. xiaolongmenensis Davis & Guo, 1986: in Davis et al., 1986b
Jinhongia jinhongensis (Guo & Gu, 1985): in Davis et al., 1986b [Type species of genus]
Gammatricula chinensis Davis, Liu & Chen, 1990: in Davis et al., 1990 [Type species of genus]
Wuconchona niuzhuangensis Kang, 1983: in Davis & Kang, 1990a [Type species of genus]

APPENDIX 2. Factor loading of characters for the ten principal components that collectively account for 85% of the variation in this study of shell characters.

	PRINCIPLE COMPONENTS				
	I.	II.	III.	IV.	V.
1.	−0.0410545	−0.4614740	0.1951133	0.1102495	−0.1964896
2.	0.3371738	−0.2702949	0.6452890	−0.2870722	−0.2273258
3.	−0.5820084	0.0153342	0.2508085	0.0428066	0.5737585
4.	−0.4883084	−0.0937884	−0.3041671	0.3050418	−0.0443432
5.	0.1598786	0.6532829	−0.1058710	−0.0463305	−0.4989291
6.	−0.2746159	0.8122425	0.0071554	−0.0500111	0.1822269
7.	0.2803561	0.2844659	0.2436223	−0.6108634	−0.2804339
8.	0.1706873	−0.4612060	0.0912007	0.4000807	−0.1060740
9.	−0.6064097	0.0550309	0.4268830	0.0825438	0.4504842
10.	−0.0511060	−0.0086817	0.7289513	0.3538858	0.0138379
11.	−0.8494929	0.0619407	0.1342359	−0.1052565	0.2478488
12.	−0.6526540	0.4972618	0.2145493	−0.2189934	−0.0605389
13.	−0.7146944	0.2136463	0.0176418	−0.0641302	0.0094302
14.	0.1056108	0.2477635	−0.3376958	0.0983843	−0.0247723
15.	−0.1938874	0.2239324	0.2971711	0.4426535	−0.3136139
16.	0.3325563	−0.1555008	0.1835824	−0.7154313	0.0046761
17.	−0.6648433	−0.3846053	0.0730909	−0.3156229	−0.4205736
18.	−0.6955758	0.3660246	0.1990413	−0.2286217	0.2015936
19.	−0.6319250	−0.3369728	−0.1161682	0.0574202	−0.4591451
20.	−0.6360441	−0.1127735	−0.2589680	0.1512705	−0.3323932
21.	−0.4095072	−0.3166545	−0.2127306	−0.1982544	−0.2723410
22.	0.3875425	−0.1664845	0.1605595	−0.5852705	0.3093103
23.	−0.0710536	0.4584002	−0.2259200	0.1122301	−0.2893657
24.	−0.7326382	−0.1977977	0.0873077	−0.2158382	0.1143209
25.	−0.0983867	0.3013054	−0.2336317	0.1312115	−0.1079600
26.	0.0980229	−0.0845837	0.8104326	0.3794045	−0.1045079
27.	0.1178917	0.2651106	0.7510733	0.1976523	−0.3326711
28.	0.1214556	0.5956626	0.1896647	−0.1906758	−0.4167448
29.	−0.6648433	−0.3846053	0.0730909	−0.3156229	−0.4205736
	VI.	VII.	VIII.	IX.	X.
1.	0.3384070	−0.5698774	0.0460096	−0.1038296	−0.2015172
2.	−0.1341500	−0.1682082	0.1296563	0.2262901	0.1179613
3.	0.1338242	0.0179137	0.0716831	0.1584757	0.0337647
4.	0.1847772	−0.0621649	−0.3912900	0.3915480	−0.0423710
5.	0.1626572	−0.0789925	0.2185103	0.1225756	−0.0940029
6.	−0.1021466	0.0043270	0.0444586	−0.0901887	0.2147945
7.	−0.0002180	0.1959912	−0.1031375	0.0608091	−0.2179681
8.	0.0615272	0.1587772	−0.2981737	−0.4940681	−0.0164338
9.	−0.2213138	−0.0213113	0.1639645	−0.1460116	−0.2374873
10.	−0.2431751	0.0326452	0.1561172	0.0089133	−0.0482282
11.	−0.1235609	0.0485087	−0.0126241	0.0552378	−0.3203997
12.	0.1602039	0.0045610	−0.0563521	−0.0245823	−0.0996069
13.	0.2771966	−0.1739794	−0.0983610	0.0695070	0.4416130
14.	0.2559430	−0.1571185	0.7337301	0.0273879	0.1133017
15.	−0.0909669	0.2889332	−0.2158527	0.4116663	0.2163310
16.	−0.3295022	0.0224967	−0.0264935	0.2984503	0.0080422
17.	0.1965575	−0.1292952	−0.0028319	−0.0987587	0.1400116
18.	−0.0673200	−0.1059933	−0.1987022	−0.2522537	0.2059356
19.	−0.1305618	0.1619921	−0.0220588	0.1714101	−0.1204920
20.	−0.4444652	0.1209360	0.1189897	−0.0587002	−0.0058012
21.	−0.4959528	0.1709711	0.2976215	−0.1487671	0.1337223
22.	−0.1349609	−0.2227013	−0.2268552	−0.0828126	0.1662128
23.	−0.5534215	−0.2637156	−0.0907283	−0.2368980	0.0500118
24.	0.1807102	0.1188745	0.2030360	0.0449544	−0.2547120
25.	−0.3337661	−0.6962163	−0.1929729	0.1613878	−0.2710739
26.	−0.0871736	−0.1570683	0.1745502	0.0772054	0.1175377
27.	0.0513585	−0.0302295	−0.0577648	−0.1412964	−0.0056331
28.	0.3292032	0.2276822	−0.1024080	−0.2274468	−0.2240125
29.	0.1965575	−0.1292952	−0.0028319	−0.0987587	0.1400116

APPENDIX 3. Factor loading of characters for the ten principal components that collectively account for 90% of the variation in this study of anatomical characters. Only 41 characters are used as no missing data were allowed in the PCA analysis.

	PRINCIPLE COMPONENTS				
	I.	II.	III.	IV.	V.
2.	−0.0971430	−0.6013535	0.5959546	0.0668697	0.2552416
3.	0.2857560	−0.0616901	−0.4464561	0.1288039	0.6460538
5.	0.2334109	0.0746406	0.4689891	0.5445427	0.1455881
6.	−0.6159816	0.2368112	−0.1616069	0.3824686	0.3790016
9.	−0.1030642	0.2758602	0.2265553	0.1676757	0.3476608
10.	0.3783801	0.2220442	0.5730512	0.1711390	−0.4213342
12.	0.2808698	−0.3578114	0.3977414	0.2035502	−0.4838175
13.	−0.5800852	0.2057583	0.3564111	0.3719478	0.3222399
14.	−0.2141655	−0.0802545	0.1442952	−0.5024069	−0.1107264
15.	−0.0625617	0.6955844	0.1884190	−0.0751765	0.0585363
16.	0.1441796	−0.2877685	−0.1940611	0.0395566	0.0007327
17.	0.9340978	−0.0764409	−0.0112246	−0.1052855	0.1197626
18.	0.8379920	−0.1581357	−0.2415173	−0.2205638	0.2052664
19.	0.0948649	−0.7225091	0.5135236	−0.0776931	0.1336098
20.	−0.0477885	−0.8711195	0.2605822	−0.1511693	0.1926126
21.	0.6492946	0.4411572	0.2990977	−0.2707346	0.3700605
22.	0.2164818	0.6650421	0.3564631	−0.3670552	0.2019860
23.	0.6580347	0.2659786	0.1374653	−0.1748385	0.4240264
24.	0.7339792	0.1832732	−0.1162168	−0.3264529	0.1854340
25.	−0.3732890	−0.4181728	0.5697897	−0.3883381	−0.1400759
26.	0.5188465	−0.1851264	0.0220450	0.4697214	−0.1053183
27.	−0.6784778	0.1793504	0.0918947	−0.1980585	−0.2374376
28.	0.6098325	0.1973294	0.6315968	0.2793996	−0.1918658
29.	0.6098325	0.1973294	0.6315968	0.2793996	−0.1918658
30.	−0.5456913	0.1716460	0.4846009	0.5285202	0.0935103
31.	−0.0988049	0.8467538	−0.0251339	−0.2078032	−0.2906712
32.	0.4414210	0.0242099	0.4463780	−0.3216799	−0.0195030
33.	0.3388348	−0.4707434	−0.3449156	0.2567195	−0.0462704
34.	−0.3332398	−0.5745382	0.5893458	−0.3239226	0.1852541
35.	0.5994937	0.3691855	0.3543632	−0.0498222	0.3475240
36.	−0.6232941	0.2722790	0.2957349	−0.2475745	0.0005819
37.	−0.6437625	0.1028952	0.3961242	−0.3618655	0.0745969
38.	0.5793707	−0.1093442	−0.1040323	−0.1968725	−0.3085475
39.	0.2811599	−0.4485988	−0.3590495	0.0503694	−0.3279842
40.	−0.3332398	−0.5745382	0.5893458	−0.3239226	0.1852541
41.	−0.4597675	0.4187379	0.0153485	0.3484048	−0.0427419
42.	−0.1782957	0.5215056	0.2159982	−0.1292289	0.0143310
43.	−0.0840292	0.1112269	0.1647247	−0.0415819	−0.3936273
44.	0.1616456	0.1293033	−0.1539454	−0.6310220	−0.2087496
45.	0.0864995	−0.7839667	0.0446516	0.1787427	0.0927740
46.	0.6098325	0.1973294	0.6315968	0.2793996	−0.1918658
	VI.	VII.	VIII.	IX.	X.
2.	−0.1394164	−0.3474175	−0.0792670	0.1056858	0.0854577
3.	0.0093270	−0.0592813	−0.2851638	0.1587237	−0.0517160
5.	0.0449117	−0.4425233	−0.2218537	0.3159829	0.1471501
6.	0.1163917	0.0395406	−0.1044403	−0.0334291	0.2700133
9.	0.1417184	0.6167990	0.2681562	0.4167362	0.1386042
10.	−0.1248724	0.2536923	−0.3529955	−0.0161008	0.1129820
12.	−0.1854555	−0.0913738	0.0851108	0.1708288	0.1926282
13.	0.2550922	−0.1352908	0.1456703	−0.1650157	−0.1249281
14.	0.2836786	−0.1617582	0.3841972	−0.0299036	0.5384613
15.	−0.0788765	0.2099368	0.2237864	0.0080864	0.3954614
16.	−0.4354456	−0.3648156	−0.2176404	−0.6109018	0.1593562
17.	−0.1534960	0.0609385	0.1527720	0.0182737	0.1012241
18.	−0.1997098	0.1097419	0.1298337	0.0507008	0.1254707

(*continued*)

APPENDIX 3. (Continued)

	PRINCIPLE COMPONENTS				
	VI.	VII.	VIII.	IX.	X.
19.	0.1677881	0.2533934	0.1785646	0.0104447	−0.0195058
20.	0.0126496	0.1760192	0.0752291	−0.1513470	0.0383810
21.	0.1104381	−0.0205072	−0.0538776	−0.1350167	−0.0573354
22.	0.2026985	0.0578036	−0.3427233	−0.0726498	−0.0024815
23.	0.3357801	−0.0910891	−0.2196621	0.1255442	0.1376799
24.	−0.1652149	0.2716005	−0.1927697	−0.0061319	0.0910426
25.	0.0315530	0.1971248	−0.2439671	−0.0636229	−0.0579249
26.	0.4822483	0.2524238	0.0512107	−0.0957911	−0.0476433
27.	−0.0037041	0.0253443	0.1257655	0.2416408	−0.0378403
28.	0.0709616	−0.1122485	0.1196700	−0.0827769	−0.0295994
29.	0.0709616	−0.1122485	0.1196700	−0.0827769	−0.0295994
30.	0.1328322	−0.1671411	−0.2060764	0.1016164	0.0785346
31.	0.1569631	0.0579261	0.1100781	−0.2140089	−0.0485999
32.	−0.4554683	0.1161356	0.0894265	0.0458263	−0.2058747
33.	0.5295037	0.3717229	−0.1185204	−0.0160033	0.0198906
34.	0.1115931	0.0793780	0.1069966	−0.0967904	−0.0698220
35.	0.0258687	0.0397086	−0.0296042	−0.2666091	−0.2045914
36.	0.1449843	0.1298960	−0.2864864	−0.1526312	−0.0600707
37.	0.2668363	−0.1405495	−0.3199402	0.0507502	0.0056072
38.	0.4748601	−0.1419334	0.0072793	0.2376274	−0.0643782
39.	0.5829850	0.0145123	−0.1912881	0.0057201	−0.1940589
40.	0.1115931	0.0793780	0.1069966	−0.0967904	−0.0698220
41.	−0.0477399	0.3526877	0.0829260	−0.2145180	−0.0505431
42.	−0.3470802	−0.0603708	0.1326352	0.5233748	−0.3710022
43.	−0.2444863	0.4647836	−0.6101984	0.0604030	0.1866010
44.	0.3225032	−0.4169769	−0.1464836	0.2691902	0.0783850
45.	−0.3467677	0.1343245	−0.2636901	0.3034776	0.0343297
46.	0.0709616	−0.1122485	0.1196700	−0.0827769	−0.0295994